

UNCLASSIFIED

AD NUMBER
AD843985
NEW LIMITATION CHANGE
TO Approved for public release, distribution unlimited
FROM Distribution authorized to U.S. Gov't. agencies and their contractors; Critical Technology; MAR 1968. Other requests shall be referred to Air Force Materials Lab., Attn: MANL, Wright-Patterson AFB, OH 45433.
AUTHORITY
Air Force Materials Lab. ltr dtd 7 Dec 1972

THIS PAGE IS UNCLASSIFIED

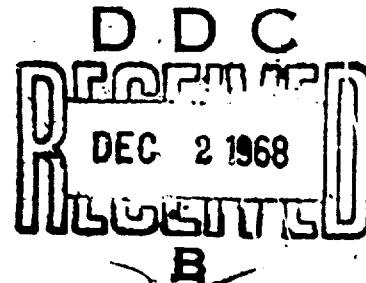
PHYSICAL AND CHEMICAL PROPERTIES OF FLUIDS, LUBRICANTS AND RELATED MATERIALS

AD843985

A. A. Krawetz
J. Krawetz
G. A. Krawetz, et al.

Phoenix Chemical Laboratory, Inc.

TECHNICAL REPORT AFML-TR-67-133, PART II
March 1968



This document is subject to special export controls and each transmittal to foreign governments or foreign nationals may be made only with prior approval of the Fluid and Lubricant Materials Branch, MANL, Nonmetallic Materials Division, Air Force Materials Laboratory, Wright-Patterson Air Force Base, Ohio 45433

Air Force Materials Laboratory
Air Force Systems Command
Wright-Patterson Air Force Base, Ohio

AFML-TR-67-133
Part II

PHYSICAL AND CHEMICAL PROPERTIES OF FLUIDS, LUBRICANTS AND RELATED MATERIALS

A. A. Krawetz
J. Krawetz
G. A. Krawetz, et al.

This document is subject to special export controls and each transmittal to foreign governments or foreign nationals may be made only with prior approval of the Fluid and Lubricant Materials Branch, MANL, Nonmetallic Materials Division, Air Force Materials Laboratory, Wright-Patterson Air Force Base, Ohio 45433

FOREWORD

This report was prepared by Phoenix Chemical Laboratory, Inc. under USAF Contract No. AF 33(615)-3416. This contract was initiated under Project No. 7343 "Aerospace Lubricants", Task No. 734303 "Fluid Lubricant Materials". This work was administered under the direction of the Air Force Materials Laboratory, Air Force Systems Command, Wright-Patterson Air Force Base, Ohio, with Mr. Keith W. Burris as project engineer.

This report covers work performed between 1 November 1966 and 31 October 1967. The manuscript was released by the author in January 1968 for publication as a technical report.

The authors acknowledge the special contributions of Jo Anne Winiecki in the preparation of this report.

The following individuals contributed significantly to the experimental phases of this program: B. Hellman, T. Tovrog, S. Gumushian, E. O'Hagan, R. Gleason and G. Kroma.

This technical report has been reviewed and is approved.



R. L. ADAMCZAK, Chief
Fluid and Lubricant Materials Branch
Nonmetallic Materials Division
Air Force Materials Laboratory

ABSTRACT

Spontaneous ignition phenomena have been evaluated for eight experimental hydraulic fluids. The technique of thermo-electric flame detection has been used to determine the minimum spontaneous ignition temperature for each system in air at one atmosphere pressure. Differential thermal analysis has been employed for the study of the thermal and oxidative degradation of two experimental lubricants in the presence of several metal oxide catalysts. Six other lubricant systems without added catalytic agents have been subjected to differential thermal analysis to evaluate their resistance to thermal and oxidative decomposition. The standard MIL-H-27601A constant temperature thermal stability apparatus has been modified to permit the measurement and recording of pressures developed during the course of the test. Several materials have been evaluated by means of the modified procedure. The chemical and physical properties of various lubricants and hydraulic fluids have been determined. Emphasis has been directed but not exclusively confined to the study of properties which are related to the attainment of effective lubrication at elevated temperatures.

This document is subject to special export controls and each transmittal to foreign governments or foreign nationals may be made only with prior approval of the Fluid and Lubricant Materials Branch, MANL, Nonmetallic Materials Division, Air Force Materials Laboratory, Wright-Patterson Air Force Base, Ohio 45433

TABLE OF CONTENTS

Section	Subject	Page No.
1.	Spontaneous Ignition of Experimental Hydraulic Fluids	1
1.1	Introduction	1
1.2	Apparatus and Procedures	2
1.3	Experimental Results and Discussion.	3
1.3.1	MLO-64-4.	3
1.3.2	MLO-64-5.	3
1.3.3	ELO-66-51	18
1.3.4	ELO-67-16	16
1.3.5	ELO-66-109.	40
1.3.6	ELO-67-23	40
1.3.7	ELO-67-49	58
1.3.8	ELO-67-55	77
1.4	Summary.	77
2.	Differential Thermal Analysis	77
2.1	Introduction	77
2.2	Apparatus and Procedure.	88
2.3	Experimental Data.	94
2.3.1	Thermal and Oxidative Degradation in the Presence of Metal Oxide Catalysts	94
2.3.1.1	Blank. Pyrex Microbeads plus Metal Oxide Catalysts. Nitrogen Atmosphere	95
2.3.1.2	MLO-64-8. Pyrex Microbeads plus Metal Oxide Catalysts. Nitrogen Atmosphere	95
2.3.1.3	ELO-65-48. Pyrex Microbeads plus Metal Oxide Catalysts. Nitrogen Atmosphere	103

LIST OF ILLUSTRATIONS

Figure		Page No.
1	MLO-64-4. Spontaneous Ignition Temperature. Run 12.	5
2	MLO-64-4. Spontaneous Ignition Temperature. Run 14.	6
3	MLO-64-4. Spontaneous Ignition Temperature. Run 5	7
4	MLO-64-4. Spontaneous Ignition Temperature. Run 21.	8
5	MLO-64-4. Spontaneous Ignition Temperature. Run 2	9
6	MLO-64-4. Spontaneous Ignition Temperature. Run 26.	10
7	MLO-64-4. Minimum Spontaneous Ignition Temperature	11
8	MLO-64-5. Spontaneous Ignition Temperature. Run 2	13
9	MLO-64-5. Spontaneous Ignition Temperature. Run 13.	14
10	MLO-64-5. Spontaneous Ignition Temperature. Run 4	15
11	MLO-64-5. Spontaneous Ignition Temperature. Run 20.	16
12	MLO-64-5. Minimum Spontaneous Ignition Temperature	17
13	EL0-66-51. Spontaneous Ignition Temperature. Run 7	21
14	EL0-66-51. Spontaneous Ignition Temperature. Run 30.	22
15	EL0-66-51. Spontaneous Ignition Temperature. Run 36.	23
16	EL0-66-51. Spontaneous Ignition Temperature. Run 2	24
17	EL0-66-51. Spontaneous Ignition Temperature. Run 31.	25
18	EL0-66-51. Spontaneous Ignition Temperature. Run 22.	26
19	EL0-66-51. Spontaneous Ignition Temperature. Run 25.	27
20	EL0-66-51. Spontaneous Ignition Temperature. Run 5	28
21	EL0-66-51. Spontaneous Ignition Temperature. Run 5	29
22	EL0-66-51. Minimum Spontaneous Ignition Temperature	30
23	EL0-67-16. Spontaneous Ignition Temperature. Run 15.	33
24	EL0-67-16. Spontaneous Ignition Temperature. Run 16.	34
25	EL0-67-16. Spontaneous Ignition Temperature. Run 8	35
26	EL0-67-16. Spontaneous Ignition Temperature. Run 23.	36
27	EL0-67-16. Spontaneous Ignition Temperature. Run 25.	37
28	EL0-67-16. Spontaneous Ignition Temperature. Run 26.	38
29	EL0-67-16. Minimum Spontaneous Ignition Temperature	39

TABLE OF CONTENTS-CONTINUED

Section	Subject	Page No.
2.3.1.4	Blank. Pyrex Microbeads plus Metal Oxide Catalysts. Air Atmosphere. .	109
2.3.1.5	MLO-64-8. Pyrex Microbeads plus Metal Oxide Catalysts. Air Atmosphere.	109
2.3.1.6	ELO-65-48. Pyrex Microbeads plus Metal Oxide Catalysts. Air Atmosphere.	117
2.3.2	Comparison of DTA and Oxidative-Corrosion Studies.	117
2.3.3	Experimental Lubricants.	122
2.3.3.1	ELO-67-13. Nitrogen Atmosphere . .	122
2.3.3.2	ELO-67-13. Air Atmosphere.	126
2.3.3.3	ELA-67-32. Nitrogen Atmosphere . .	126
2.3.3.4	ELA-67-32. Air Atmosphere.	131
2.3.3.5	ELA-67-33. Nitrogen Atmosphere . .	131
2.3.3.6	ELA-67-33. Air Atmosphere.	134
2.3.3.7	ELA-67-34. Nitrogen Atmosphere . .	134
2.3.3.8	ELO-67-45. Nitrogen Atmosphere . .	138
2.3.3.9	ELO-67-45. Air Atmosphere.	140
2.3.3.10	ELO-67-51. Nitrogen Atmosphere . .	140
2.3.3.11	ELO-67-51. Air Atmosphere.	143
2.4	Conclusion.	143
3.	Thermal Stability.	145
3.1	Introduction.	145
3.2	Apparatus and Procedures.	146
3.3	Results and Discussion.	147
4.	Chemical and Physical Properties of Experimental Lubricants. .	167
5.	Future Work.	167
	References.	169

LIST OF ILLUSTRATIONS-CONTINUED

Figure		Page No.
30	ELO-66-109. Spontaneous Ignition Temperature. Run 5	42
31	ELO-66-109. Spontaneous Ignition Temperature. Run 15. . . .	43
32	ELO-66-109. Spontaneous Ignition Temperature. Run 18. . . .	44
33	ELO-66-109. Spontaneous Ignition Temperature. Run 22. . . .	45
34	ELO-66-109. Spontaneous Ignition Temperature. Run 21. . . .	46
35	ELO-66-109. Spontaneous Ignition Temperature. Run 24. . . .	47
36	ELO-66-109. Minimum Spontaneous Ignition Temperature	48
37	ELO-67-23. Spontaneous Ignition Temperature. Run 2	50
38	ELO-67-23. Spontaneous Ignition Temperature. Run 18. . . .	51
39	ELO-67-23. Spontaneous Ignition Temperature. Run 8	52
40	ELO-67-23. Spontaneous Ignition Temperature. Run 16. . . .	53
41	ELO-67-23. Spontaneous Ignition Temperature. Run 5	54
42	ELO-67-23. Spontaneous Ignition Temperature. Run 13. . . .	55
43	ELO-67-23. Spontaneous Ignition Temperature. Run 20. . . .	56
44	ELO-67-23. Minimum Spontaneous Ignition Temperature	57
45	ELO-67-49. Spontaneous Ignition Temperature. Run 24. . . .	61
46	ELO-67-49. Spontaneous Ignition Temperature. Run 38. . . .	62
47	ELO-67-49. Spontaneous Ignition Temperature. Run 13. . . .	63
48	ELO-67-49. Spontaneous Ignition Temperature. Run 14. . . .	64
49	ELO-67-49. Spontaneous Ignition Temperature. Run 10. . . .	65
50	ELO-67-49. Spontaneous Ignition Temperature. Run 25. . . .	66
51	ELO-67-49. Spontaneous Ignition Temperature. Run 7	67
52	ELO-67-49. Spontaneous Ignition Temperature. Run 22. . . .	68
53	ELO-67-49. Spontaneous Ignition Temperature. Run 16. . . .	69
54	ELO-67-49. Spontaneous Ignition Temperature. Run 33. . . .	70
55	ELO-67-49. Spontaneous Ignition Temperature. Run 39. . . .	71
56	ELO-67-49. Spontaneous Ignition Temperature. Run 17. . . .	72
57	ELO-67-49. Spontaneous Ignition Temperature. Run 41. . . .	73
58	ELO-67-49. Spontaneous Ignition Temperature. Run 19. . . .	74
59	ELO-67-49. Spontaneous Ignition Temperature. Run 34. . . .	75
60	ELO-67-49. Minimum Spontaneous Ignition Temperature	76

LIST OF ILLUSTRATIONS-CONTINUED

Figure		Page No.
61	ELO-67-55. Spontaneous Ignition Temperature. Run 7	81
62	ELO-67-55. Spontaneous Ignition Temperature. Run 31.	82
63	ELO-67-55. Spontaneous Ignition Temperature. Run 42.	83
64	ELO-67-55. Spontaneous Ignition Temperature. Run 41.	84
65	ELO-67-55. Spontaneous Ignition Temperature. Run 36.	85
66	ELO-67-55. Spontaneous Ignition Temperature. Run 47.	86
67	ELO-67-55. Minimum Spontaneous Ignition Temperature	87
68	Differential Thermal Analysis. Blank (Pyrex Microbeads) Thermocouple Pair T-7	89
69	Differential Thermal Analysis. Blank (Pyrex Microbeads) Air Atmosphere	90
70	Differential Thermal Analysis. Blank (Pyrex Microbeads) Nitrogen Atmosphere.	91
71	Differential Thermal Analysis. Blank (Pyrex Microbeads) Thermocouple Pair T-10 Compensated	92
72	Differential Thermal Analysis. Blank (Pyrex Microbeads) Thermocouple Pair T-11	93
73	Differential Thermal Analysis. Blank (Pyrex Microbeads plus Iron Oxide and Titanium Dioxide in Nitrogen)	96
74	Differential Thermal Analysis. Blank (Pyrex Microbeads plus Cuprous Oxide and Cupric Oxide in Nitrogen).	97
75	Differential Thermal Analysis. MLO-64-8	99
76	Differential Thermal Analysis. MLO-64-8 plus Iron Oxide and Titanium Dioxide in Nitrogen	100
77	Differential Thermal Analysis. MLO-64-8 plus Cuprous Oxide and Cupric Oxide in Nitrogen	101
78	Differential Thermal Analysis. MLO-64-8 plus Copper, Titanium and Iron	102
79	Differential Thermal Analysis. ELO-65-48.	103
80	Differential Thermal Analysis. ELO-65-48 plus Iron Oxide and Titanium Dioxide in Nitrogen	106
81	Differential Thermal Analysis. ELO-65-48 plus Cuprous Oxide and Cupric Oxide in Nitrogen	107
82	Differential Thermal Analysis. ELO-65-48 plus Copper, Titanium and Iron	108
83	Differential Thermal Analysis. Blank (Pyrex Microbeads plus Iron Oxide and Titanium Dioxide in Nitrogen)	110

LIST OF ILLUSTRATIONS-CONTINUED

Figure		Page No.
84	Differential Thermal Analysis. Blank (Pyrex Microbeads plus Cuprous Oxide and Cupric Oxide in Air.	111
85	Differential Thermal Analysis. MLO-64-8 and ELO-65-48 in Air	113
86	Differential Thermal Analysis. MLO-64-8 plus Iron Oxide and Titanium Dioxide in Air	114
87	Differential Thermal Analysis. MLO-64-8 plus Cuprous Oxide and Cupric Oxide in Air	115
88	Differential Thermal Analysis. MLO-64-8 plus Copper, Titanium and Iron in Air	116
89	Differential Thermal Analysis. ELO-65-48 plus Iron Oxide and Titanium Dioxide in Air	119
90	Differential Thermal Analysis. ELO-65-48 plus Cuprous Oxide and Cupric Oxide in Air	120
91	Differential Thermal Analysis. ELO-65-48 plus Copper, Titanium and Iron in Air	121
92	Differential Thermal Analysis. ELO-67-17 in Nitrogen	125
93	Differential Thermal Analysis. ELO-67-13 in Air.	127
94	Differential Thermal Analysis. ELO-67-13 in Air.	128
95	Differential Thermal Analysis. Blank. Air Atmosphere.	129
96	Differential Thermal Analysis. ELA-67-32. Nitrogen Atmosphere	130
97	Differential Thermal Analysis. ELA-67-32. Air Atmosphere.	132
98	Differential Thermal Analysis. ELA-67-33. Nitrogen Atmosphere	133
99	Differential Thermal Analysis. ELA-67-33. Air Atmosphere.	135
100	Differential Thermal Analysis. ELA-67-34. Nitrogen Atmosphere	136
101	Differential Thermal Analysis. ELA-67-34. Nitrogen Atmosphere	137
102	Differential Thermal Analysis. ELO-67-45. Nitrogen Atmosphere	139
103	Differential Thermal Analysis. ELO-67-45. Air Atmosphere.	141
104	Differential Thermal Analysis. ELO-67-51. Nitrogen Atmosphere	142
105	Differential Thermal Analysis. ELO-67-51. Air Atmosphere.	144
106	Schematic of Modified Thermal Stability Test Cell	148
107	MLO-64-8. Thermal Stability at 700 Deg. F.	150
108	ELO-64-68. Thermal Stability at 700 Deg. F.	152
109	ELO-65-48. Thermal Stability at 700 Deg. F.	154

LIST OF ILLUSTRATIONS-CONTINUED

Figure		Page No.
110	ELO-66-20. Thermal Stability at 650 Deg. F.	156
111	ELO-66-31. Thermal Stability at 600 Deg. F.	158
112	ELO-66-31. Thermal Stability at 650 Deg. F.	160
113	ELO-66-31. Thermal Stability at 700 Deg. F.	162
114	ELO-66-51. Thermal Stability at 700 Deg. F.	164
115	ELO-67-49. Thermal Stability at 700 Deg. F.	166
116	Vapor Pressure of ELO-66-51.	187

LIST OF TABLES

Table		Page No.
I	MLO-64-4. Spontaneous Ignition Temperature.	4
II	MLO-64-5. Spontaneous Ignition Temperature.	12
III	ELO-66-51. Spontaneous Ignition Temperature	19
IV	ELO-67-16. Spontaneous Ignition Temperature	31
V	ELO-66-109. Spontaneous Ignition Temperature.	41
VI	ELO-67-23. Spontaneous Ignition Temperature	49
VII	ELO-67-49. Spontaneous Ignition Temperature	59
VIII	ELO-67-55. Spontaneous Ignition Temperature	78
IX	Spontaneous Ignition Summary	80
X	Differential Thermal Analysis. MLO-64-8 plus Metal Oxide Catalysts in Nitrogen Atmosphere	98
XI	Differential Thermal Analysis. ELO-65-48 plus Metal Oxide Catalysts in Nitrogen Atmosphere	104
XII	Differential Thermal Analysis. MLO-64-8 plus Metal Oxide Catalysts in Air Atmosphere.	112
XIII	Differential Thermal Analysis. ELO-65-48 plus Metal Oxide Catalysts in Air Atmosphere.	118
XIV	MLO-64-8. Corrosion and Oxidation Stability (Micro Method).	123
XV	MLO-64-8. Corrosion and Oxidation Stability (Micro Method).	124
XVI	Thermal Stability of MLO-64-8.	149
XVII	Thermal Stability of ELO-64-68	151
XVIII	Thermal Stability of ELO-65-48	153
XIX	Thermal Stability of ELO-66-20	155
XX	Thermal Stability of ELO-66-31	157
XXI	Thermal Stability of ELO-66-51	163
XXII	Thermal Stability of ELO-67-49	165
XXIII	Properties of MLO-64-4	170
XXIV	Properties of MLO-64-5	172
XXV	Properties of ELO-66-20.	174

LIST OF TABLES-CONTINUED

Table		Page No.
XXVI	Properties of ELO-66-24 and ELO-66-25.	176
XXVII	Properties of ELO-66-30.	177
XXVIII	Properties of ELO-66-34.	181
XXIX	Properties of ELO-66-51.	184
XXX	Properties of ELO-66-109	188
XXXI	Properties of ELO-66-117	190
XXXII	Properties of ELO-67-15.	193
XXXIII	Properties of ELO-67-16.	194
XXXIV	Properties of ELO-67-21.	195
XXXV	Properties of ELO-67-22.	196
XXXVI	Properties of ELO-67-23.	197
XXXVII	Properties of ELO-67-35.	199
XXXVIII	Properties of ELO-67-49.	200
XXXIX	Properties of ELO-67-50.	201
XL	Properties of ELO-67-54.	205
XLI	Properties of MCG-66-303	207
XLII	Properties of MCG-66-334	211
XLIII	Properties of MCG-66-335	215
XLIV	Properties of MCG-66-336	219

1. SPONTANEOUS IGNITION OF EXPERIMENTAL HYDRAULIC FLUIDS

1.1 Introduction:

During the past reporting period the spontaneous ignition properties of eight experimental hydraulic fluids have been studied. The current investigations comprise part of a larger program of study, portions of which have been described in previous reports in this series. The design and construction of the spontaneous ignition apparatus and discussion of the technique of thermoelectric flame detection may be found in Reference 2. Various applications of the apparatus and methods described therein to a variety of experimental and operational hydraulic fluid systems are described in References 3, 4 and 5.

It has been found useful as well as convenient to define several terms which relate to spontaneous ignition. These have been published previously (Reference 3) but are repeated at this point for the convenience of the reader.

- (1) The spontaneous ignition temperature (SIT) is the lowest temperature at which hot-flame ignition is found for a given sample volume in an ignition chamber of specified size.
- (2) For a given ignition chamber volume the lowest (SIT) for any sample size is $(SIT)_s$.
- (3) For a given sample size the lowest (SIT) for any chamber volume is $(SIT)_v$.
- (4) The lowest (SIT) for any chamber volume and sample size is $(SIT)_{sv}$.
- (5) The reaction threshold is the lowest temperature for a given sample size and chamber volume at which a measurable exothermic effect can be observed subsequent to the introduction of the sample.

The usual term fuel/air or sample/air ratio has not been employed in these studies because, although a measured volume of the liquid sample may be introduced into the ignition system, it is unusual for complete volatilization to occur. The most common occurrences are the partial evaporation of the sample followed by the ignition of the gaseous components or the thermal degradation of the fluid to produce gaseous decomposition products which then ignite if they are exposed to a temperature sufficiently high to cause their spontaneous combustion. In either case the determination of the actual volume of vapor formed would be a fairly difficult procedure which would be of small benefit in the overall assessment of resistance to spontaneous ignition. The effort required to obtain fuel/air ratios under these circumstances is not justified by the information yielded therefrom. Instead the liquid sample volume used and the ignition chamber capacity are recorded for each system which has been studied.

The investigation of the spontaneous ignition properties of the eight systems described in this report has been confined to a single chamber size. The properties (SIT) and $(SIT)_s$ have been determined for each sample. In addition the reaction threshold has been measured for one sample size in a chamber of the same volume used for the other determinations.

1.2 Apparatus and Procedures:

The apparatus procedures and definitions used are the same as those which have been described in earlier reports (References 2, 3, 4, 5). Air at 1.0 atm. pressure was the oxidizing medium in all experiments. A one-liter borosilicate glass combustion chamber was used. The combustion chamber was removed and cleaned after each experimental run in which visible deposits were observed subsequent to the completion of combustion reactions. This necessitated replacement of the chamber after virtually every experimental run.

Sample introduction was accomplished by means of an automatic repeating pipet with an 18" stainless steel hypodermic needle. The needle for all experiments had a 0.109" O.D. with 0.085 I.D. The end of the needle was constricted to an opening approximately 0.010" x 0.085". This needle has been identified in the experiments to follow as, "Needle A."

All experimental runs were accomplished with an iron-constantan element in the thermoelectric flame detection system. In no case was there evidence of interaction either catalytic or otherwise between the thermocouple materials and any of the samples which were investigated.

1.3 Experimental Results and Discussion:

1.3.1 MLO-64-4. See Table I and Figures 1 through 7.

Runs made with sample sizes of 0.2, 0.5 and 1.0 ml. in the 1000 ml. combustion chamber were found to exhibit typical hot-flame, cool-flame, and pre-ignition type reactions. Runs 12 and 14, Figures 1 and 2 are representative of the pre-ignition reactions. Runs 5 and 21, Figures 3 and 4, illustrate the cool-flames while Runs 2 and 26, Figures 5 and 6 show typical hot-flame ignitions.

The minimum temperature at which hot-flame ignition may be expected to occur is determined from the plot of observed spontaneous ignition temperature vs. sample size shown in Figure 7. The minimum spontaneous ignition temperature, $(SIT)_s$, is found to be 670 deg. F. The reaction threshold for the 0.2 ml. sample series is 423 deg. F.

1.3.2 MLO-64-5. See Table II and Figures 8 through 12.

In the processes involved in the spontaneous ignition of sample MLO-64-5 no cool-flame reactions were observed. The transition from pre-ignition reactions to hot-flames as the temperature of the combustion chamber is increased apparently proceeds without the occurrence of intermediate cool-flames. Runs 2 and 13, Figures 8 and 9 illustrate the pre-ignition reactions. Runs 4 and 20 are typical of the observed hot-flame ignitions.

TABLE I

SAMPLE NUMBER MLO-64-4

SPONTANEOUS IGNITION TEMPERATURE

Needle A

1000 ml. chamber - Iron-Constantan Thermocouple

Run	Sample Size, ml.	Initial Temp., deg. F.	Max. Rise, deg. F.	TYPE OF REACTION			Delay, Sec.	Observations
				Pre- Ignition	Cool Flame	Hot Flame		
1	1.0	670	46		X		43	
2		676	170			X	22	Orange flame, explosion
3		678	53		X		48	
4		682	178			X	20	Orange flame, explosion
5	0.5	667	57		X		47	
6		670	173			X	15	Orange flame, explosion
7		676	127			X	17	Orange flame, explosion
8	0.2	423	0	X				
9		435	5	X				
10		476	8	X				
11		495	14	X				
12		505	21	X				
13		540	30	X			166	
14		543	31	X			184	
15		560	44		X		80	
16		572	45		X		62	
17		595	49		X		52	
18		605	45		X		50	
19		615	34		X		45	
20		635	41		X		46	
21		645	51		X		62	
22		647	44		X		45	
23		670	42		X		47	
24		675	265			X	11	Orange flame, explosion
25		682	179			X	14	Orange flame, explosion
26		685	227			X	13	Orange flame, explosion

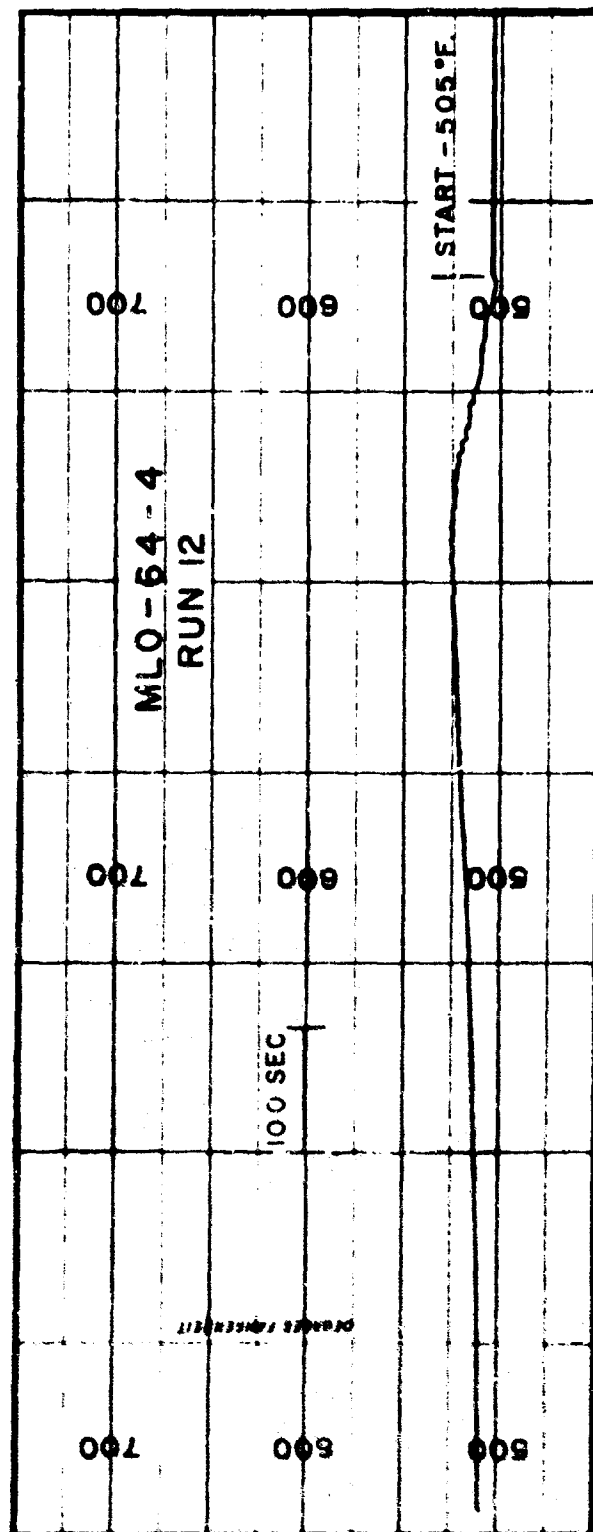


FIGURE 1. MLO-64-4. SPONTANEOUS IGNITION TEMPERATURE. RUN 12.

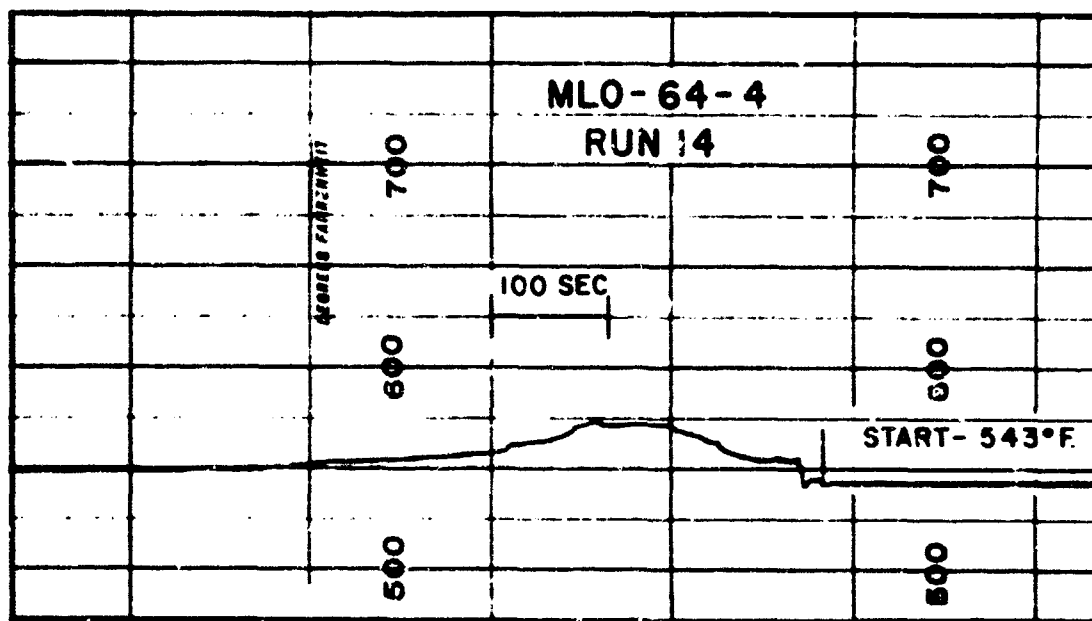


FIGURE 2. MLO-64-4. SPONTANEOUS IGNITION TEMPERATURE. RUN 14.

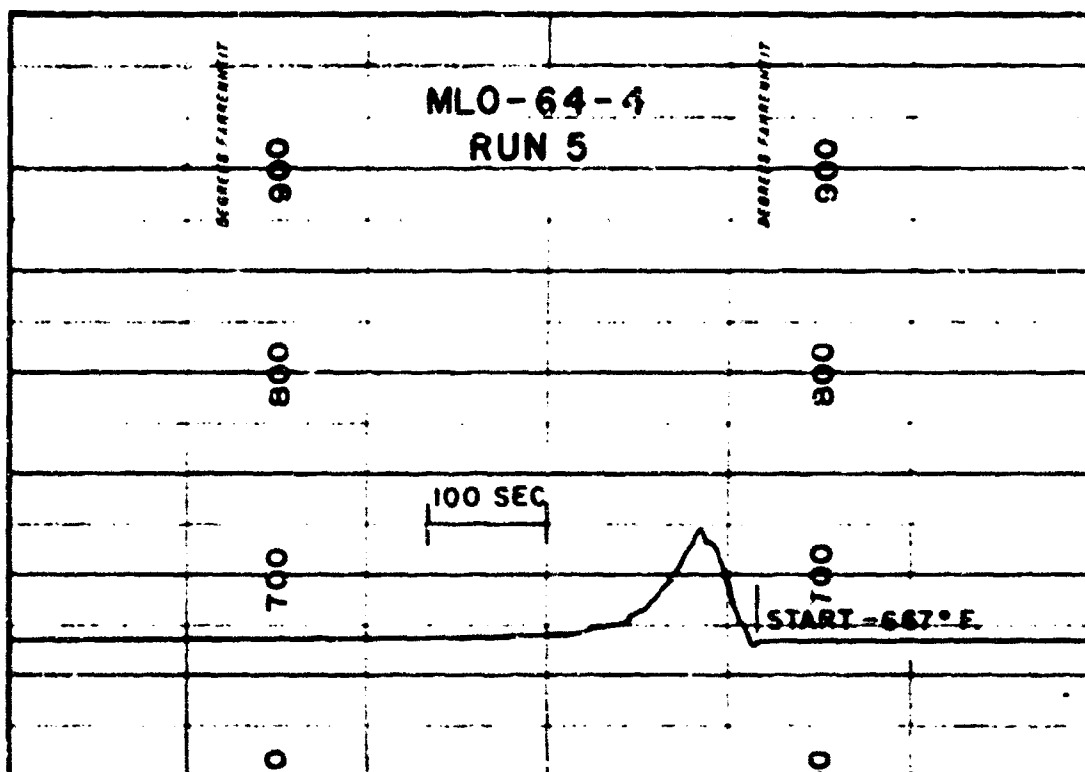


FIGURE 3. MLO-64-4. SPONTANEOUS IGNITION TEMPERATURE. RUN 5.

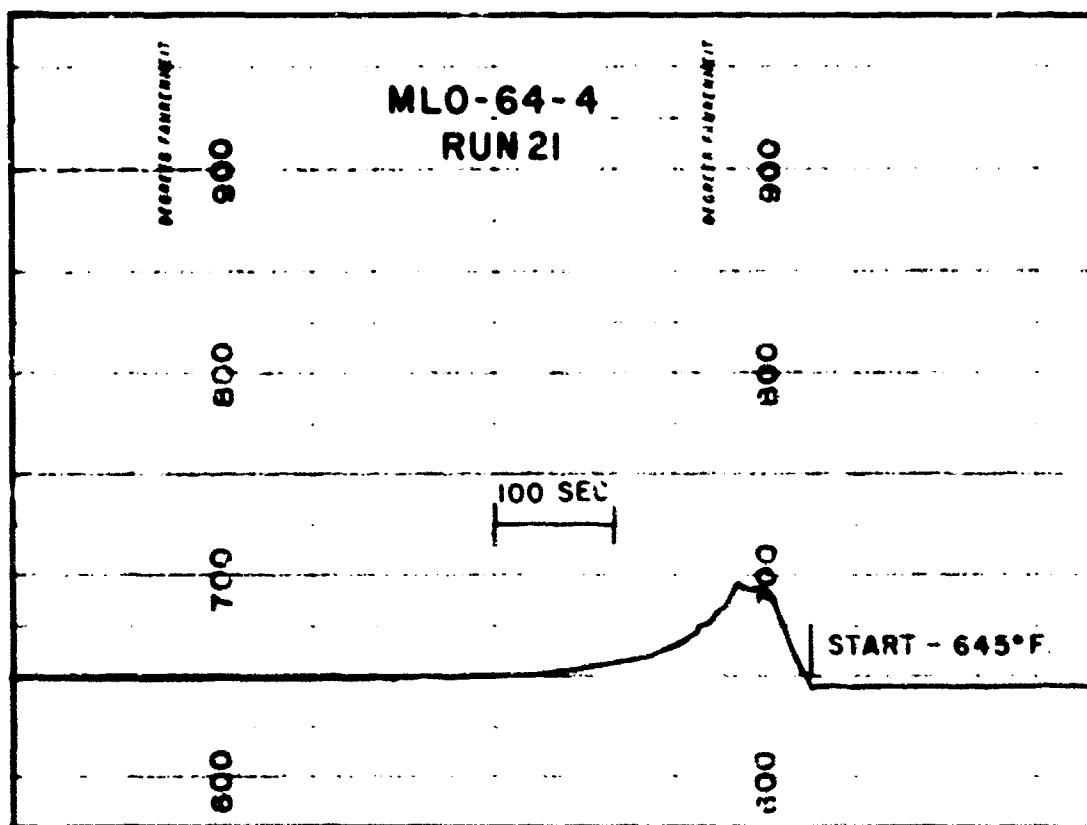


FIGURE 4. MLO-64-4. SPONTANEOUS IGNITION TEMPERATURE. RUN 21.

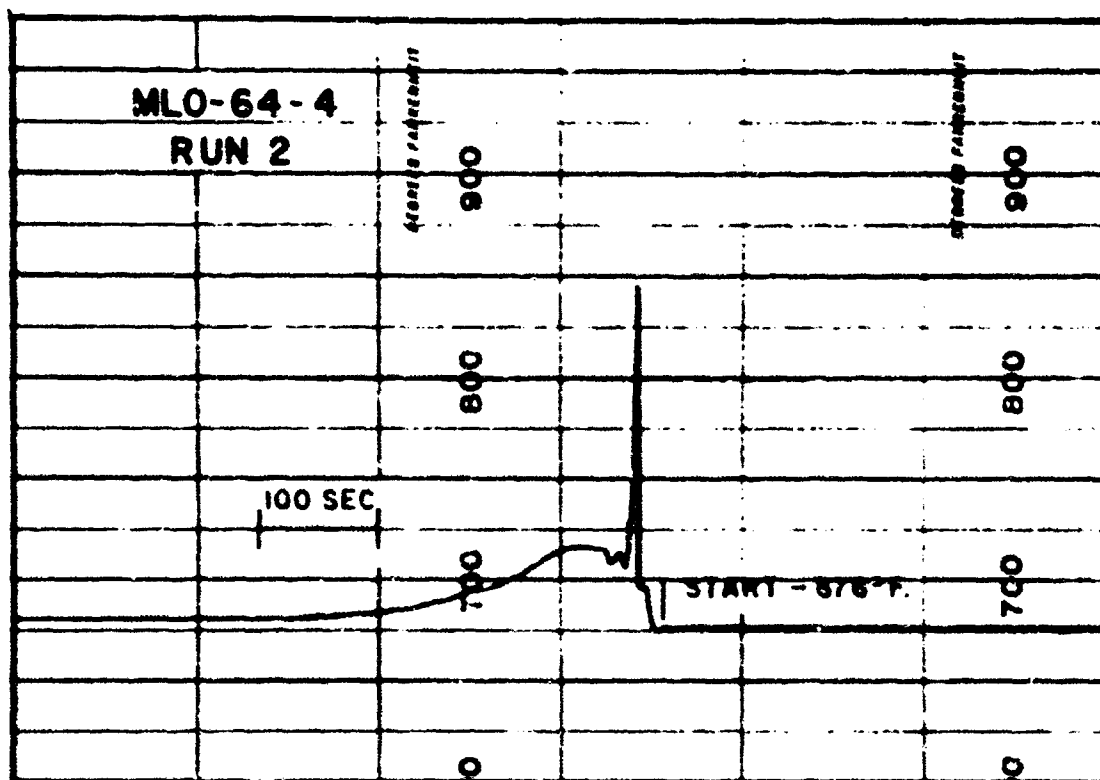


FIGURE 5. MLO-64-4. SPONTANEOUS IGNITION TEMPERATURE. RUN 2.

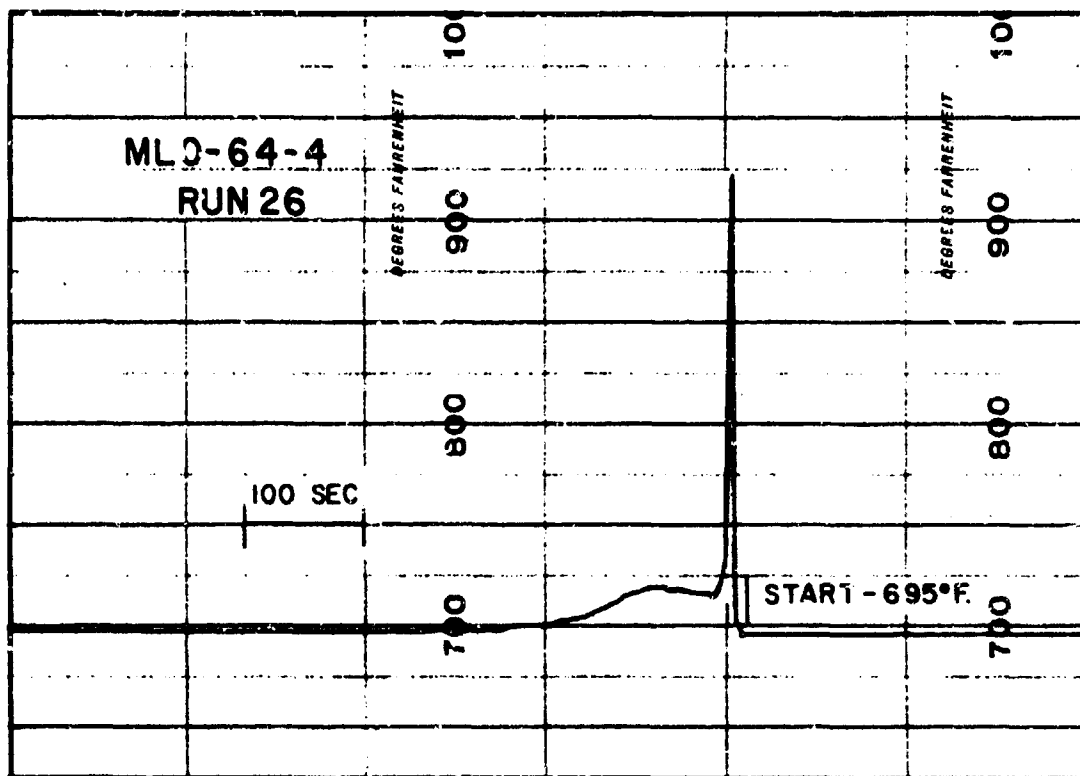


FIGURE 6. MLO-64-4. SPONTANEOUS IGNITION TEMPERATURE. RUN 26.

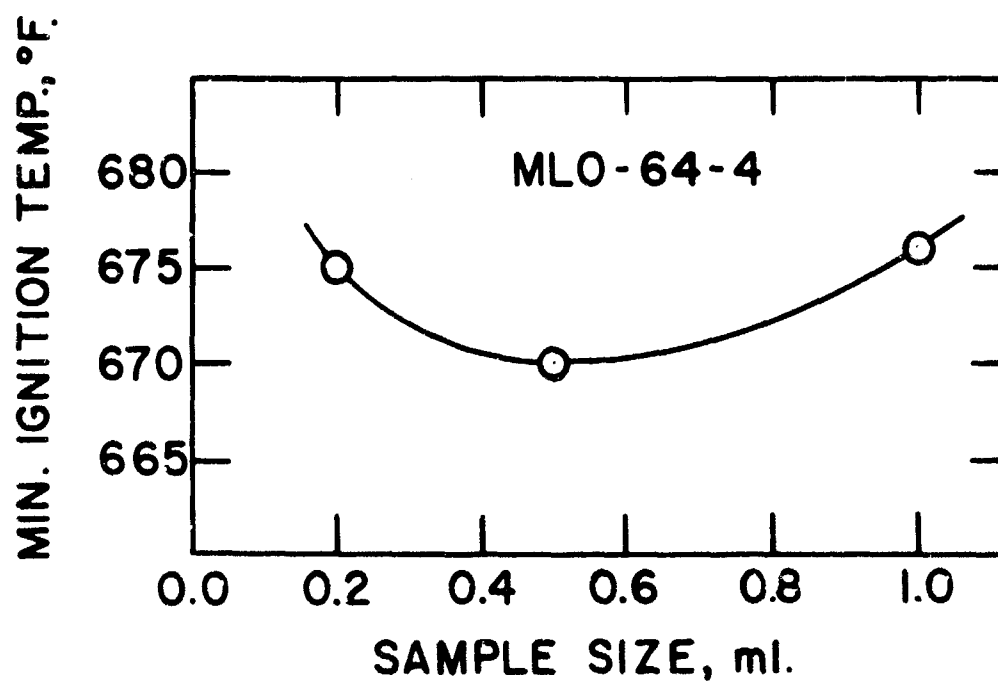


FIGURE 7. MLO-64-4. MINIMUM SPONTANEOUS IGNITION TEMPERATURE.

TABLE II

SAMPLE NUMBER MLO-64-5

SPONTANEOUS IGNITION TEMPERATURE

Needle A

1000 ml. chamber - Iron-Constantan ThermocoupleTYPE OF REACTION

Run	Sample Size, ml.	Initial Temp., deg. F.	Max. Rise, deg. F.	Pre-Ignition	Cool Flame	Hot Flame	Delay, Sec.	Observations
1	1.0	431	9	X				
2		449	13	X				
3		455	100			X	156	Orange flame, explosio
4		462	314			X	95	Orange flame, explosio
5	0.5	451	13	X				
6		455	185			X	129	Orange flame, explosio
7	0.2	421	0	X				
8		424	2	X				
9		430	7	X				
10		438	10	X				
11		443	12	X				
12		448	8	X				
13		450	12	X				
14		455	127			X	128	Orange flame, explosio
15		455	156			X	125	Orange flame, explosio
16		459	61			X	104	Orange flame, explosio
17		476	161			X	30	Orange flame, explosio
18	0.1	446	9	X				
19		449	7	X				
20		455	151			X	115	Smoke, orange flame

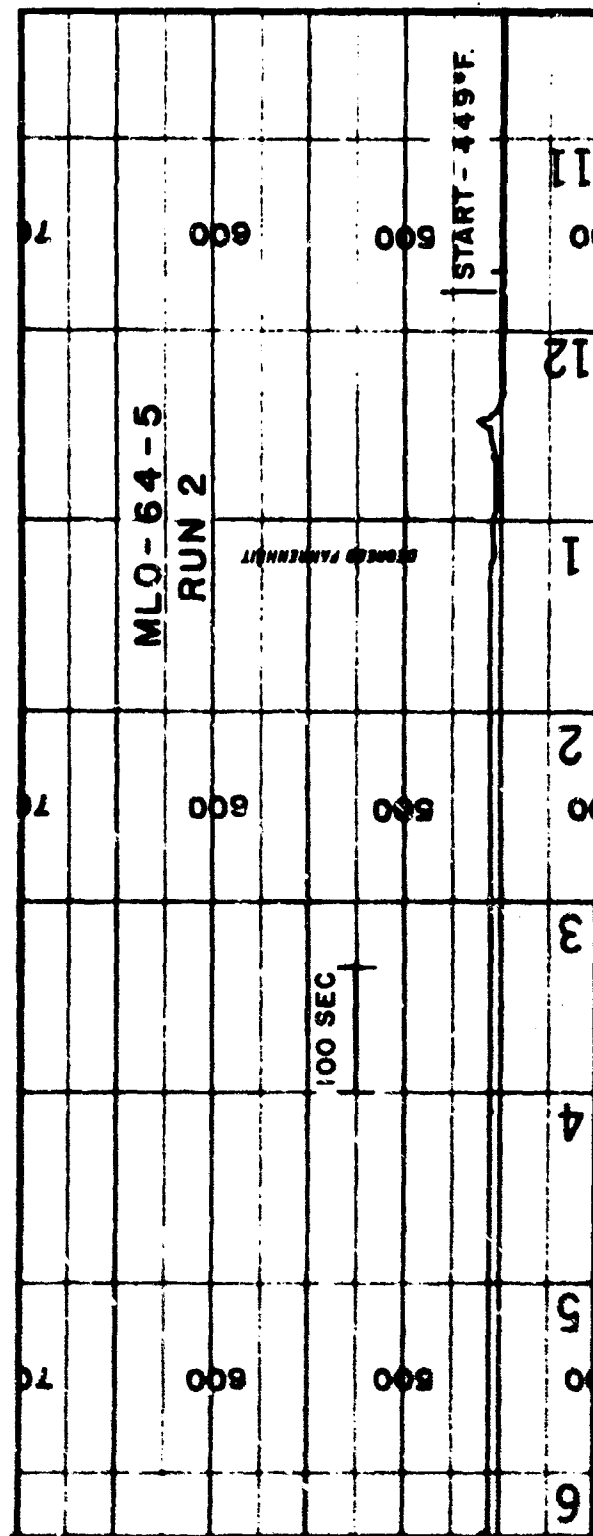


FIGURE 8. MLO-64-5. SPONTANEOUS IGNITION TEMPERATURE. RUN 2.

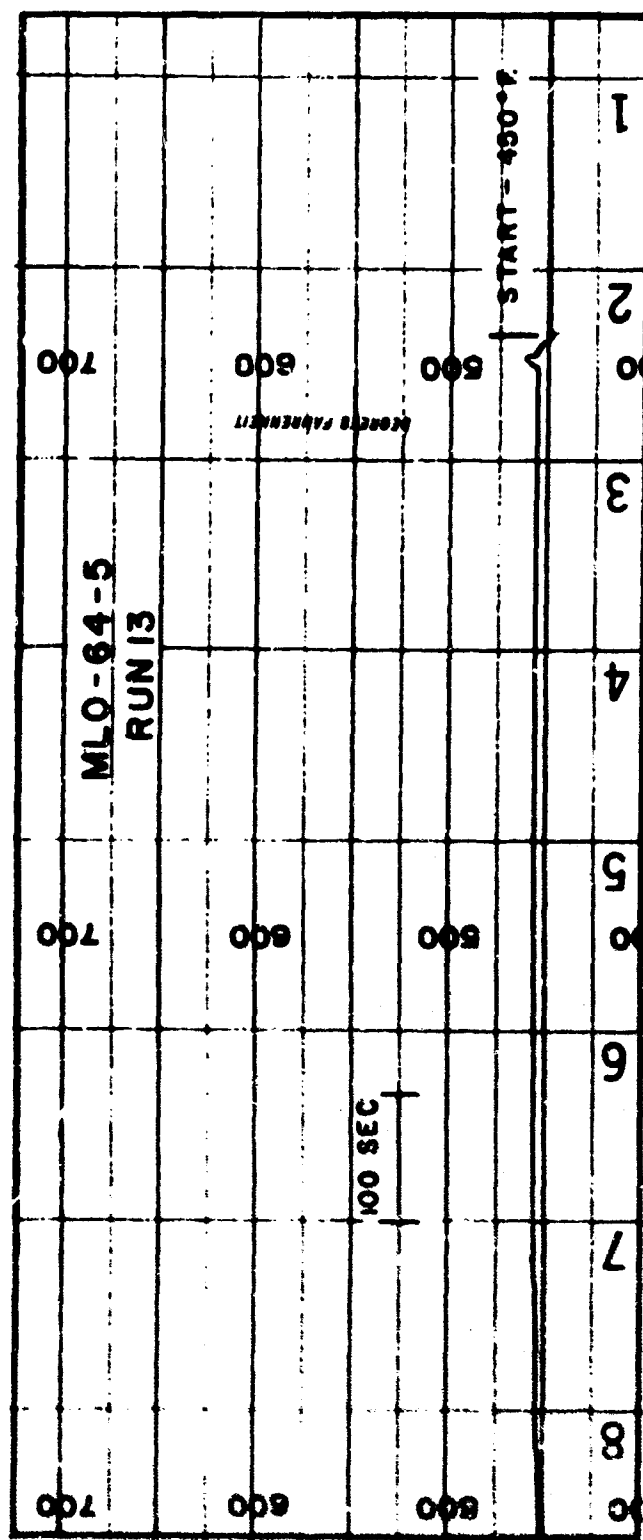


FIGURE 9. MLO-64-5. SPONTANEOUS IGNITION TEMPERATURE. RUN 13.

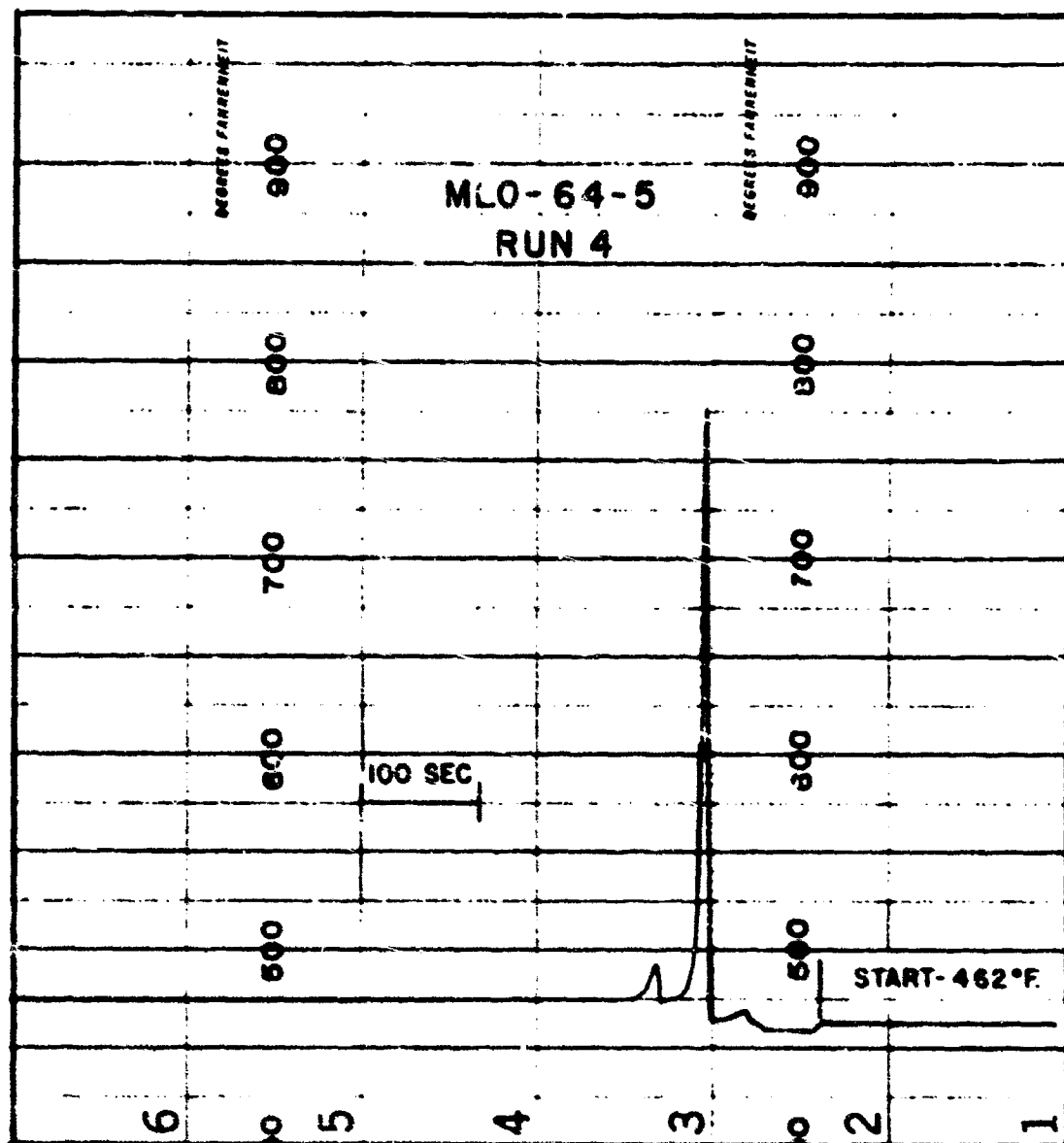


FIGURE 10. MLO-64-5. SPONTANEOUS IGNITION TEMPERATURE. RUN 4.

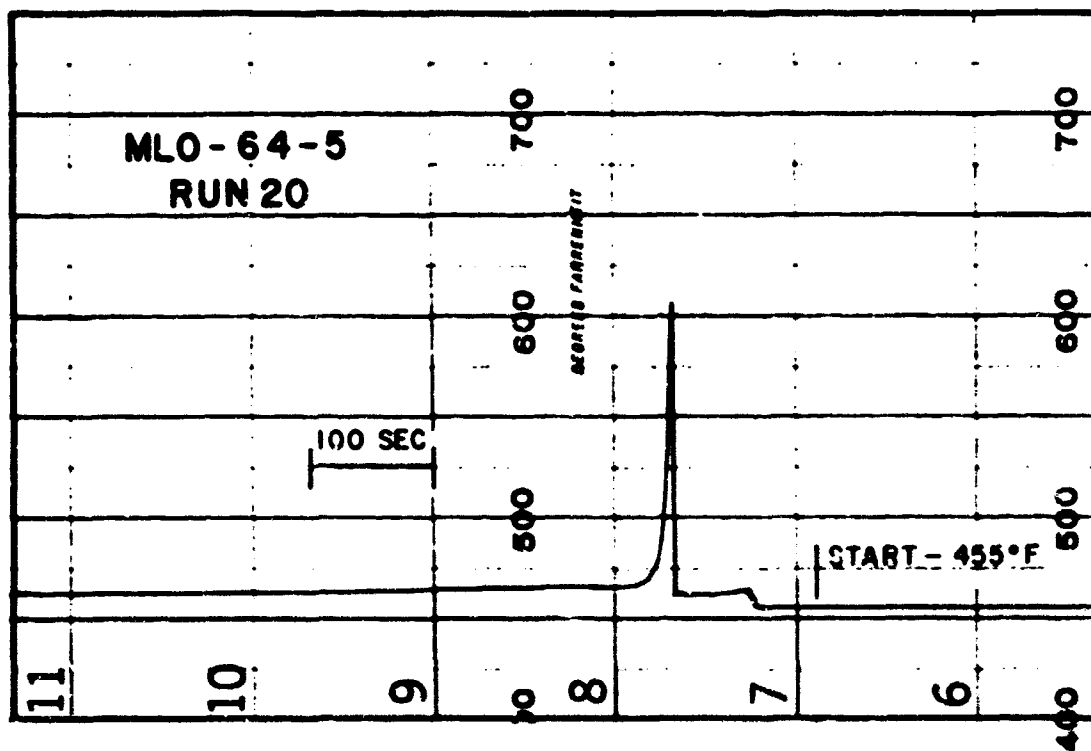


FIGURE 11. MLO-64-5. SPONTANEOUS IGNITION TEMPERATURE. RUN 20.

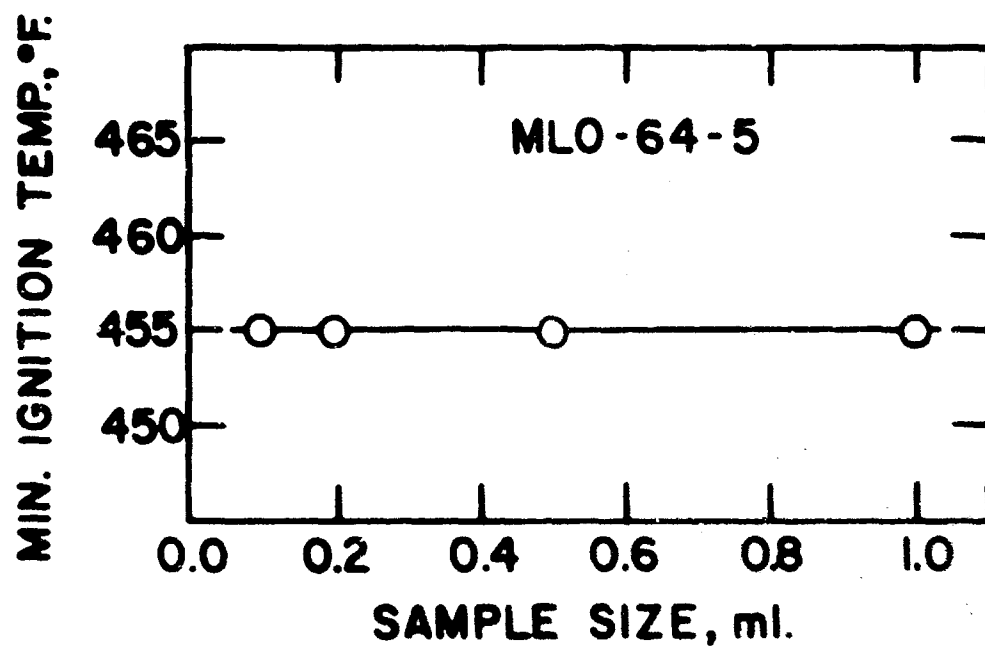


FIGURE 12. MLO-64-5. MINIMUM SPONTANEOUS IGNITION TEMPERATURE.

The lowest temperature for which a hot-flame ignition may be expected is determined from Figure 12 in which spontaneous ignition temperature is plotted as a function of sample size. It may be seen that the spontaneous ignition temperature does not vary over the range of sample sizes from 0.1 to 1.0 ml. The minimum spontaneous ignition temperature, $(SIT)_s$, is therefore 455 deg. F. The reaction threshold for the 0.2 ml. sample series is 421 deg. F.

1.3.3 ELO-66-51. See Table III and Figures 13 through 22.

In the study of the spontaneous ignition of sample ELO-66-51 cool-flame reactions were observed only for the 0.2 and 0.5 ml. sample sizes. In the runs made with 0.1 and 0.05 ml. of sample in the 1000 ml. combustion chamber pre-ignition reactions were followed directly by hot-flames. No intermediate reactions were observed. Runs 7, 30 and 36 illustrate typical hot-flame ignitions. See Figures 13, 14 and 15. Runs 2 and 31 are typical of the cool-flame ignitions. See Figures 16 and 17. Examples of some of the more energetic pre-ignition reactions are shown by Runs 22 and 25, Figures 18 and 19. The transition from cool-flame to hot-flame is especially gradual in the case of the 0.05 ml. sample series. In some cases the time-temperature plots possess properties common to both flame classes. These runs have been designated by "?" in Table III and have been included under the general classification of cool-flames. Runs 3 and 5, Figures 20 and 21 illustrate this phenomenon.

Figure 22 is a plot of observed spontaneous ignition temperature against sample size. The minimum spontaneous ignition temperature, $(SIT)_s$, determined from that plot is 1002 deg. F. The reaction threshold for the 0.2 ml. sample series is 833 deg. F.

1.3.4 ELO-67-16. See Table IV and Figures 23 through 29.

In three experimental series using 0.2, 0.5 and 1.0 ml. of sample both cool- and hot-flame reactions were detected. In the 0.2 ml. series runs were made at temperatures low enough to delineate the temperature range within which pre-ignition reactions may be expected. The ignition phenomena observed for this sample are quite typical. No unusual features were noted during the study of its self-ignition properties. Runs 15 and 16,

SAMPLE NUMBER ELO-66-51

SPONTANEOUS IGNITION TEMPERATURE

Needle A

1000 ml. chamber - Iron-Constantan Thermocouple

TYPE OF REACTION

Run	Sample Size, ml.	Initial Temp., deg. F.	Max. Rise, deg. F.	Pre- Ignition	Cool Flame	Hot Flame	Delay, Sec.	Observations
1	0.5	1001	36		X		16	Smoke
2		1007	37		X		17	
3		1015	47		X?		17	Smoke
4		1020	55			X	11	Smoke
5		1025	45		X?		11	Smoke
6		1030	39		X?		9	Smoke
7		1045	56			X	10	Smoke
8	0.2	447	0	X				
9		470	0	X				
10		484	0	X				
11		533	0	X				
12		594	0	X				
13		514	0	X				
14		672	0	X				
15		735	0	X				
16		780	0	X				
17		833	0	X				
18		837	2	X				
19		841	2	X				
20		845	3	X				
21		876	5	X				
22		909	10	X				
23		916	10	X				
24		958	11	X				

TABLE 1 - CONTINUED

SAMPLE NUMBER ELO-66-51

SPONTANEOUS IGNITION TEMPERATURE

Needle A

1000 ml. chamber - Iron-Constantan Thermocouple

TYPE OF REACTION

Run	Sample Size, ml.	Initial Temp., deg. F.	Max. Rise, deg. F.	Pre- Ignition	Cool Flame	Hot Flame	Delay, Sec.	Observations
25	0.2	972	22	X				
26		1000	27	X			9	
27		1003	32			X	3	Smoke
28		1008	63			X	2	Smoke
29		1016	60			X	7	Smoke
30		1022	105			X	5	Smoke
31		1031	39		X		9	Smoke
32		1052	47			X	4	Smoke
33	0.1	997	8	X				
34		1001	9	X				
35		1002	55			X	5	Smoke
36		1005	65			X	9	Smoke
37	0.05	1005	15	X				
38		1008	7	X				
39		1015	74			X	7	Smoke

X Indicates reaction which has both cool-flame and hot-flame characteristics.

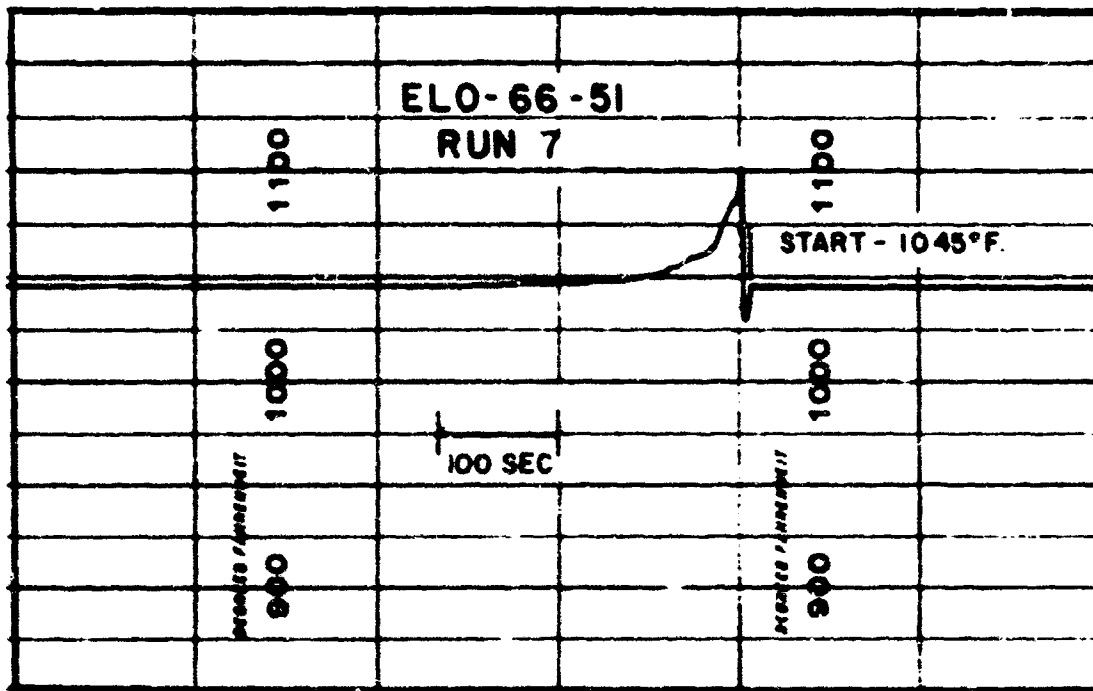


FIGURE 13. ELO-66-51. SPONTANEOUS IGNITION TEMPERATURE. RUN 7.

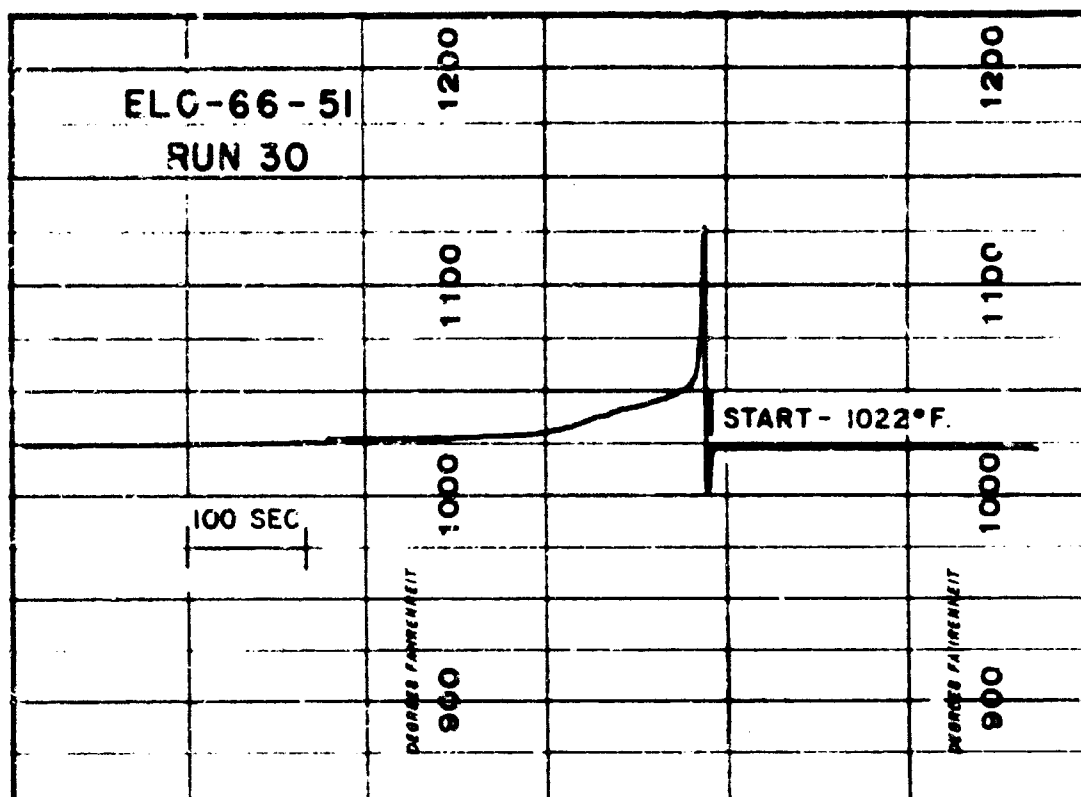


FIGURE 14. ELC-66-51. SPONTANEOUS IGNITION TEMPERATURE. RUN 30.

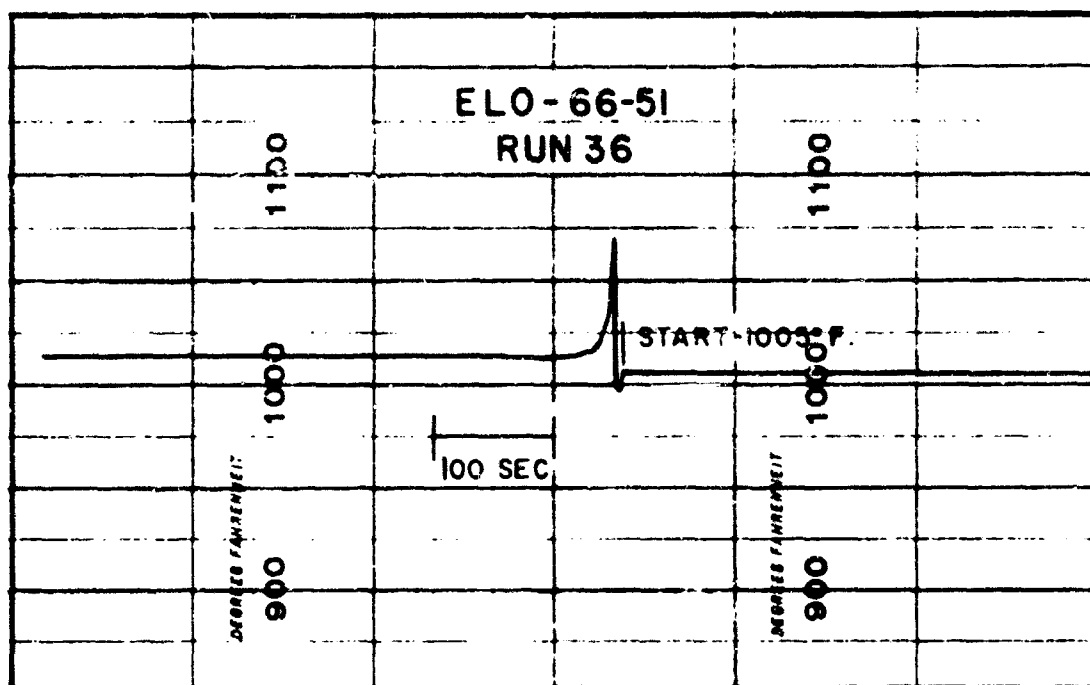


FIGURE 15. ELO-66-51 SPONTANEOUS IGNITION TEMPERATURE. RUN 36.

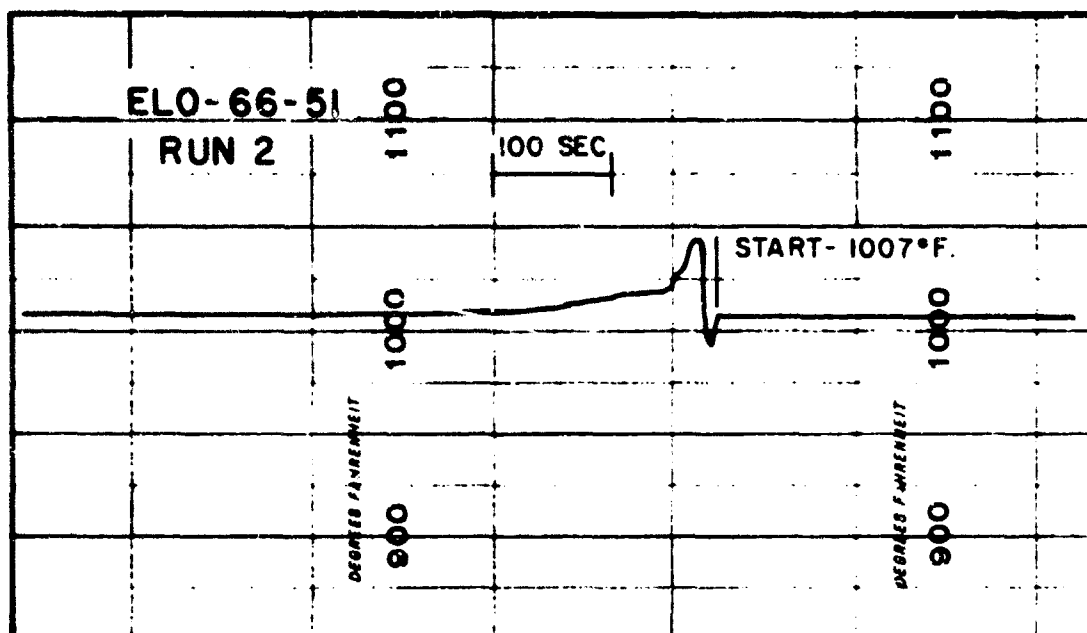


FIGURE 16. ELO-66-51. SPONTANEOUS IGNITION TEMPERATURE. RUN 2.

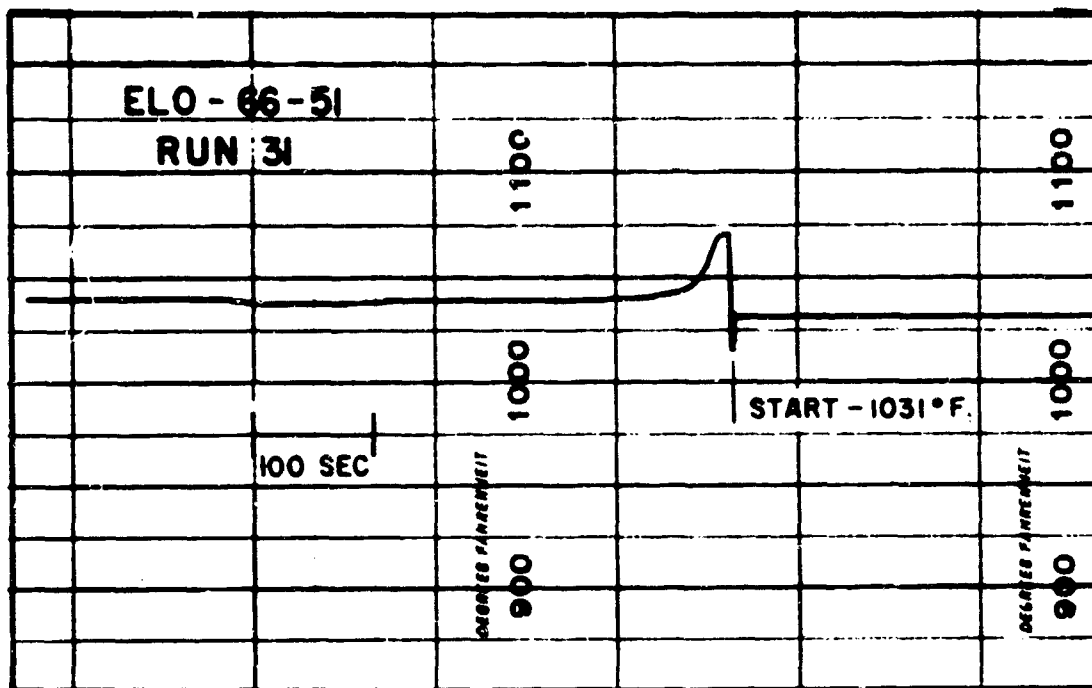


FIGURE 17. ELO-66-51. SPONTANEOUS IGNITION TEMPERATURE. RUN 31.

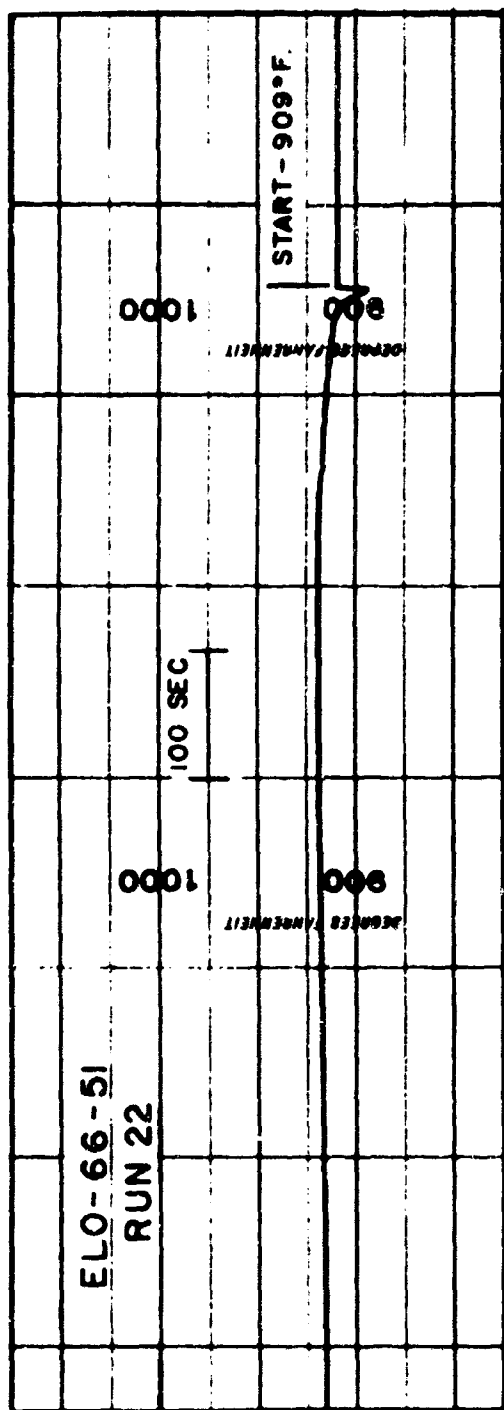


FIGURE 18. ELO-66-51. SPONTANEOUS IGNITION TEMPERATURE. RUN 22.

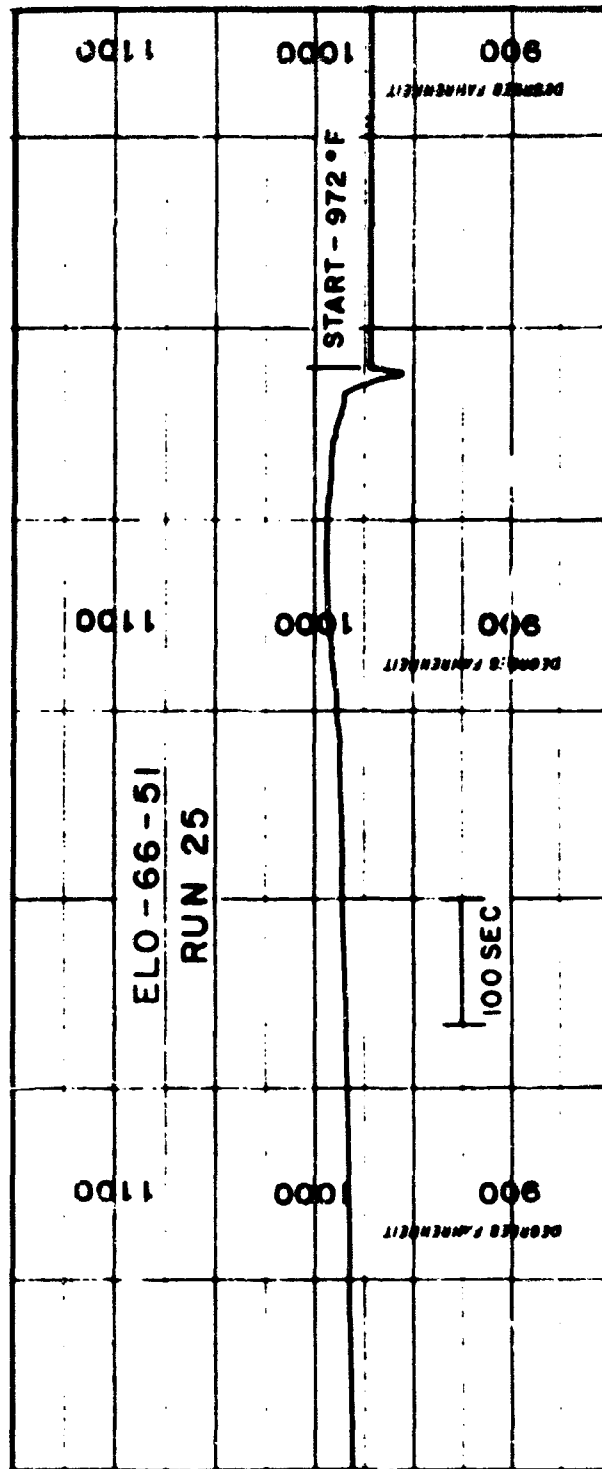


FIGURE 19. ELO-66-51. SPONTANEOUS IGNITION TEMPERATURE. RUN 25.

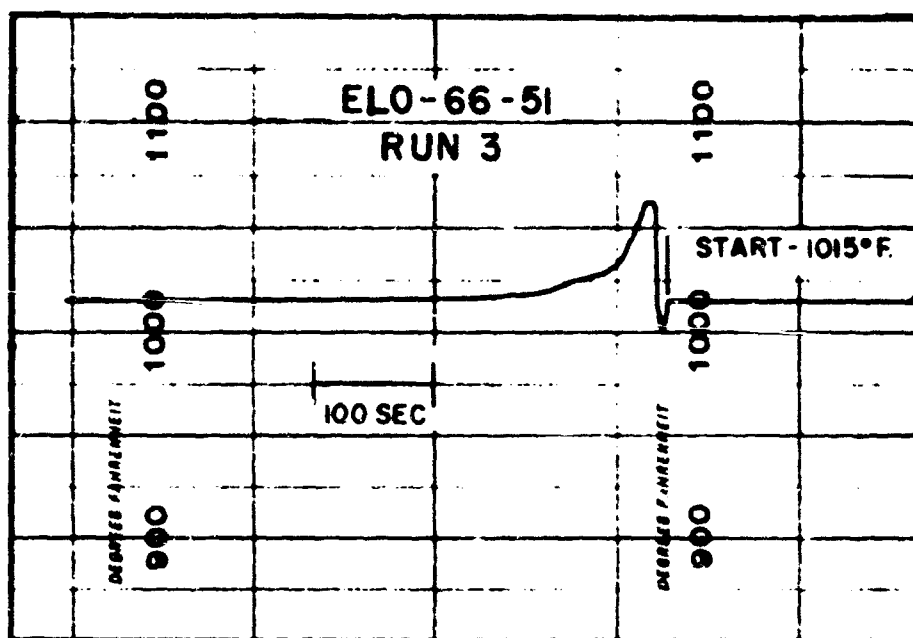


FIGURE 20. ELO-66-51. SPONTANEOUS IGNITION TEMPERATURE. RUN 3.

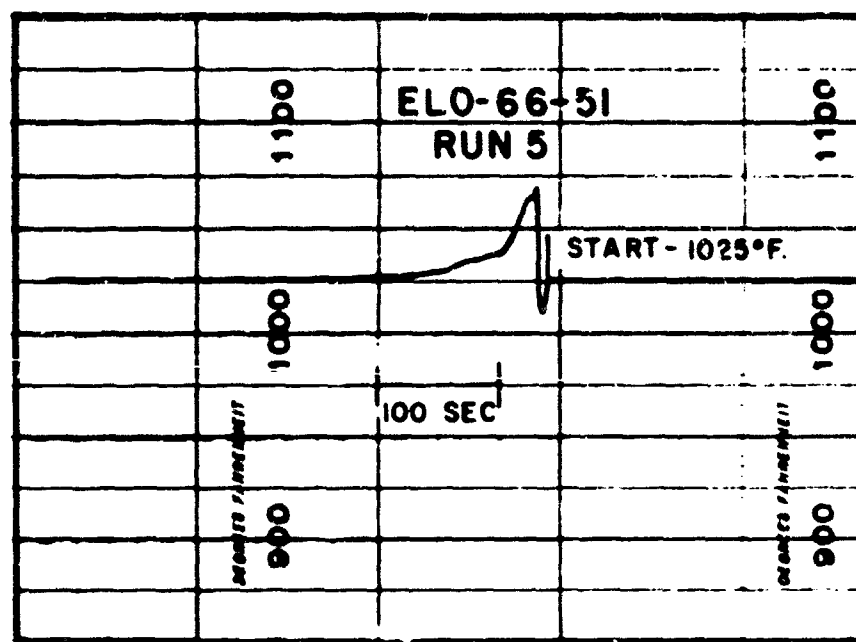


FIGURE 21. ELO-66-51. SPONTANEOUS IGNITION TEMPERATURE. RUN 5.

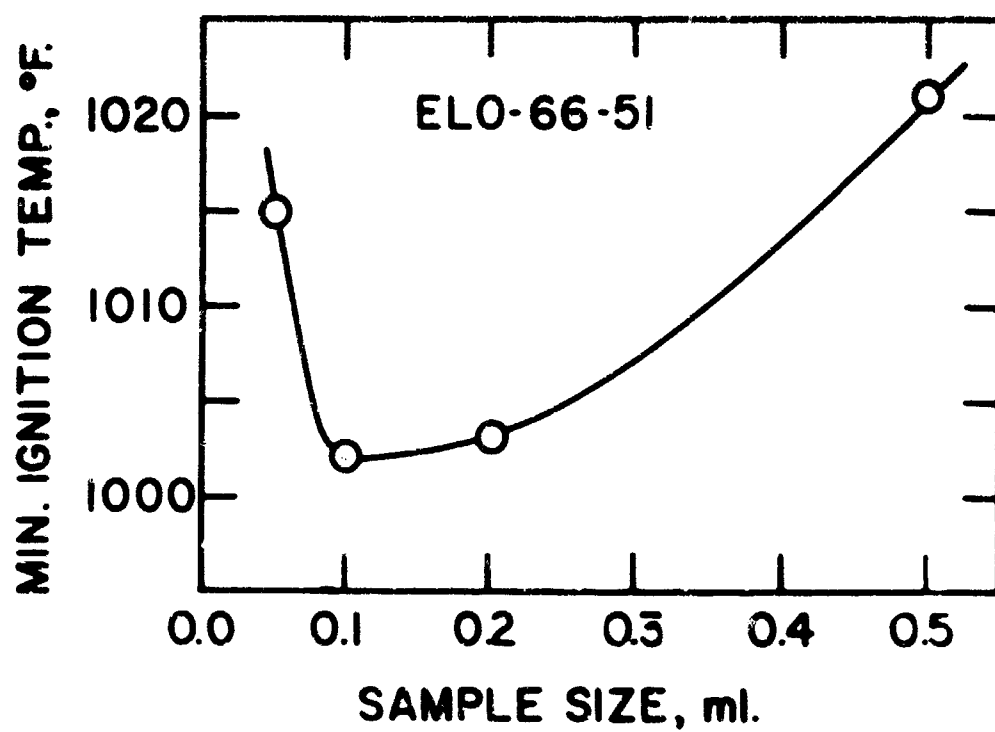


FIGURE 22. ELO-66-51. MINIMUM SPONTANEOUS IGNITION TEMPERATURE.

TABLE IV

SAMPLE NUMBER ELO-67-16

SPONTANEOUS IGNITION TEMPERATURE

Needle A

1000 ml. chamber - Iron-Constantan Thermocouple

TYPE OF REACTION

Run	Sample Size, ml.	Initial Temp., deg. F.	Max. Rise, deg. F.	Pre- Ignition	Cool Flame	Hot Flame	Delay, Sec.	Observations
1	1.0	650	45		X		32	Smoke
2		657	33			X	20	Orange flame, explosion
3		663	44		X		42	Smoke
4	0.5	595	37		X		47	
5		601	33		X		45	
6		621	36		X		43	
7		640	36		X		39	
8		647	43		X		37	Smoke
9		650	35			X	14	Orange flame, explosion
10		657	190			X	15	Orange flame, explosion
11	0.2	413	0	X				
12		435	2					
13		460	4	X				
14		485	7	X				
15		517	10	X				
16		528	14	X				
17		574	35		X		72	
18		593	33		X		47	
19		594	32		X		55	
20		615	36		X		44	

TABLE IV-CONTINUED

SAMPLE NUMBER KLO-67-16

SPONTANEOUS IGNITION TEMPERATURE

Needle A

1000 ml. chamber - Iron-Constantan Thermocouple

TYPE OF REACTION

Run	Sample Size, ml.	Initial Temp., deg. F.	Max. Rise, deg. F.	Pre-Ignition	Cool Flame	Hot Flame	Delay, Sec.	Observations
21	0.2	632	38		X			
22		641	44		X		42	
23		651	66		X		41	Smoke
24		657	40		X		40	
25		662	243			X	11	Orange flame
26		665	261			X	12	Orange flame
27		667	101			X	12	Orange flame
28		676	91			X	8	Orange flame
29		695	61			X	8	Orange flame

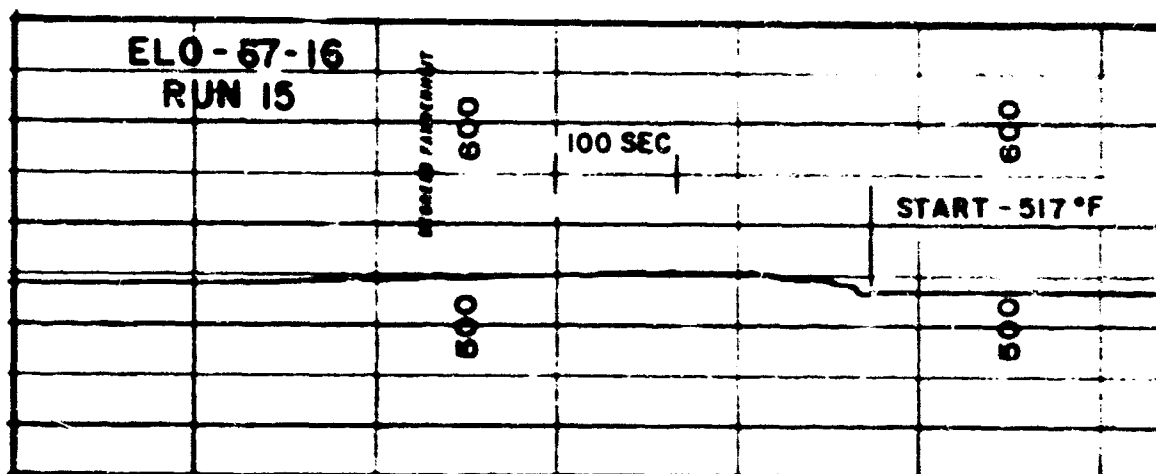


FIGURE 23. ELO-67-16. SPONTANEOUS IGNITION TEMPERATURE. RUN 15.

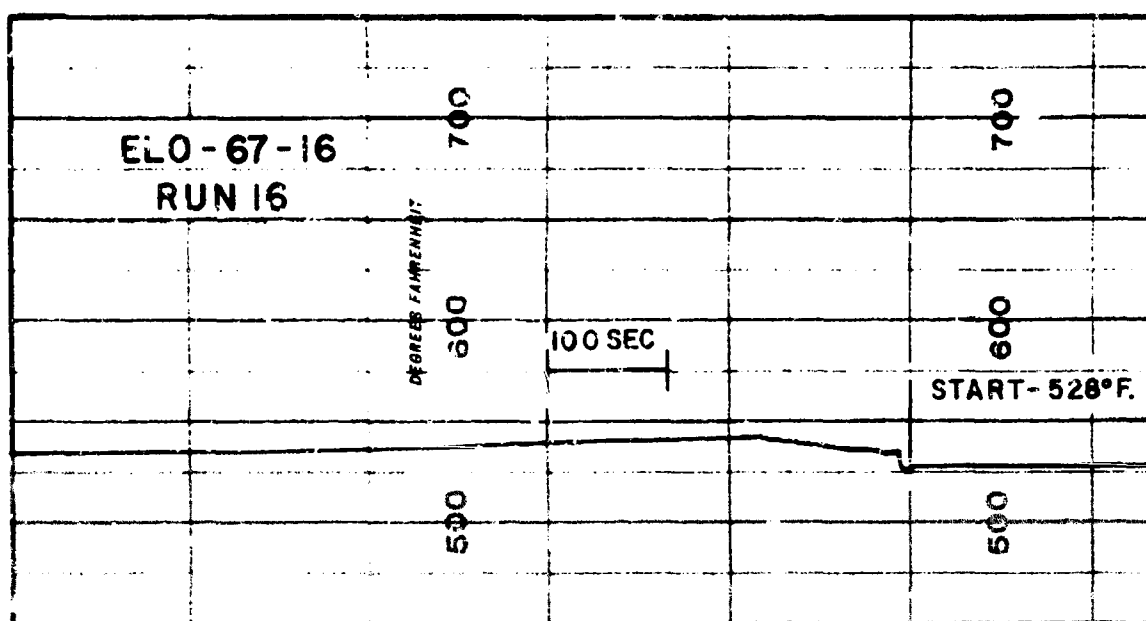


FIGURE 24. ELO-67-16. SPONTANEOUS IGNITION TEMPERATURE. RUN 16.

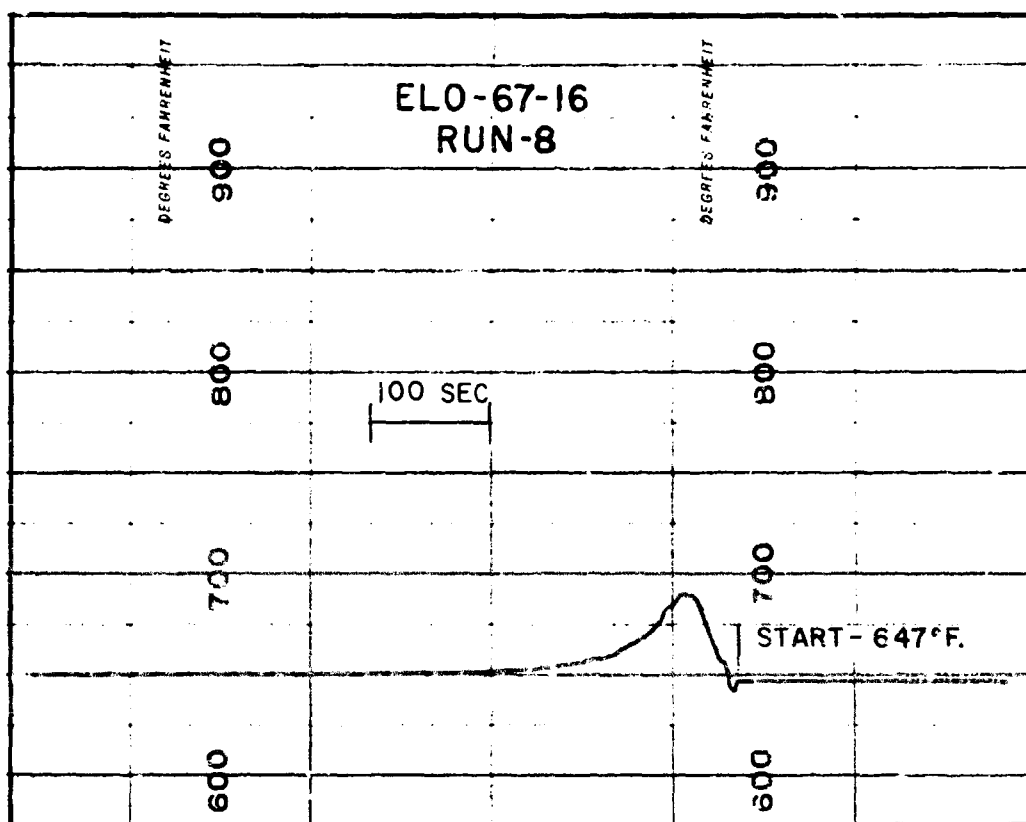


FIGURE 25. ELC-67-16. SPONTANEOUS IGNITION TEMPERATURE. RUN 8.

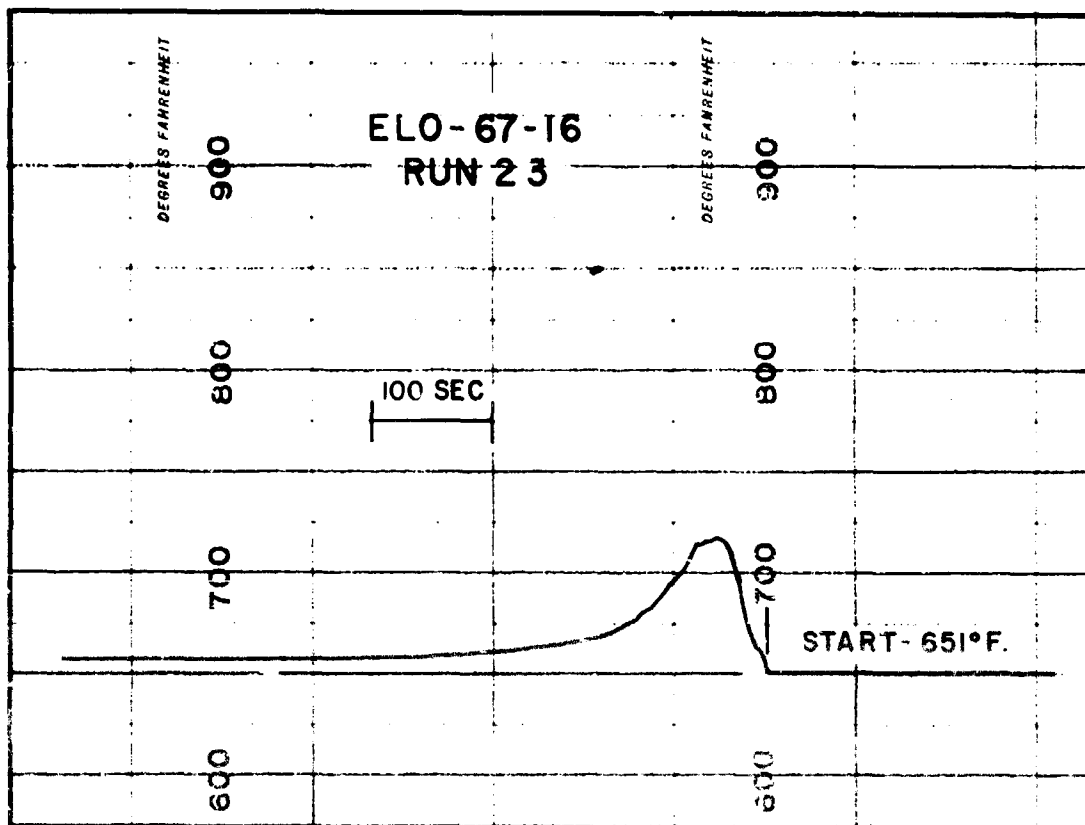


FIGURE 26. ELO-67-16. SPONTANEOUS IGNITION TEMPERATURE. RUN 23.

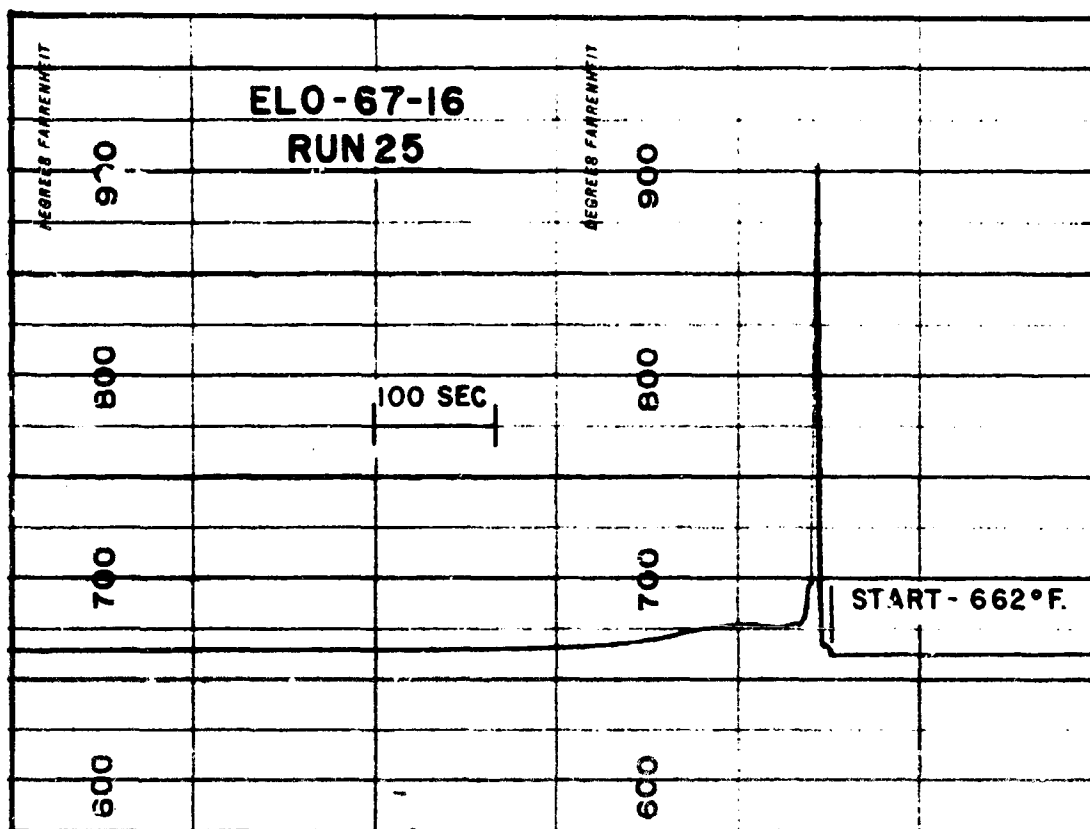


FIGURE 27. ELO-67-16. SPONTANEOUS IGNITION TEMPERATURE. RUN 25.

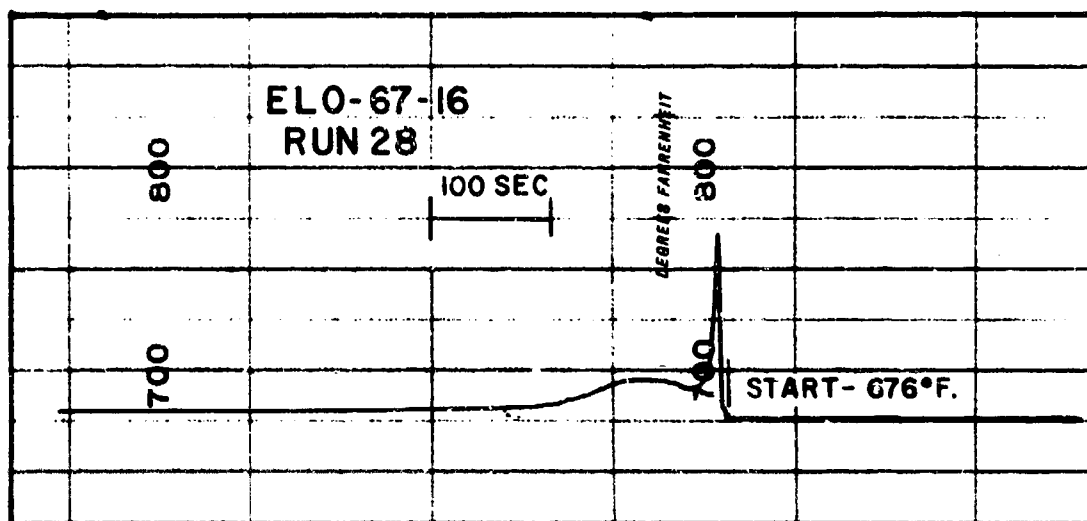


FIGURE 28. ELO-67-16. SPONTANEOUS IGNITION TEMPERATURE. RUN 28.

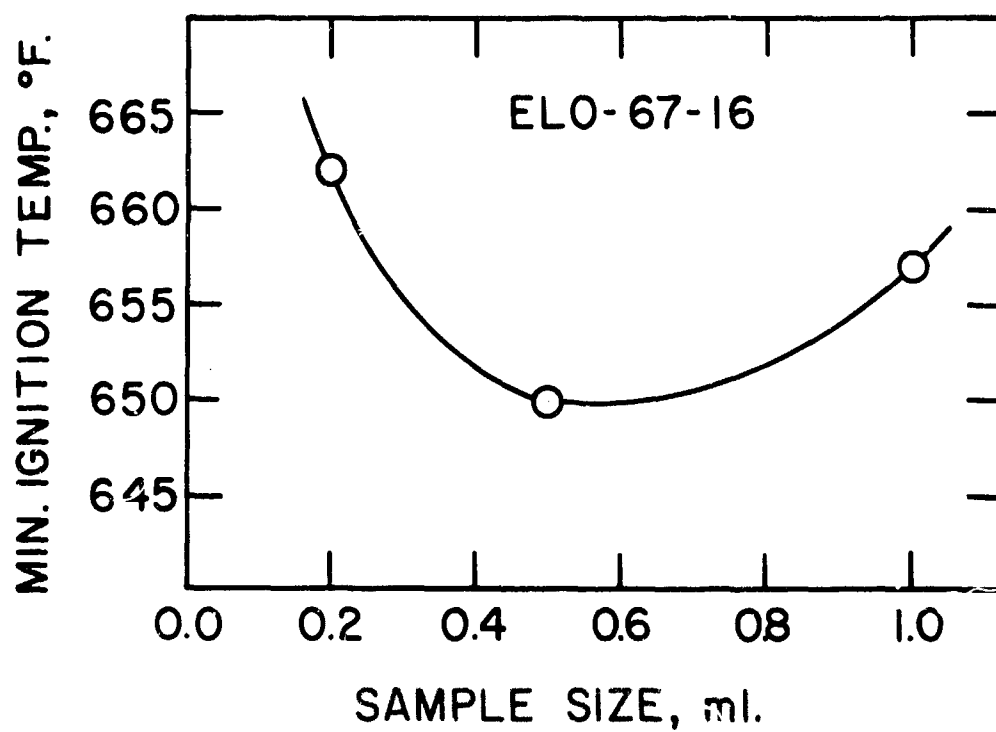


FIGURE 29. ELO-67-16. MINIMUM SPONTANEOUS IGNITION TEMPERATURE.

Figures 23 and 24, illustrate the pre-ignition reactions; Runs 8 and 23, Figures 25 and 26, the cool-flames; and Runs 25 and 28, Figures 27 and 28, the hot-flames.

The minimum spontaneous ignition temperature, $(SIT)_s$, determined from Figure 29 is 650 deg. F. The reaction threshold for the 0.2 ml. sample series is 413 deg. F.

1.3.5 ELO-66-109. See Table V and Figures 30 through 36.

In the study of the spontaneous ignition of sample ELO-66-109 pre-ignition, cool-flame and hot-flame reactions were observed for all sample sizes which were investigated. Pre-ignition reactions are illustrated by Run 5, Figure 30, and Run 15, Figure 31. Typical cool-flame ignitions are shown by Run 18, Figure 32, and Run 22, Figure 33; hot-flame ignitions, by Run 21, Figure 34, and Run 24, Figure 35.

Figure 36 is a plot of observed spontaneous ignition temperature against sample size. The minimum spontaneous ignition temperature, $(SIT)_s$, determined from that plot is 650 deg. F. The reaction threshold for the 0.2 ml. sample series is 451 deg. F.

1.3.6 ELO-67-23. See Table VI and Figures 37 through 44.

In the processes involved in the spontaneous ignition of sample ELO-67-23 typical hot-flame and pre-ignition reactions were observed. Runs 2 and 18, Figures 37 and 38, are representative of these hot-flame ignitions. In some cases more complex hot-flame ignitions occur. This kind of reaction is distinguished by the series of sharp, intense peaks which are produced by the multiple ignitions which occur. Runs 8 and 16, Figures 39 and 40, are illustrative. Typical pre-ignition reactions occur in Runs 5 and 13 -- See Figures 41 and 42. Some reactions resembling cool-flame ignitions are evident at the higher temperatures studied for the 0.2 ml. sample series. Run 20, Figure 43, is illustrative.

Observed spontaneous ignition temperatures are plotted against sample size in Figure 44. The minimum spontaneous ignition temperature, $(SIT)_s$, determined from that plot is 471 deg. F. The reaction threshold for the 0.2 ml. series is 420 deg. F.

TABLE V

SAMPLE NUMBER KLO-66-109

SPONTANEOUS IGNITION TEMPERATURE

Needle A

1000 ml. chamber - Iron-Constantan ThermocoupleTYPE OF REACTION

Run	Sample Size, ml.	Initial Temp., deg. F.	Max. Rise, deg. F.	Pre-Ignition	Cool Flame	Hot Flame	Delay, Sec.	Observations
1	0.2	451	1	X			--	
2		465	4	X			--	
3		522	10	X			--	
4		542	14	X			--	
5		559	17	X			--	
6		580	23		X		55	
7		604	29		X		48	
8		617	26		X		50	
9		643	31		X		39	
10		645	30		X		38	
11		650	33		X		53	
12	0.1	656	179			X	4	Orange flame, explosion
13		666	198			X	6	Orange flame, explosion
14		495	10	X			--	
15	0.05	532	11	X			--	
16		580	26	X			--	
17		610	27		X		38	
18		645	30		X		36	
19		650	156			X	4	Orange flame
20		655	140			X	5	Orange flame
21		660	175			X	7	Orange flame
22		650	27		X		36	
23		652	24		X		37	
24		657	129			X	5	Orange flame

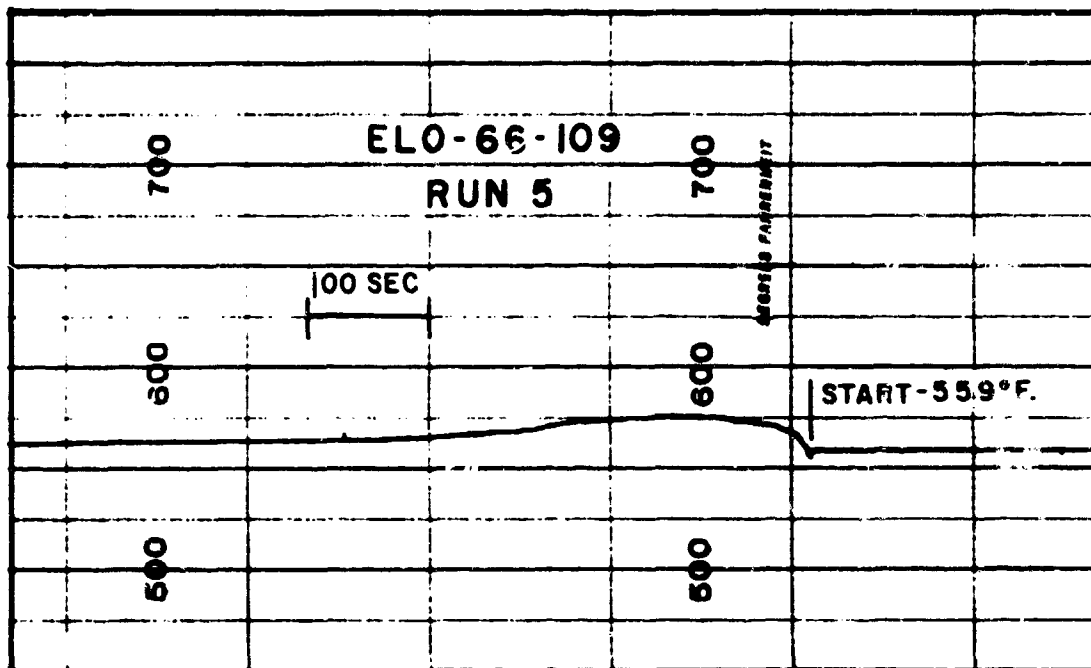


FIGURE 30. ELO-66-109. SPONTANEOUS IGNITION TEMPERATURE. RUN 5.

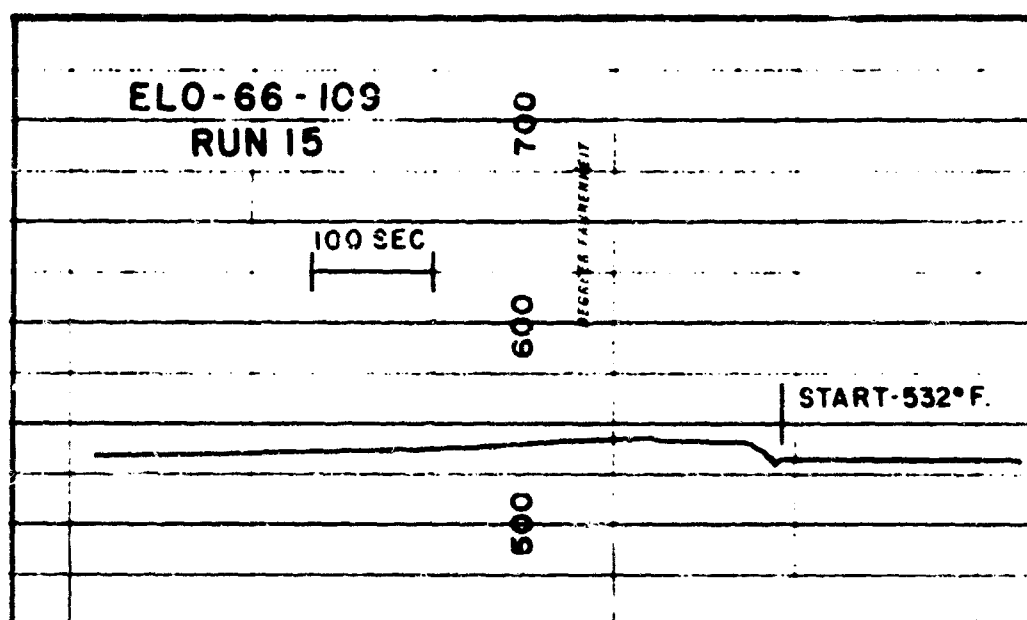


FIGURE 31. ELO-66-109. SPONTANEOUS IGNITION TEMPERATURE. RUN 15.

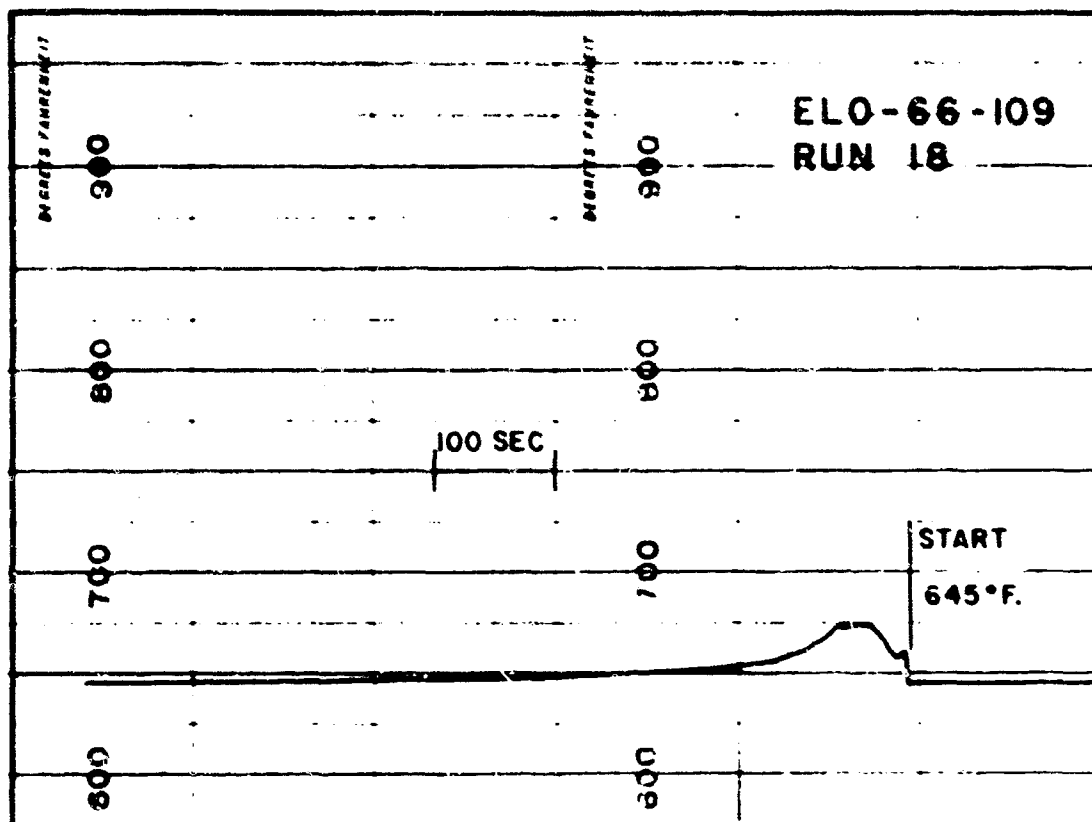


FIGURE 32. ELO-66-109. SPONTANEOUS IGNITION TEMPERATURE. RUN 18.

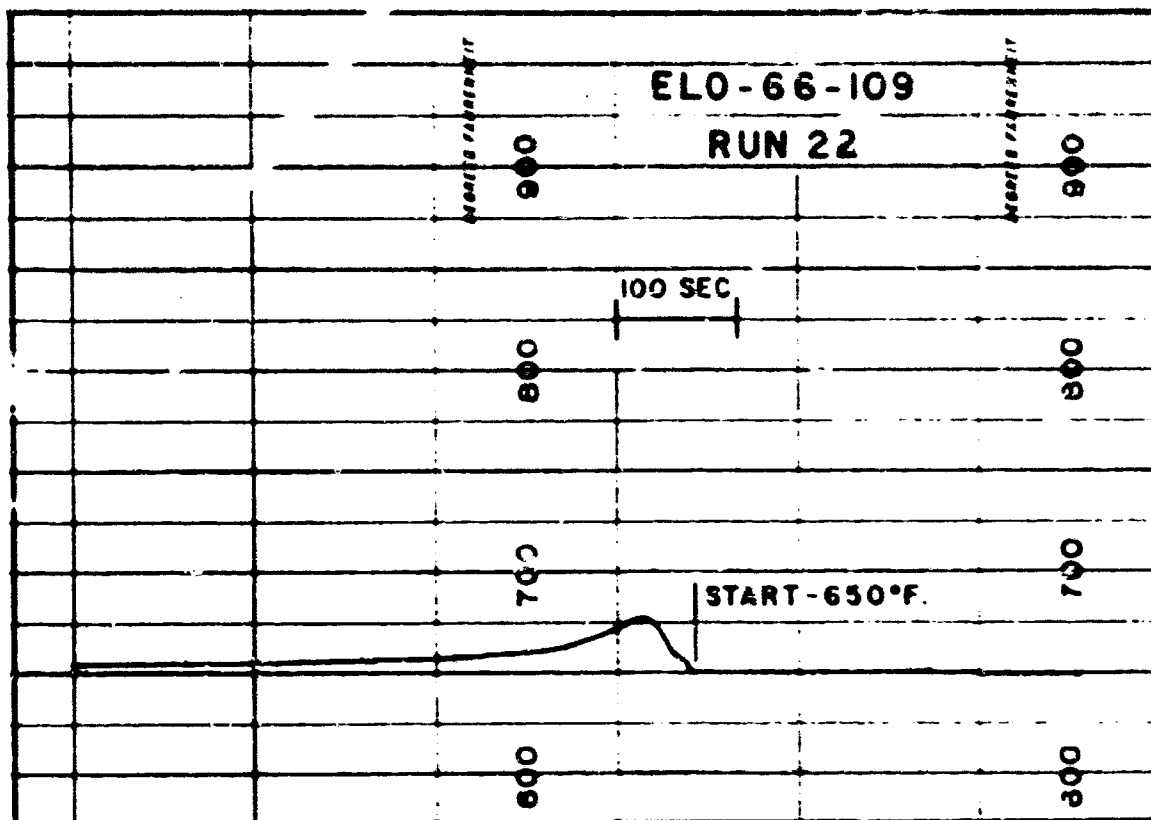


FIGURE 33. ELO-66-109. SPONTANEOUS IGNITION TEMPERATURE. RUN 22.

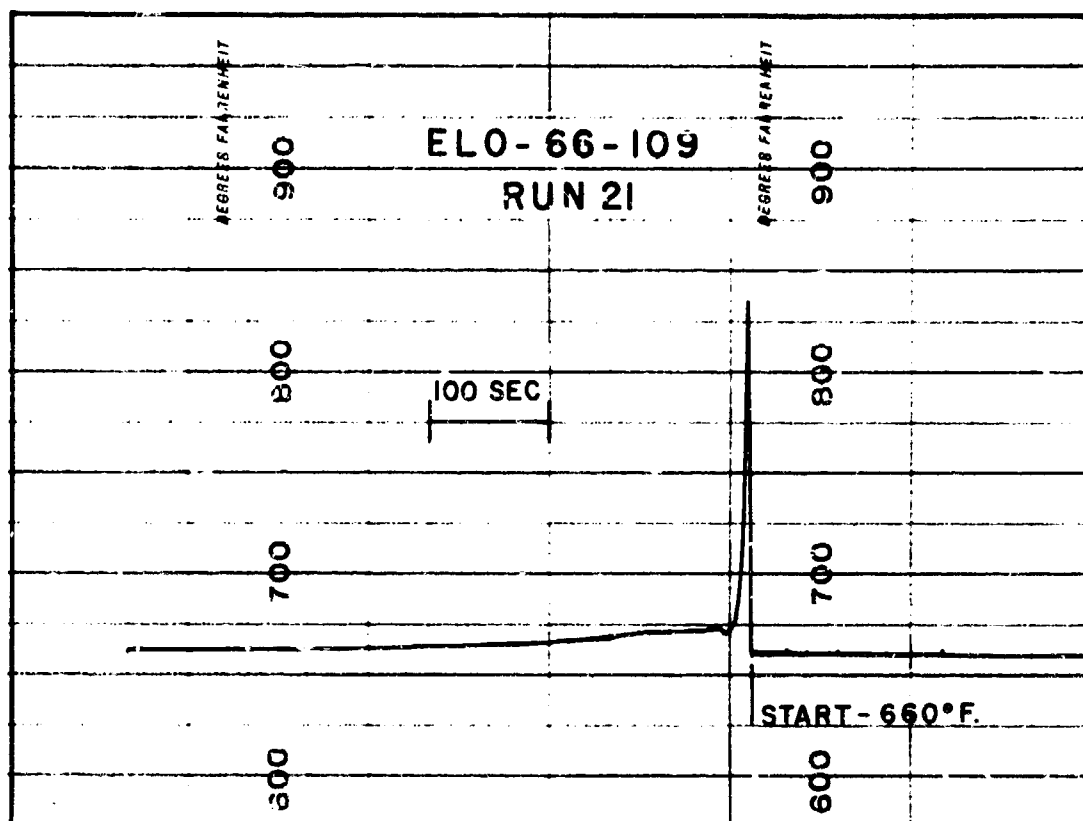


FIGURE 34. ELO-66-109. SPONTANEOUS IGNITION TEMPERATURE. RUN 21.

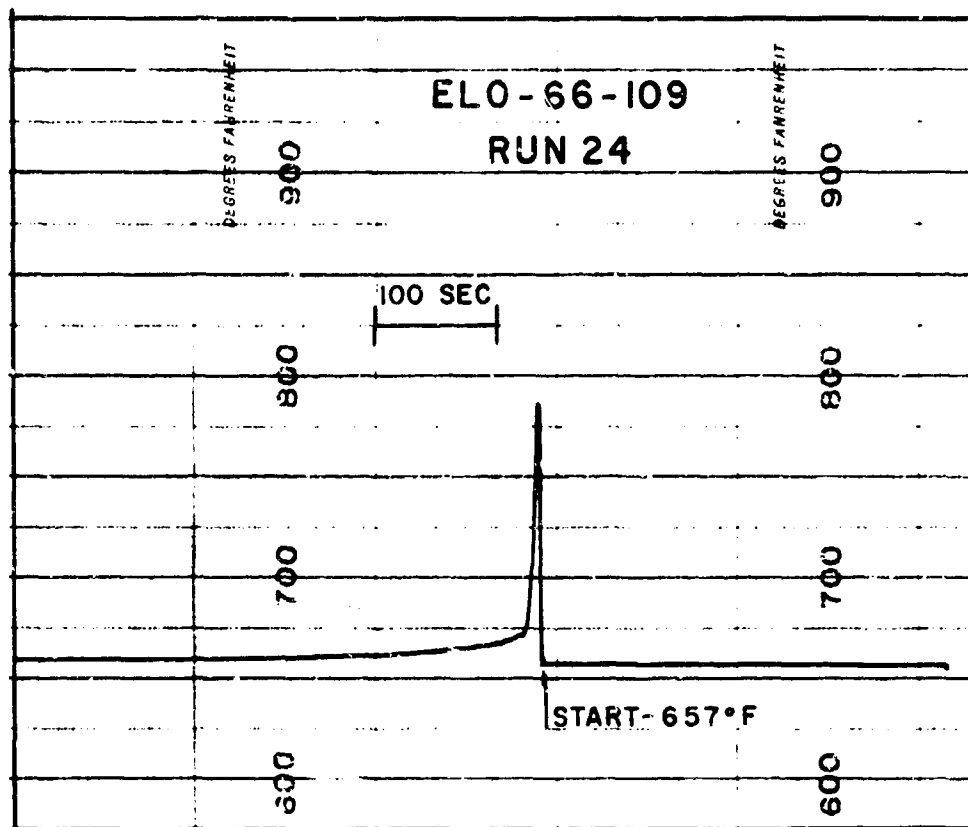


FIGURE 35. ELO-66-109. SPONTANEOUS IGNITION TEMPERATURE. RUN 24.

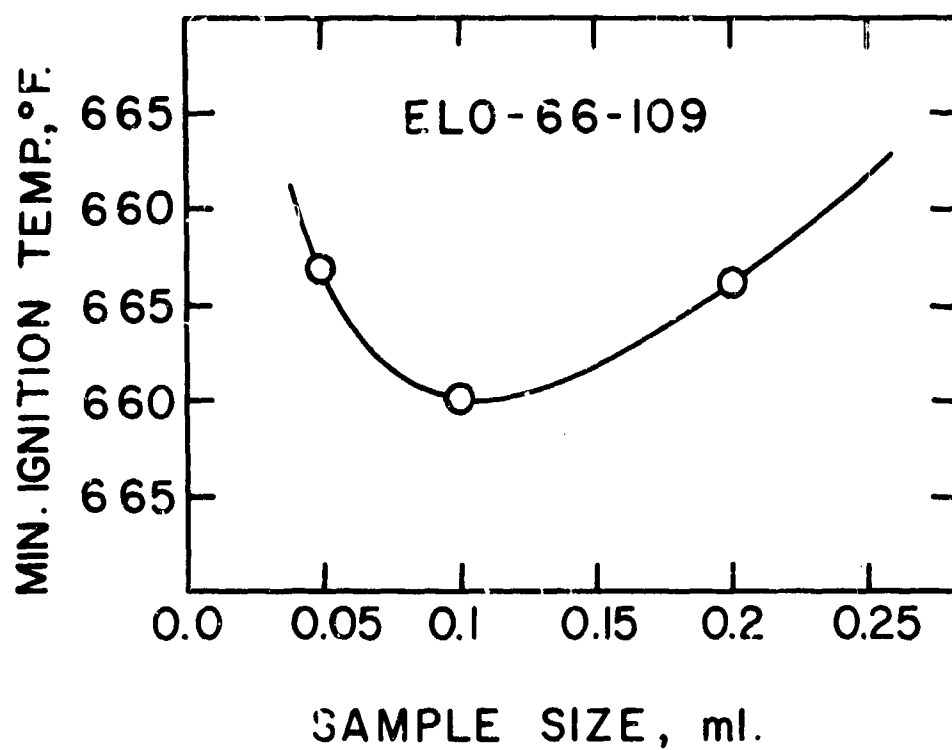


FIGURE 36. ELO-66-109. MINIMUM SPONTANEOUS IGNITION TEMPERATURE.

TABLE VI

SAMPLE NUMBER ELO-67-23

SPONTANEOUS IGNITION TEMPERATURE

Needle A

1000 ml. chamber - Iron-Constantan ThermocoupleTYPE OF REACTION

Run	Sample Size, ml.	Initial Temp., deg. F.	Max. Rise, deg. F.	Pre- Ignition	Cool Flame	Hot Flame	Delay, Sec.	Observations
1	1.0	475	10	X			--	Smoke
2		482	100			X	220	Heavy explosion, orange flame
3	0.5	425	1	X			--	
4		456	4	X			--	
5		465	15	X			--	
6		471	80			X	203	Heavy explosion, orange flame
7		476	74			X	196	Heavy explosion, orange flame
8		491	215			X	133	Heavy explosion, orange flame
9	0.2	420	0	X			--	
10		425	5	X			--	
11		433	6	X			--	
12		442	8	X			--	
13		455	7	X			--	
14		462	7	X			--	
15		468	14	X			--	
16		474	228			X	138	Heavy explosion, smoke
17		488	204			X	78	Heavy explosion, smoke
18		519	198			X	51	Heavy explosion, smoke
19		520	26		X		--	
20		567	40		X		55	

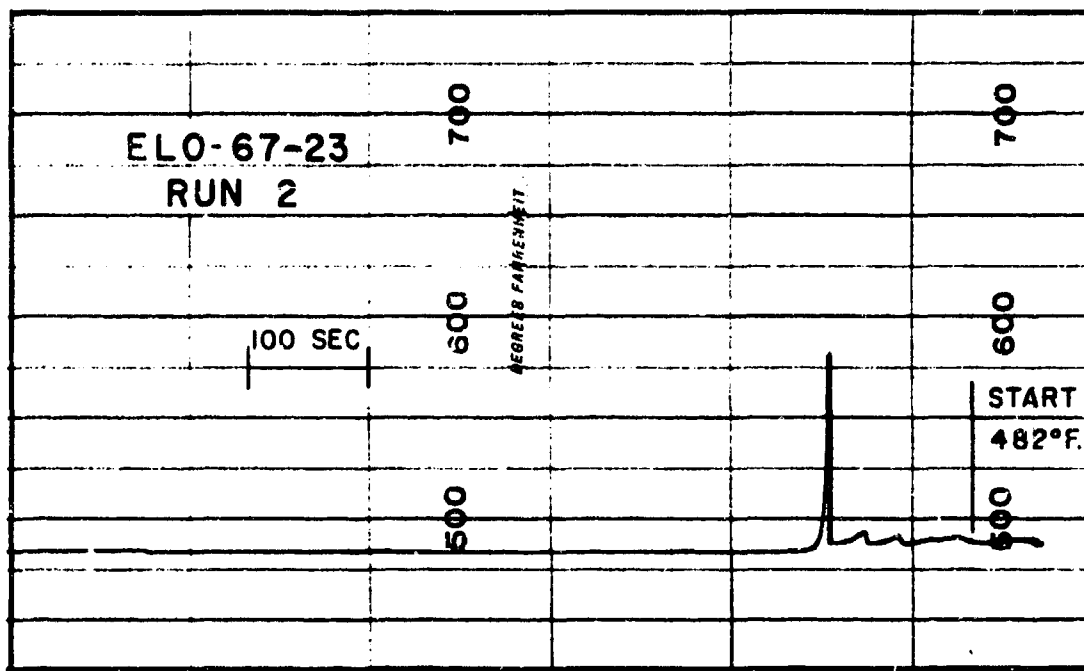


FIGURE 37. ELO-67-23. SPONTANEOUS IGNITION TEMPERATURE. RUN 2.

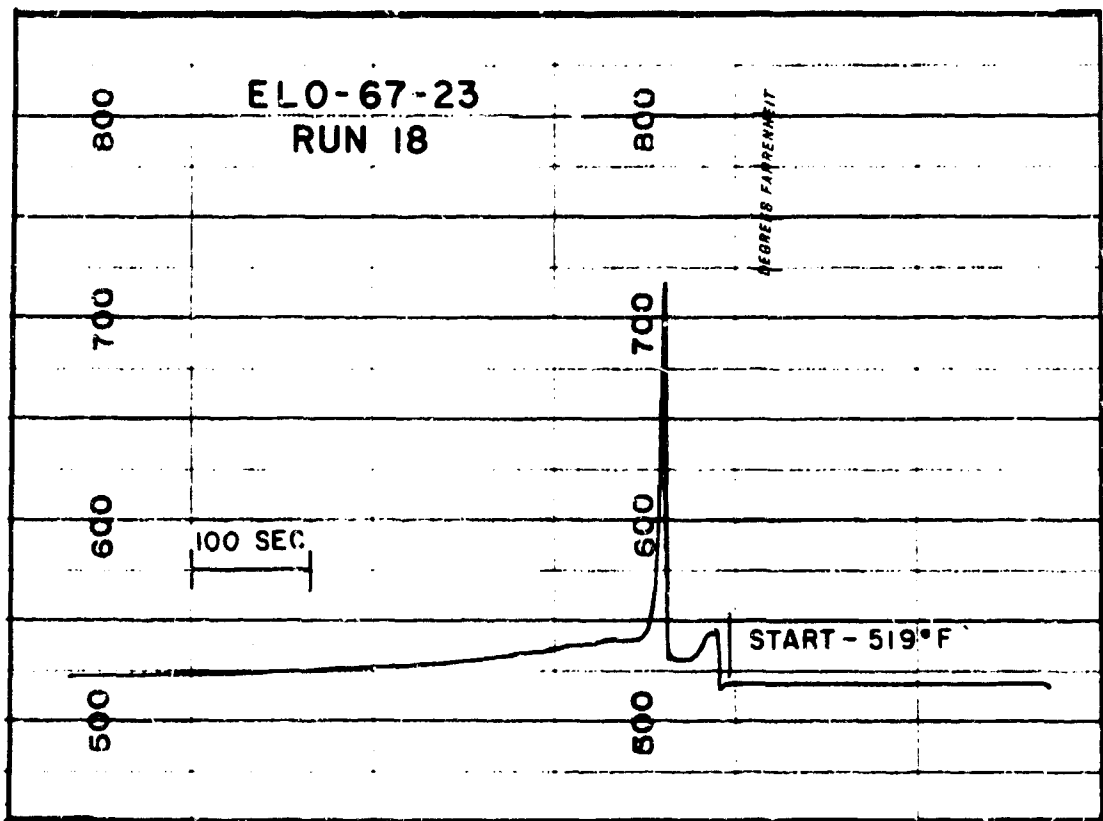


FIGURE 38. ELO-67-23. SPONTANEOUS IGNITION TEMPERATURE. RUN 18.

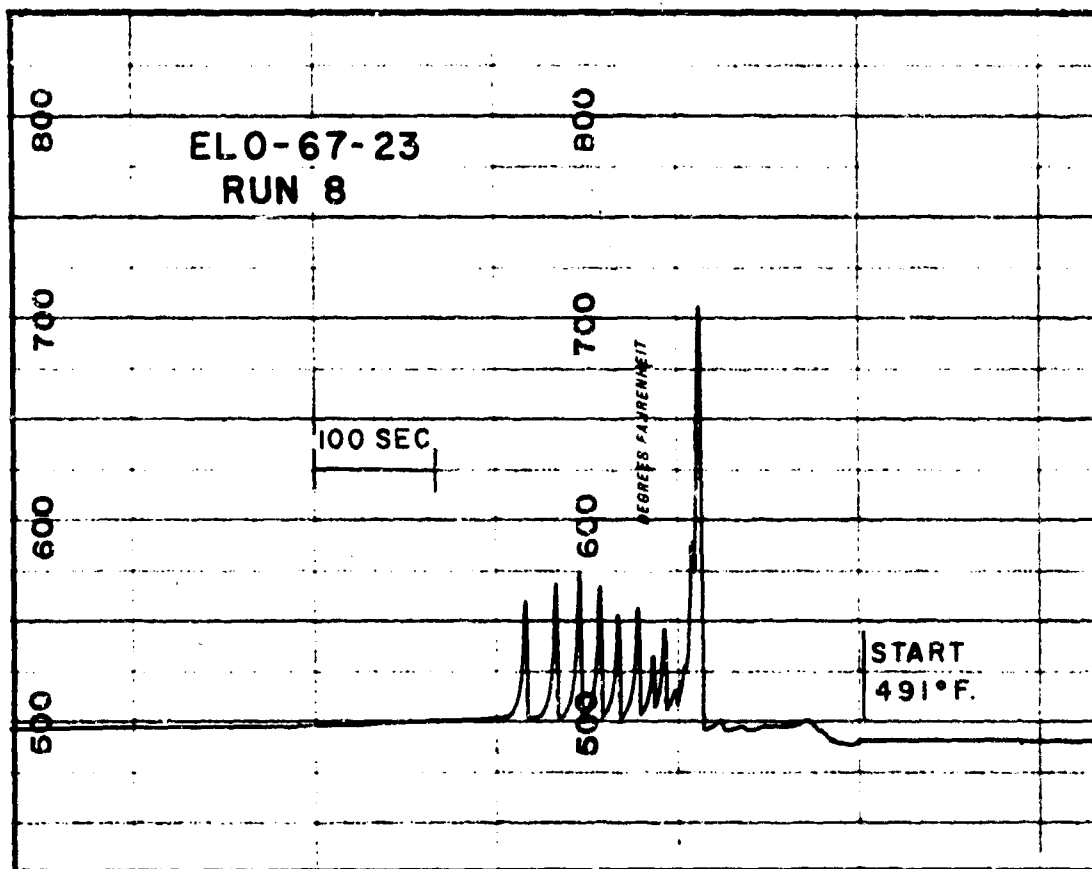


FIGURE 39. ELO-67-23. SPONTANEOUS IGNITION TEMPERATURE. RUN 8.

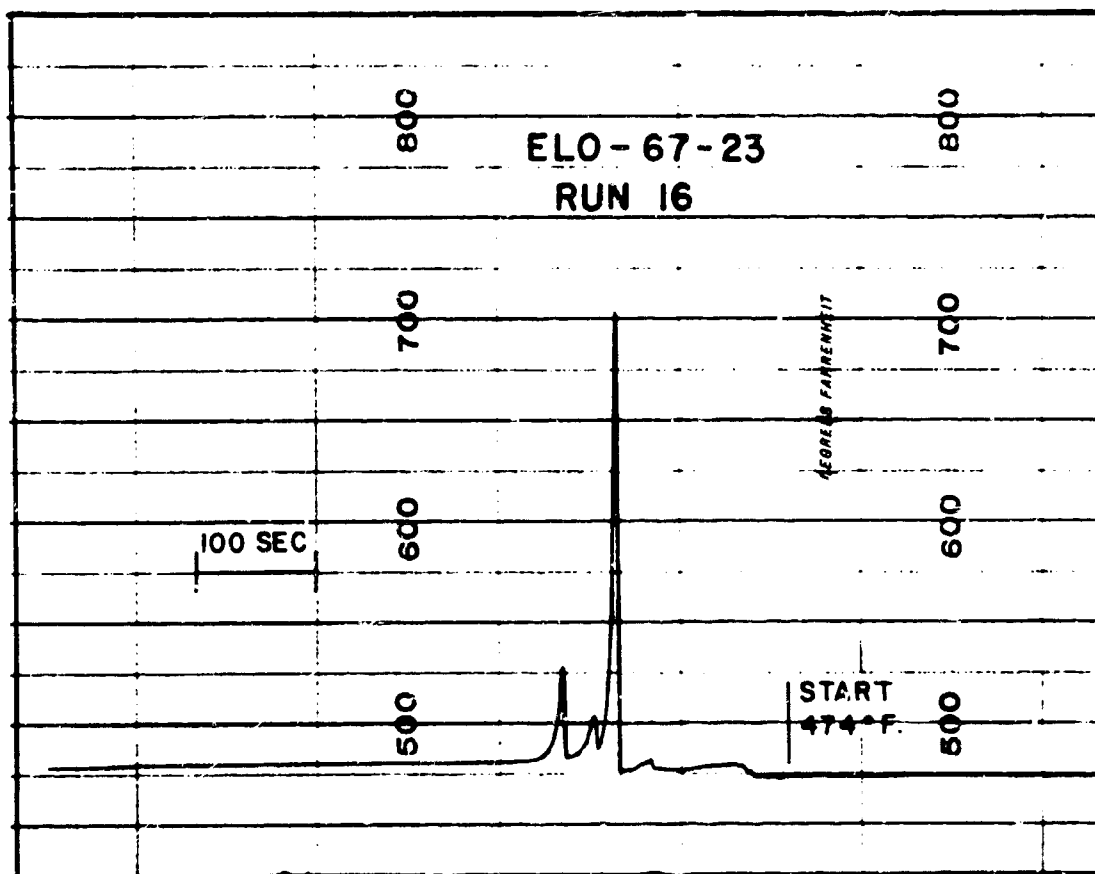


FIGURE 40. ELO-67-23. SPONTANEOUS IGNITION TEMPERATURE. RUN 16.

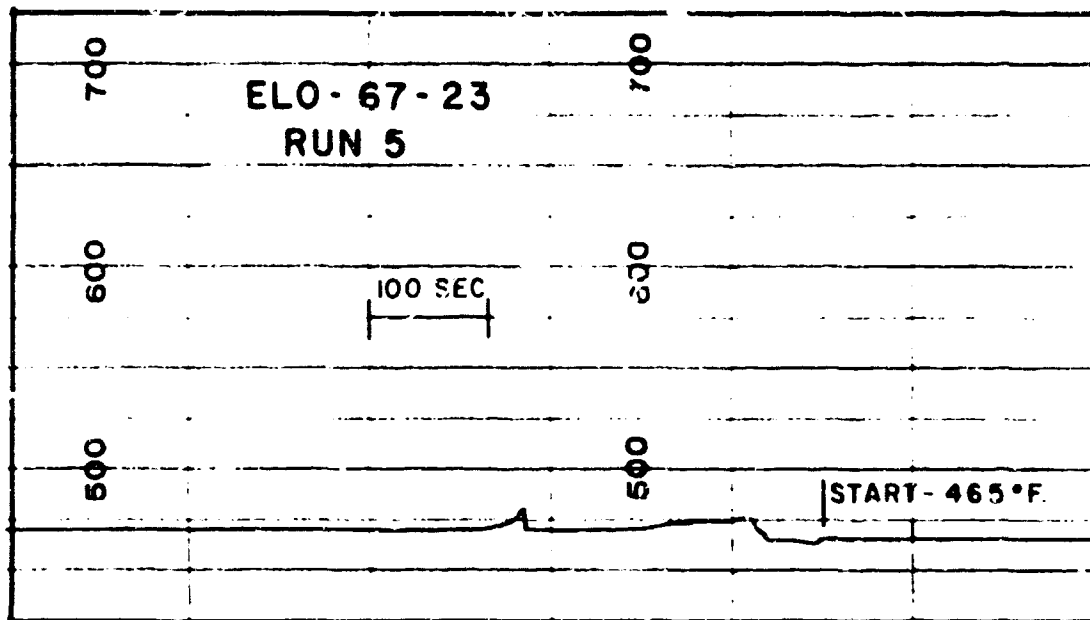


FIGURE 41. ELO-67-23. SPONTANEOUS IGNITION TEMPERATURE. RUN 5.

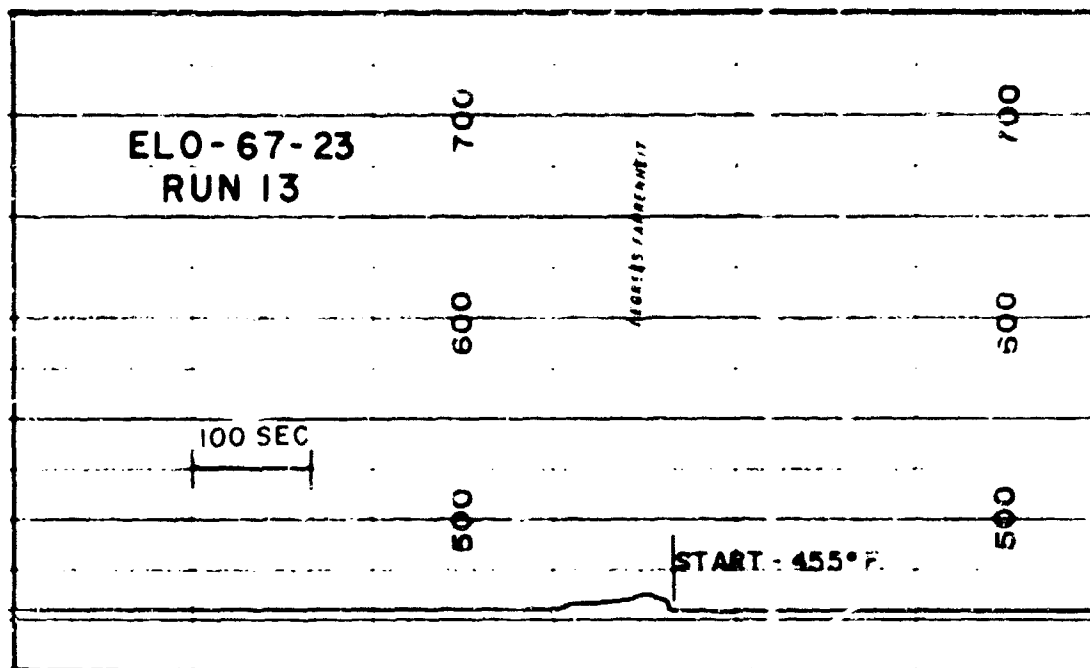


FIGURE 42. ELO-67-23. SPONTANEOUS IGNITION T. SPONTANEOUS IGNITION. RUN 13.

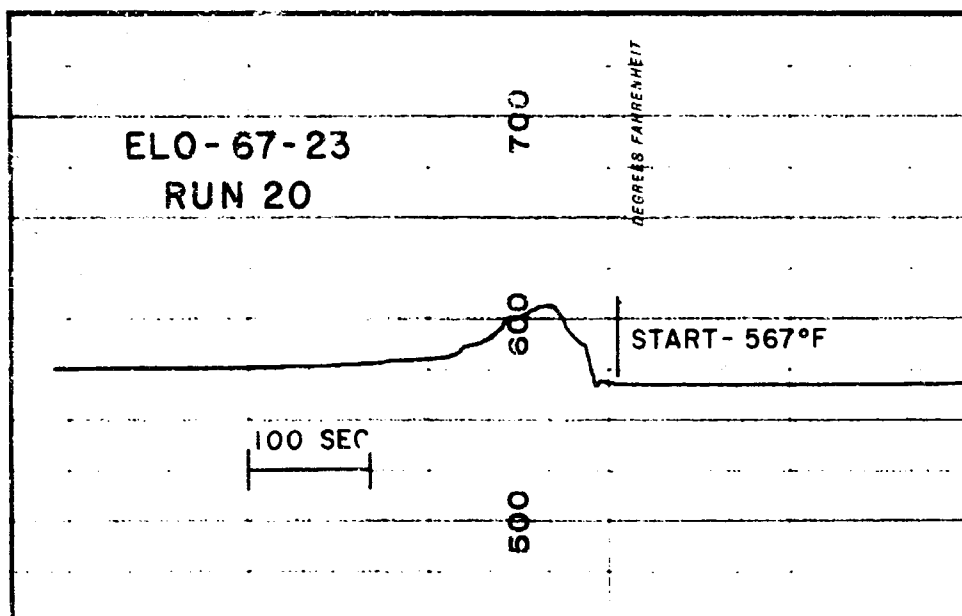


FIGURE 43. ELO-67-23. SPONTANEOUS IGNITION TEMPERATURE. RUN 20.

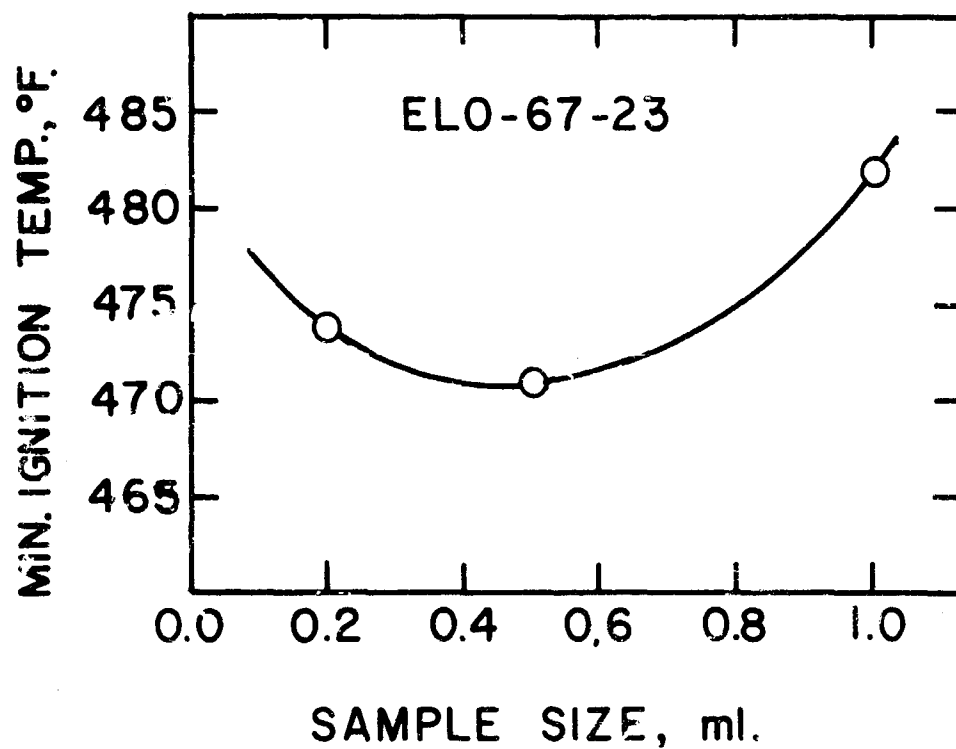


FIGURE 44. ELO-67-23. MINIMUM SPONTANECUS IGNITION TEMPERATURE.

1.3.7 ELO-67-49. See Table VII and Figures 45 through 60.

At temperatures below 500 deg. F. the spontaneous ignition of the sample apparently proceeds without complication. Both pre-ignition and hot-flame ignitions occur. In some cases the hot-flame ignitions lead to the formation of multiple peaks in the time-temperature record. In other cases single sharp peaks are observed alone or followed by broad peaks due to slow oxidation. The occurrence of multiple ignitions with the larger sample sizes is observed at temperatures just above the transition point from pre-ignition reactions to hot-flame ignitions. The following runs are illustrative of the various hot-flames observed. Simple hot-flame ignition, Run 24 and 38, Figures 45 and 46; simple hot-flame followed by slow oxidation, Run 13 and 14, Figures 47 and 48; multiple hot-flame, Run 10 and 25, Figures 49 and 50. Characteristic pre-ignition reactions are found at lower temperatures. Runs 7 and 22, Figures 51 and 52 are representative.

The pattern of ignition undergoes an unexpected change as the temperature of the ignition chamber is increased. After a transitional region of pseudo-hot-flame ignitions which are observed for the 0.2 and 0.1 ml. sample sizes (See Runs 16 and 33, Figures 53 and 54) and energetic-pre-ignition reactions which are observed for the 0.05 ml. series (See Run 39, Figure 55) rather typical cool-flame ignitions are found. Runs 17 and 41, Figures 56 and 57, are good examples. At higher temperatures hot-flames again appear. See Runs 19 and 34, Figures 58 and 59. The exact cause of this behavior cannot be determined from the available data. However, the phenomenon is consistent with the supposition that the sample undergoes decomposition or chemical rearrangement at temperatures above 500 deg. F. to produce a changed material which is somewhat less flammable than the original.

The minimum temperatures required to produce hot-flame ignitions of both classifications are plotted against sample sizes in Figure 60. The minimum spontaneous ignition temperature (SIT)_s is taken to be the minimum point in the lower of the two curves shown in that Figure. It is 466 deg. F. The minimum temperature required to produce the reaction represented by the upper curve is 608 deg. F. The reaction threshold for the 0.2 ml. sample series is 415 deg. F.

TABLE VII

SAMPLE NUMBER ELO-67-49

SPONTANEOUS IGNITION TEMPERATURE

Needle A

1000 ml. chamber - Iron-Constantan ThermocoupleTYPE OF REACTION

Run	Sample Size, ml.	Initial Temp., deg. F.	Max. Rise, deg. F.	Pre- Ignition	Cool Flame	Hot Flame	Delay, Sec.	Observations
1	0.2	415	1	X			--	
2		418	3	X			--	
3		420	4	X			--	
4		424	4	X			--	
5		431	4	X			--	
6		445	7	X			--	
7		457	13	X			--	
8		470	186			X	125	Explosion
9		479	197			X	78	Orange flame
10		482	189			X	59	Orange flame, explosion
11		489	141			X	31	Orange flame, explosion
12		495	180			X	30	Orange flame, explosion
13		509	166			X	20	Orange flame
14		525	170			X	7	Orange flame
15		535	153			X	5	Orange flame
16		545	75			(X)	11, 26	Smoke
17		587	58		X		43	
18		604	68		X		32	
19		610	390			X	5	Orange flame, explosion
20		618	252			X	4	Orange flame
21		624	238			X	4	Orange flame

TABLE VII-CONTINUED

SAMPLE NUMBER ELO-67-49

SPONTANEOUS IGNITION TEMPERATURE

Needle A

1000 ml. chamber - Iron-Constantan Thermocouple

TYPE OF REACTION

Run	Sample Size, ml.	Initial Temp., deg. F.	Max. Rise, deg. F.	Pre-Ignition	Cool Flame	Hot Flame	Delay, Sec.	Observations
22	0.1	459	17	X			--	
23		465	11	X			--	
24		466	227			X	169	Orange flame
25		472	96			X	91	Orange flame
26		491	2	X			--	
27		525	36		X		110	
28		535	49		X		54	
29		550	59		X		48	
30		565	60		X		50	
31		578	58		X		49	
32	0.05	595	80			(X)	39	
33		605	70			(X)	6, 36	
34		608	254			X	5	Orange flame, explosion
35		615	210			X	4	Orange flame, explosion
36		619	236			X	5	Orange flame, explosion
37		465	12	X			--	
38		472	88			X	68	Orange flame
39		599	16	X!			9	
40		607	13	X!			9	
41		614	66		X		43	
42		620	146			X	3	Orange flame

(X) Indicates transitional reaction with apparent cool-flame and hot-flame characteristics.

X! Indicates energetic pre-ignition reaction.

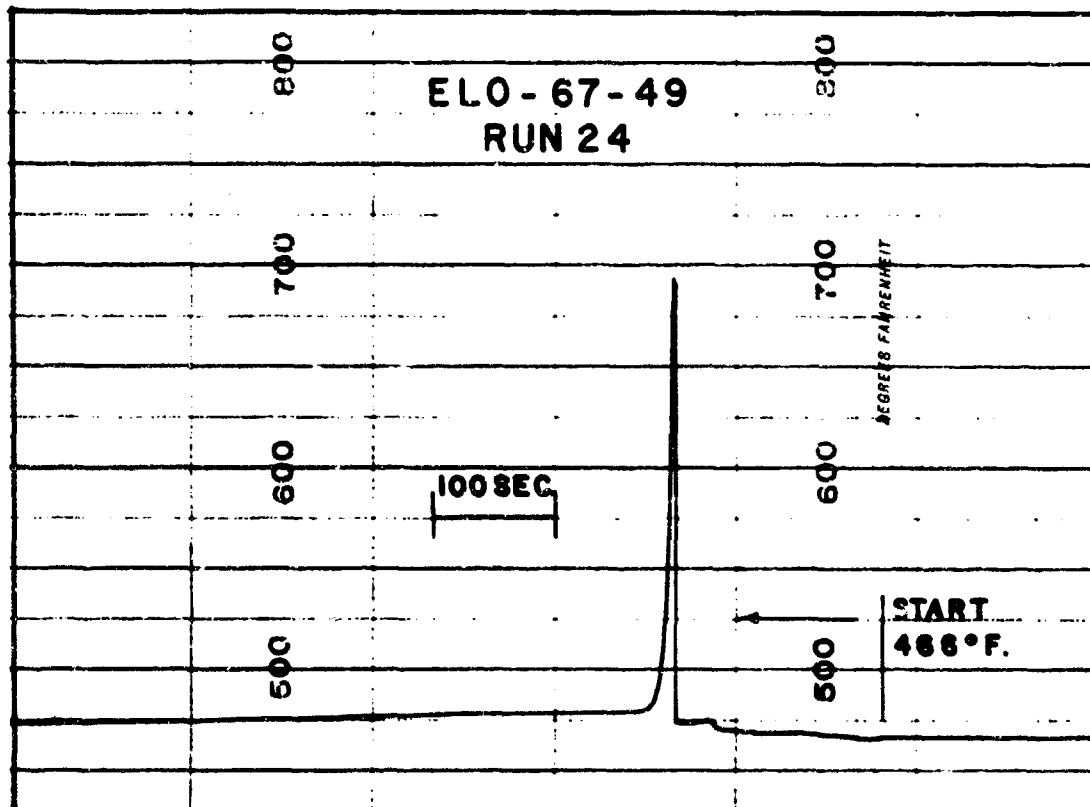
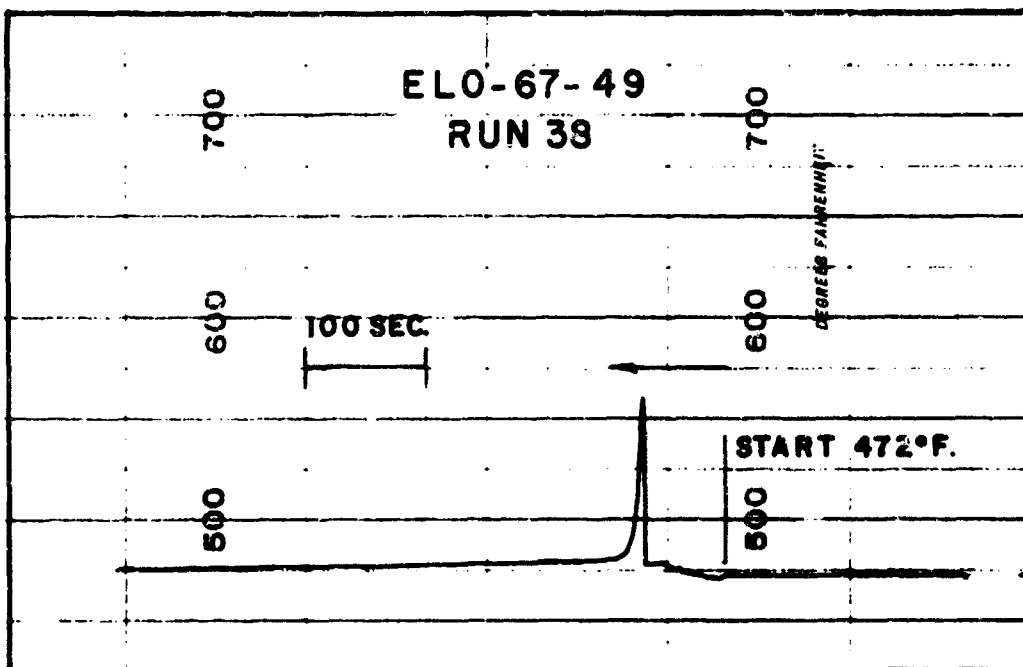


FIGURE 45. ELO-67-49. SPONTANEOUS IGNITION TEMPERATURE. RUN 24.



4

FIGURE 46. ELO-67-49. SPONTANEOUS IGNITION TEMPERATURE. RUN 38.

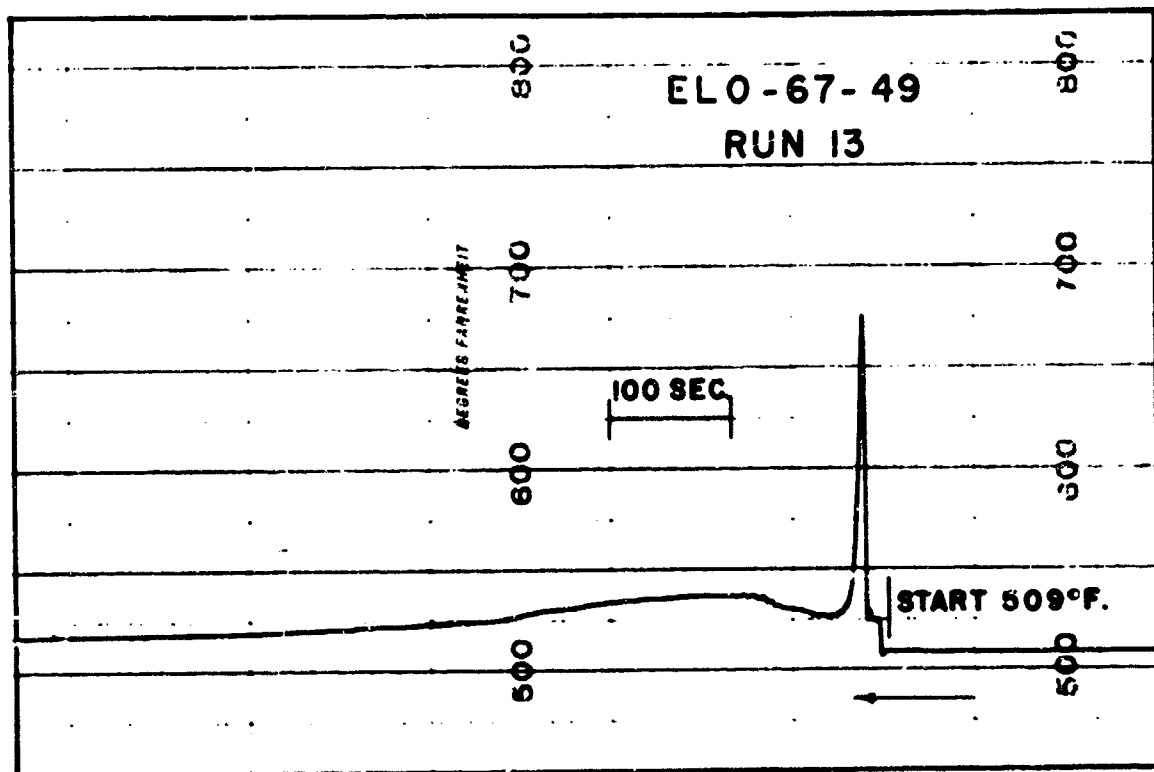


FIGURE 47. ELO-67-49. SPONTANEOUS IGNITION TEMPERATURE. RUN 13.

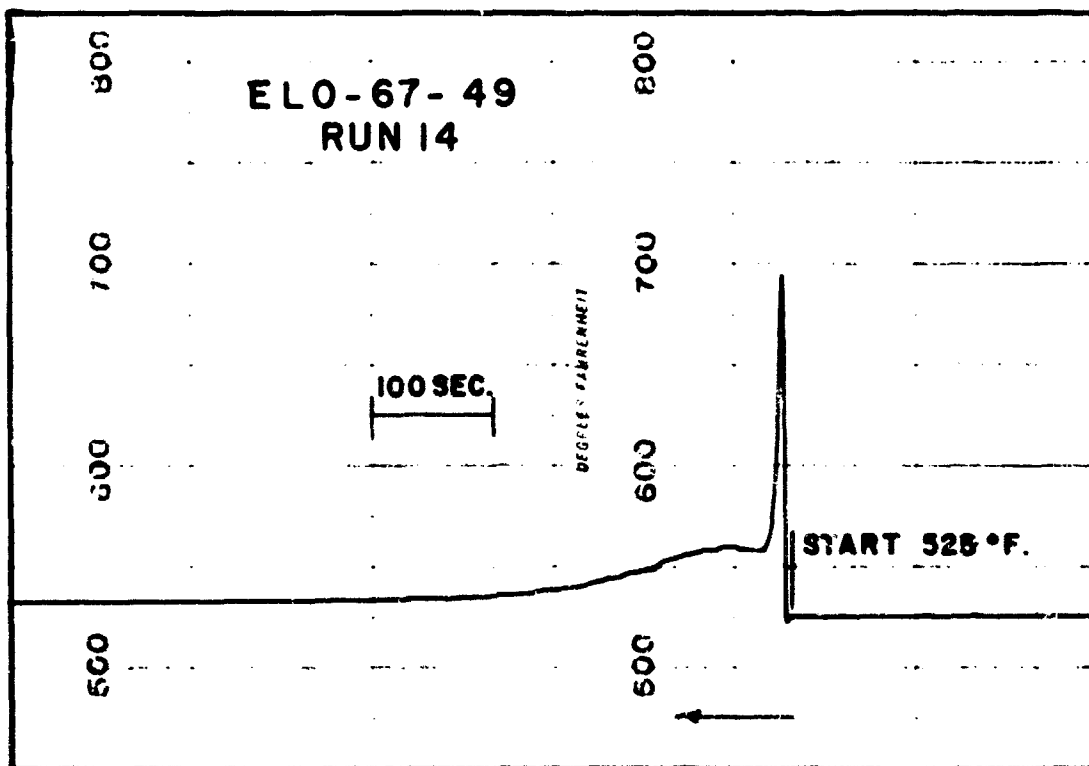


FIGURE 48. SPONTANEOUS IGNITION TEMPERATURE. RUN 14.

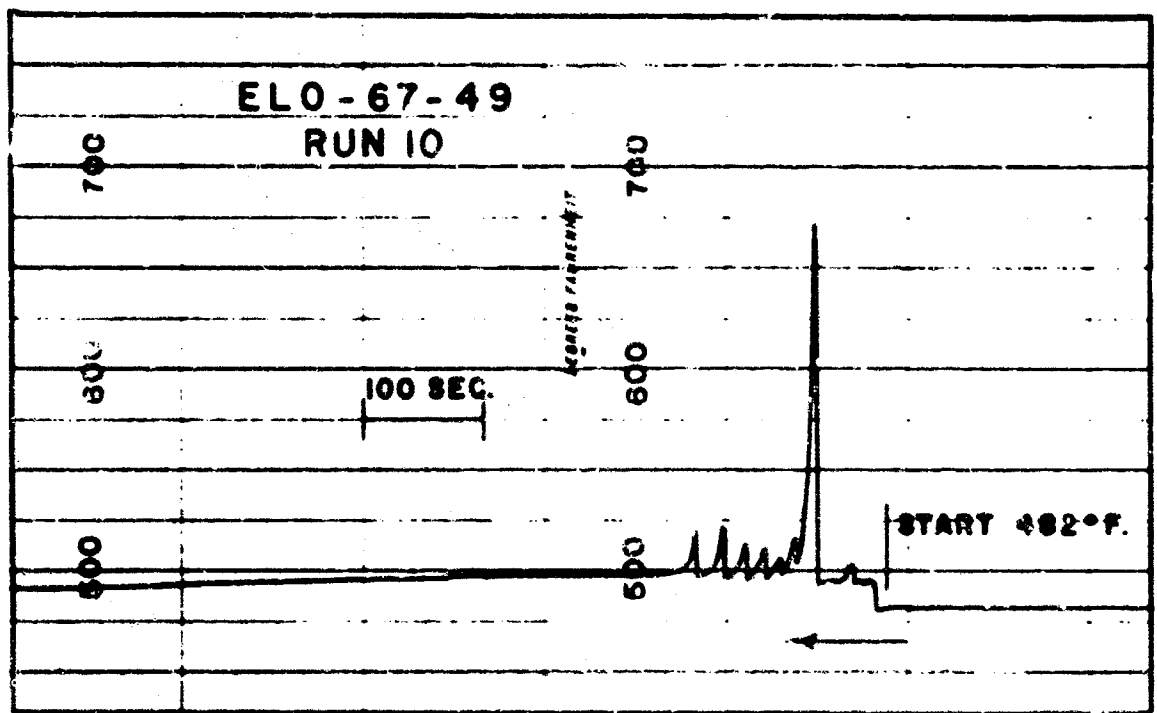


FIGURE 49. ELO-67-49 SPONTANEOUS IGNITION TEMPERATURE. RUN 10.

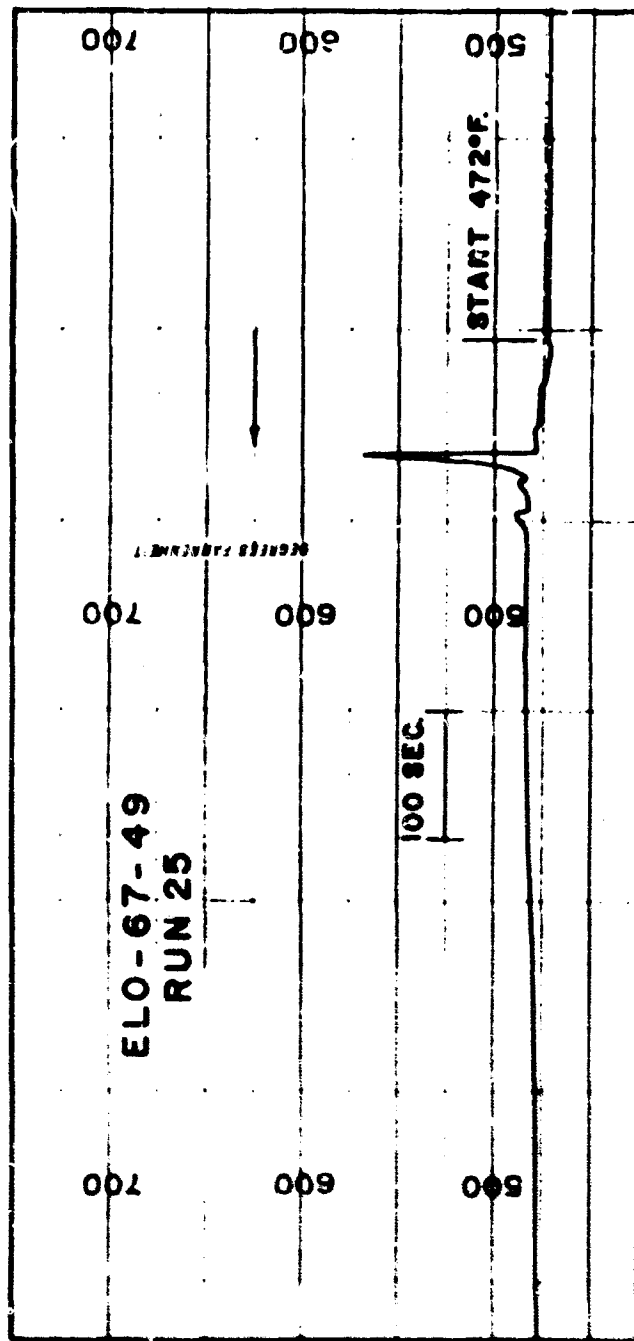


FIGURE 50. ELO-67-49. SPONTANEOUS IGNITION TEMPERATURE. RUN 25.

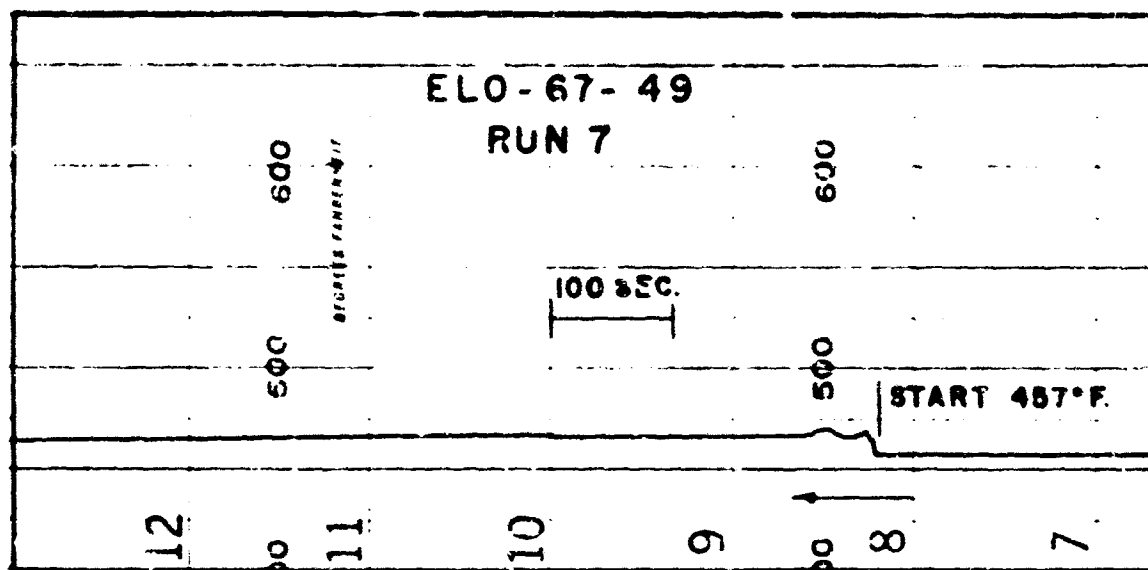


FIGURE 51. ELO-67-49. SPONTANEOUS IGNITION TEMPERATURE. RUN 7.

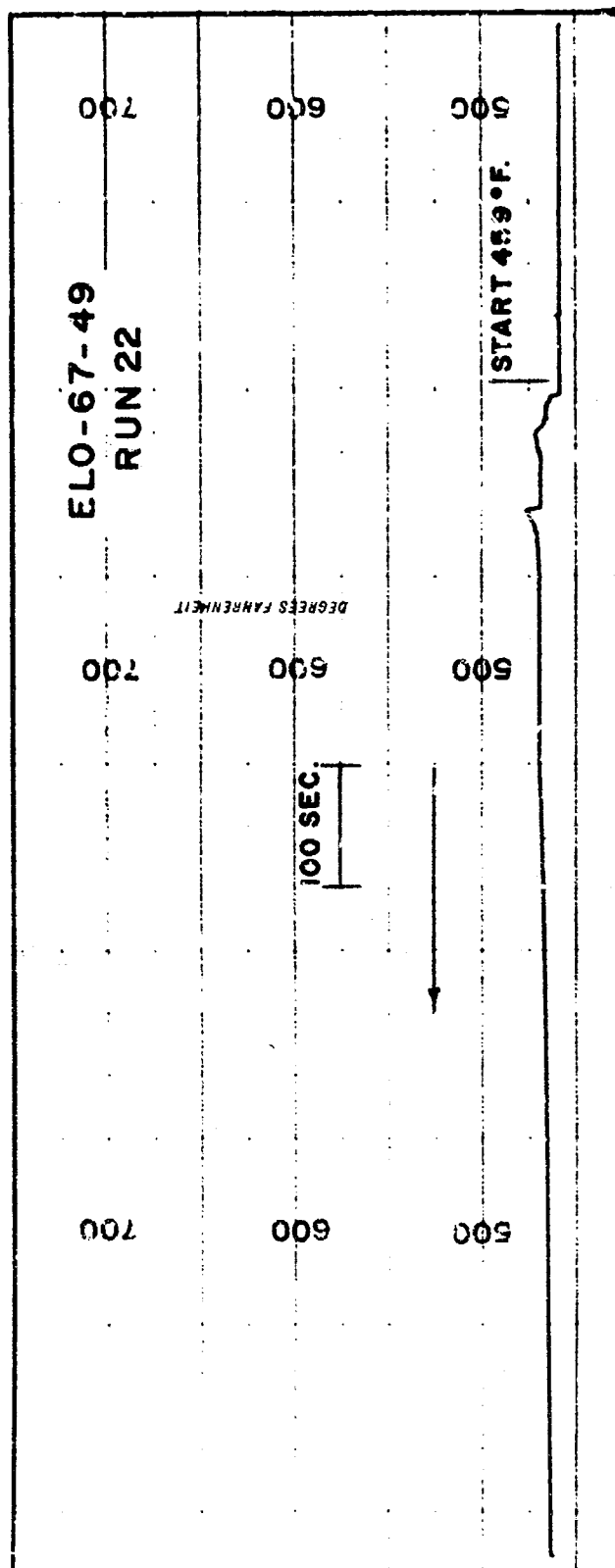


FIGURE 52. ELO-67-49. SPONTANEOUS IGNITION TEMPERATURE. RUN 22.

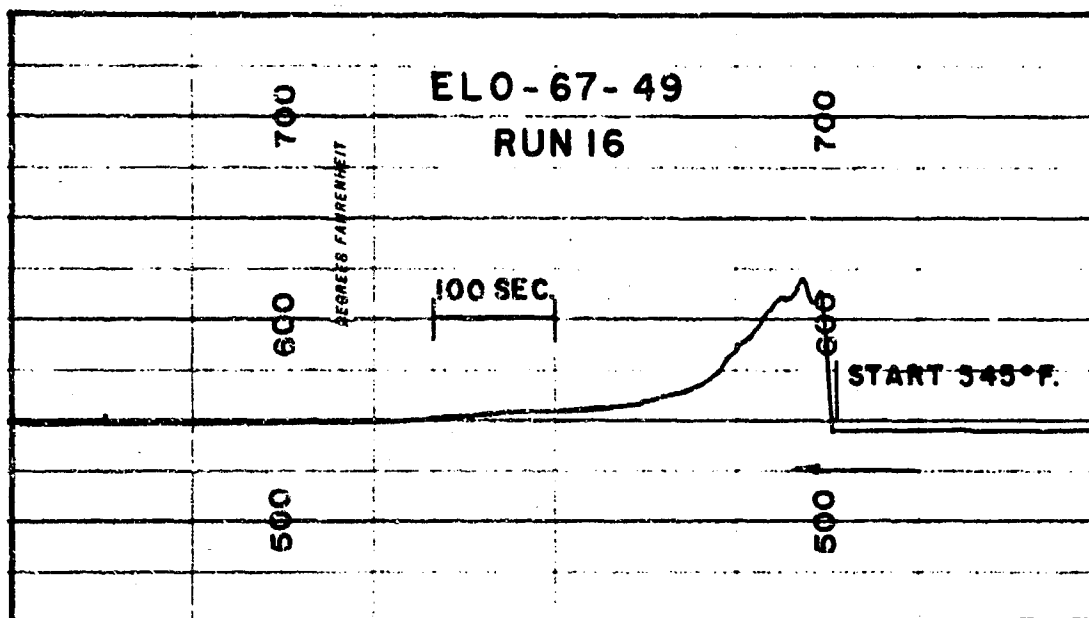


FIGURE 53. ELO-67-49. SPONTANEOUS IGNITION TEMPERATURE. RUN 16.

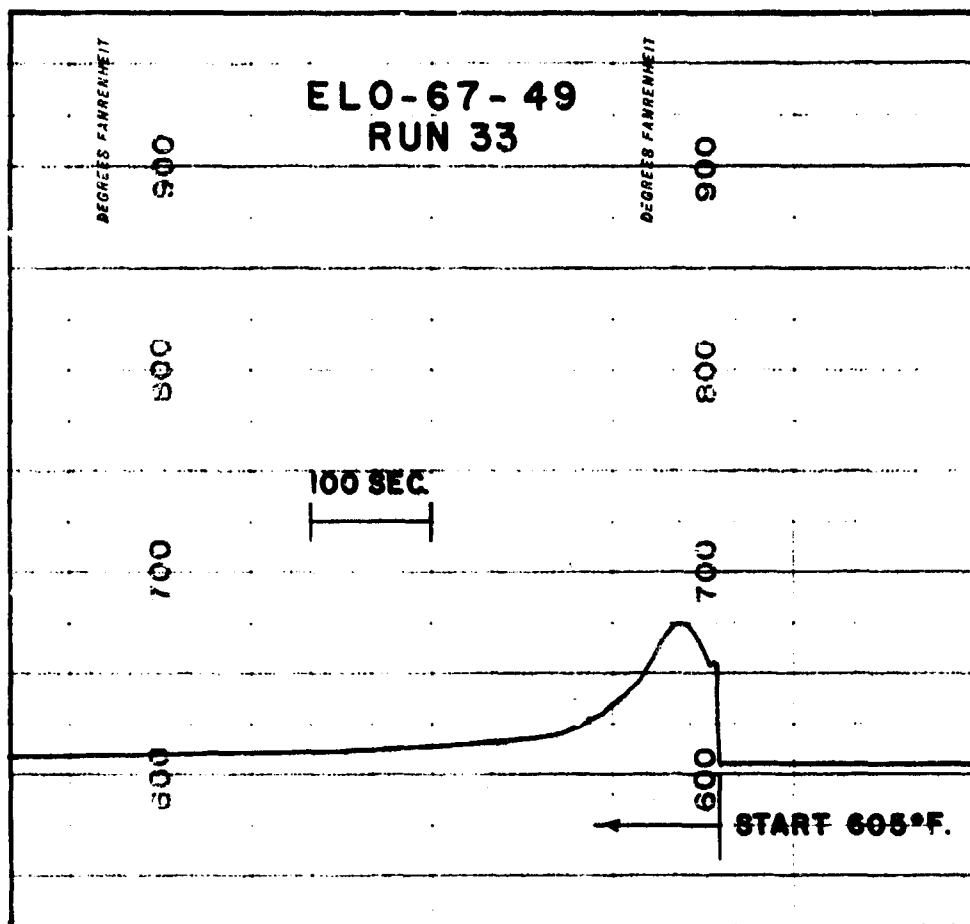


FIGURE 54. ELO-67-49. SPONTANEOUS IGNITION TEMPERATURE. RUN 33.

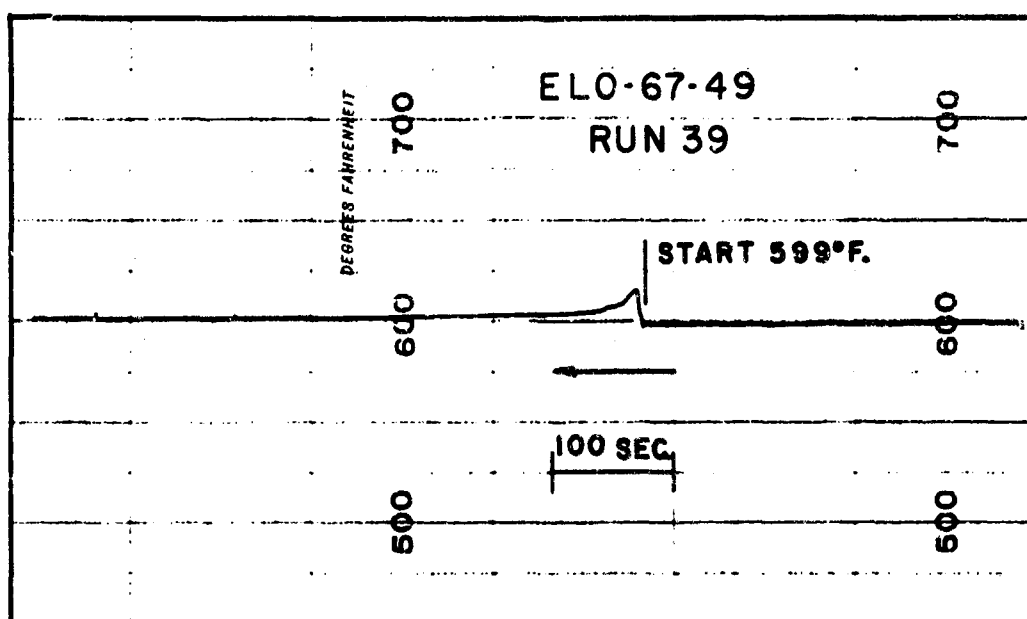


FIGURE 55. ELO-67-49. SPONTANEOUS IGNITION TEMPERATURE. RUN 39.

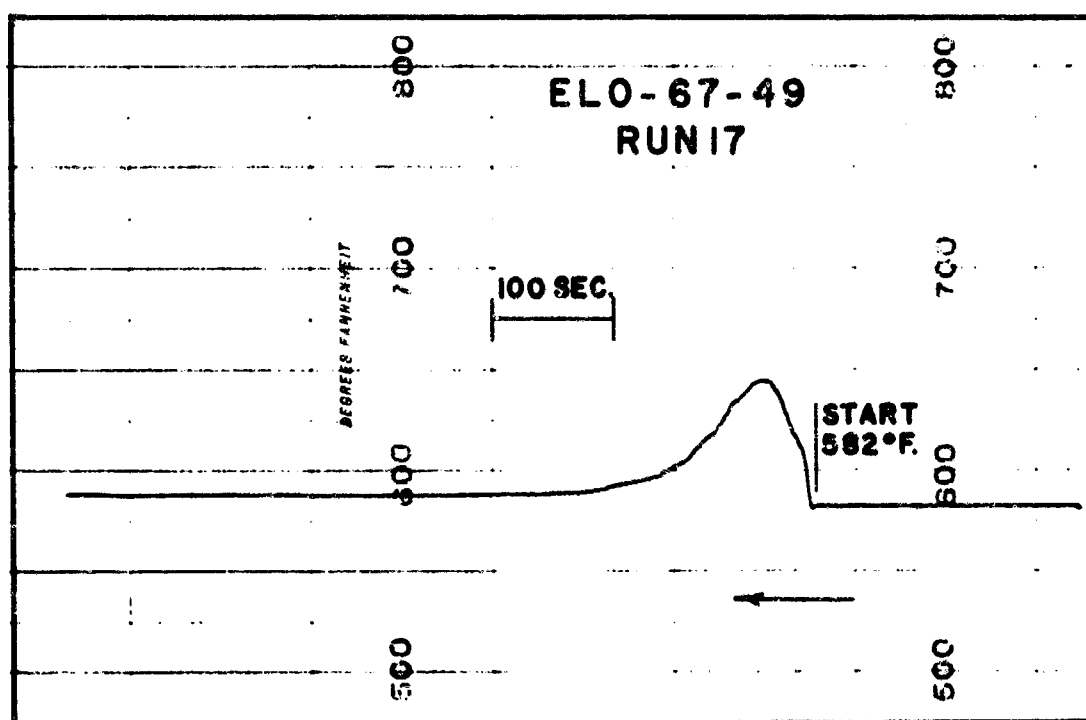


FIGURE 56. ELO-67-49. SPONTANEOUS IGNITION TEMPERATURE. RUN 17.

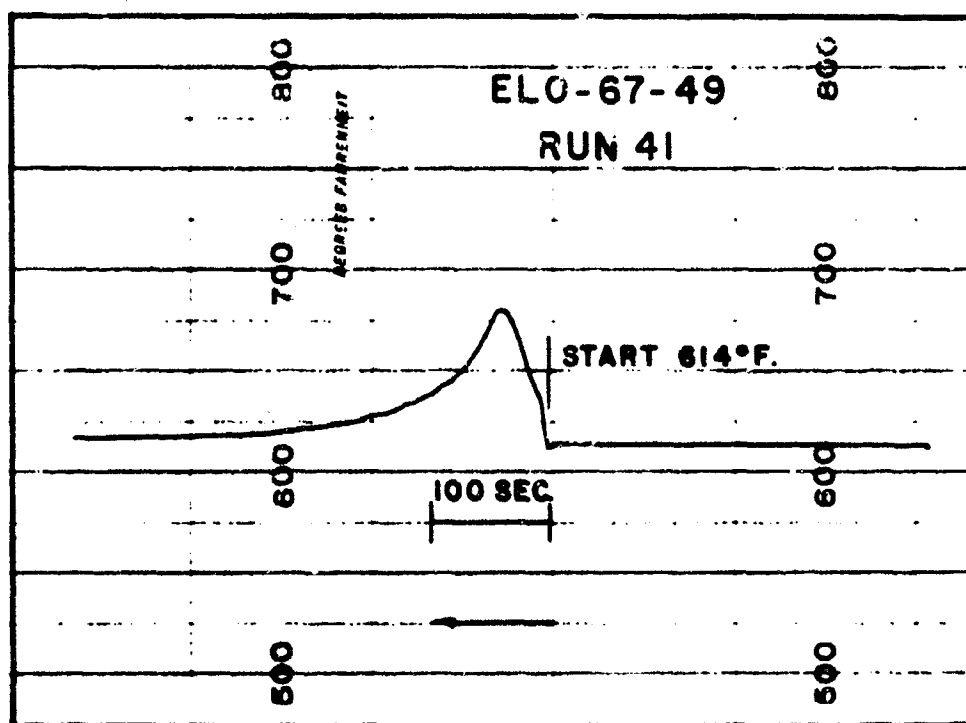


FIGURE 57. ELO-67-49. SPONTANEOUS IGNITION TEMPERATURE. RUN 41.

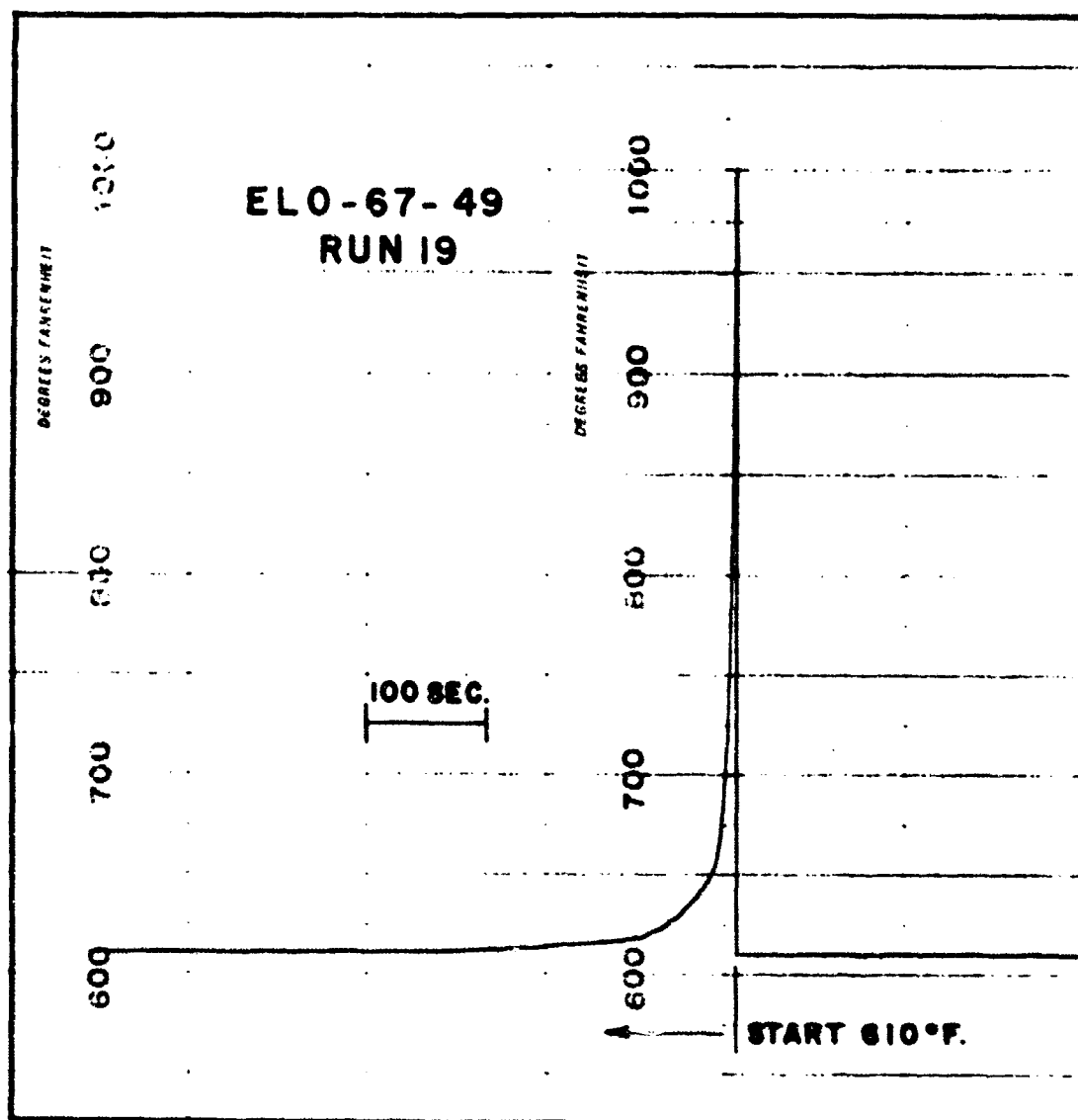


FIGURE 58. ELO-67-45. SPONTANEOUS IGNITION TEMPERATURE. RUN 19.

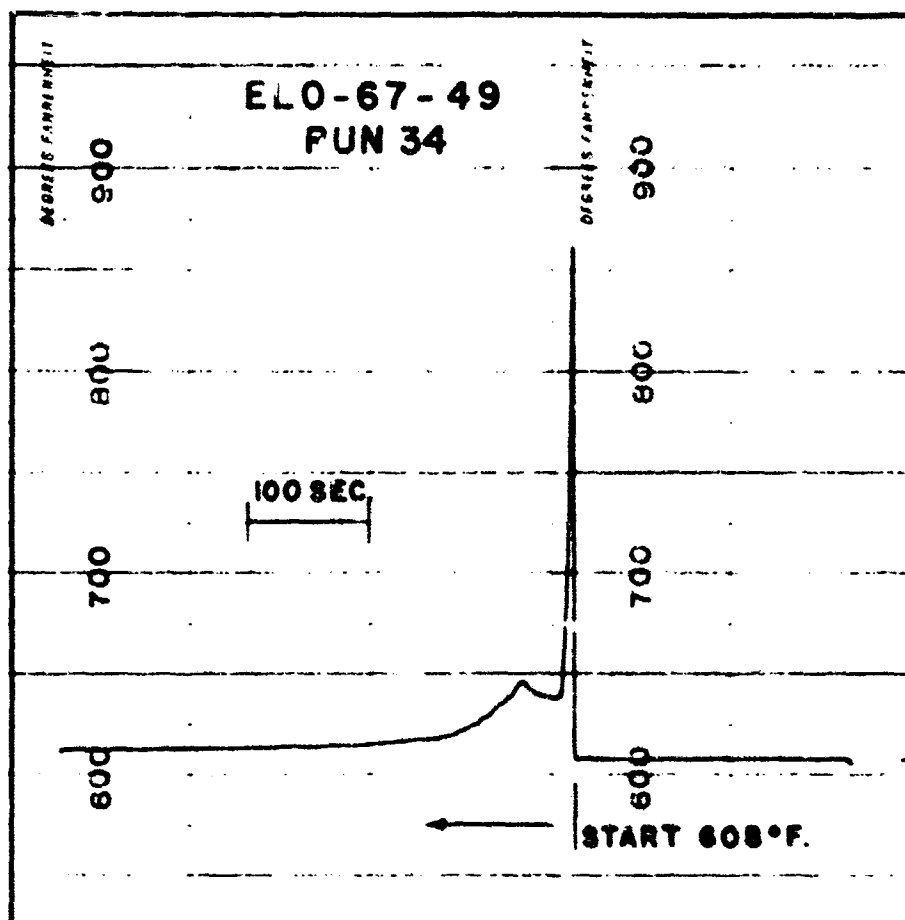


FIGURE 59. ELO-67-49. SPONTANEOUS IGNITION TEMPERATURE. RUN 34.

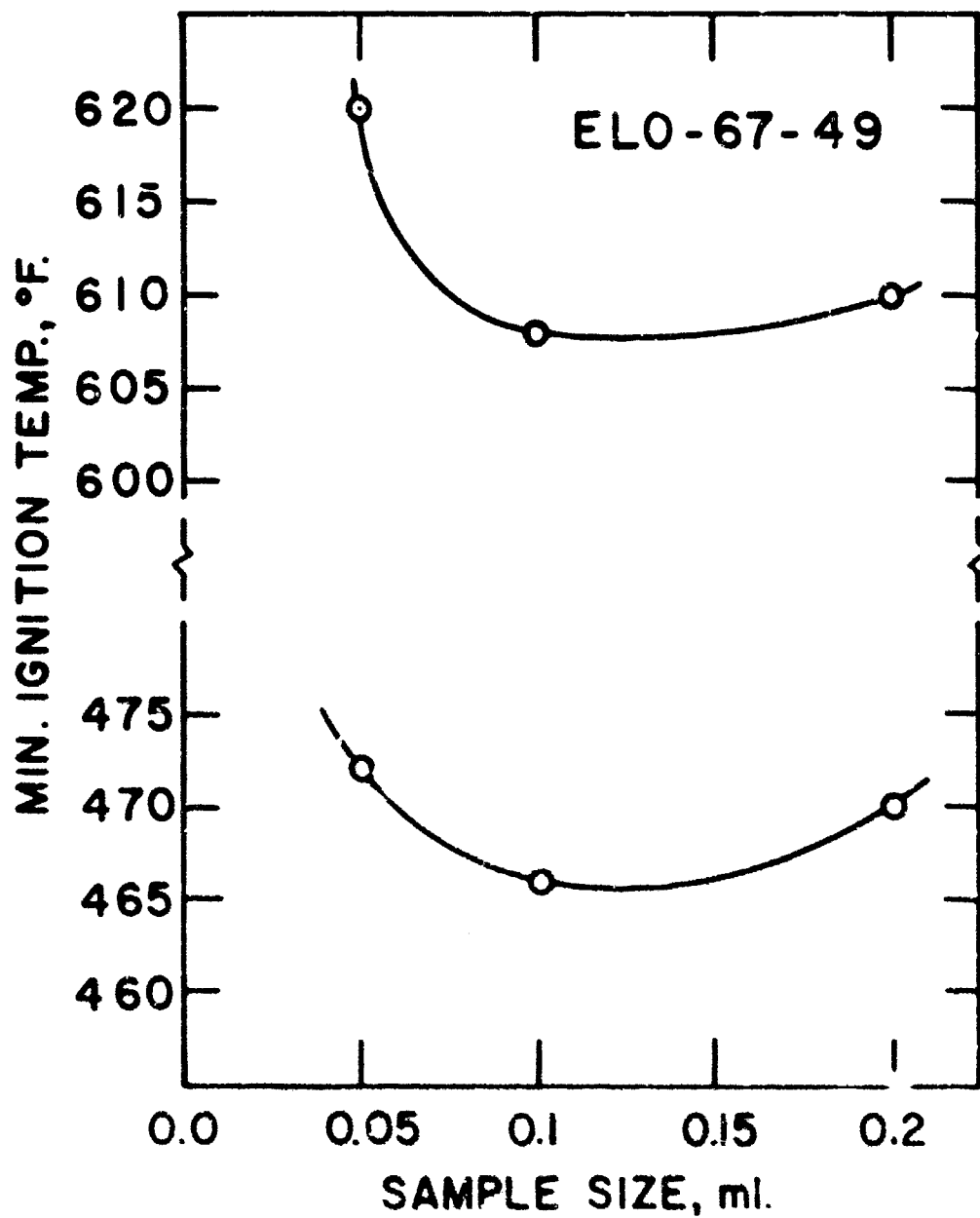


FIGURE 60. ELO-67-49. MINIMUM SPONTANEOUS IGNITION TEMPERATURE.

1.3.8 ELO-67-55. See Table VIII and Figures 61 through 67.

Experiments made with sample sizes of 0.1, 0.2, 0.5 and 1.0 ml. in a 1000 ml. combustion chamber indicate the ignition of sample ELO-67-55 proceeds directly from the pre-ignition stage to hot-flames. No cool-flame ignitions were observed in any instance. Both pre-ignition and hot-flame reactions were found to be typical. No complications were observed. Runs 7, 31 and 42, Figures 61, 62 and 63, are illustrative of the pre-ignition reactions. Runs 11, 36 and 47, Figures 64, 65 and 66, are examples of the hot-flame ignitions.

The minimum spontaneous ignition temperature of the sample, (SIT)_s, was found to be 730 deg. F. See Figure 67. The reaction threshold for the 0.2 ml. sample series was 520 deg. F.

1.4 Summary:

The results of the evaluations of the spontaneous ignition properties of the eight samples studied in the current reporting period are summarized in Table IX. The minimum spontaneous ignition temperatures found varied from 455° to 1005 deg. F. Hot-flame reactions were observed in every case. The reaction thresholds ranged from 415° to 833 deg. F.

2. DIFFERENTIAL THERMAL ANALYSIS

2.1 Introduction:

The use of differential thermal analysis (DTA) for the investigation of the processes involved in the thermal and oxidative degradation of organic fluid systems including experimental lubricants and hydraulic fluid systems has been discussed previously. (References 1, 2, 3, 4, 5). The effects of metallic and non metallic catalysts on the decomposition of such systems have also been described (References 4, 5). In the present work the effects of several metal oxide catalysts on the decomposition of two samples have been studied in both nitrogen and air atmospheres. In addition, the thermal and oxidative degradation of six other samples have been investigated.

TABLE VIII

SAMPLE NUMBER ELO-57-55

SPONTANEOUS IGNITION TEMPERATURE

Needle A

1000 ml. chamber - Iron-Constantan ThermocoupleTYPE OF REACTION

Run	Sample Size, ml.	Initial Temp., deg. F.	Max. Rise, deg. F.	Pre-Ignition	Cool Flame	Hot Flame	Delay, Sec.	Observations
1	1.0	727	5	X				
2		732	170			X	95	Orange flame, explosion
3		740	175			X	81	Orange flame, explosion
4	0.5	730	0	X				
5		730	0	X				
6		730	120			X	115	Orange flame, explosion
7		733	14	X				
8		740	105			X	59	Orange flame, explosion
9		740	100			X	56	Orange flame, explosion
10		771	127			X	37	Orange flame, explosion
11		750	100			X	27	Orange flame, explosion
12	0.2	650	0	X				
13		650	0	X				
14		7	0	X				
15		600	0	X				
16		610	0	X				
17		620	1	X				
18		637	0	X				
19		641	0	X				
20		670	1	X				
21		680	1	X				
22		680	1	X				
23		681	0	X				
24		680	1	X				
25		680	0	X				

TABLE VIII-CONTINUED

SAMPLE NUMBER ELO-57-55

SPONTANEOUS IGNITION TEMPERATURE

Needle A

1000 ml. chamber - Iron-Constant n Thermocouple

TYPE OF REACTION

Run	Sample Size, ml.	Initial Temp., deg. F.	Max. Rise, deg. F.	Pre-Ignition	Cool Flame	Hot Flame	Delay, Sec.	Observations
26	0.2	673	2	X				
27		690	1	X				
28		700	4	X				
29		705	13	X				
30		717	5	X				
31		735	14	X				
32		749	11	X				
33		755	200			X	80	Orange flame, explosion
34		756	*			X	*	Orange flame, explosion
35		756	*			X	*	Orange flame, explosion
36		763	307			X	45	
37	1.1	735	1	X				
38		757	10	X				
39		759		X				
40		760		X				
41		765		X				
42		770		X				
43		782	3	X				
44		783	2	X				
45		785	5	X				
46		786	130			X	13	Orange flame, explosion
47		787	125			X	13	Orange flame, explosion

* Sample temperature and delay could not be determined because recorder pen stopped writing.

TABLE IX

SPONTANEOUS IGNITION SUMMARY

<u>SAMPLE NUMBER</u>	<u>REACTION THRESHOLD, DEG. F.</u>	<u>MINIMUM SPONTANEOUS IGNITION TEMPERATURE (SIT)_s, DEG. F. 1000 ml. chamber</u>
MLQ-64-4	423	670
MLQ-64-5	421	455
ELO-66-51	833	1002
ELO-66-109	451	650
ELO-67-16	413	650
ELO-67-23	420	471
ELO-67-40	415	465, 548
ELO-67-45	500	773

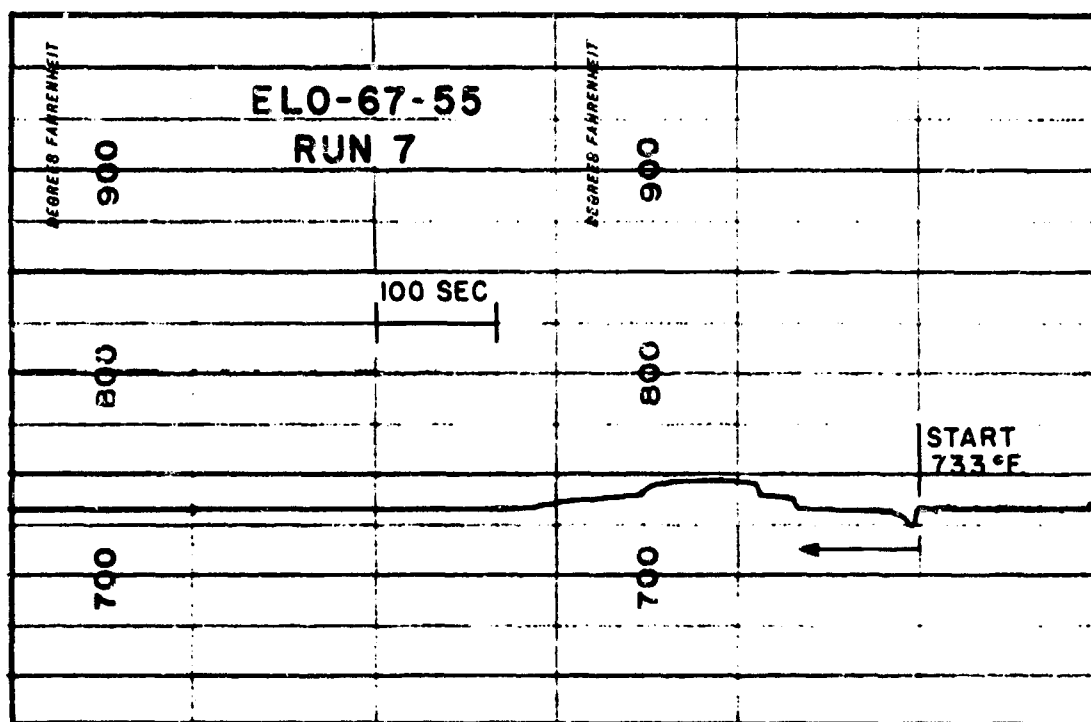


FIGURE 61. ELO-67-55. SPONTANEOUS IGNITION TEMPERATURE. RUN 7.

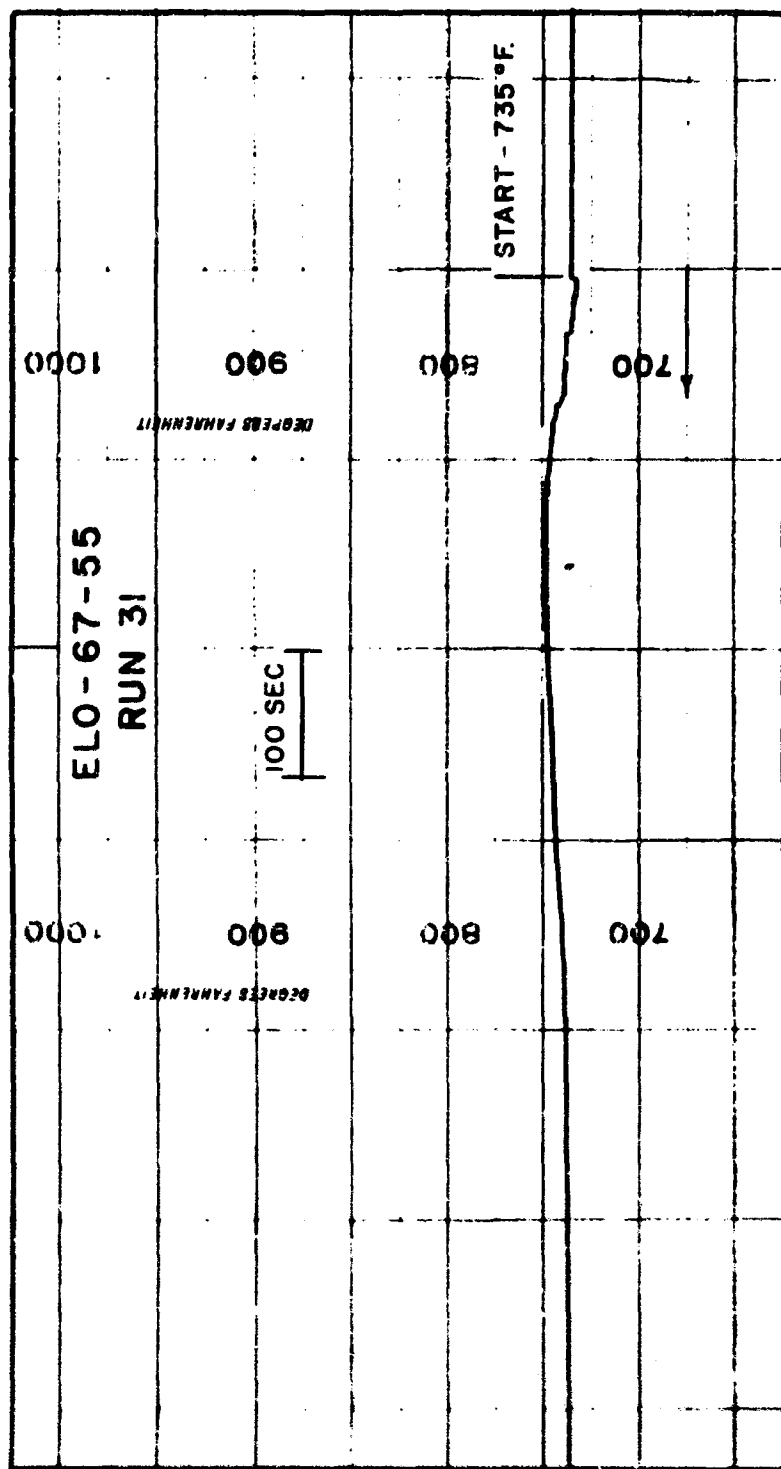


FIGURE 62. ELO-67-55. SPONTANEOUS IGNITION TEMPERATURE. RUN 31.

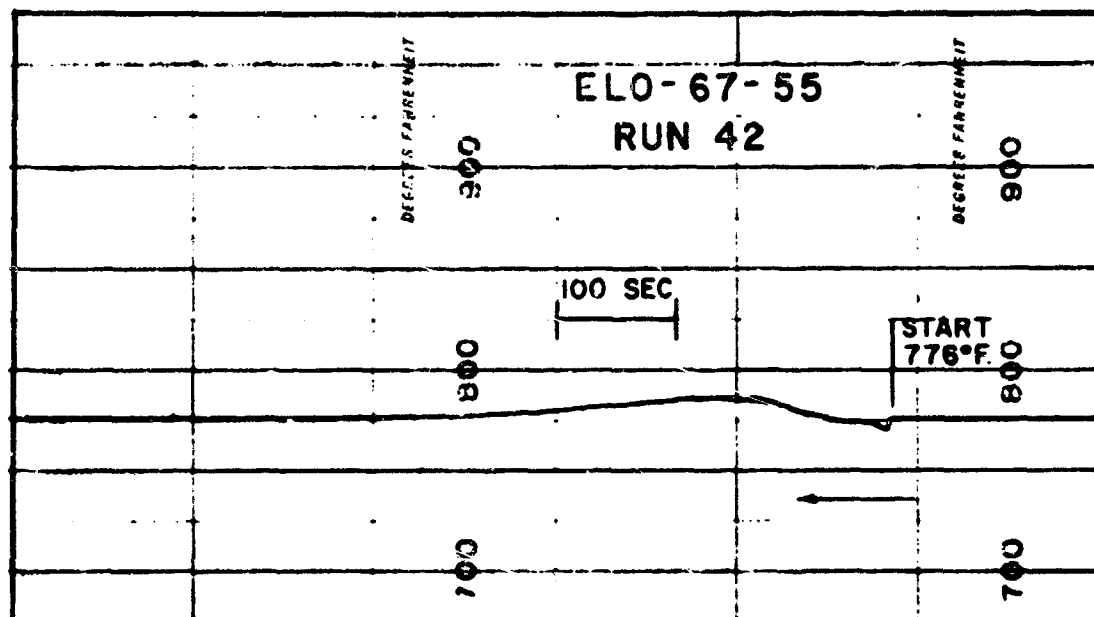


FIGURE 63. ELO-67-55. SPONTANEOUS IGNITION TEMPERATURE. RUN 42.

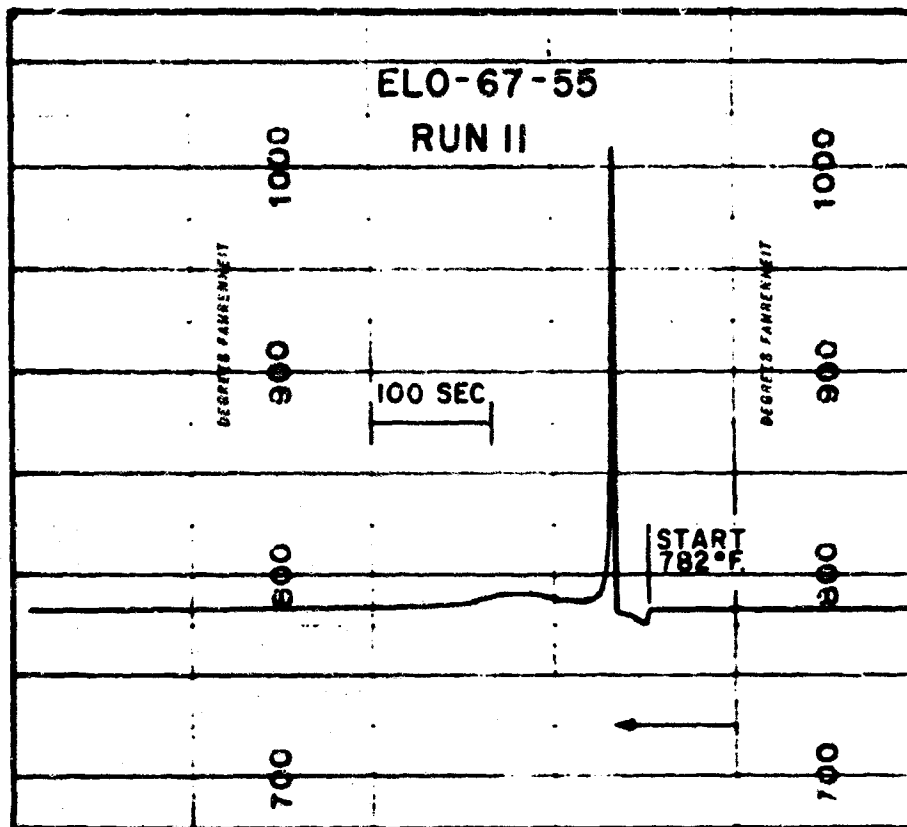


FIGURE 64. ELO-67-55. SPONTANEOUS IGNITION TEMPERATURE. RUN II.

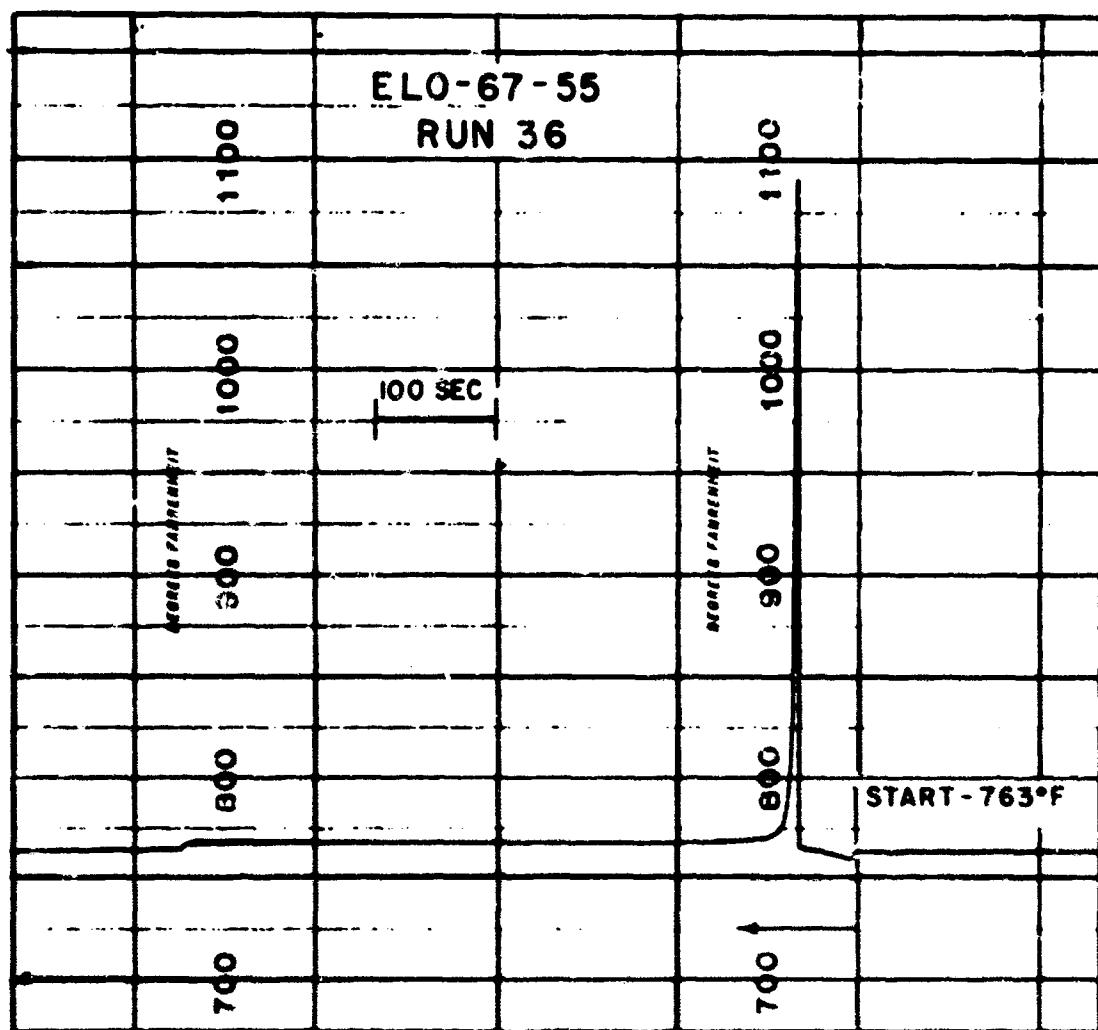


FIGURE 65. ELO-67-55. SPONTANEOUS IGNITION TEMPERATURE. RUN 36.

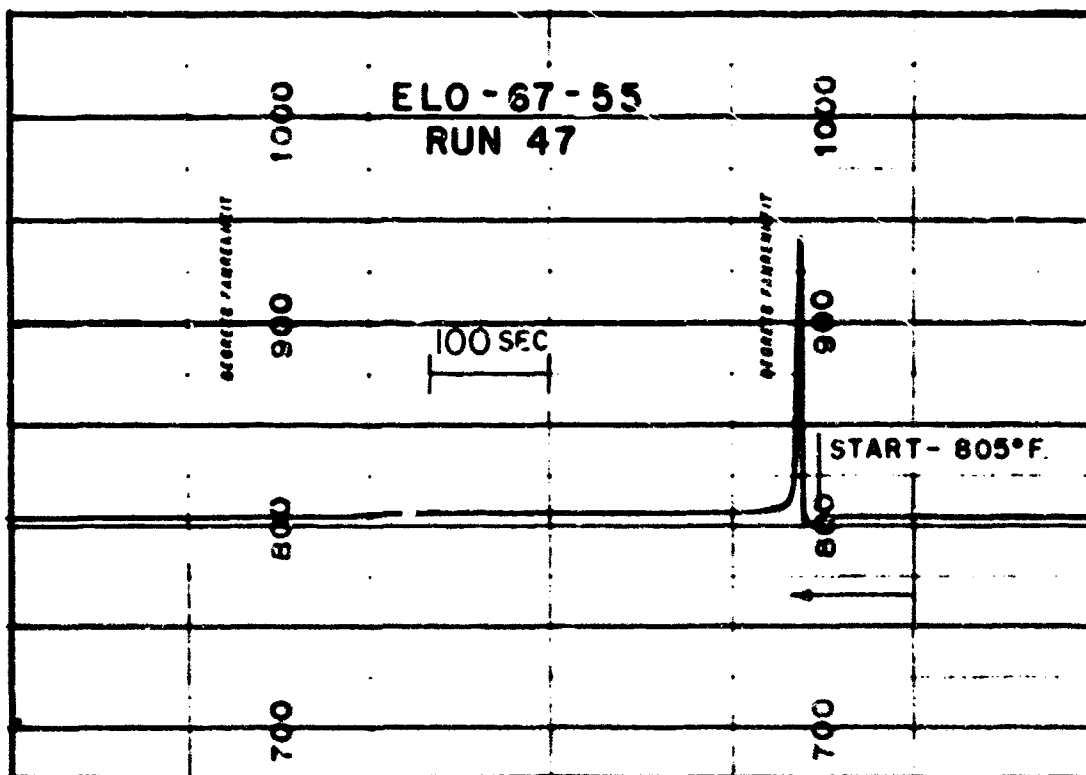


FIGURE 66. ELO-67-55. SPONTANEOUS IGNITION TEMPERATURE. RUN 47.

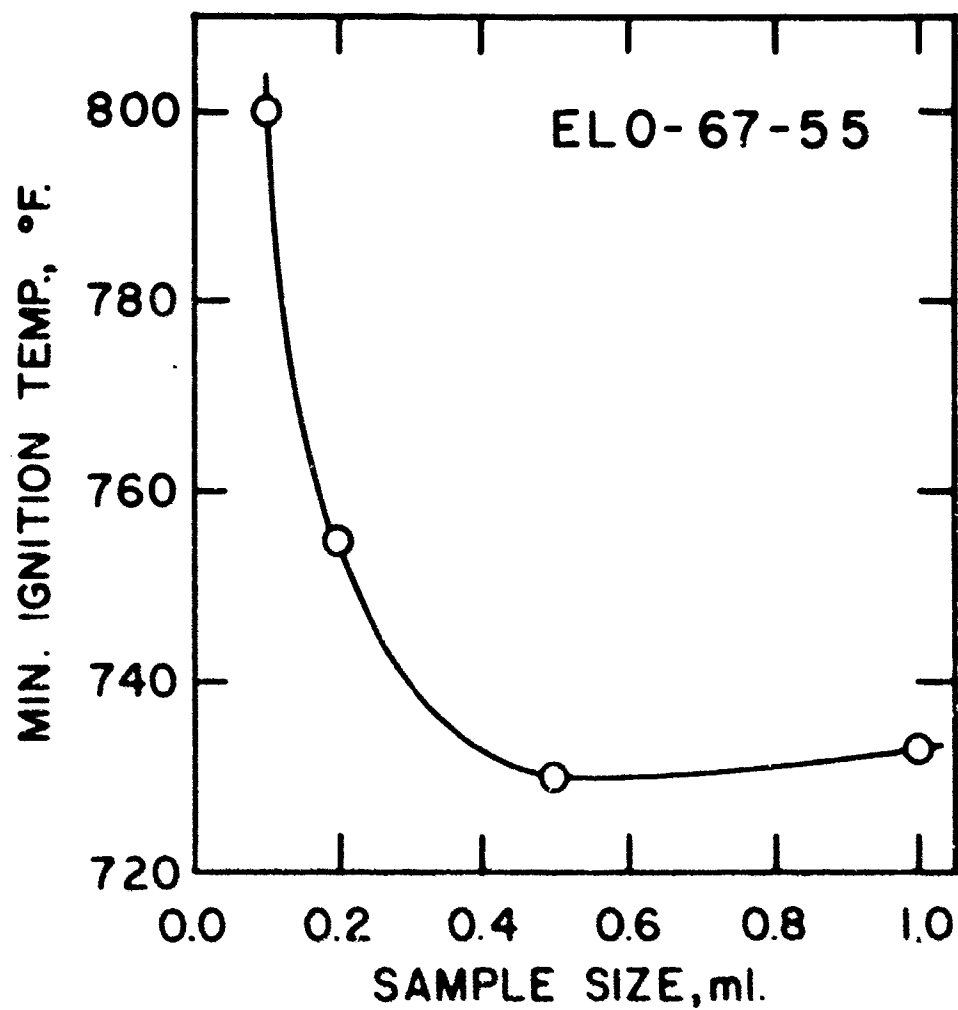


FIGURE 67. ELO-67-55. MINIMUM SPONTANEOUS IGNITION TEMPERATURE.

2.2 Apparatus and Procedure:

The apparatus and procedures used in these studies are the same as those which have been described in detail in the previous reports in this series. (References 1, 2, 3, 4, 5). The matched thermocouple assemblies and temperature programming system are those illustrated in Reference 4.

Borosilicate glass microbeads (170-230 mesh) have been used as the DTA reference standard. The microbeads have, in addition, been added to the sample side of the DTA cell in order to equalize the heat capacities and the thermal conductivities of the sample and reference sides. Instrumental blanks which illustrate the net thermal balance of the several different measuring thermocouples and the DTA system itself are shown in Figures 68, 69, 70, 71, 72 and 95. For measurements in which catalytic agents have been used DTA reference blanks of mixtures containing 10% by weight of each catalyst with borosilicate glass microbeads have also been run. (cf. Figures 73, 74, 83 and 84 which appear in Sections 2.3.1.1 and 2.3.1.4) Similar mixtures of 10% catalyst with microbeads have been added to various samples to study the effects of the catalysts on the degradation of the samples.

The data obtained in these studies are described and interpreted in the following text. A comment is required with regard to those experiments which involve potential catalysis. Many effects which have been attributed to the action of added substances have been categorized under the generic term "catalysis". True catalysis may or may not be involved. For example, it may be that in some cases an effect may be the result of a corrosion-like process leading to the formation of complex or higher oxides from the simple oxides initially employed. DTA alone does not distinguish between such reactions and purely catalytic interactions in the accepted sense of the word.

In the thermograms presented on the following pages the ordinate represents temperature difference in microvolts as measured by iron-constantan thermocouples. An arrow in the key to each thermogram indicates the endothermic direction of each ordinate. The length of the arrows supplies the voltage scale to be applied to the ordinate. In order to

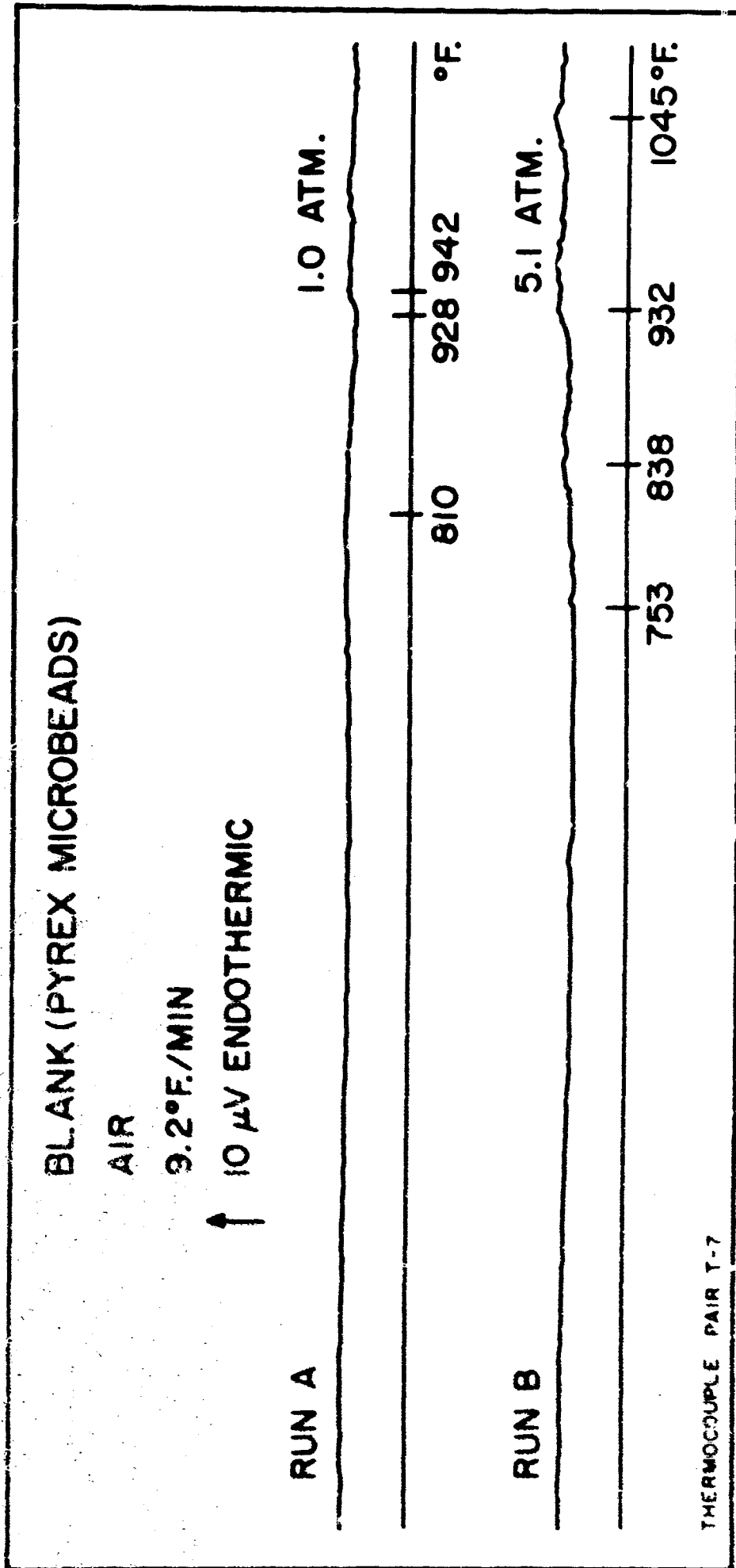


FIGURE 68. DIFFERENTIAL THERMAL ANALYSIS. BLANK (PYREX MICROBEADS). THERMOCOUPLE PAIR T-7.

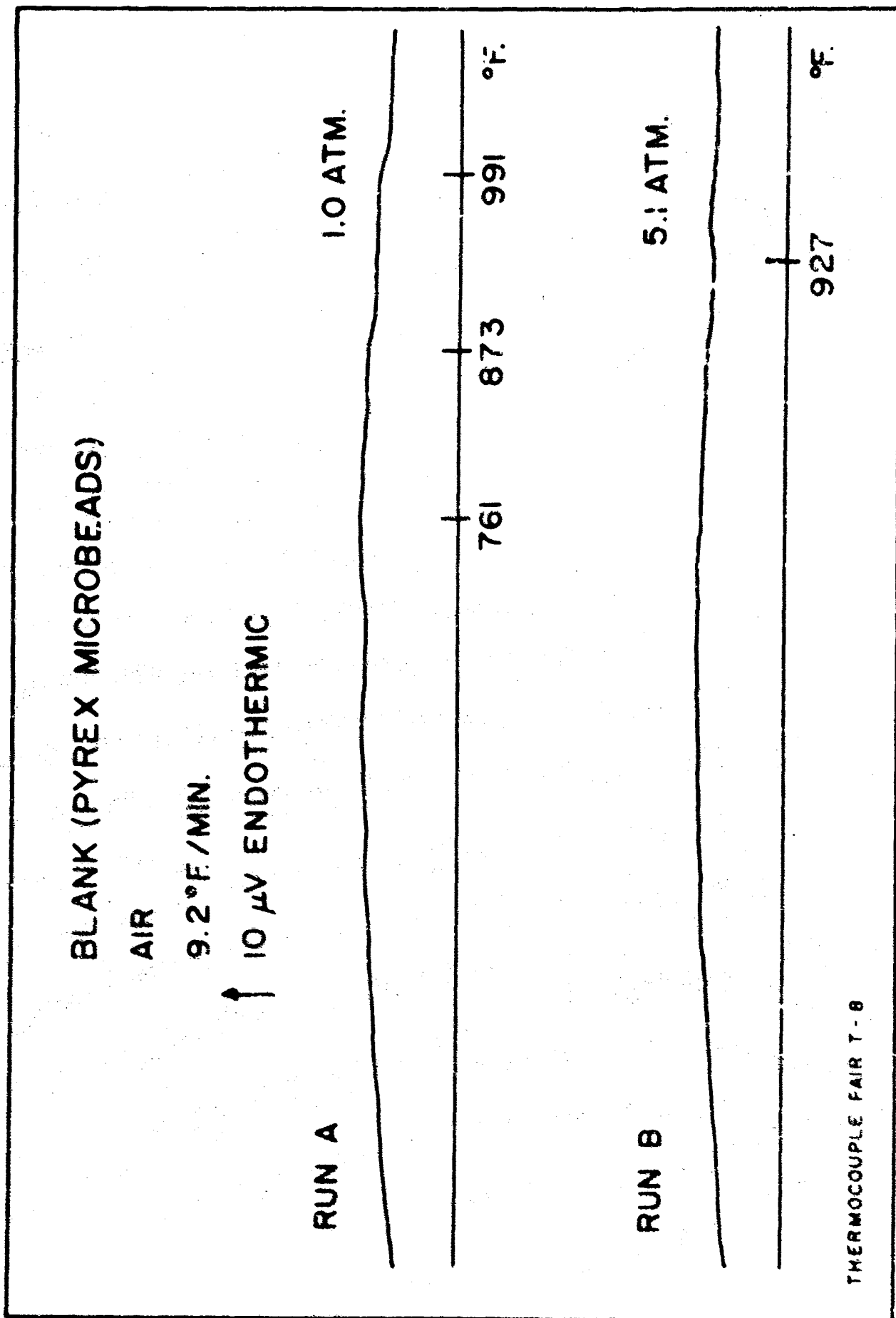


FIGURE 69. DIFFERENTIAL THERMAL ANALYSIS. BLANK (PYREX MICROBEADS). AIR ATMOSPHERE.

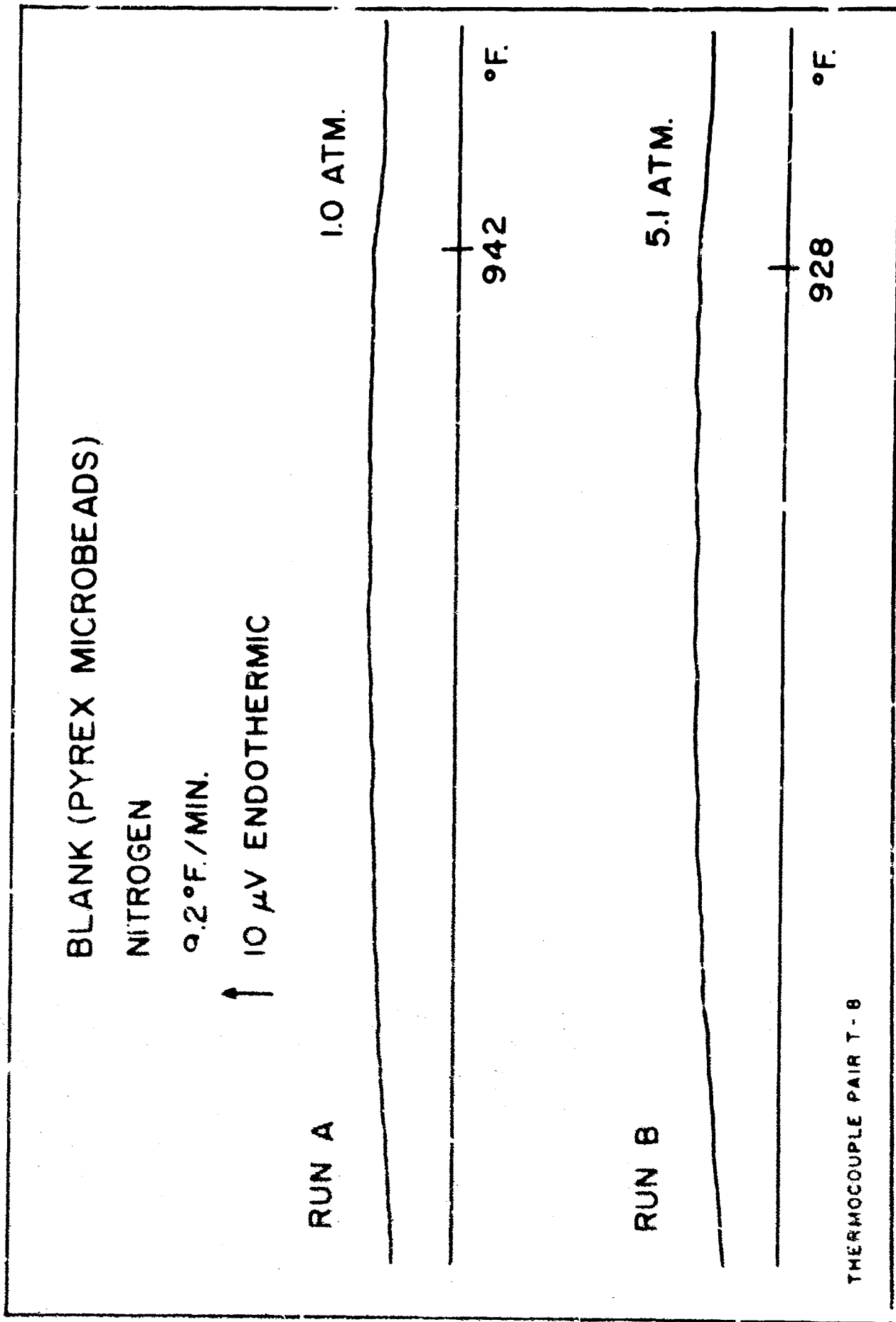


FIGURE 70. DIFFERENTIAL THERMAL ANALYSIS. BLANK (PYREX MICROBEADS). NITROGEN ATMOSPHERE.

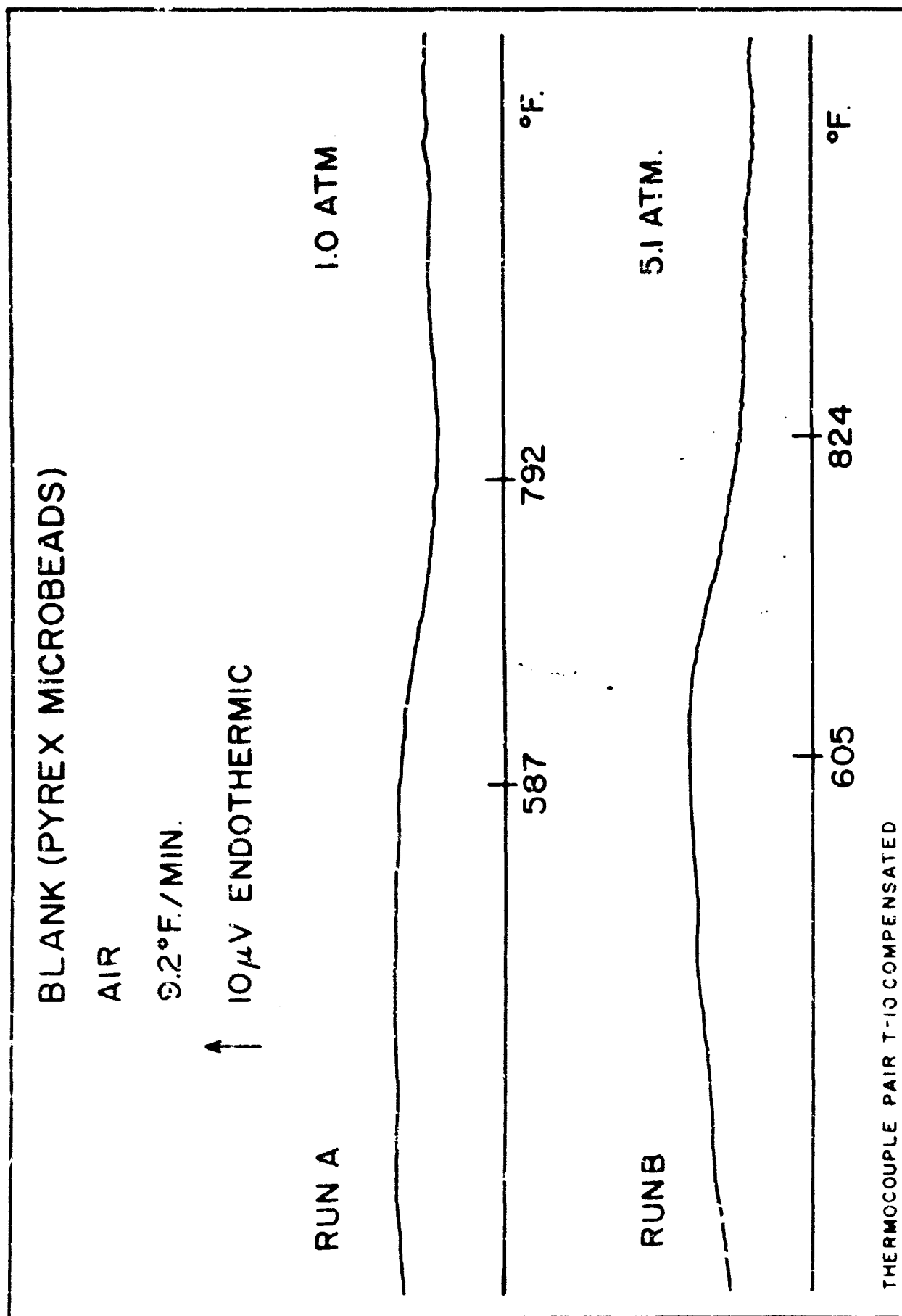


FIGURE 71. DIFFERENTIAL THERMAL ANALYSIS. BLANK (PYREX MICROBEADS). THERMOCOUPLE PAIR T-10 COMPENSATED.

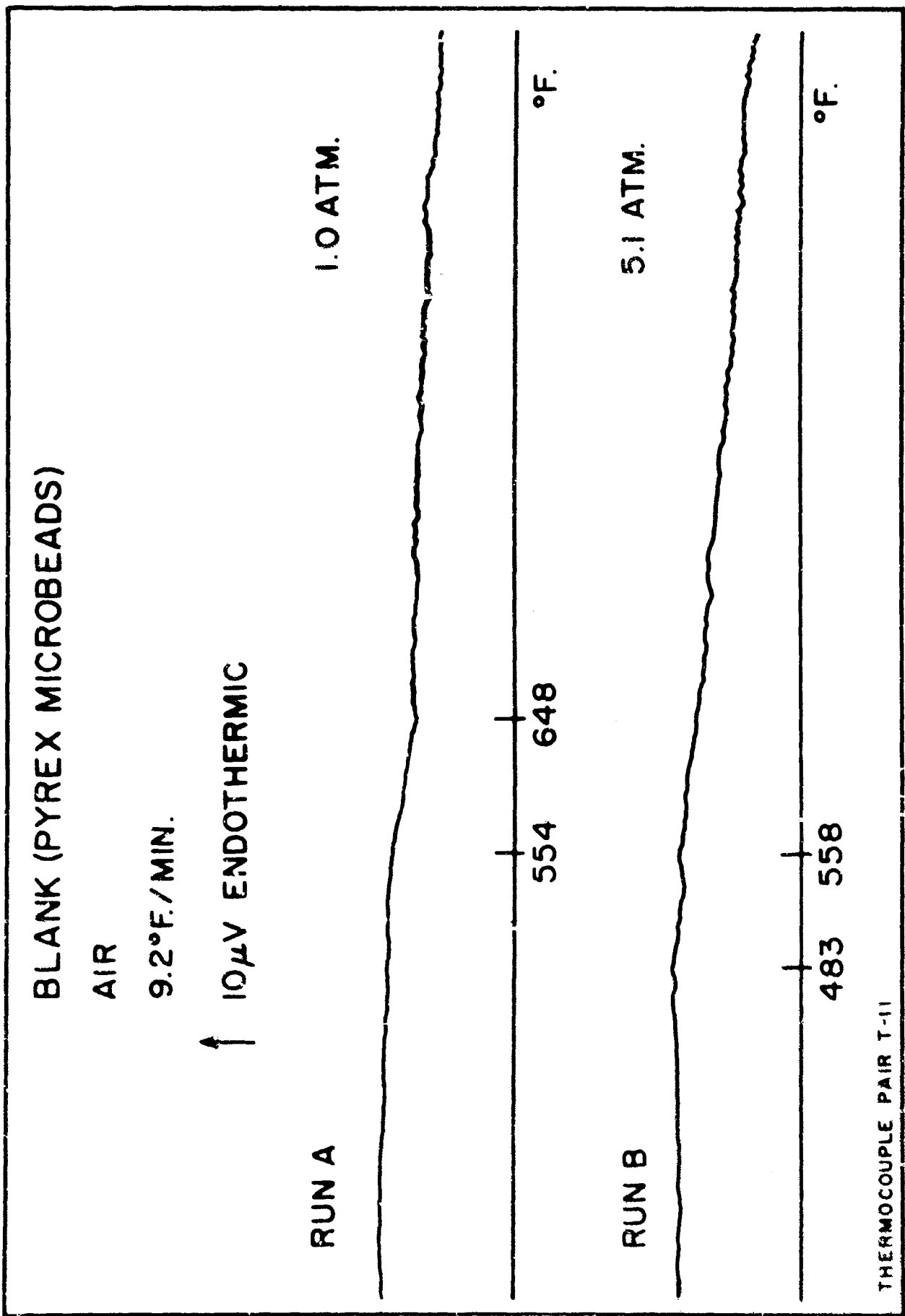


FIGURE 72. DIFFERENTIAL THERMAL ANALYSIS. BLANK (PYREX MICROBEADS). THERMOCOUPLE PAIR T-11.

convert temperature differences measured in microvolts to degrees Fahrenheit it is necessary to consult the appropriate conversion tables. No constant factor can be used since the voltage response of the thermocouples is not the same at various temperatures but varies from point to point over the range of temperatures encountered during a DTA run. Temperature measured in degrees Fahrenheit is recorded on the abscissa. The scale is nearly linear. Small departures from linearity may occur from time to time. These reflect the fact that, in some instances, the temperature of the interior of the DTA cell does not always track exactly the linear program called for by the temperature programming control system.

In the lower left-hand corner of each thermogram may be found a notation which identifies the thermocouple-pair used for the measurements displayed thereon. Where applicable the use of baseline compensation is also noted in the same location. Comparison of sample thermograms to the appropriate instrumental and reference blanks is thus facilitated.

2.3 Experimental Data:

2.3.1 Thermal and Oxidative degradation in the presence of metal oxide catalysts.

The application of DTA to the study of lubricant systems in the presence of various metal catalysts has been discussed in detail in an earlier report (Reference 5). In that work DTA was employed for the investigation of the thermal decomposition and oxidation of two samples, MLC-64-8 and ELO-65-48, in the presence of fifteen different metals and several types of activated and unactivated carbon and molecular sieve. The effects due to the presence of these various substances were clearly demonstrated by DTA. Several of these materials, notably the activated carbons, were found to exert profound catalytic influences upon the degradation of the samples.

In the course of the preceeding experiments it was noted that some of the metals did not behave as expected under DTA in the presence of the samples. Of particular importance were the findings that copper was inactive in the presence of ELO-65-48 and that titanium had little influence on the decomposition of MLC-64-8 in air. Since these findings

were somewhat at odds with data obtained from oxidation and corrosion testing (Reference 6), it was felt that additional studies were needed to elucidate the roles played by these metals in the thermal and oxidative degradation of the two lubricant systems. In the earlier studies the metals used for catalysts were all reagent grade powders. Since in practice such powders are often coated with a layer of their oxides, it was decided to determine whether the various metal oxides might be more active with respect to the samples than the pure metals themselves. In the present study thermograms of mixtures of MLO-64-8 and of ELO-65-48 with oxides of iron, titanium and copper have been run and the results compared with those previously obtained for mixtures with the corresponding pure metals. Reagent grade oxides have been used for all determinations. In the case of cuprous oxide a stabilizer is customarily present even in the reagent grade chemical to prevent oxidation to the cupric oxide. This agent was removed prior to the use of cuprous oxide in these studies.

2.3.1.1 Blank. Pyrex Microbeads plus Metal Oxide Catalysts.

Nitrogen Atmosphere. Thermocouple Pair T-7.

9.2°F./Min. Scan Rate. See Figures 73 and 74.

Thermograms run for mixtures of pyrex microbeads plus iron, titanium and copper oxides were found to contain no important features not contained in blank runs made for the thermocouple pair used.

2.3.1.2 MLO-64-8. Pyrex Microbeads plus Metal Oxide Catalysts.

Nitrogen Atmosphere. Thermocouple Pair T-7.

9.2°F./Min. Scan Rate. See Figures 75, 76, 77 and 78 and Table X.

The run made with pure iron catalyst indicated a moderate degree of activity of iron with respect to the sample. The thermogram displays only a relatively small amount of exothermic reactivity above and beyond that seen in the thermogram of the pure sample. In comparison the thermogram run for iron oxide is completely different. The familiar twin decomposition peaks of the pure sample are no longer present and in their place is a single large exotherm occurring at a much lower temperature. A similar phenomenon is observed in the thermograms of mixtures of the sample with cuprous oxide and pure copper. Cupric oxide, on the other hand, appears to be essentially

BLANK (PYREX MICROBEADS + Fe_2O_3 & TiO_2)

NITROGEN

9.2°F./MIN

↑ 10 μV ENDOTHERMIC 5.1 ATM.

Fe_2O_3



TiO_2



T-7

FIGURE 73. DIFFERENTIAL THERMAL ANALYSIS. BLANK (PYREX MICROBEADS PLUS IRON OXIDE AND TITANIUM DIOXIDE IN NITROGEN).

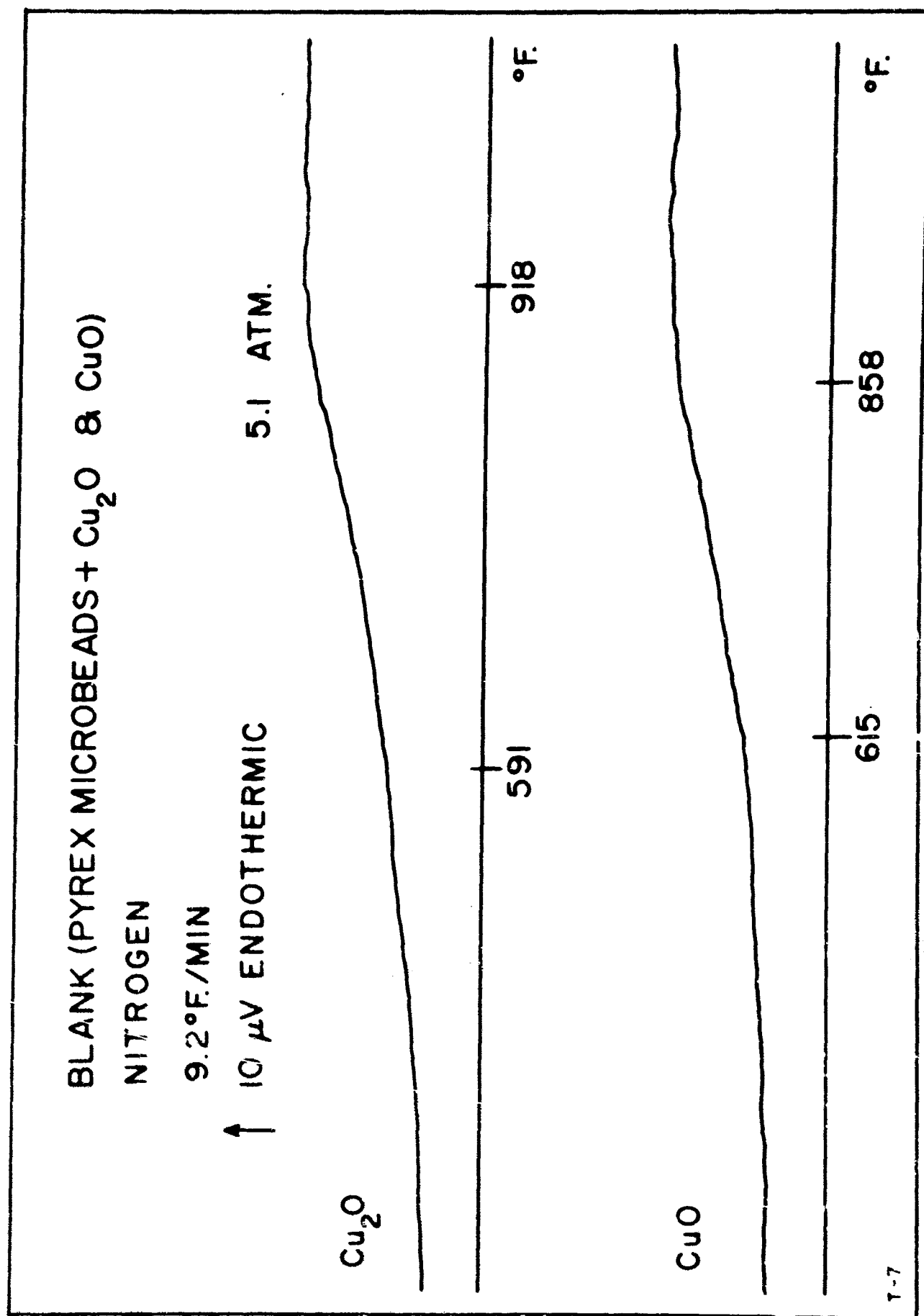


FIGURE 74. DIFFERENTIAL THERMAL ANALYSIS. BLANK (PYREX MICROBEADS PLUS CUPROUS OXIDE AND CUPRIC OXIDE IN NITROGEN).

TABLE X

DIFFERENTIAL THERMAL ANALYSIS: MLO-64-8 PLUS
METAL OXIDE CATALYSTS IN NITROGEN ATMOSPHERE
(5.1 ATM. TOTAL PRESSURE)

CATALYST	FIGURE	ENDOTHERMS, DEG. F.*		EXOTHERMS, DEG. F.*		
No Catalyst	75			917	964!	995!
Iron Oxide (Fe ₂ O ₃)	76		800	938!!	958	
Iron	78		808	923	968!	990!
Titanium Dioxide (TiO ₂)	76		864!	925!	968!!	
Titanium	78	595	(810)	893	965!	993! 1014!
Cuprous Oxide (Cu ₂ O)	77		800	857	955!!	
Cupric Oxide (CuO)	77				964!	984!
Copper	78			894	967!	997!

Those thermal effects which may be attributed solely to the reactions of the catalysts have not been included in this tabulation.

Key to symbols:

- () weak thermal effect
! strong thermal effect
!! very strong thermal effect

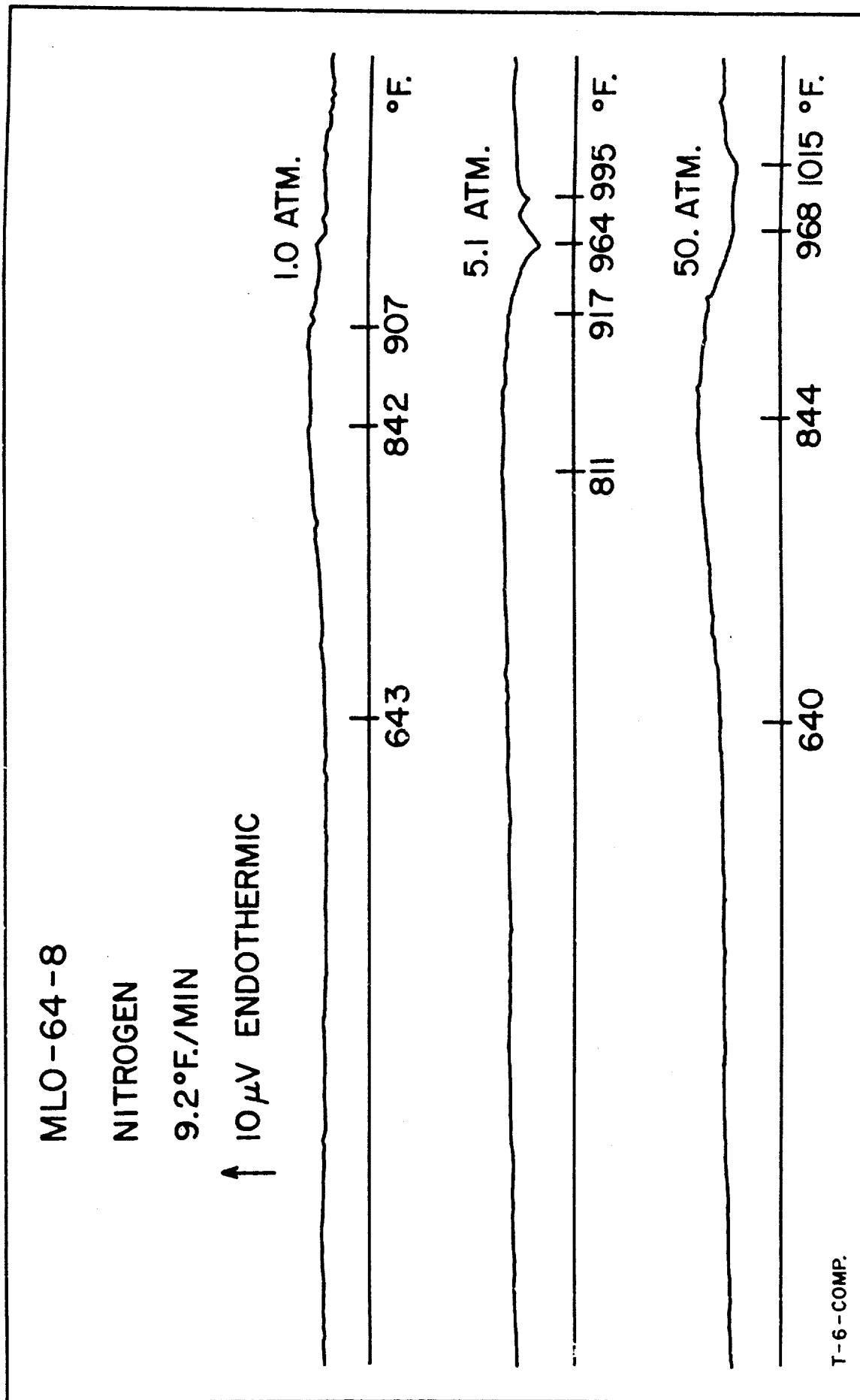


FIGURE 75. DIFFERENTIAL THERMAL ANALYSIS: MLO-64-8.

MLO 64-8 + Fe_2O_3 & TiO_2 CATALYST

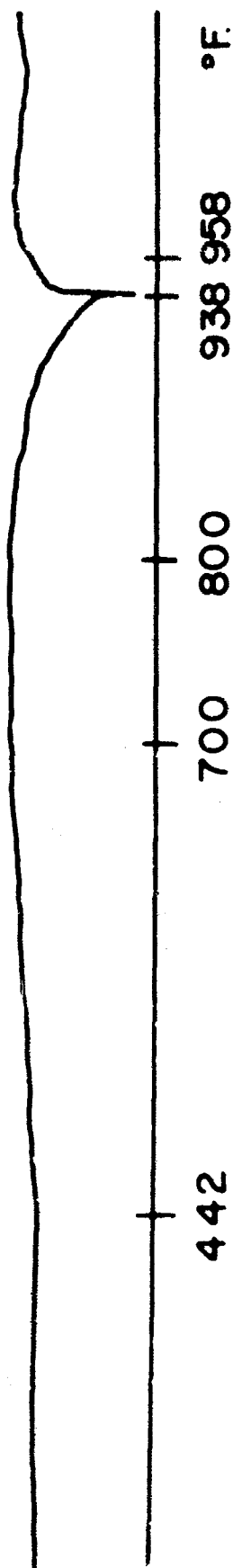
NITROGEN

9.2 °F/MIN

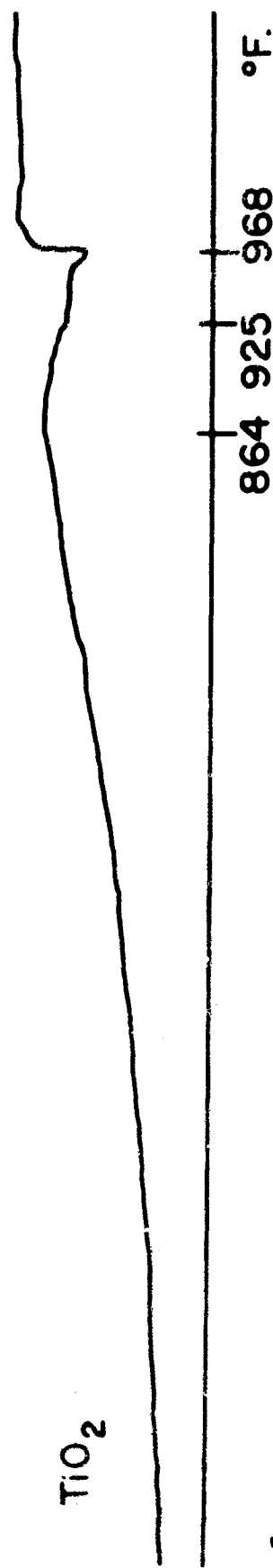
5.1 ATM.

↑ 10 μV ENDOTHERMIC

Fe_2O_3



TiO_2



T-7

FIGURE 76. DIFFERENTIAL THERMAL ANALYSIS. MLO-64-8 PLUS IRON OXIDE AND TITANIUM DIOXIDE IN NITROGEN.

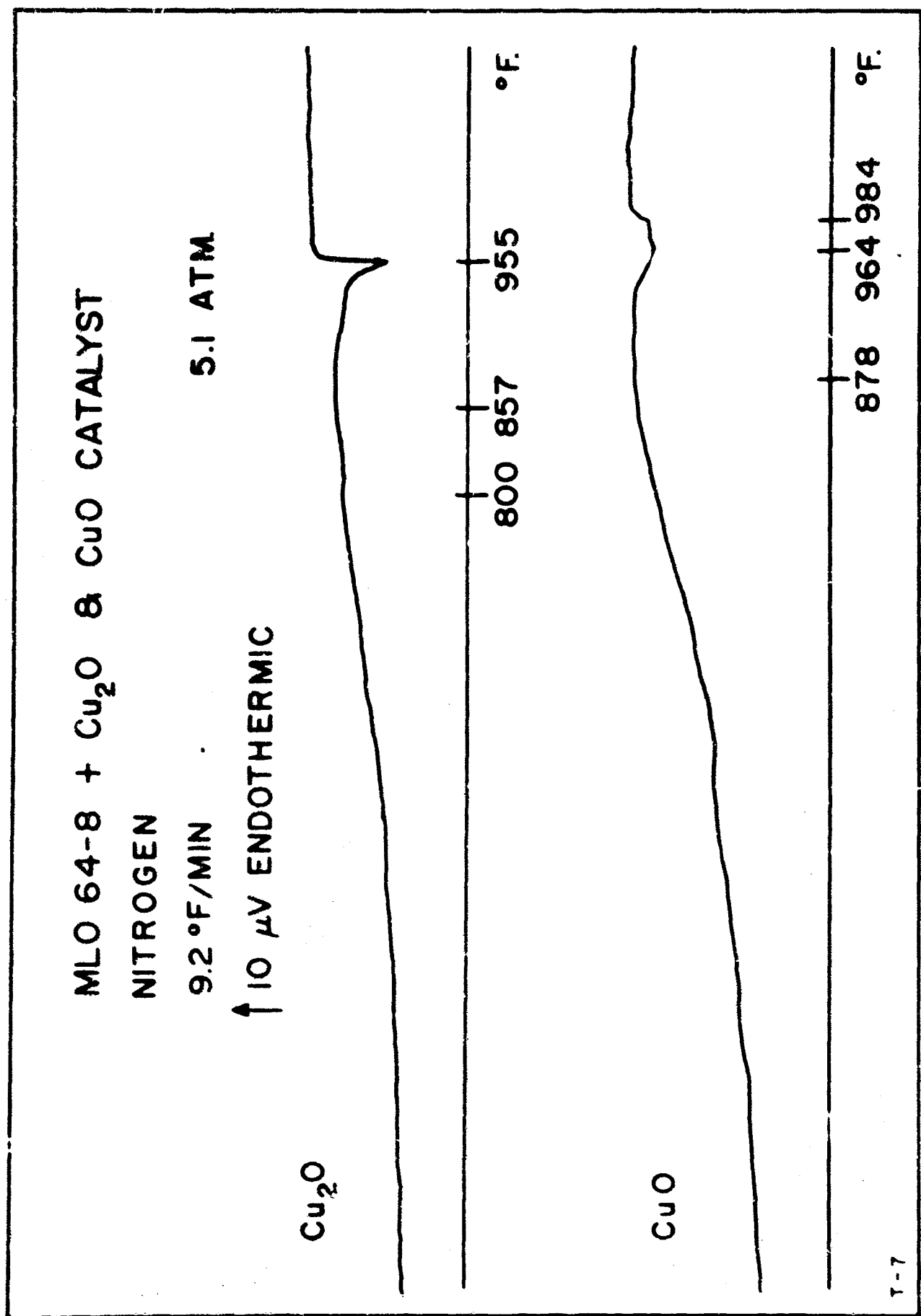


FIGURE 77. DIFFERENTIAL THERMAL ANALYSIS. MLO-64-8 PLUS CUPROUS OXIDE AND CUPRIC OXIDE IN NITROGEN.

MLO -64-8 + METAL CATALYSTS

NITROGEN

9.2°F./MIN

↑ 10 μV ENDOTHERMIC

5.1 ATM.

Cu

816 354 967 997 °F.

Ti

595

810 893 965 1014 °F.
993

Fe

808 923 958 990 °F.

T-6-COMP

FIGURE 72. DIFFERENTIAL THERMAL ANALYSIS: MLO-64-8 PLUS
COPPER, TITANIUM AND IRON.

inactive; its mixtures lead to thermograms which are essentially identical with those obtained for the sample alone. Titanium dioxide appears much more active under the nitrogen atmosphere than does metallic titanium itself. The principal effect produced by pure titanium was the enhancement of the decomposition of sample residues left after the initial decomposition. In that case a pair of exothermic peaks at 965 and 993 deg. F. were followed by an extremely intense exotherm at 1014 deg. F. In the case of titanium dioxide a different situation is found. The characteristic pair of exotherms is absent and a single strong exotherm at 968 deg. F. is preceded by a broad thermal decomposition peak which occurs after 864 deg. F.

2.3.1.3 ELO-65-48. Pyrex Microbeads plus Metal Oxide Catalysts.

Nitrogen Atmosphere. Thermocouple Pair T-7.

9.2°F./Min. Scan Rate. See Figures 79, 80, 81 and 82 and Table XI.

The thermogram for pure ELO-65-48 exhibits a strong boiling endotherm with a peak at 852 deg. F. A similar feature appears in the thermograms run with added iron, copper and titanium powders. It occurs at virtually the same temperature in each case. The endotherm in the thermogram for the iron mixture is a single peak like that for the pure sample; those for the copper and titanium mixtures are slightly split at the maximum. Only in the case of titanium is any decomposition evident. There it is seen mainly as a roughness which appears in the thermogram at temperatures above the boiling point of the sample. While the metals themselves seem to have only a small effect on the decomposition of the sample under nitrogen, inspection of Figures 80 and 81 reveals that a different situation prevails with respect to the oxide mixtures. In the presence of iron oxide a pronounced boiling endotherm is present; however, its maximum occurs at a temperature much lower than that of the boiling endotherm for the pure sample. The truncated appearance of the peak suggests that a strong exothermic reaction, presumably decomposition, also occurs at temperatures well below the boiling point. A like phenomenon is seen in the run made for titanium dioxide where the boiling peak has virtually been cancelled by the heat effect due to the simultaneous decomposition. Small boiling endotherms are observed for mixtures with cuprous and cupric oxide. These are displaced toward lower temperatures and reduced in magnitude as a result of decomposition. Cupric oxide seems less active in this regard than iron oxide, cuprous oxide or titanium dioxide.

TABLE XI

DIFFERENTIAL THERMAL ANALYSIS: ELO-65-42 PLUS
METAL OXIDE CATALYSTS IN NITROGEN ATMOSPHERE
(5.1 ATM. TOTAL PRESSURE)

CATALYST	FIGURE	ENDOTHERMS, DEC. F.*		EXOTHERMS, DEC. F.*	
No Catalyst	19	623	852!	(673)	
Iron Oxide (Fe_2O_3)	20		814! 842!		
Iron	20		846!	(722)	
Titanium Dioxide (TiO_2)	21		833 864	775	
Titanium	22	604	838! 843!	756	876
Cuprous Oxide (Cu_2O)	24		(833)		
Cupric Oxide (CuO)	25		840		
Copper	26	(812)	846! 853!	(855)	

* Those thermal effects which may be attributed solely to the reactions of the catalysts have not been included in this tabulation.

Key to symbols:

() weak thermal effect

! strong thermal effect

!! very strong thermal effect

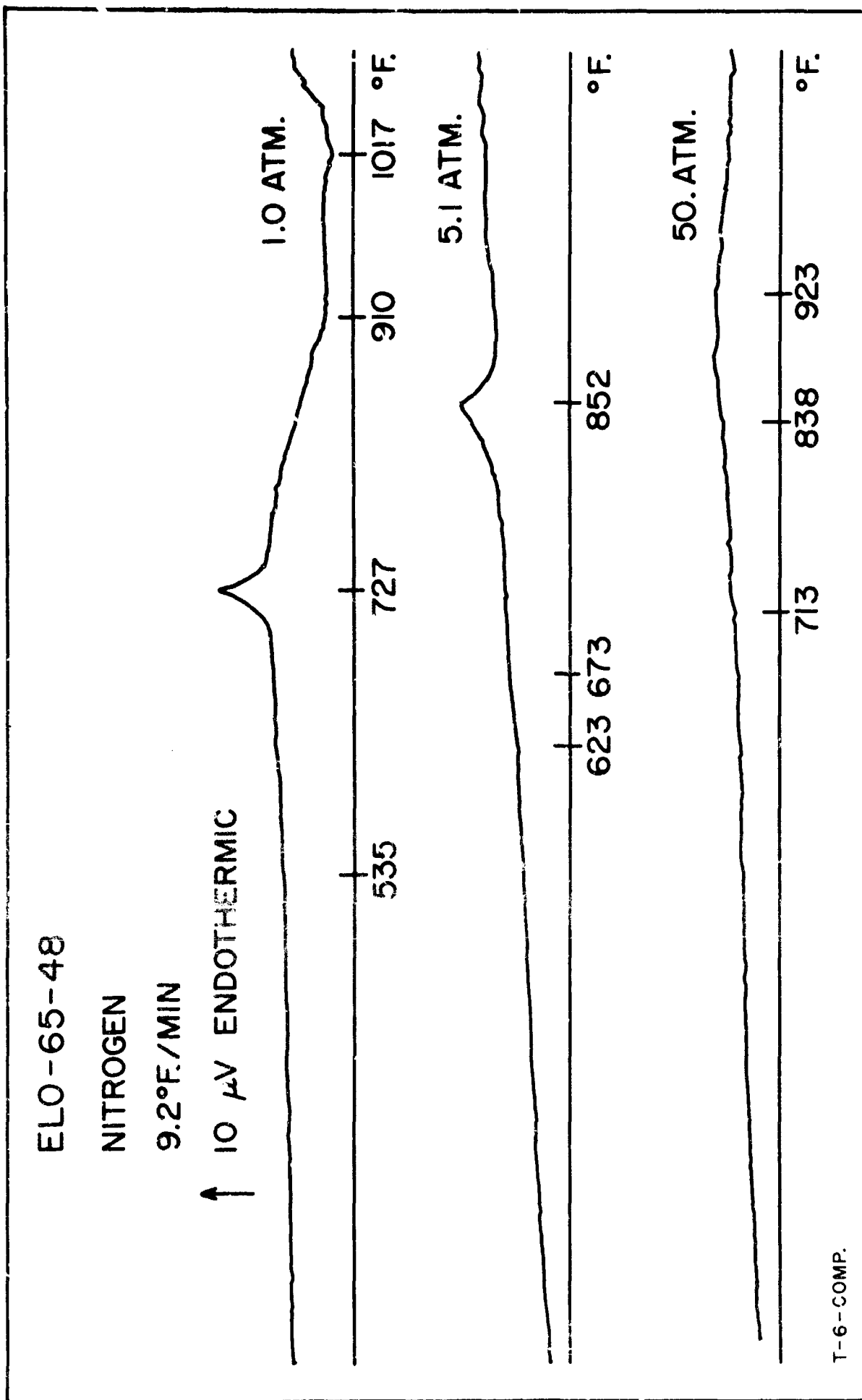


FIGURE 79. DIFFERENTIAL THERMAL ANALYSIS. ELO-65-48.

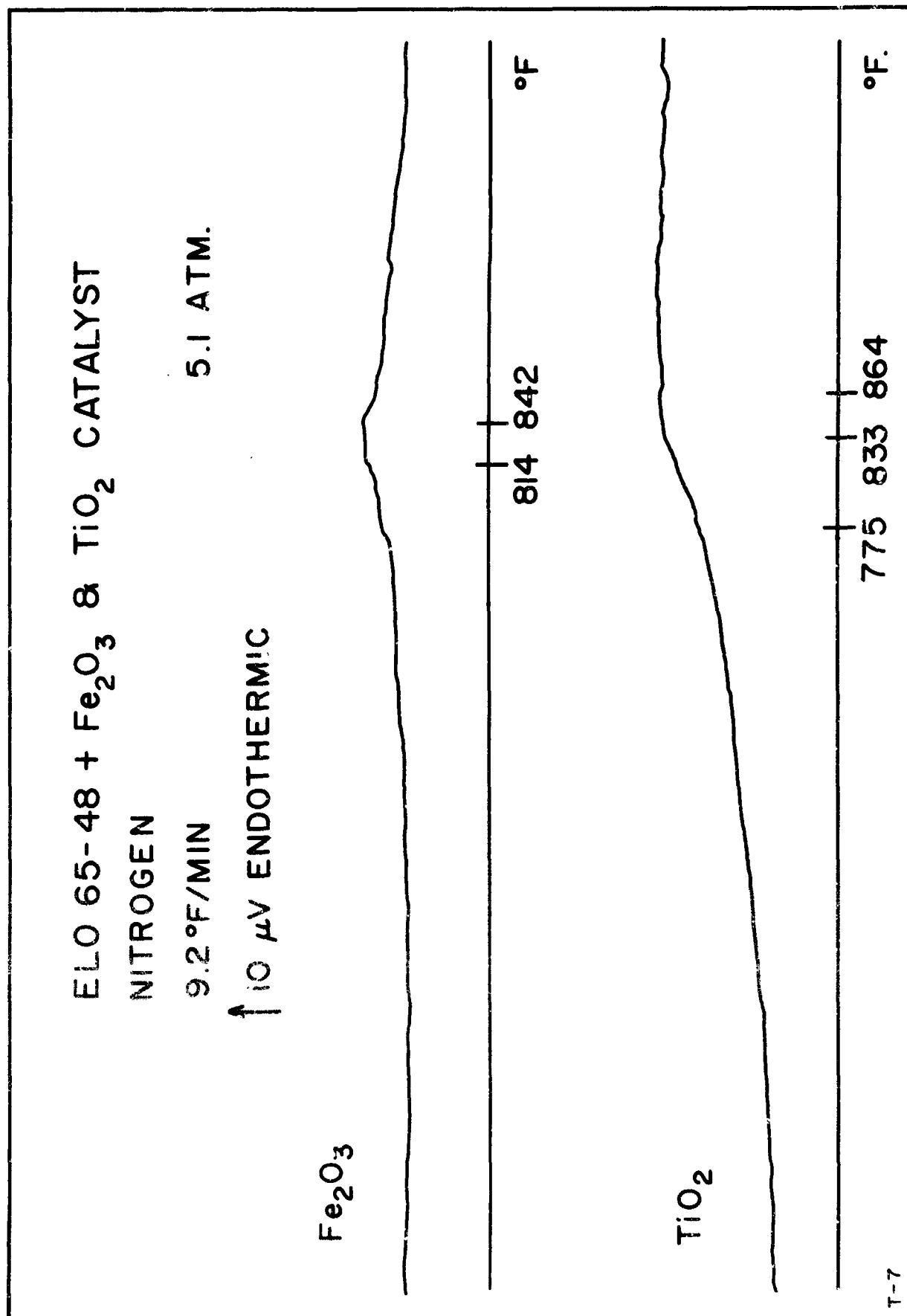


FIGURE 30. DIFFERENTIAL THERMAL ANALYSIS. ELO-65-48 PLUS IRON OXIDE AND TITANIUM DIOXIDE IN NITROGEN.

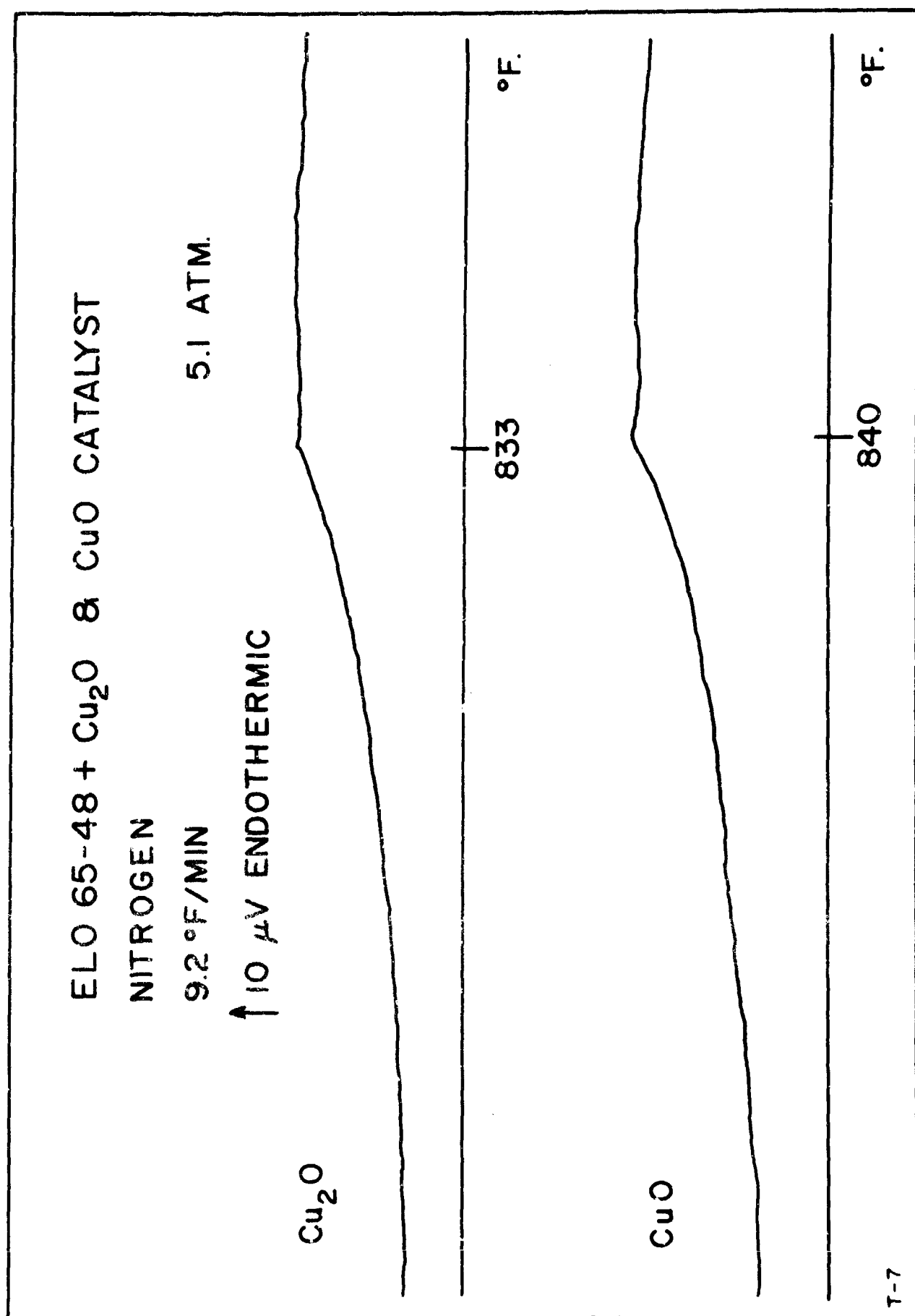


FIGURE 81. DIFFERENTIAL THERMAL ANALYSIS. ELO-65-48 PLUS CUPROUS OXIDE AND CUPRIC OXIDE IN NITROGEN.

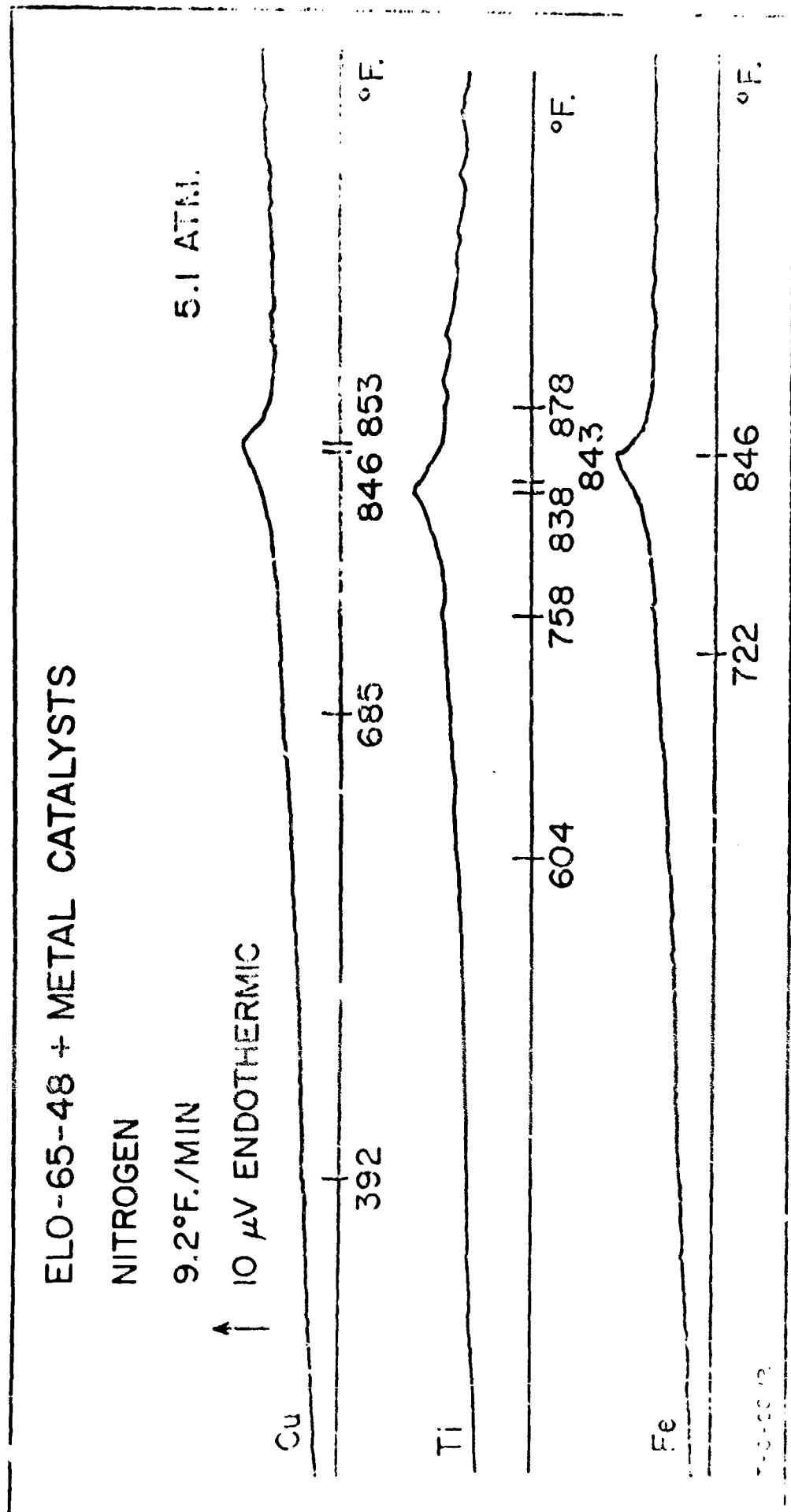


FIGURE 82. DIFFERENTIAL THERMAL ANALYSIS: ELO-65-48 PLUS
COPPER, TITANIUM AND IRON.

2.3.1.4 Blank. Pyrex Microbeads plus Metal Oxide Catalysts.

Air Atmosphere. Thermocouple Pair T-7.

9.2°F./Min. Scan Rate. See Figures 83 and 84.

The thermograms of four metal oxide-microbead mixtures run in air are essentially the same as those determined for the same oxides under nitrogen. There is, however, one exception: In the thermogram for cupric oxide a small, sharp exotherm occurs at 414 deg. F. in an air atmosphere. A like effect is not observed under nitrogen. The blank run for iron oxide was terminated at approximately 840 deg. F. by a thermocouple failure. The broken line in Figure 83 is an approximation of what the remainder of the thermogram would be had it been run.

2.3.1.5 MLO-64-8. Pyrex Microbeads plus Metal Oxide Catalysts.

Air Atmosphere. Thermocouple Pair T-7.

9.2°F./Min. Scan Rate. See Figures 85, 86, 87 and 88 and Table XII.

In air iron powder was found to affect mainly the decomposition of residues left after the initial breakdown of the sample. Iron oxide (Fe_2O_3) is more active. The thermogram obtained in air is different from that for either the pure sample or the mixture of the sample with iron powder. In general the pattern of decomposition in the presence of iron oxide in air is similar to that found previously for the same system under a nitrogen atmosphere. Titanium metal exhibited only slight catalytic action towards MLO-64-8 in air. The oxide, in contrast, produces severe degradation in the sample and its residues at temperatures well below those at which decomposition had previously been detected. Both oxides of copper also exhibit increased activity in air over that found in nitrogen. Cuprous oxide increases decomposition of sample residues at about 1000 deg. F. in addition to the enhancement of the earlier decomposition-an effect which was also observed in nitrogen. In the nitrogen atmosphere cupric oxide seemed fairly inert. In air its activity parallels that of cuprous oxide. That is, the decomposition exotherm appearing at about 960 deg. F. is greatly intensified and a new exotherm at 979 deg. F. is produced. Although these occur at temperatures approximately the same as those at which exotherms were also observed for the pure sample and for mixtures of the sample with copper.

BLANK (PYREX MICROBEADS + Fe_2O_3 & TiO_2)

AIR

9.2°F./MIN.

↑ 10 μV ENDOTHERMIC

5.1 ATM.

Fe_2O_3

THERMOCOUPLE
BREAK

448

635

915 962

°F.

TiO_2

460

660

923

°F.

T-7

FIGURE 83. DIFFERENTIAL THERMAL ANALYSIS. BLANK (PYREX MICROBEADS PLUS IRON OXIDE AND TITANIUM DIOXIDE IN AIR).

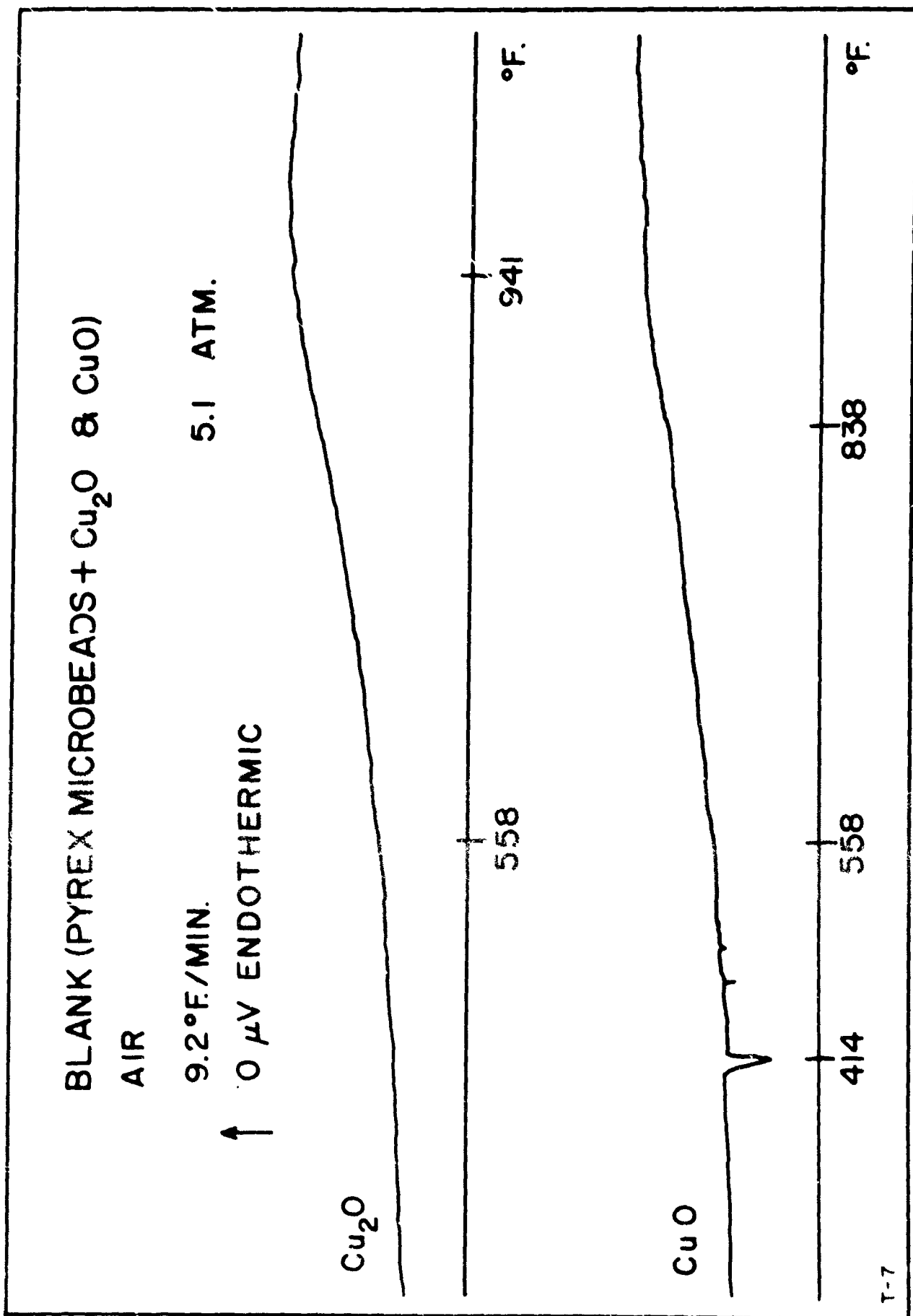


FIGURE 84. DIFFERENTIAL THERMAL ANALYSIS. BLANK (PYREX MICROBEADS PLUS CUPROUS OXIDE AND CUPRIC OXIDE IN AIR).

TABLE XII

DIFFERENTIAL THERMAL ANALYSIS: MLO-64-2 PLUS
METAL OXIDE CATALYSTS IN AIR ATMOSPHERE
(5.1 ATM. TOTAL PRESSURE)

CATALYST	FIGURE	EXOTHERMS, DEG. F.*			
Pt Catalyst	25	808	961!	992!	
Iron Oxide (Fe_2O_3)	26	(742)	870	943!!	950
Iron	28	742	960!	977!	994!!
Titanium Dioxide (TiO_2)	29	(858)	910!!	954!!	1002!!
Titanium	29	(765)	887	958!	979! (1050)
Cuprous Oxide (Cu_2O)	27	(813)	840	960!!	995!!
Cupric Oxide (CuO)	27	(843)	879	963!	975!!
Copper	27	898	921	945!	964!

* Those thermal effects which may be attributed solely to the reactions of the catalysts have not been included in this tabulation.

Key to symbols:

() weak thermal effect

! strong thermal effect

!! very strong thermal effect

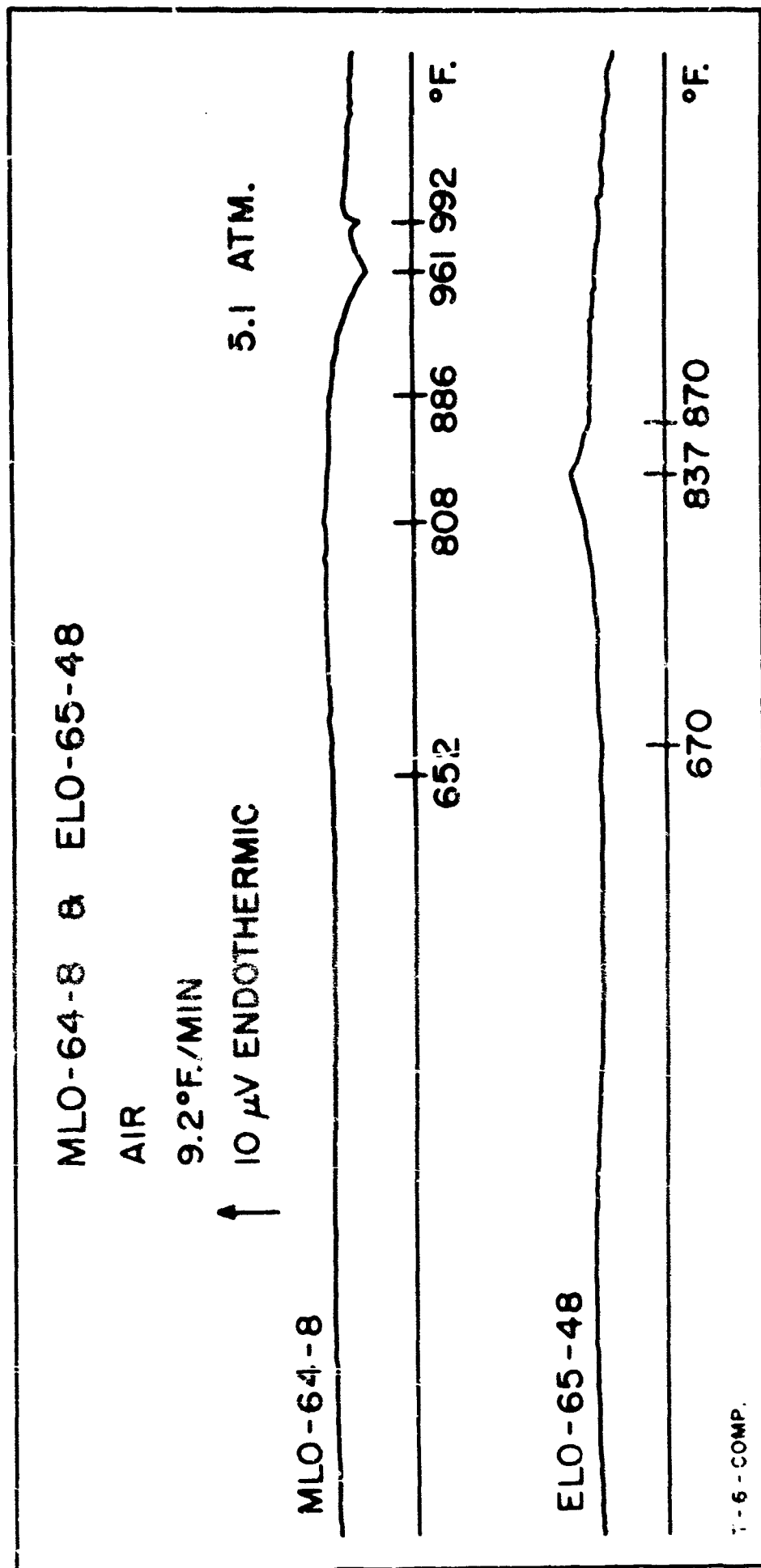


FIGURE 85. DIFFERENTIAL THERMAL ANALYSIS.
MLO-64-8 AND ELO-65-48 IN AIR.

MLO 64-8 + Fe_2O_3 & TiO_2 CATALYST

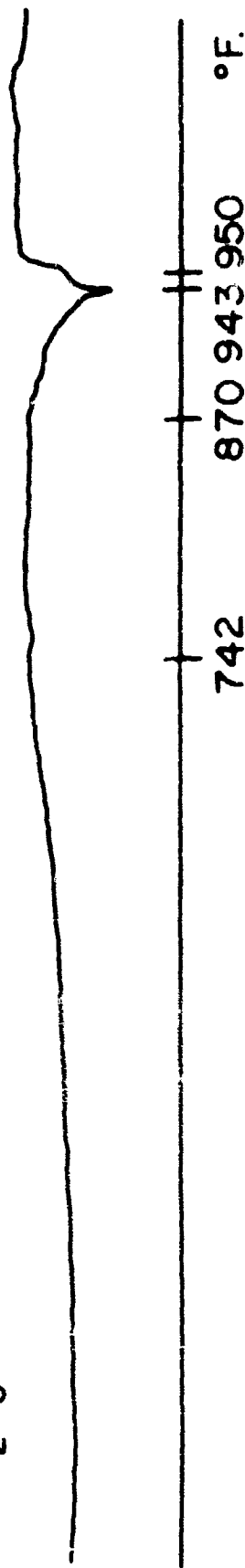
AIR

92 °F/MIN.

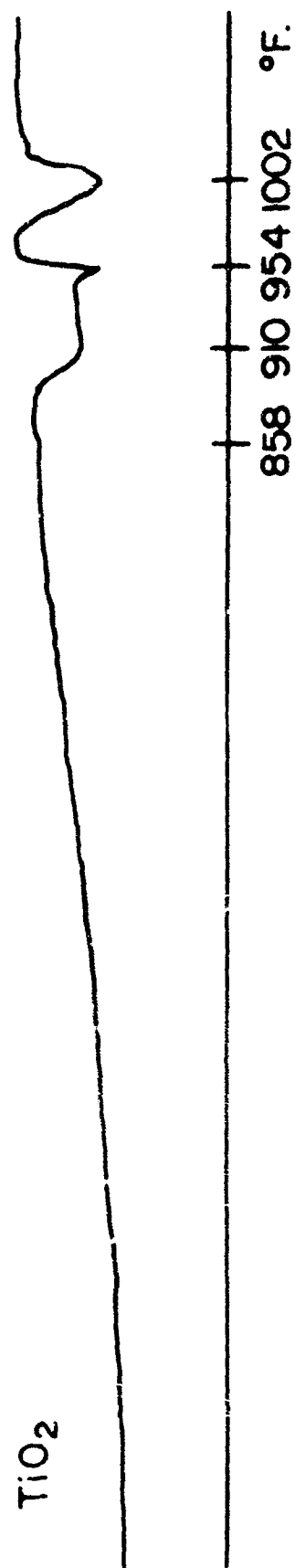
5.1 ATM.

↑ 10 μV ENDOTHERMIC

Fe_2O_3



TiO_2



T-7

FIGURE #6. DIFFERENTIAL THERMAL ANALYSIS. MLO-64-8 PLUS IRON OXIDE AND TITANIUM DIOXIDE IN AIR.

MLO 64-8 + Cu_2O & CuO CATALYST

AIR

9.2 °F/MIN.

5.1 ATM.

↑ 10 μV ENDOTHERMIC

Cu_2O



813 840 960 995 °F.

CuO



843 879 963 979 °F.

T-7

FIGURE 8. DIFFERENTIAL THERMAL ANALYSIS. MLO-64-8 PLUS CUPROUS OXIDE AND CUPRIC OXIDE IN AIR.

MLO-64-8 + METAL CATALYSTS

AIR

9.2°F./MIN

10 μV ENDOTHERMIC

5.1 ATM.

Cu

600

723

898 945

921 964

°F.

Ti

765

887

953

1050

978

°F.

Fe

742

960 994

977

°F.

FIGURE 88. DIFFERENTIAL THERMAL ANALYSIS. MLO-64-8 PLUS COPPER, TITANIUM AND IRON IN AIR.

their configuration and relative intensities suggest that they are the result of different reactions rather than the same reactions in which thermal effects are amplified by the adsorption-retention effect observed for molecular sieve and some non-activated carbon powders.

2.3.1.6 ELO-65-48. Pyrex Microbeads plus Metal Oxide Catalysts.

Air Atmosphere. Thermocouple Pair T-7.

9.2°F./Min. Scan Rate. See Figures 85, 89, 90 and 91 and Table XIII.

Each of the metal oxide catalysts studied exhibits considerable activity with respect to ELO-65-48 in air atmosphere. In nitrogen the decomposition of the sample was affected to an extent such that the prominent boiling endotherm was weakened considerably by the simultaneous occurrence of an exothermic decomposition. In air the same phenomenon occurs to a greater degree. Only in the run made with added iron oxide does any evidence whatever of the boiling endotherm remain. Decomposition of residues left at temperatures above that of the absent or reduced boiling endotherm is especially noticeable in each case. Similar exotherms appear also in the thermograms for mixtures of the sample with pure iron and titanium but are absent from the thermogram for the copper mixture.

2.3.2 Comparison of DTA and Oxidative-Corrosion Studies.

Examination of the data in Section 2.3.1 reveals that the effects of metal oxides on both the thermal and oxidative decomposition of samples MLO-64-8 and ELO-65-48 are very different from those produced by the corresponding metals. In general the oxides appear to be much more active with respect to the enhancement of existing decomposition processes and with respect to the opening of new pathways by which the degradation process may occur. The systems comprising MLO-64-8 in admixture with titanium and titanium dioxide in both air and nitrogen are especially noteworthy examples of this phenomenon.

Since under the conditions of differential thermal analysis titanium metal was found to be relatively inactive by comparison with its oxide the following experiments were conducted in order to determine whether a similar situation existed under the conditions of the corrosion and oxidation test.

TABLE XIII

DIFFERENTIAL THERMAL ANALYSIS: ELO-65-48 PLUS
METAL OXIDE CATALYSTS IN AIR ATMOSPHERE
(5.1 ATM. TOTAL PRESSURE)

CATALYST	FIGURE	ENDOTHERMS, DEG. F.*			EXOTHERMS, DEG. F.*		
No Catalyst	85	670	837!		870		
Iron Oxide (Fe ₂ O ₃)	89	775	809		854	947	1081!!
Iron	91	(664)	727	834!	842!	902	1034!!
Titanium Dioxide (TiO ₂)	89		(832)		863	989	1000!! 1007!!
Titanium	91			831!		964	974!!
Cuprous Oxide (Cu ₂ O)	90	609			892	985	
Cupric Oxide (CuO)	90	656			898	977	
Copper	91	721	832!	842!	862		

* Those thermal effects which may be attributed solely to the reactions of the catalysts have not been included in this tabulation.

Key to symbols:

() weak thermal effect

! strong thermal effect

!! very strong thermal effect

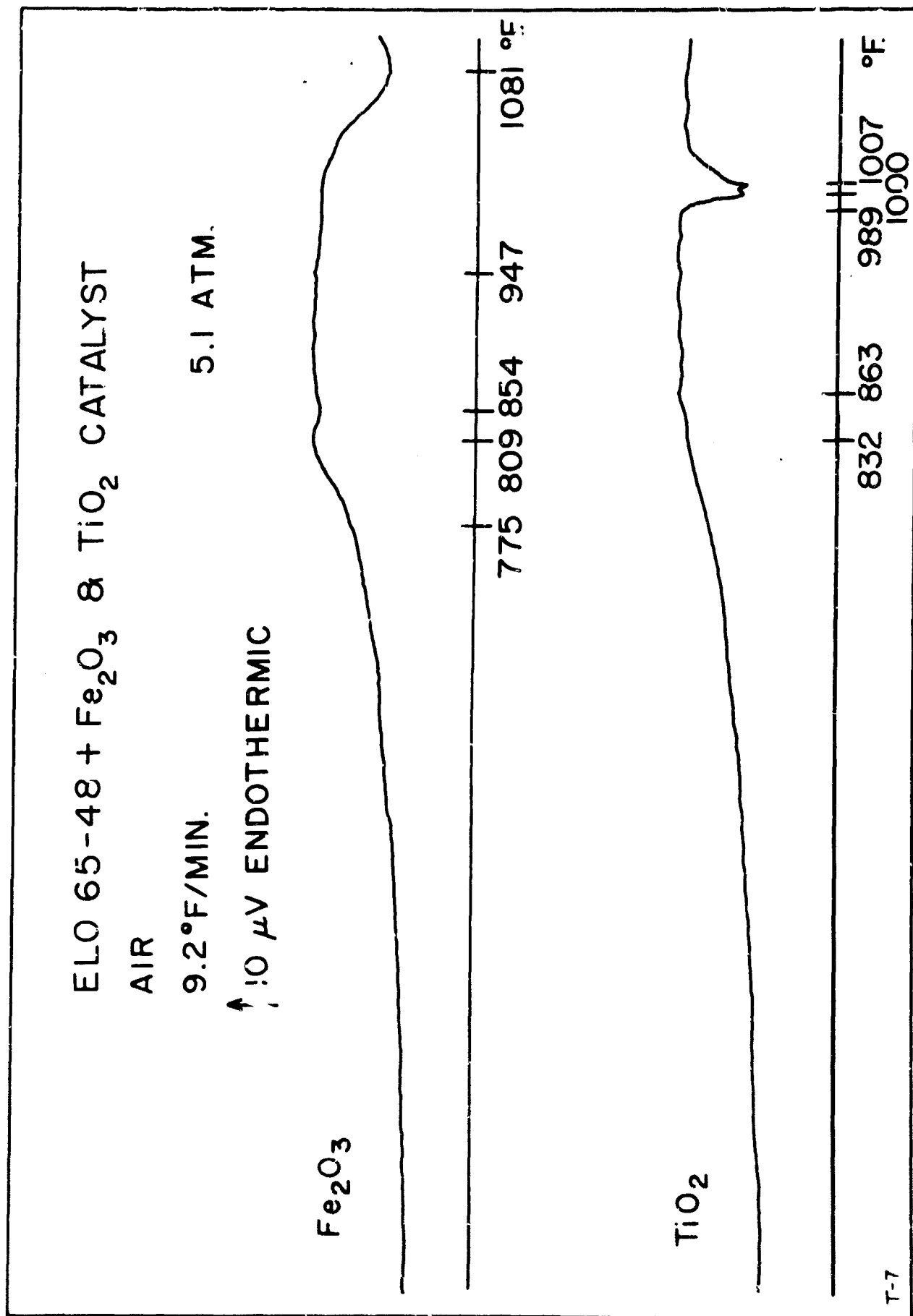


FIGURE 89. DIFFERENTIAL THERMAL ANALYSIS. ELO-65-18 PLUS
 IRON OXIDE AND TITANIUM DIOXIDE IN AIR.

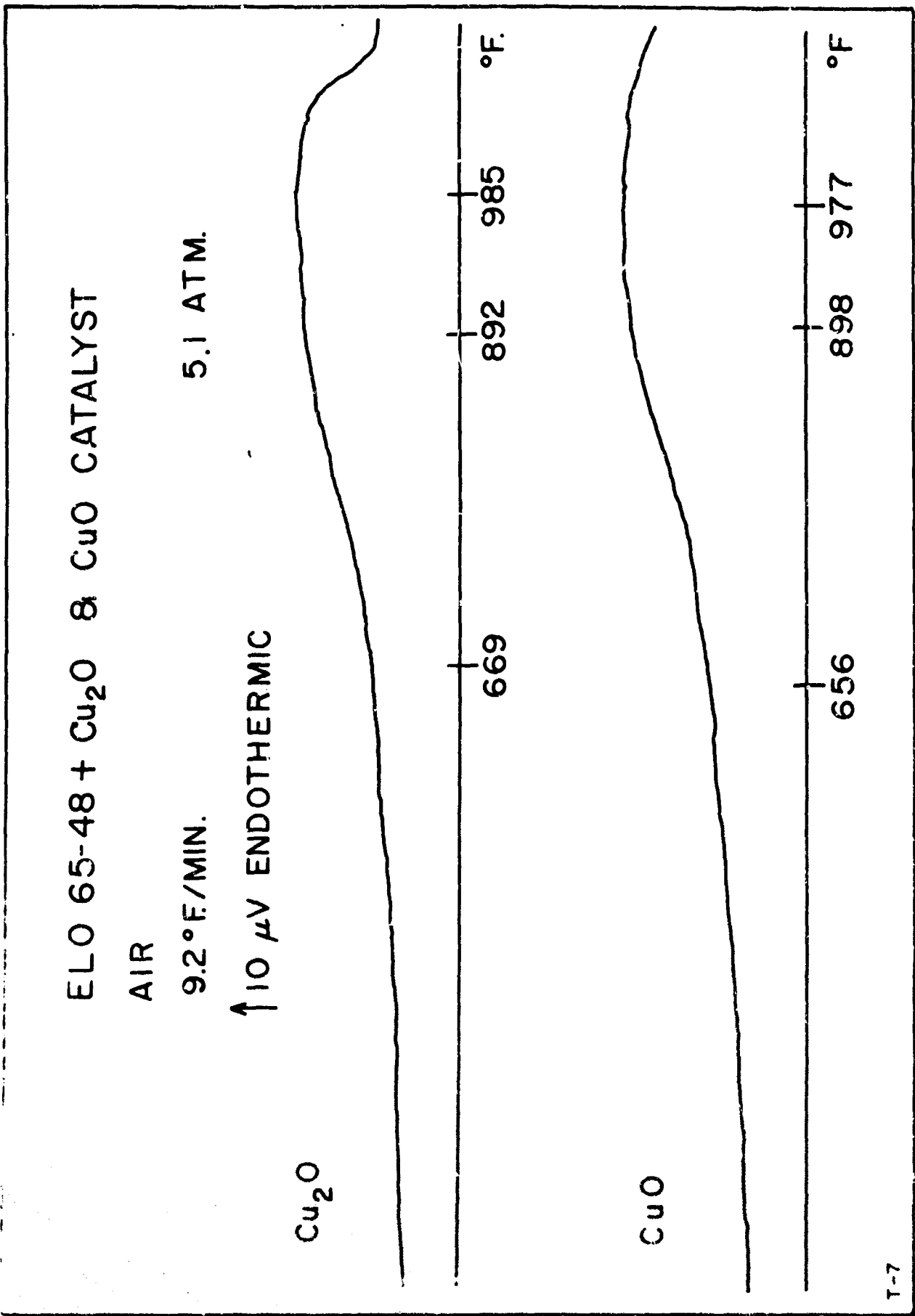


FIGURE 90. DIFFERENTIAL THERMAL ANALYSIS. ELO-65-48 PLUS CUPROUS OXIDE AND CUPRIC OXIDE IN AIR.

ELO-65-48 + METAL CATALYSTS

AIR

9.2°F./MIN.

↑ 10 μV ENDOTHERMIC

5.1 ATM.

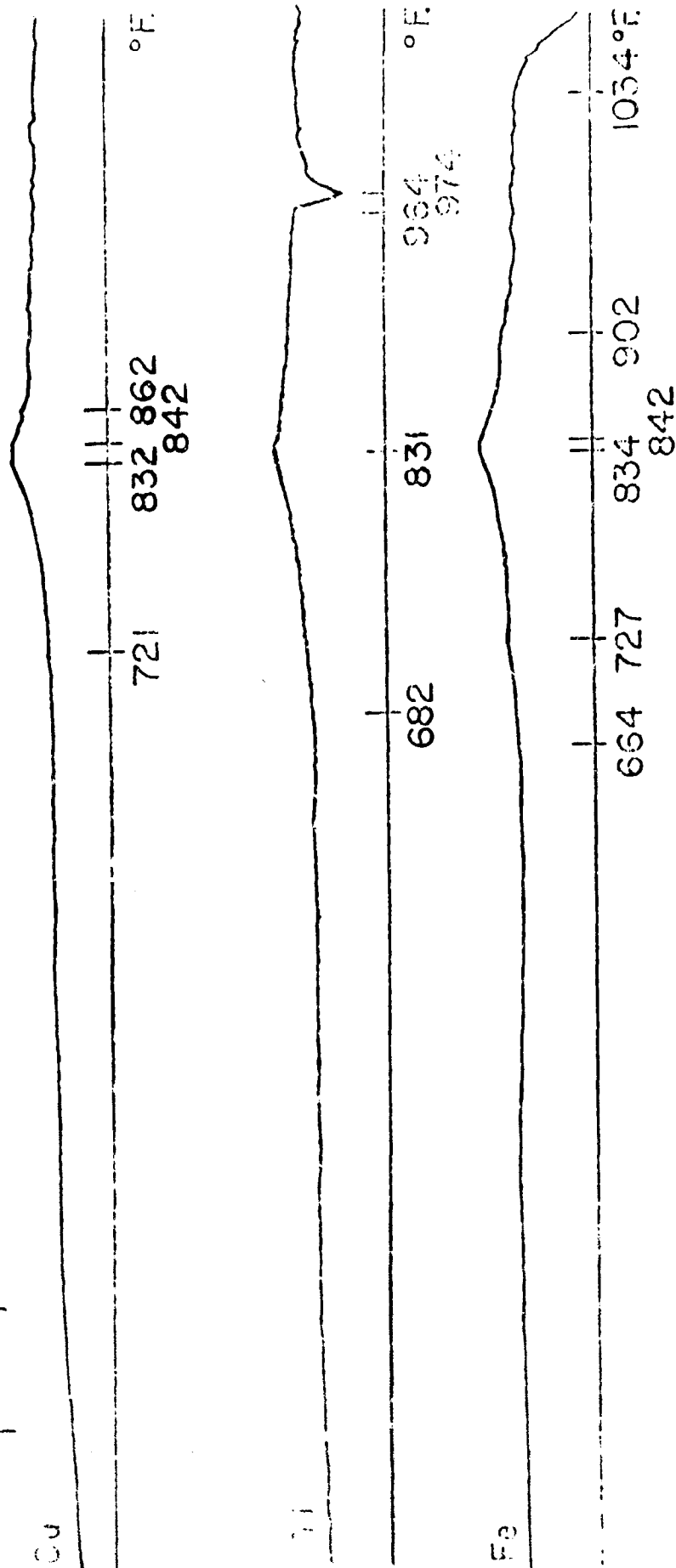


FIGURE 91. DIFFERENTIAL THERMAL ANALYSIS. ELO-65-48 PLUS COPPER, TITANIUM AND IRON IN AIR.

Standard micro corrosion and oxidation tests were run in duplicate on MLO-64-8 using two different titanium alloys. Upon completion of the above evaluations the exposed oils were analyzed in the prescribed manner and the alloy specimens weighed. Each alloy specimen was then placed without additional polishing into a fresh portion of the test oil and exposed again under the conditions of the micro corrosion-oxidation test. The data obtained from these experiments are given in Tables XIV and XV. Duplicate runs using the standard procedure are shown under the column headed "Polished Specimen"; the second series of measurements are found under the heading, "Pre-exposed Specimen".

It is clear that somewhat different corrosion and oxidation results are obtained depending on the mode of preparation of the alloy test piece. However, because of the disastrous nature of the decomposition of MLO-64-8 in the presence of either of the two alloys used, it is felt that the available data do not permit any distinction to be made between the stability of the fluid in the presence of a freshly polished titanium alloy test pieces and the stability in the presence of alloy test pieces subjected to the corrosive action of the fluid before the test exposure. Probably the test pieces corrode so rapidly in the presence of the sample that in either case the net effect of the specimen on the bulk or the bulk oil sample is nearly the same as that found for the pre-exposed test pieces.

Similar corrosion and oxidation studies with copper, iron, steel or pure titanium specimens might prove to be more enlightening than the above measurements have been. Such studies could not be performed during the present reporting period due to shortage of the test fluid. It is expected that further investigations of this nature will be included in future work.

2.3.3 Experimental Lubricants:

2.3.3.1 ELO-67-13. Nitrogen Atmosphere. Thermocouple Pair T-10-compensated. 9.2°F./Min. Scan Rate. See Figure 92.

The thermograms of the sample were run under nitrogen at 1.0 and 5.1 atm. total pressure. Virtually identical results were obtained at each pressure. The main features of each thermogram are strongly exothermic. A very strong exotherm is found at 357 to 358 deg. F. A second, exotherm

TABLE XIV

SAMPLE NUMBER MLO-64-8

CORROSION AND OXIDATION STABILITY (MICRO METHOD)
72 hours @ 600 deg. F. - Air Flow 1 liter/hour

	Polished Specimen		Pre-exposed Specimen	
	Run 1	Run 2	Run 1	Run 2
Tests on the Original Oil:				
Viscosity @ 100 deg. F., cs.	308.0	308.0	308.0	308.0
Neutralization Number, mg.KOH/g.	LT 0.001	LT 0.001	LT 0.001	LT 0.001
Tests on the Oxidized Oil:				
Viscosity @ 100 deg. F.	11.21	13.02	110.1	7.41
Neutralization Number, mg.KOH/g.	3.34	3.46	0.88	2.19
Evaporation Loss, %	46.4	39.8	27.1	57.1
Appearance	Water white, with white precipitate	Water white, with white precipitate	Water white, with white precipitate	Water white, with white precipitate
Decrease in Viscosity, %	96.4	95.8	64.2	97.6
Increase in Neutralization Number, mg.KOH/g.	3.34	3.46	0.88	2.19
Loss of Weight of Titanium - 6% Al - 4% V Alloy	0.26 *	0.26*	0.91*	0.77*

* Dark Grey

TABLE XV

SAMPLE NUMBER MLO-64-8CORROSION AND OXIDATION STABILITY (MICRO METHOD)
72 hours @ 600 deg. F. - Air Flow 1 liter/hour

	Polished Specimen		Pre-exposed Specimen	
	Run 1	Run 2	Run 1	Run 2
Tests on the Original Oil:				
Viscosity @ 100 deg. F., cs.	308.0	308.0	308.0	308.0
Neutralization Number, mg.KOH/g.	LT 0.001	LT 0.001	LT 0.001	LT 0.001
Tests on the Oxidized Oil:				
Viscosity @ 100 deg. F.	48.50	34.70	89.2	73.50
Neutralization Number, mg.KOH/g.	0.75	1.46	1.01	0.98
Evaporation loss, %	35.8	42.0	22.0	31.2
Appearance	Water white, with white precipitate	Water white, with white precipitate	Water white, with white precipitate	Water white, with white precipitate
	84.2	88.7	71.0	76.1
Decrease in Viscosity, %	0.75	1.46	1.01	0.98
Increase in Neutralization Number, mg.KOH/g.				
Loss of Weight of Titanium - 4% Al - 4% Mn Alloy	1.96*	2.47*	2.31*	2.39*

* Dark Grey

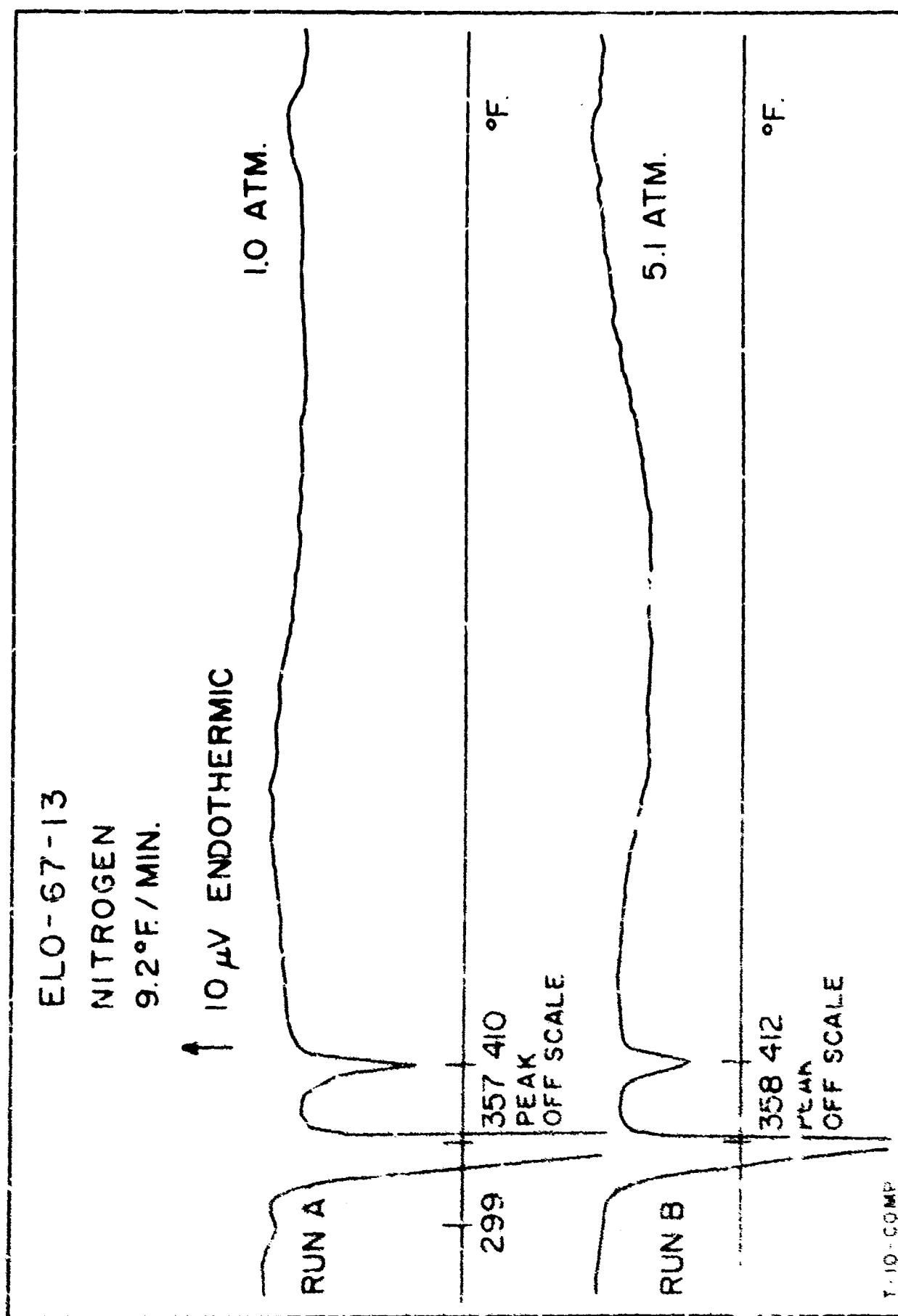


FIGURE 92. DIFFERENTIAL THERMAL ANALYSIS, ELO-67-13 IN NITROGEN.

which occurs at a slightly higher temperature 410° to 412 deg. F. - is weaker than the first, but must still be classified as a very strong effect. At 1.0 atm. a weak exotherm is seen at 299 deg. F. as well. Apparent thermal effects which occur after the main exotherms have not been classified because the degradation of the sample at lower temperatures seems to have been so complete that any such evaluation would be meaningless. On the basis of the DTA data it must be concluded that the sample is highly unstable even in an inert atmosphere.

2.3.3.2 EL0-67-13. Air Atmosphere. Thermocouple Pair T-11 and T-11-compensated. 9.2°F./Min. Scan Rate. See Figures 93, 94 and 95.

The thermograms of the sample were run in an air atmosphere under total pressures of 1.0, 5.1 and 50.0 atm. The data obtained at all pressures are substantially identical and, indeed, are the same as those obtained for the runs made under nitrogen. A very strong exotherm in the region 353° to 370 deg. F. is followed by a weaker but still prominent effect at 409° to 412 deg. F. These data are shown in Figures 93 and 94. For ease in reference the instrumental blank for the 50.0 atm. run is shown in Figure 95. The stability of the sample in air is completely comparable to that observed under nitrogen.

2.3.3.3 ELA-67-32. Nitrogen Atmosphere. Thermocouple Pair T-10-compensated. 9.2°F./Min. Scan Rate. See Figure 96.

At 1.0 atm. sharp, intense endotherms are observed at 288° and 417 deg. F. A broad endotherm between 827° and 938 deg. F. with peak at 898 deg. F. is also seen. At 5.1 atm. the only significant feature is the intense endotherm at 297 deg. F. which corresponds to the one observed at 288 deg. F. at 1.0 atm. The large exothermic shift seen after 600 deg. F. is not due to the sample but reflects a change in the thermocouple matching at that temperature. (See Figure 71) The sharp endotherm at 417 deg. F. and the broad endotherm between 827° and 938 deg. F. which are seen only in the run made at 1.0 atm. are due to the boiling of various sample components. Possibly some decomposition occurs at the same time as the initial boiling so that the latter effect reflects only the slow volatilization of sample residues. It is also possible that the sample contains a volatile and

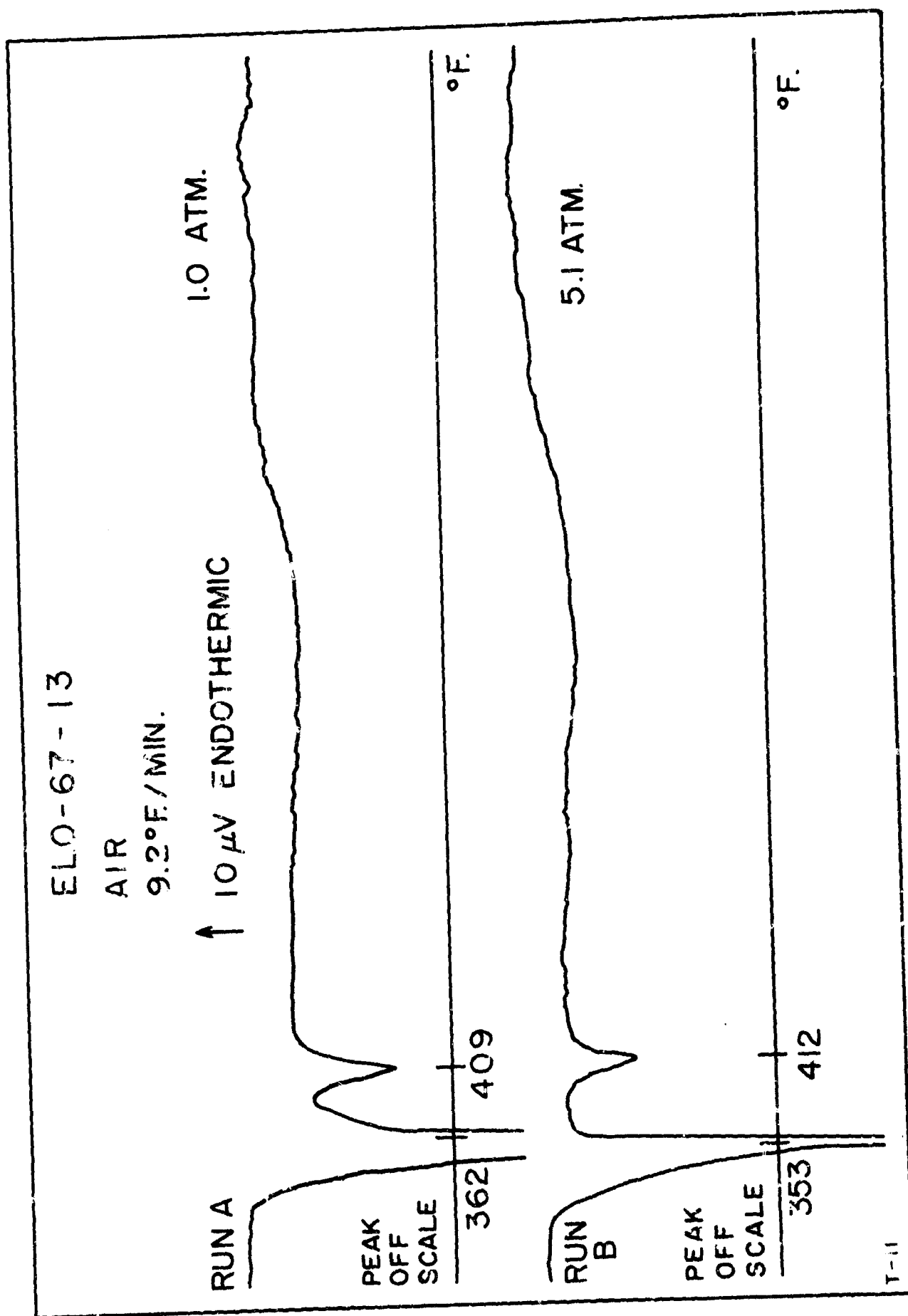


FIGURE 93. DIFFERENTIAL THERMAL ANALYSIS. ELO-67-13 IN AIR.

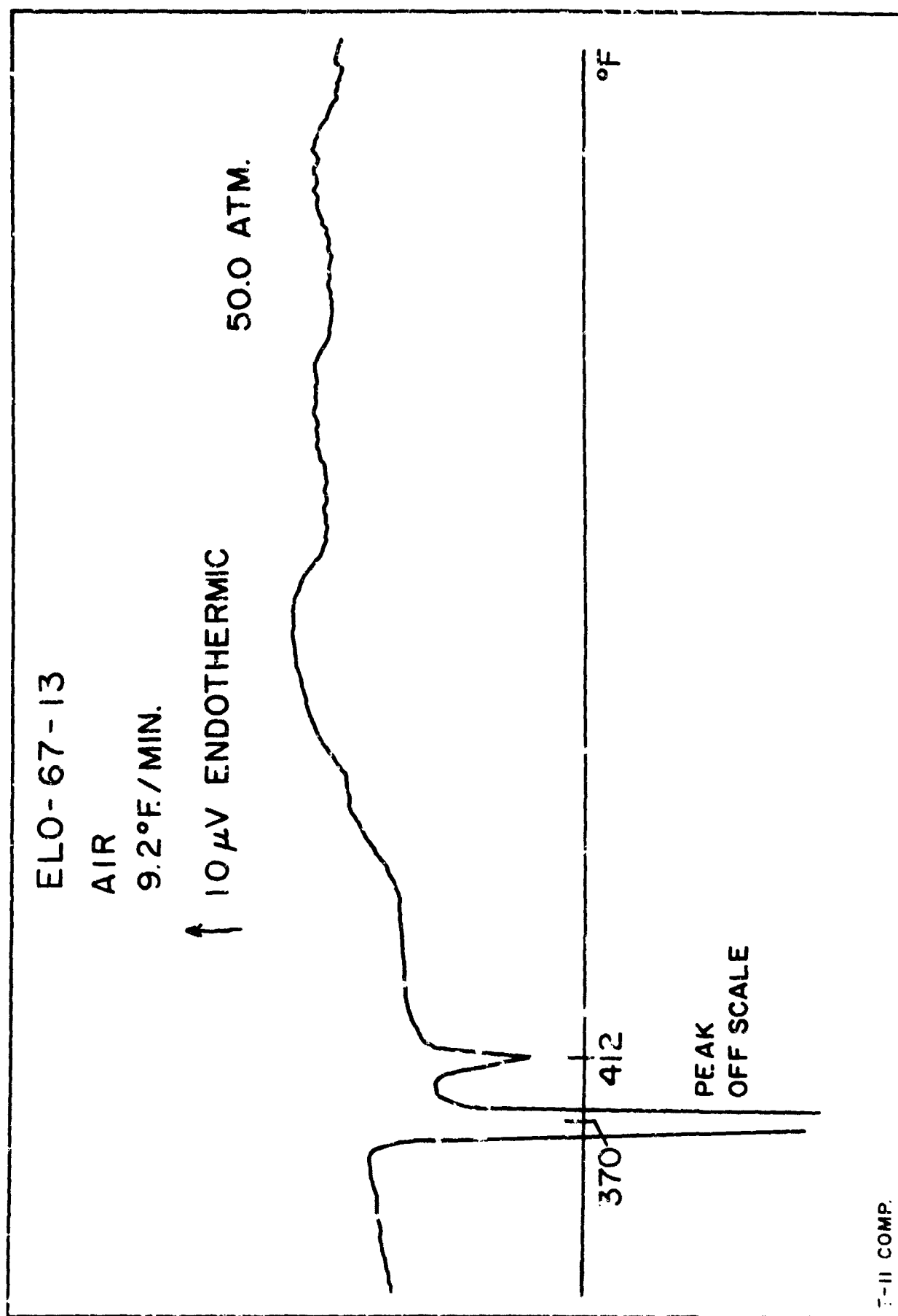


FIGURE 94. DIFFERENTIAL THERMAL ANALYSIS. ELO-67-13 IN AIR.

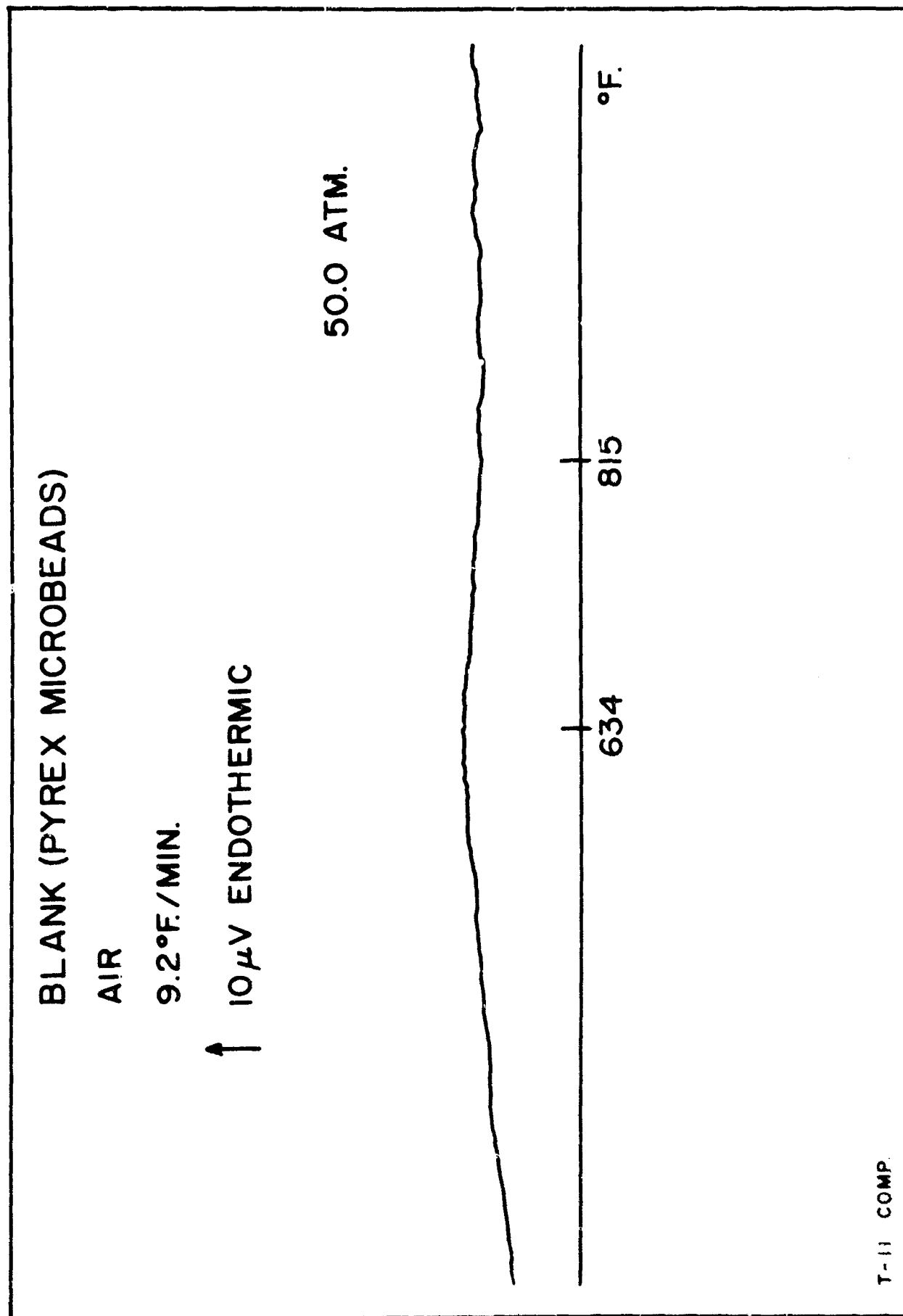


FIGURE 95. DIFFERENTIAL THERMAL ANALYSIS. BLANK. NITROGEN ATMOSPHERE.

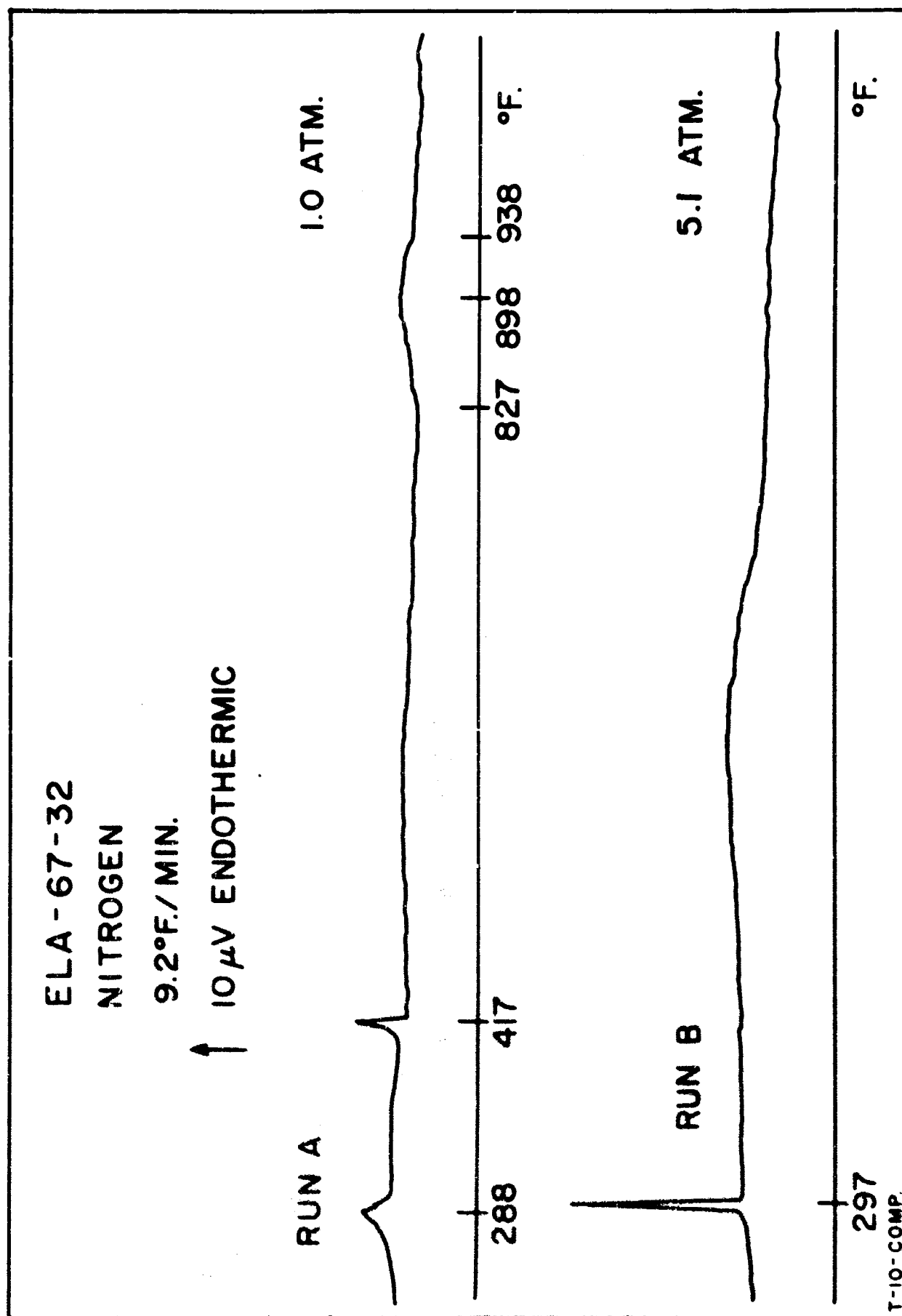


FIGURE 96. DIFFERENTIAL THERMAL ANALYSIS. ELA-67-32. NITROGEN ATMOSPHERE.

relatively non-volatile constituents boiling at widely separated temperatures. The endotherms which are observed at 288° and 297 deg. F. respectively are due presumably to the melting of the sample. The pressure dependence of the effect, however, is unusually large for a transition such as melting. The explanation for this is not clear. However, other pressure dependent-phase changes in addition to melting may occur at the same time. Alternatively the melting process may simply have an unusually large pressure coefficient.

2.3.3.4 ELA-67-32. Air Atmosphere. Thermocouple Pair T-8.

9.2°F./Min. Scan Rate. See Figure 97.

The thermogram obtained for sample ELA-67-32 under an air atmosphere is in many respects very similar to that obtained for the same material under nitrogen. Melting endotherms are found at 285° and 297 deg. F. respectively for the 1.0 and 5.1 atm. runs. At 1.0 atm. two boiling endotherms appear at 423 deg. F. and between 768° and 924 deg. F. with a peak at 857 deg. F. The principal difference between the runs made in air and in nitrogen lies in the fact that in the thermogram for air atmosphere an exothermic effect begins at 506 deg. F. and reaches a maximum at 547 deg. F. This effect is seen only in the run made at 5.1 atm. Presumably the oxidation which the exotherm reflects is that of a volatile fraction which boils at 423 deg. F. at 1.0 atm. and which at that pressure is lost to the system before oxidation can be detected in the condensed phase in contact with the differential thermocouple.

2.3.3.5 ELA-67-33. Nitrogen Atmosphere. Thermocouple Pair T-10-compensated. 9.2°F./Min. Scan Rate. See Figure 98.

At 1.0 atm. the thermogram of the sample exhibits a sharp, intense endotherm with peak at 328 deg. F. A similar peak is also seen at 324 deg. F. for the run made at 5.1 atm. total pressure. These endotherms are produced by the fusion of the sample. At 1.0 atm. the slope of the thermogram assumes an endothermic trend after 767 deg. F. This endotherm is due to evaporation and leads into a major endothermic boiling peak with maximum at 847 deg. F. The boiling peak is quite symmetric. There is no evidence of decomposition during the boiling process at 1.0 atm. A slightly different situation is observed at 5.1 atm. The suppression of both evaporation and boiling at the

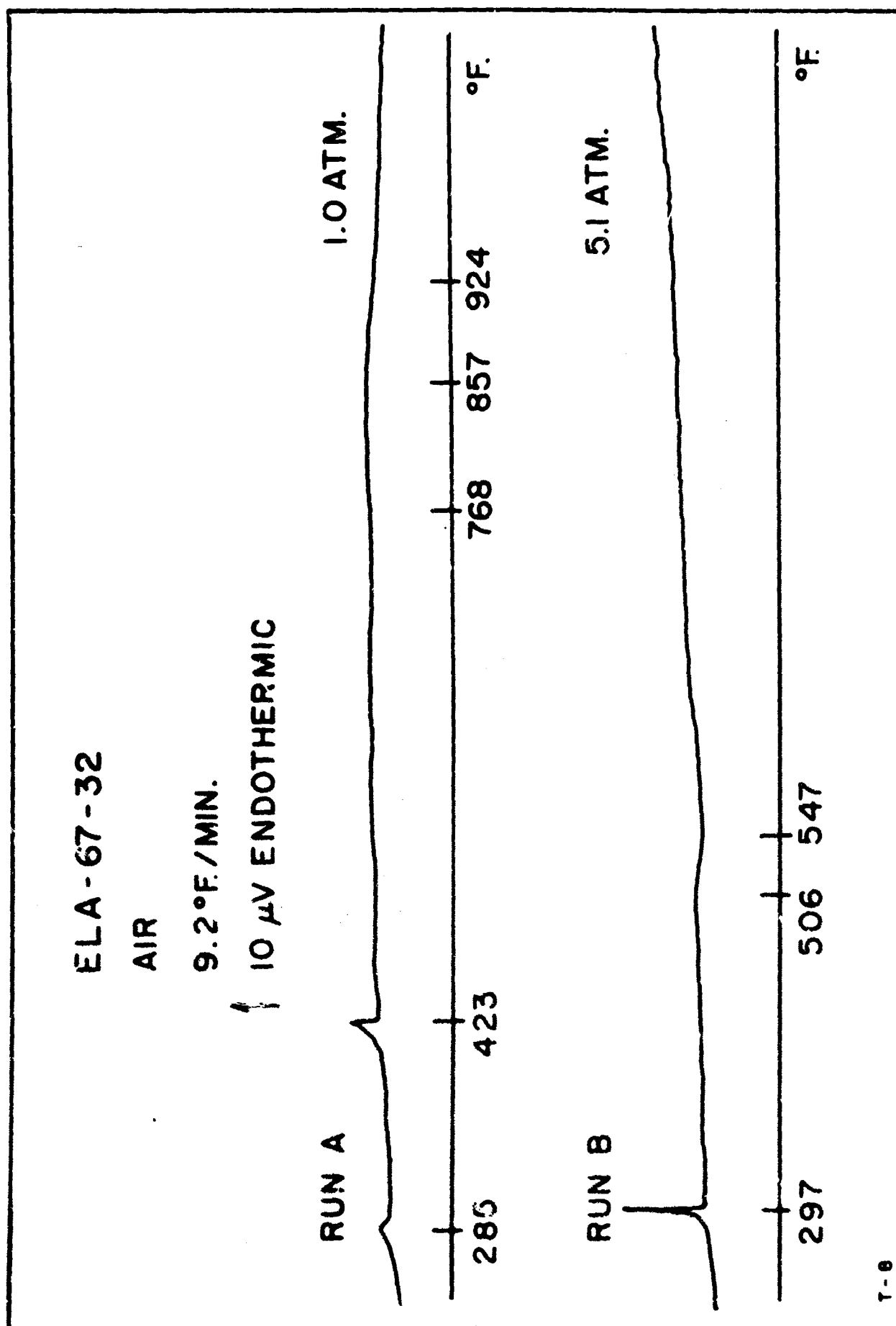


FIGURE 97. DIFFERENTIAL THERMAL ANALYSIS. ELA-67-32. AIR ATMOSPHERE.

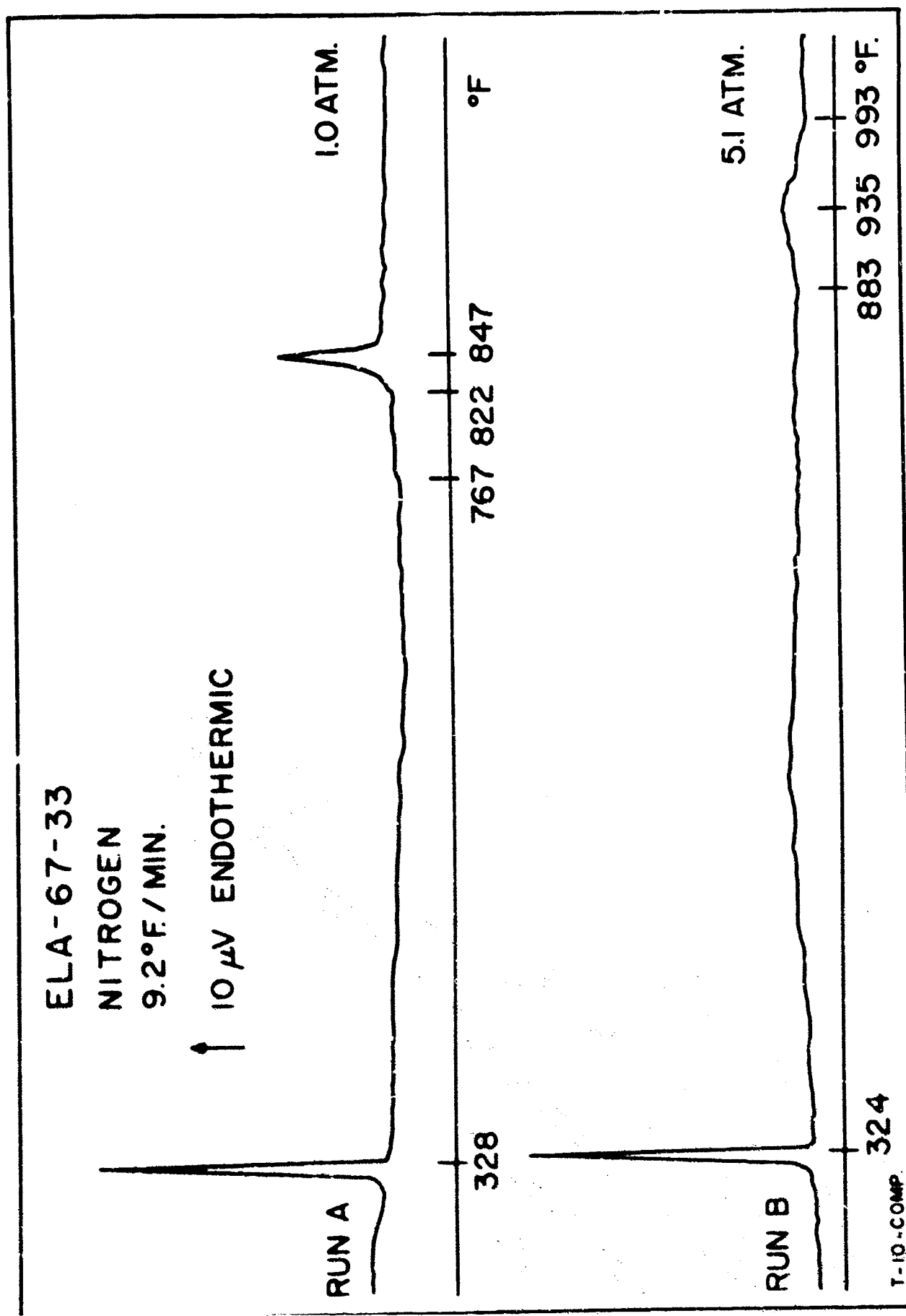


FIGURE 98. DIFFERENTIAL THERMAL ANALYSIS. ELA-67-33. NITROGEN ATMOSPHERE.

increased pressure are quite pronounced. The onset of evaporation is first detected at 883 deg. F. A boiling peak of moderate intensity follows at 935 deg. F. A small exotherm at 993 deg. F. may reflect the decomposition of residues left over after completion of boiling. The sample appears to be quite stable over a wide range of temperature in a nitrogen atmosphere.

2.3.3.6 ELA-67-33. Air Atmosphere. Thermocouple Pair T-8.

9.2°F./Min. Scan Rate. See Figure 99.

The main features of the thermogram for ELA-67-33 in air are similar to those observed for the material under nitrogen. Intense, sharp melting endotherms are found at 325 deg. F. for the runs made at 1.0 and 5.1 atm. At 1.0 atm. evaporation endotherm begins at 715 deg. F. and leads into a strong, symmetrical boiling endotherm at 843 deg. F. A small exotherm at 914 deg. F. suggests the decomposition of residues left after the boiling of the sample. At 5.1 atm. the boiling endotherm at 947 deg. F. is preceded by a moderate decomposition exotherm which begins at 806 deg. F. and reaches its maximum at 882 deg. F. A small exotherm at 988 deg. F. again suggests the further decomposition of sample residues. The presence of air apparently leads to an oxidative degradation after 806 deg. F. which does not appear in the oxygen-free system. While the relative stability of the sample in an air atmosphere is less than it is in nitrogen, the material is obviously still quite stable.

2.3.3.7 ELA-67-34. Nitrogen Atmosphere. Thermocouple Pair T-8.

9.2°F./Min. Scan Rate. See Figures 100 and 101.

The sample was found to be extremely viscous and tacky. For this reason it was extremely difficult to load the sample into the DTA cell in a proper manner so as to achieve good thermal contact between the sample and the measuring thermocouples. As a result the repeatability of the DTA runs was poor. Indeed, it is felt that many of the features observed in the several thermograms reflect movement of the sample and changing degree of contact between the sample and thermocouple. This is particularly true of the many short-term periodic fluctuations observed in the runs made at 1.0 atm. Several runs were made at each pressure. All data are presented in Figures 100 and 101 to enable the reader to grasp the general pattern of the decomposition

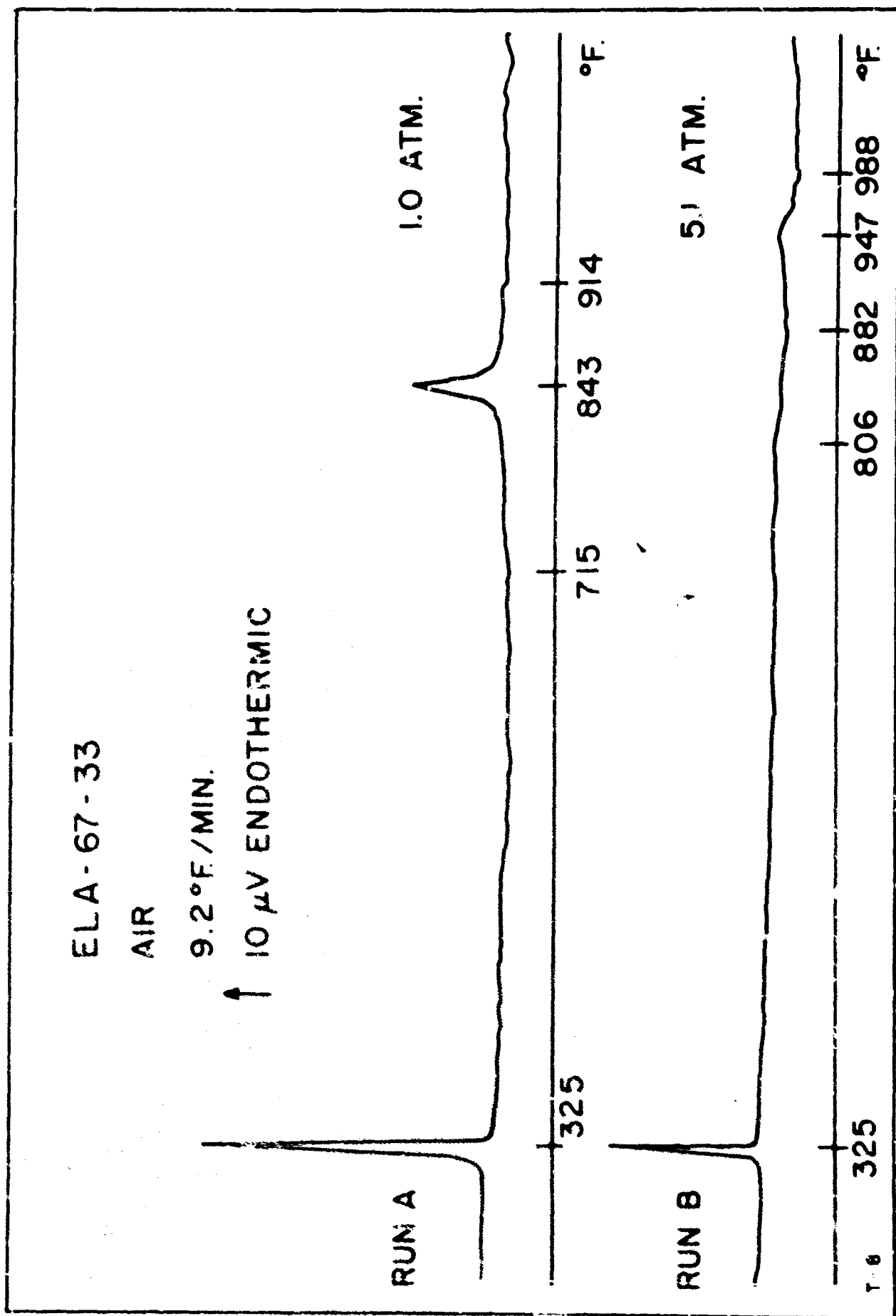


FIGURE 99. DIFFERENTIAL THERMAL ANALYSIS. ELA-67-33. AIR ATMOSPHERE.

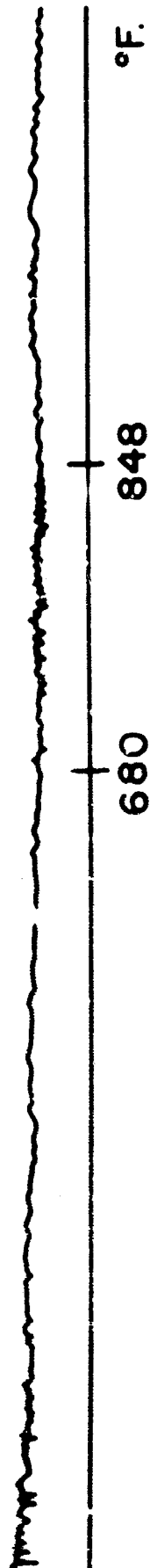
ELA-67-34

NITROGEN

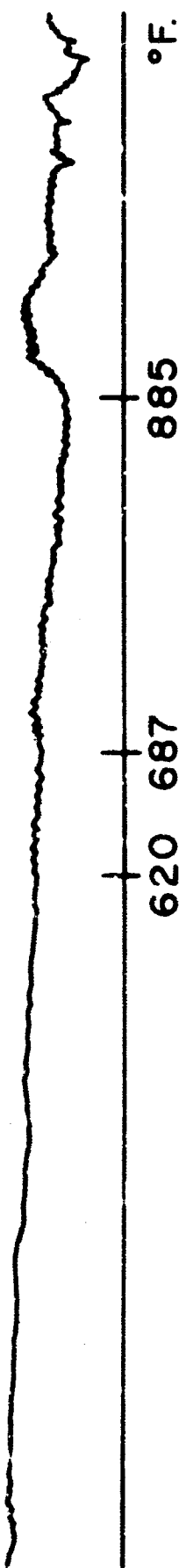
9.2 °F./MIN.

↑ 10 μV ENDOTHERMIC 1.0 ATM.

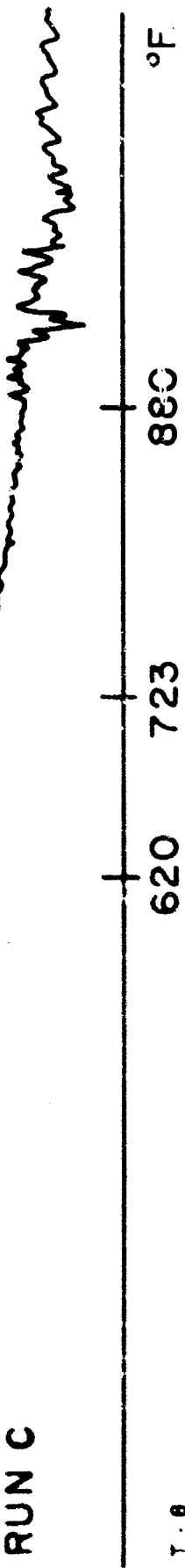
RUN A



RUN B



RUN C



T. 6

EL 1-67-34

NITROGEN

5.1 °F./MIN.

↑ 10 μV ENDOTHERMIC 5.1 ATM.

RUN A

770 875 958 °F.

RUN B

735 830 977 °F.

T-6

FIGURE 101. DIFFERENTIAL THERMAL ANALYSIS. ELA-67-34. NITROGEN ATMOSPHERE.

and the other processes which affect the DTA runs.

Motion of the sample in the DTA cell occurs when the liquid layer is pushed upward under the influence of the pressure of sample vapors and/or entrapped air. An increment of sample is pushed upward by the vapors until the liquid film breaks. At that point the liquid flows back to the lower regions of the sample container and the process is repeated. The repression of sample vaporization at higher pressures causes a marked reduction in such oscillation of the sample level.

At 1.0 atm. an increase in oscillation occurs after 620 deg. F. One may conclude as a consequence that sample vaporization increased markedly when that temperature was reached. Additional changes are observed in the 848° to 885 deg. F. region - either change in slope or degree and nature of sample oscillation. This may indicate further changes in the character of the sample. At 5.1 atm. volatilization induced processes in the 620 deg. F. region are not observed. Rather smooth thermograms without pronounced oscillations are obtained. A rather slight exothermic break occurs in the 830° to 875 deg. F. region. On the basis of the foregoing the following general conclusions can be reached: 1) Sample volatilization becomes important above 620 deg. F. and continues over a wide range of temperatures. 2) Decomposition of sample and/or sample residues occur above 800 deg. F.

2.3.3.8 ELO-67-45. Nitrogen Atmosphere. Thermocouple Pair T-11.
9.2°F./Min. Scan Rate. See Figure 102.

The sample is comparatively low boiling. At 1.0 atm. an intense boiling endotherm at 417 deg. F. is preceded by a boiling endotherm at 406 deg. F. A slight exotherm is observed at temperatures below the boiling point at 397 deg. F. A similar peak also occurs after the boiling endotherm at 523 deg. F. After 523 deg. F. the trend of the thermogram is endothermic. Peaks occur at 715° and 772 deg. F. These are due to the evaporation and boiling of heavier components or residues from earlier decomposition. At 5.1 atm. the main boiling endotherm is shifted to 509 deg. F. A small satellite peak is seen at 537 deg. F. A broad, weak exotherm precedes the boiling peak. It begins at 350 deg. F. and reaches its maximum at 410 deg. F.

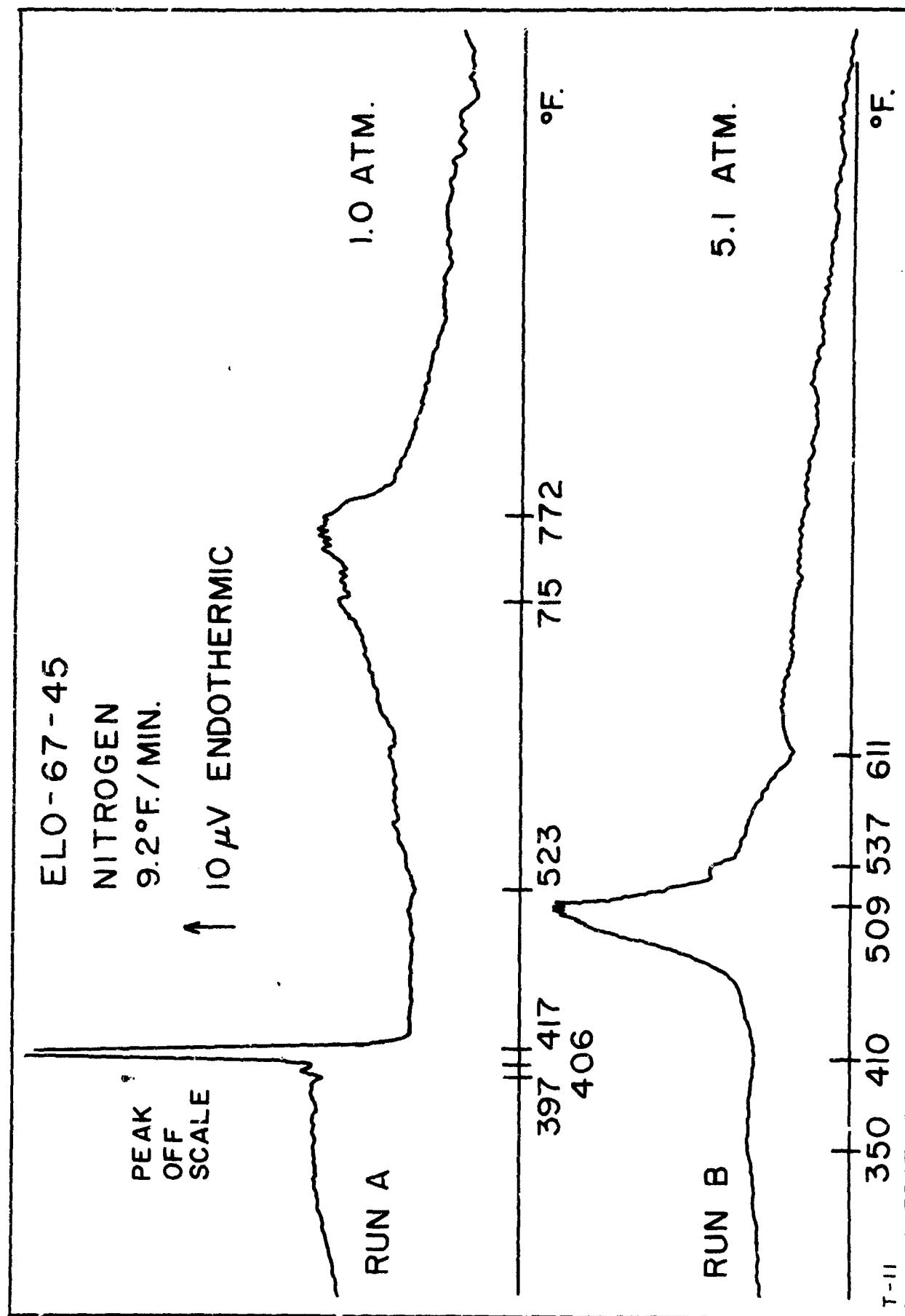


FIGURE 102. DIFFERENTIAL THERMAL ANALYSIS. ELO-67-45. NITROGEN ATMOSPHERE.

After the boiling peak a small exotherm at 611 deg. F. is suggestive of a decomposition reaction. At 5.1 atm. the endotherms which occur after 523 deg. F. at 1.0 atm. are completely suppressed.

2.3.3.9 ELO-67-45. Air Atmosphere. Thermocouple Pair T-8.
9.2°F./Min. Scan Rate. See Figure 103.

The thermogram for sample ELO-67-45 in air is quite similar to that obtained in a nitrogen atmosphere. One of the main differences is that at 1.0 atm. a slight periodic instability is observed to begin at 371 deg. F. just before the main boiling endotherm at 417 deg. F. A second periodic instability, more pronounced than the first, occurs between 443° and 775 deg. F. The former effect is probably due to sample motion produced by the rapid evaporation of the sample. However, the latter effect may be the result of any one of several causes. These include: motion of sample residues under the influence of their own vapor pressures; refluxing of the more volatile components of sample residues; rapid degradation of sample residues to produce small amounts of volatile materials which are rapidly lost in the manner which is commonly observed for silicones; and the return and rapid re-evaporation of major components originally lost below 435 deg. F. These pressure dependent processes are suppressed at 5.1 atm. At that pressure evaporation endotherms which occur between 410° and 500 deg. F. are followed by a strong boiling endotherm at 522 deg. F. A small endotherm at 720 deg. F. probably corresponds to the endotherm seen at 775 deg. F. in the run made at 1.0 atm. under air and at 772 deg. F. in the run made at 1.0 atm. under nitrogen. The most probable effect of the presence of air is to produce an oxidation reaction which leads to the evolution of small amounts of volatile components whose presence is marked by the periodic instability recorded between 443° and 775 deg. F. at 1.0 atm.

2.3.3.10 ELO-67-51. Nitrogen Atmosphere. Thermocouple Pair T-10-compensated. 9.2°F./Min. Scan Rate. See Figure 104.

At 1.0 atm. the thermogram of the sample exhibits a weak endothermic drift between 708° and 787 deg. F. which is the result of evaporation of the sample. After 787 deg. F. an intense boiling endotherm with peak at 805 deg. F. is seen. Satellite boiling peaks occur at 853° and 865 deg. F. These are followed by a weak exotherm at 878 deg. F. which may reflect the decomposition

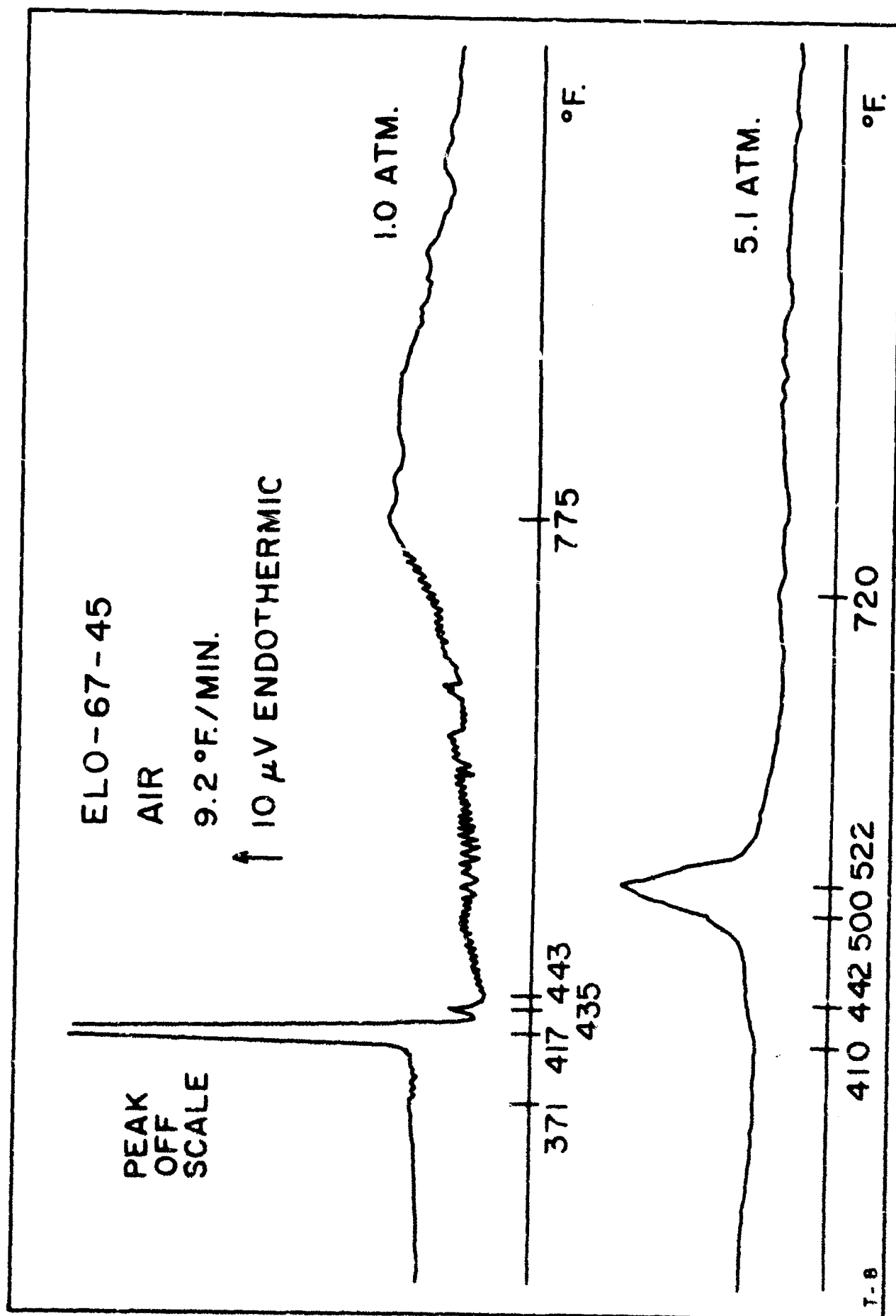


FIGURE 103. DIFFERENTIAL THERMAL ANALYSIS. ELO-67-45. AIR ATMOSPHERE.

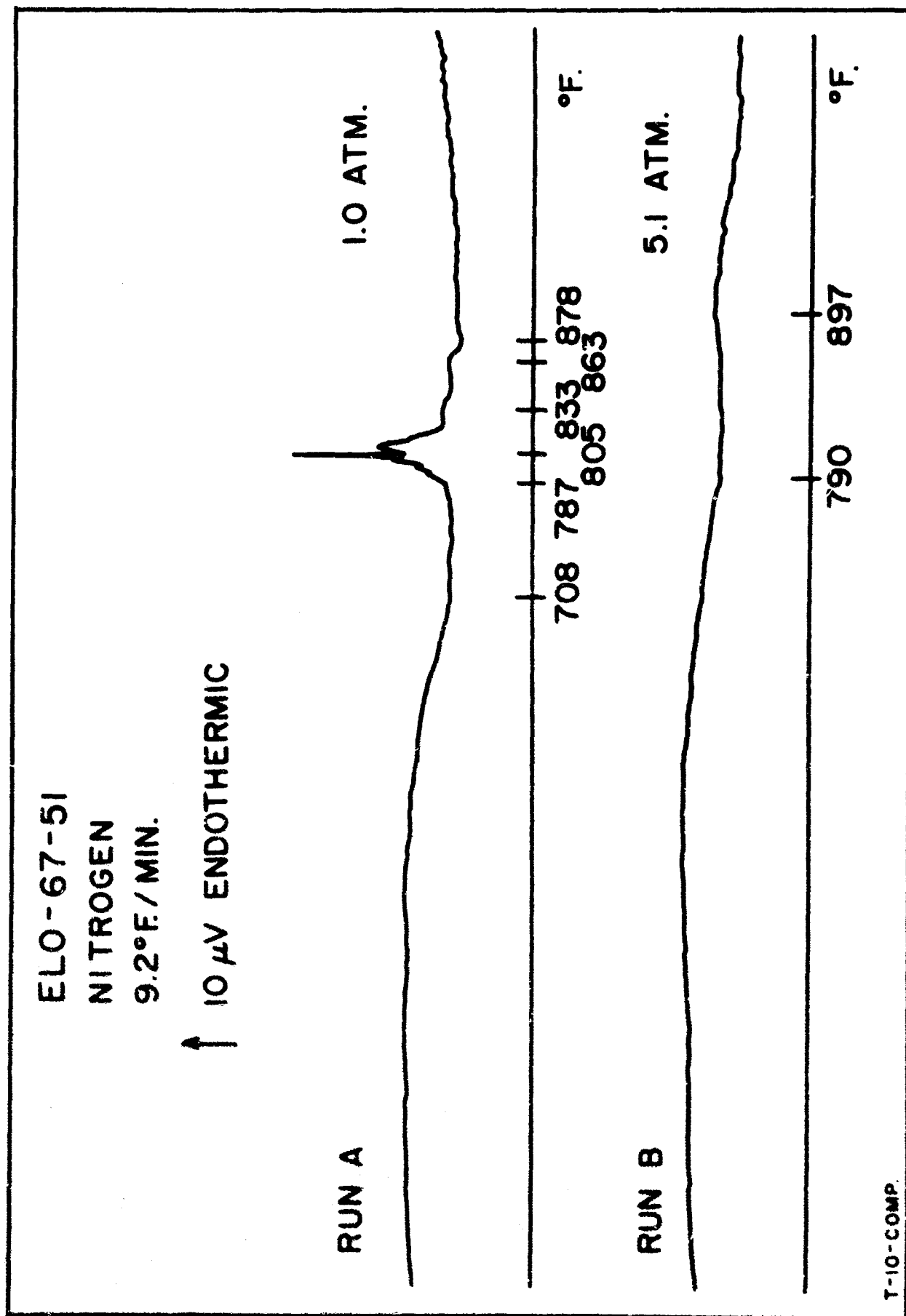


FIGURE 104. DIFFERENTIAL THERMAL ANALYSIS. ELO-67-51. NITROGEN ATMOSPHERE.

of sample residues. At 5.1 atm. the evaporation and boiling endotherms are much weaker. The onset of evaporation is observed at 790 deg. F; the boiling endotherm, at 897 deg. F. At temperatures up to and including the boiling point at 5.1 atm. the sample appears to be quite stable.

2.3.3.11 ELO-67-51. Air Atmosphere. Thermocouple Pair T-10-compensated. 9.2°F./Min. Scan Rate. See Figure 105.

In air the decomposition of ELO-67-51 appears to follow very much the same pattern as that observed to occur under nitrogen. At 1.0 atm. while a small endotherm is observed at 613 deg. F. evaporation probably does not produce a measurable endotherm until 754 deg. F. This continues until 792 deg. F. which marks the beginning of the main boiling endotherm with peak at 810 deg. F. A small endotherm is also seen at 923 deg. F. At 5.1 atm. evaporation begins at 813 deg. F. and continues until a maximum is reached at the boiling temperature 916 deg. F. A weak exotherm at 877 deg. F. probably is the result of the same process that produced a similar peak at 878 deg. F. under nitrogen at 1.0 atm. This decomposition is probably so minor that its weak exotherm is not always sufficiently strong to be detected. No significant features are seen in the thermogram of the sample in air that are not also seen in the thermogram made under a nitrogen atmosphere.

2.4 Conclusion:

Frequent thermocouple failure was experienced during the differential thermal analysis of samples ELO-67-13, ELO-67-45 and ELO-67-51. In every case failure was found to be due to a corrosive penetration of the stainless steel thermocouple sheath. Sample ELO-67-13 seemed to be a particularly bad offender during DTA studies made at 50.0 atmospheres pressure. Presumably this effect was due to the fact that at that pressure the corrosive material was kept in contact with the thermocouple sheath for a longer time before being evaporated from the test system. Because of the high rate of thermocouple failure which was encountered with these samples studies at 50.0 atm. were discontinued.

Studies now in progress to be reported in future reports in this series comprise investigation of the thermal and oxidative degradation of fluids in the presence of metal oxides other than Fe_2O_3 , TiO_2 , Cu_2O and CuO .

ELO-67-51

AIR

9.2°F./MIN.

↑ 10 μ V ENDOTHERMIC

RUN A

1.0 ATM.

RUN B

5.1 ATM.

T-10-COMP.

FIGURE 105. DIFFERENTIAL THERMAL ANALYSIS. ELO-67-51. AIR ATMOSPHERE.

3. THERMAL STABILITY:

3.1 Introduction:

Two principal techniques are currently in common use for the evaluation of the thermal stability of fluids and lubricants. Both are variants of sealed-tube methods which have been widely used over the years for this purpose. In each case the volatile decomposition products produced by decomposition are retained in the system so as to remain in continuous contact with fluid being examined.

In one method the sample is placed in a borosilicate glass cell, dried and degassed by agitation under vacuum at elevated temperature, and sealed. The sealed tube and sample are then exposed at a selected temperature for a designated time. After exposure, the sample is cooled, removed from the tube and examined for changes in its properties. No metals or catalysts are used. The procedure for this test is described in Method 25.3 of Federal Test Method Standard 791a. The usual exposure is 24 hours at 500 deg. F. These conditions are the same as those specified in Military Specification MIL-L-23699A for Lubricating Oil, Aircraft Turbine Engines, Synthetic Base. Other conditions are possible of course. The only limitation is the stability of the fluids under study and the strength of the glass tube. Both the stability of the sample and the strength of the tube decrease significantly at temperatures above 500 deg. F. In many cases useful sample stability can be maintained at temperatures above 500 deg. F. However, the strength of the glass at that temperature is such to render such measurements fairly dangerous. Another factor of importance with respect to safety is that ester-based fluids as well as various other types can be hydrolytically unstable at very high temperatures. The presence of slight traces of water in such materials can lead to excessively high decomposition pressures which may rupture the sample tube with catastrophic results.

The second type of thermal stability measurement is that described in Military Specification MIL-H-27601A, Hydraulic Fluid, Petroleum Base, High Temperature, Flight Vehicle. The stainless steel test bomb specified in that method has far greater strength than the glass reaction tube described above.

For this reason operation at higher temperatures and the use of metal catalysts are safe as well as practical. Provision is made for the use of a pressure gauge with this test cell. In the standard apparatus used in the present investigations an additional modification has been introduced to protect against excessively high pressures which may sometimes be encountered in the evaluation of unknown experimental systems. This comprises a safety head* with rupture disc with appropriate bursting characteristics to guard both the test bomb and associated instrumentation used in the system against pressure overloads.

Evaluation of thermal stability by the method of MIL-H-27601A is customarily accomplished by the determination of changes in fluid viscosity and acidity and catalyst weight loss or gain as a result of exposure. There are no current requirements in effect which limit the pressure developed as a result of the decomposition of the sample. However, the decomposition pressure produced in the standard apparatus can be monitored. This requires the taking of multiple gauge readings. That procedure is both inconvenient and unsatisfactory in that those changes in pressure which are due to the rapid breakdown of the sample after an initial induction period may not be detected until long after they have occurred. It is the purpose of the present series of measurements to investigate the decomposition pressure phenomenon as it relates to thermal stability. For this purpose an instrumented test cell has been designed to permit the continuous recording of pressure within the system.

3.2 Apparatus and Procedures:

The standard MIL-H-27601A thermal stability test cell has been modified by the substitution of a bonded strain gauge pressure transducer** for the pressure gauge. As stated above, the cell and pressure element are protected by a safety head and rupture disc. The configuration of the system

-
- * The 2S Safety Head Manufactured by Black, Sivalis and Bryson, Inc., Kansas City, Missouri, has been found to be satisfactory.
 - ** A Model 211 pressure transducer with appropriate adapter manufactured by Norwood Division of American Standard, Monrovia, California, has been found satisfactory.

has been adjusted to minimize entrapment of overhead condensate and to permit such condensate to return to the sample bomb by a direct route. The apparatus is shown schematically in Figure 106. In other respects the apparatus and techniques employed in the current studies are identical to those stipulated by the military specification.

3.3 Results and Discussion:

In the present series of investigations the thermal stabilities of seven different fluids have been evaluated. The data are presented in Figures 107 through 115, Tables XVI through XXII. In order to determine the effect if any of changes in the geometry of the experimental system occasioned by the use of the pressure transducing element, studies in each case have been made with both the standard and the modified systems. Data for sample MLO-64-8 using the standard system have been taken from an earlier report (Reference 4) but are repeated at this time for ease of comparison. Some differences may be noted in the results obtained with the different experimental systems. It is felt however, that these represent natural experimental variations. There is no evidence to suggest the existence of systematic deviations caused by the changes in the apparatus.

Pressure vs. time plots obtained with the modified apparatus are shown in Figures 107 through 115. Even in the few systems which have been studied to date certain distinctive differences in behavior may be noted. Stable samples with low vapor pressure at the test temperature show a small initial pressure rise with little or no further increase during the course of exposure. Samples MLO-64-8 at 700 deg. F., ELO-64-68 at 700 deg. F., and ELO-66-20 at 650 deg. F. are examples. Sample ELO-66-31 at 650° and 700 deg. F., is less stable than any of the foregoing. An initial rapid increase in pressure due to sample vapor pressure is followed by a continuing rise which is indicative of moderate decomposition. The pressure measurements indicate that sample ELO-65-48 at 700 deg. F. is still less stable. At 700 deg. F. the pressure in the system containing this material rises continuously at a fairly rapid rate throughout the course of exposure.

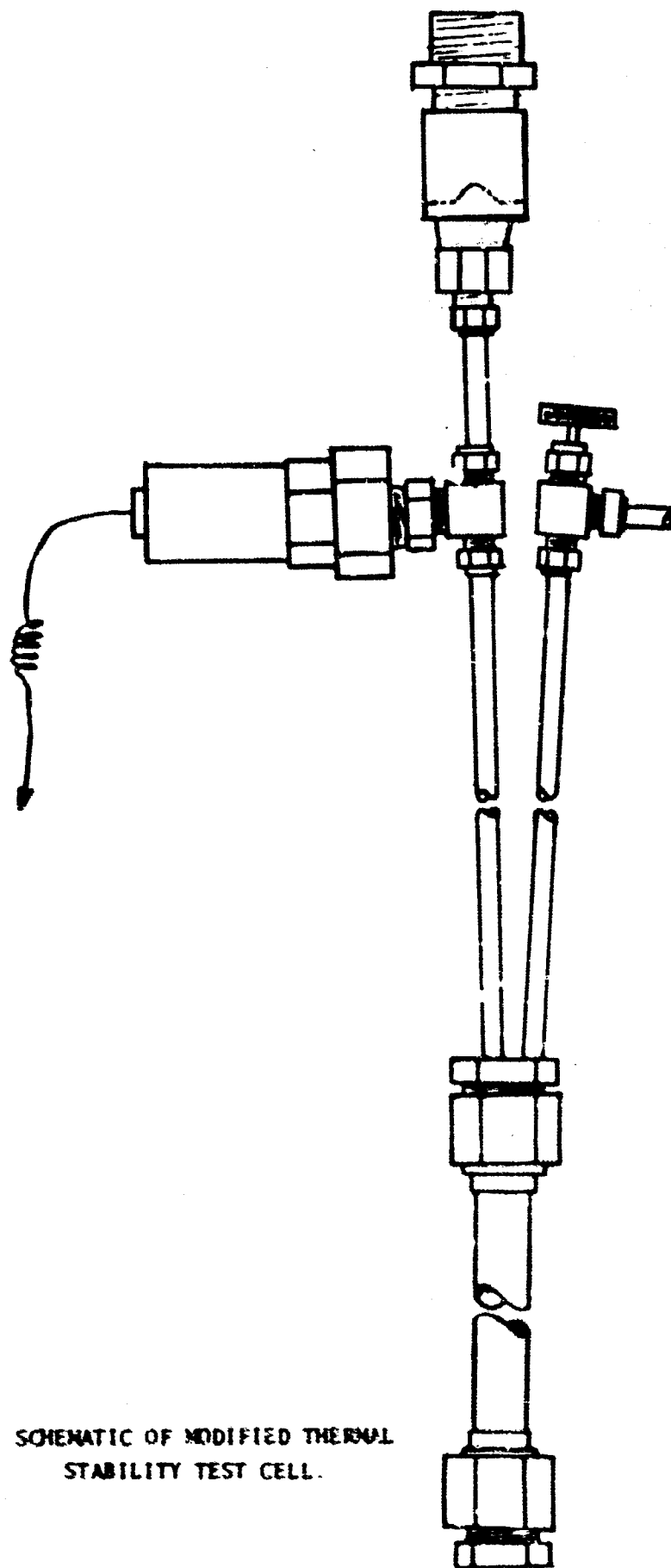


FIGURE 106. SCHEMATIC OF MODIFIED THERMAL STABILITY TEST CELL.

TABLE XVI

THERMAL STABILITY OF MLO-64-8
per MIL-B-27601A - 6 hours @ 700 deg. F.

	<u>Standard</u>	<u>Modified*</u>
Viscosity @ 100 deg. F., cs.		
Original	307.6	308.0
After exposure	302.0	304.6
% Decrease	1.8	1.1
Neutralization No., mg.KOH/g.		
Original	Less than 0.01	Less than 0.01
After exposure	Less than 0.01	0.04
Increase	0.00	0.03+
Appearance after exposure:	Cloudy	Clear, light yellow with indiscible layer
Change in Weight of Metals, mg./sq.cm:		
M-10	0.00 No change	+0.04 Moderate tarnish
Bronze	0.32 Black corrosion	+0.08 Moderate tarnish
52-100	0.06 Slight corrosion	+0.04 Moderate tarnish

* Pressure gauge replaced by pressure transducing element.

MLO-64-8 THERMAL STABILITY AT 700°F.

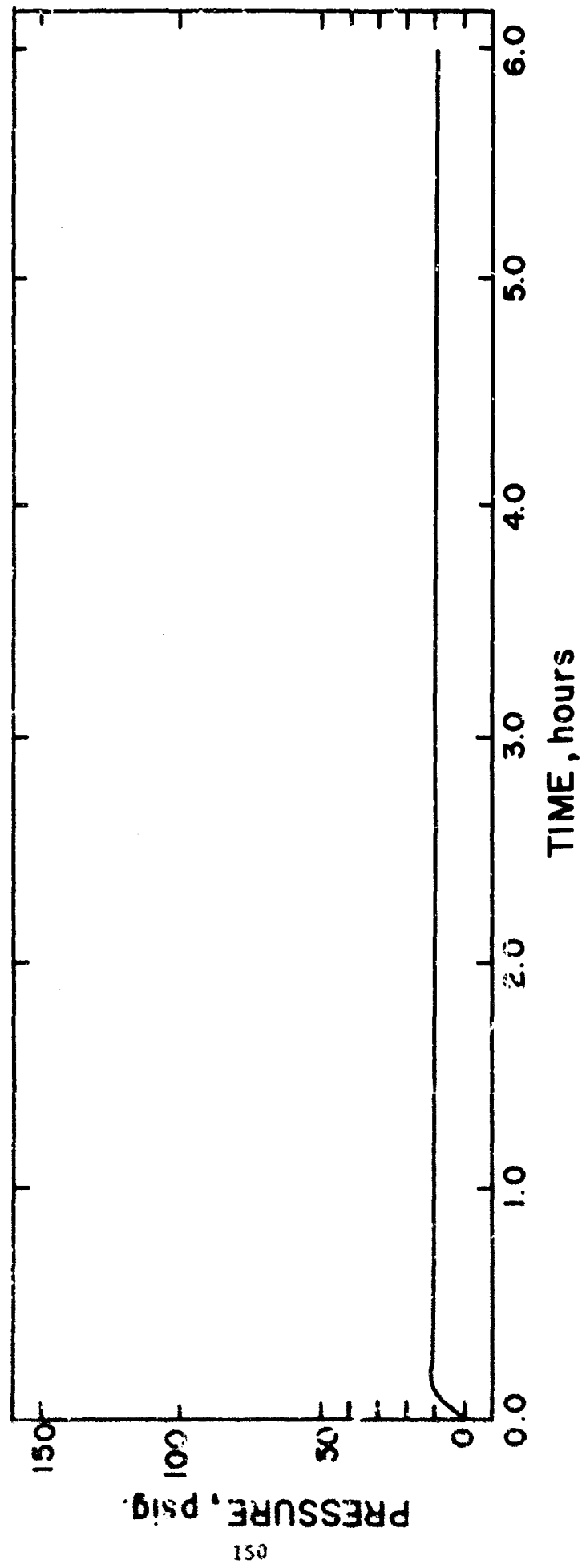


FIGURE 107. MLO-64-8. THERMAL STABILITY AT 700 DEG. F.

TABLE XVII

THERMAL STABILITY OF ELO-64-68
per MIL-H-27601A - 6 hours @ 700 deg. F.

	<u>Standard</u>	<u>Modified*</u>
Viscosity @ 100 deg. F., cs.		
Original	347.2	347.2
After exposure	338.9	345.2
% Decrease	2.4	0.6
Neutralization No., mg.KOH/g.		
Original	0.08	0.08
After exposure	0.04	0.12
Increase	-0.04	0.04
Appearance after exposure:	Slightly cloudy, yellow	Clear, light yellow
Change in Weight of Metals, mg./sq.cm:		
M-10	0.00	0.04 Slight tarnish
Bronze	0.04 Moderate tarnish	0.08 Dull tarnish
52-100	0.00	0.06 Slight tarnish

* Pressure gauge replaced by pressure transducing element.

ELO-64-68 THERMAL STABILITY AT 700°F.

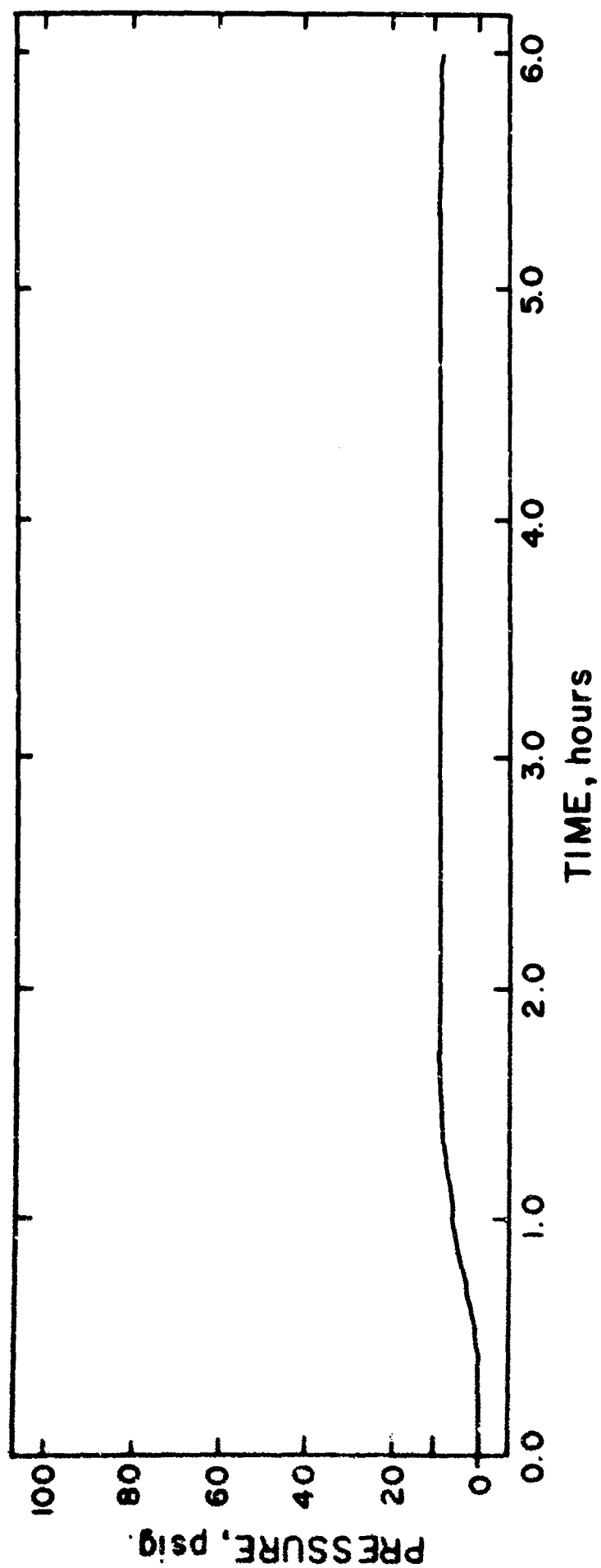


FIGURE 108. ELO-64-68. THERMAL STABILITY AT 700 DEG. F.

TABLE XVIII

THERMAL STABILITY OF ELO-65-48
per MIL-B-27601A - 6 hours @ 700 deg. F.

	<u>Standard</u>	<u>Modified*</u>
Viscosity @ 100 deg. F., cs.		
Original	15.14	15.14
After exposure	13.44	12.84
% Decrease	11.2	15.2
Neutralization No., mg.KOH/g.		
Original	0.07	0.07
After exposure	0.12	0.07
Increase	0.05	0.00
Appearance after exposure:	Slightly cloudy, yellow	Cloudy, pale yellowish gray with immiscible layer
Change in Weight of Metals, mg./sq.cm:		
M-10	0.00	0.00 Iridescent
Bronze	0.04 Moderate tarnish	0.06 Slight tarnish
52-100	0.00	0.00 Iridescent

* Pressure gauge replaced by pressure transducing element.

ELO-65-48 THERMAL STABILITY AT 700°F.

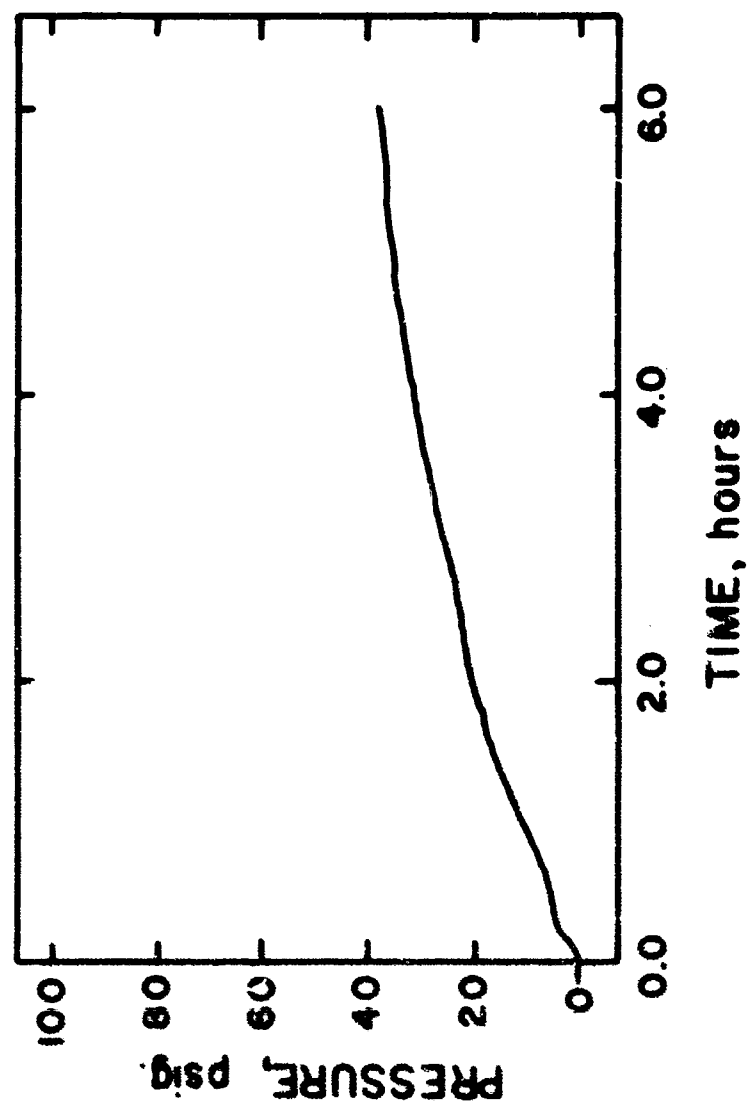


FIGURE 109. ELO-65-48. THERMAL STABILITY AT 700 DEG. F.

TABLE XIX

THERMAL STABILITY OF ELO-66-20
per MIL-H-27601A - 6 hours @ 650 deg. F.

	<u>Standard</u>	<u>Modified*</u>
Viscosity @ 100 deg. F., cs.		
Original	326.4	326.4
After exposure	314.6	315.1
% Decrease	3.5	3.5
Neutralization No., mg.KOH/g.		
Original	0.22	0.22
After exposure	0.73	0.77
Increase	0.56	0.55
Appearance after exposure:	Clear, brown	Clear, brown
Change in Weight of Metals, mg./sq.cm:		
M-10	0.00 Slight tarnish	0.00 Slight tarnish
Bronze	+0.06 Moderate tarnish	+0.04 Moderate tarnish
52-100	0.00 Slight tarnish	0.00 Slight tarnish

* Pressure gauge replaced by pressure transducing element.

ELO-66-20 THERMAL STABILITY AT 650°F.

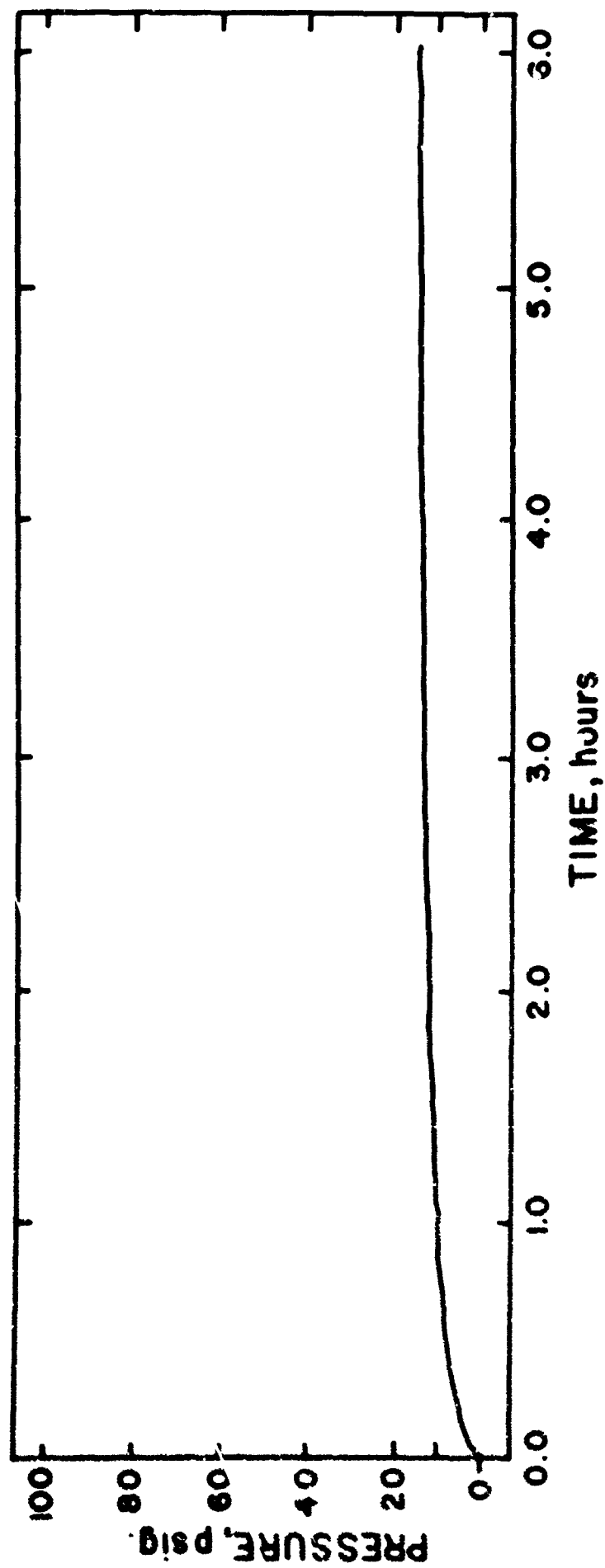


FIGURE 110. ELO-66-20. THERMAL STABILITY AT 650 DEG. F.

TABLE XX

THERMAL STABILITY OF ELO-66-31
per MIL-H-27601A - 6 hours @ 600 deg. F.

	<u>Standard</u>	<u>Modified*</u>
Viscosity @ 100 deg. F., cs.		
Original	4.67	4.67
After exposure	4.76	4.76
% Increase	1.9	1.9
Neutralization No., mg.KOH/g.		
Original	Less than 0.01	Less than 0.01
After exposure	0.01	0.01
Increase	0.01	0.01
Appearance after exposure:		
	Water white, clear	Water white, clear
Change in Weight of Metals, mg./sq.cm.		
M-10	0.00 No change	0.00 No change
Bronze	+0.04 Moderate tarnish	+0.02 Moderate tarnish
52-100	0.00 No change	0.00 No change

* Pressure gauge replaced by pressure transducing element.

ELO-66-31 THERMAL STABILITY AT 600°F.

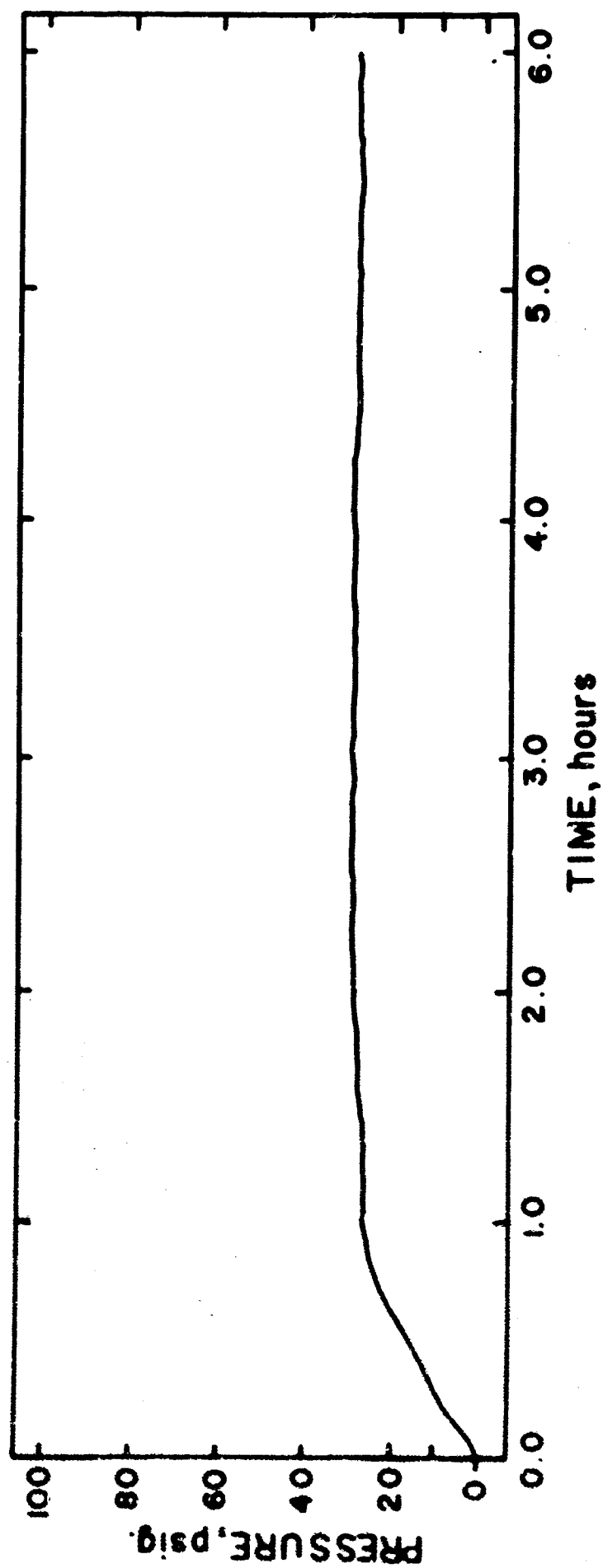


FIGURE 111. ELO-66-31. THERMAL STABILITY AT 600 DEG. F.

TABLE XX-CONTINUED

THERMAL STABILITY OF EIO-66-31
per MIL-H-27801A - 2 hours @ 650 deg. F.

	<u>Standard</u>	<u>Modified*</u>
Viscosity @ 100 deg. F., cs.		
Original	4.67	4.67
After exposure	4.65	4.67
% Decrease	0.4	0.0
Neutralization No., mg.KOE/g.		
Original	Less than 0.01	Less than 0.01
After exposure	0.01	0.01
Increase	0.01	0.01
Appearance after exposure:		
	Clear, pale yellow	Clear, pale yellow
Change in Weight of Metals, mg./sq.cm:		
M-10	0.00 No change	0.00 No change
Bronze	+0.02 Moderate tarnish	+0.06 Moderate tarnish
52-100	0.00 No change	0.00 No change

* Pressure gauge replaced by pressure transducing element.

ELO-66-31 THERMAL STABILITY AT 650°F.

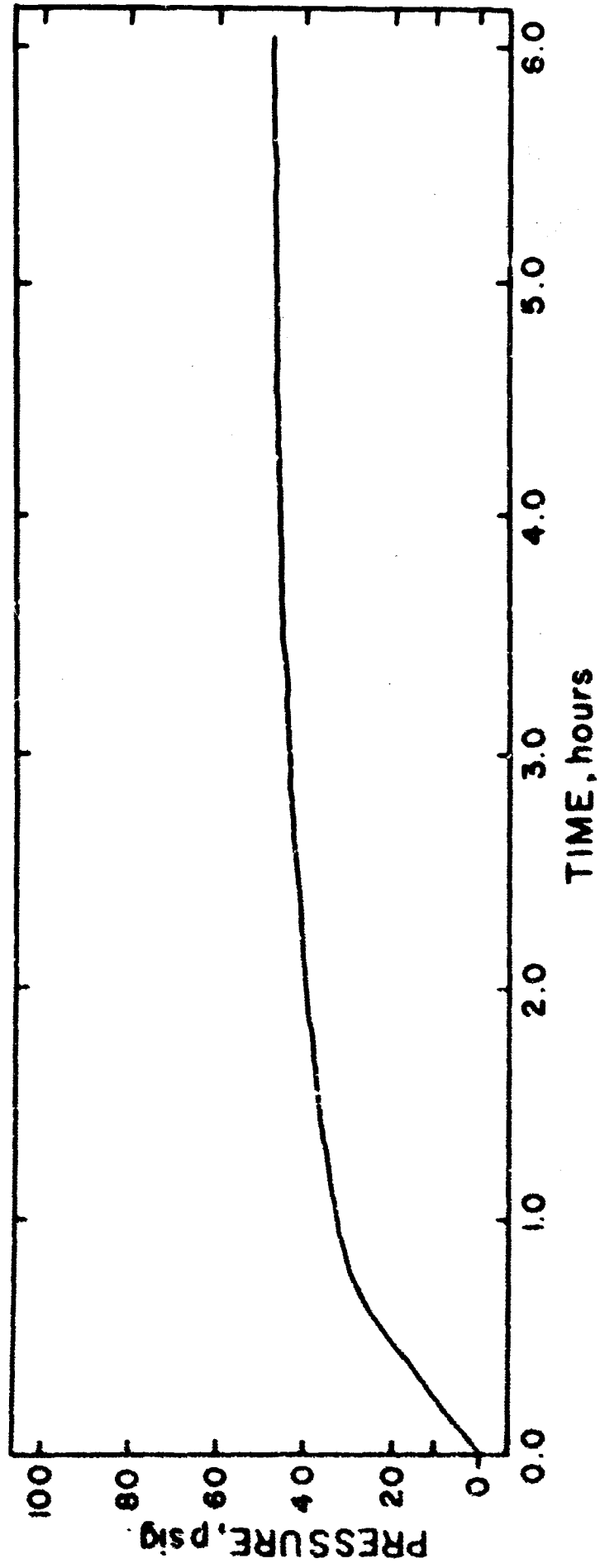


FIGURE 112. THERMAL STABILITY AT 650 DEG. F.

TABLE XX-CONTINUED

THERMAL STABILITY OF ELO-66-31
per MIL-H-27601A - 6 hours @ 700 deg. F.

	<u>Standard</u>	<u>Modified*</u>
Viscosity @ 100 deg. F., cs.		
Original	4.67	4.67
After exposure	4.80	4.70
% Increase	2.8	2.6
Neutralization No., mg.KOH/g.		
Original	Less than 0.01	Less than 0.01
After exposure	0.02	0.03
Increase	0.01	0.02
Appearance after exposure:	Clear, pale yellow	Clear, pale yellow
Change in Weight of Metals, mg./sq.cm:		
M-10	0.00 No change	0.00 No change
Bronze	+0.04 Moderate tarnish	+0.02 Moderate tarnish
52-100	0.00 No change	0.00 No change

* Pressure gauge replaced by pressure transducing element.

ELO-66-31 THERMAL STABILITY AT 700°F.

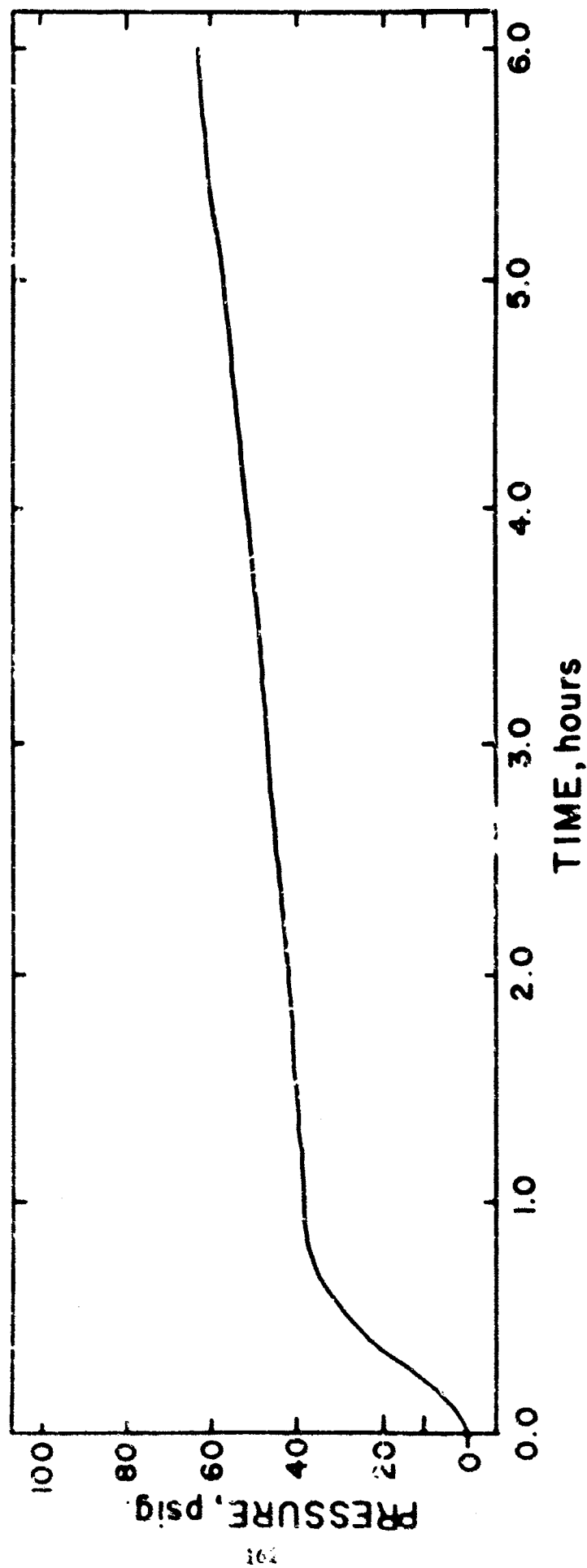


FIGURE 113. ELO-66-31. THERMAL STABILITY AT 700 DEG. F.

TABLE XXI

THERMAL STABILITY OF ELO-66-51
per MIL-H-27014 - 6 hours @ 700 deg. F.

	<u>Standard</u>	<u>Modified*</u>
Viscosity @ 100 deg. F., cs.		
Original	26.20	26.20
After exposure	26.06	26.00
% Decrease	0.5	0.8
Neutralization No., mg.KOH/g.**		
Original	33.4	33.4
After exposure	44.0	41.2
Increase	10.6	7.8
Appearance after exposure:	Clear, dark grayish brown	Clear, dark grayish brown
Change in Weight of Metals, mg./sq.cm:		
M-10	0.00 Slight tarnish	+0.02 Slight tarnish
Bronze	+0.08 Brown	+0.08 Brown
52-100	+0.04 Slight tarnish	0.00 Slight tarnish

* Pressure gauge replaced by pressure transducing element.

** Sample was immiscible in titration solvent. Best repeatability was obtained at high stirring rates.

ELO-66-51 THERMAL STABILITY AT 700°F.

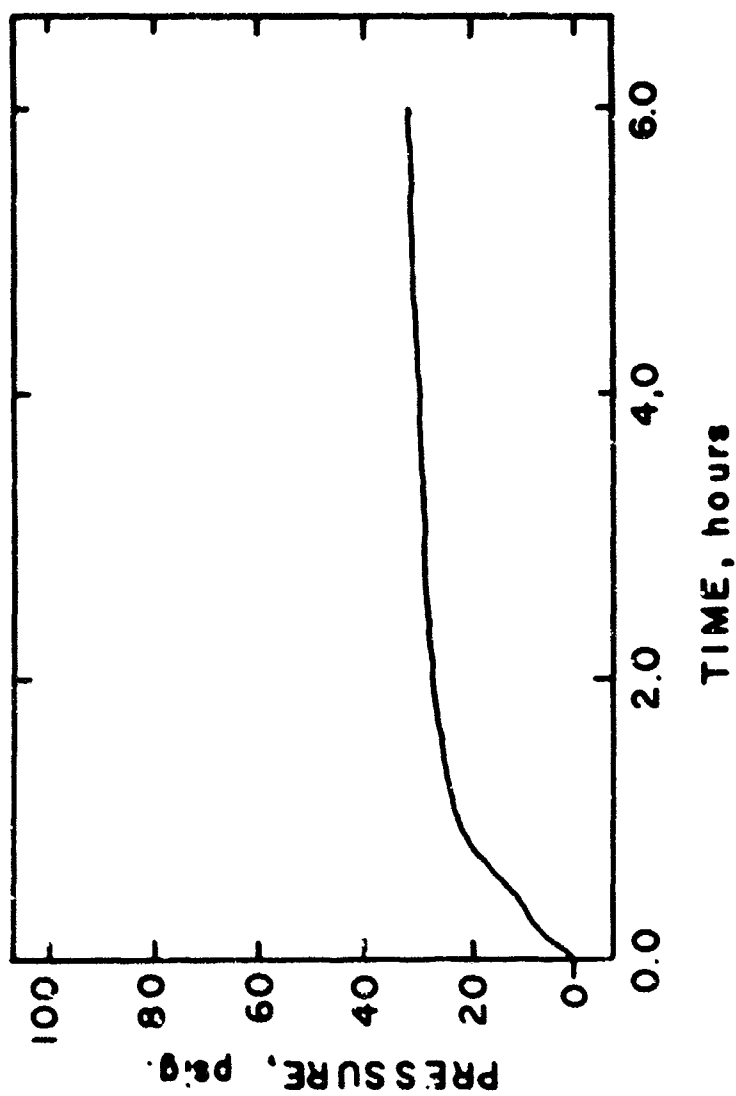


FIGURE 114. ELO-66-51. THERMAL STABILITY AT 700 DEG. F.

TABLE XXII

THERMAL STABILITY OF ELO-67-49
per MIL-H-27601A - 6 hours @ 700 deg. F.

	<u>Standard</u>	<u>Modified*</u>
Viscosity @ 100 deg. F., cs.		
Original	16.84	16.84
After exposure	12.36	12.42
% Decrease	26.6	26.2
Neutralization No., mg.KOH/g.		
Original	0.06	0.06
After exposure	0.06	0.09
Increase	0.00	+0.03
Appearance after exposure:	Slightly cloudy, light brown	Slightly cloudy, light brown
Change in Weight of Metals, mg./sq.cm:		
M-10	0.00 Slight change	0.00 Slight change
Bronze	0.08 Light brown	+0.12 Light brown
52-100	0.00 Slight change	0.00 Slight change

* Pressure gauge replaced by pressure transducing element.

ELO-67-49 THERMAL STABILITY AT 700°F.

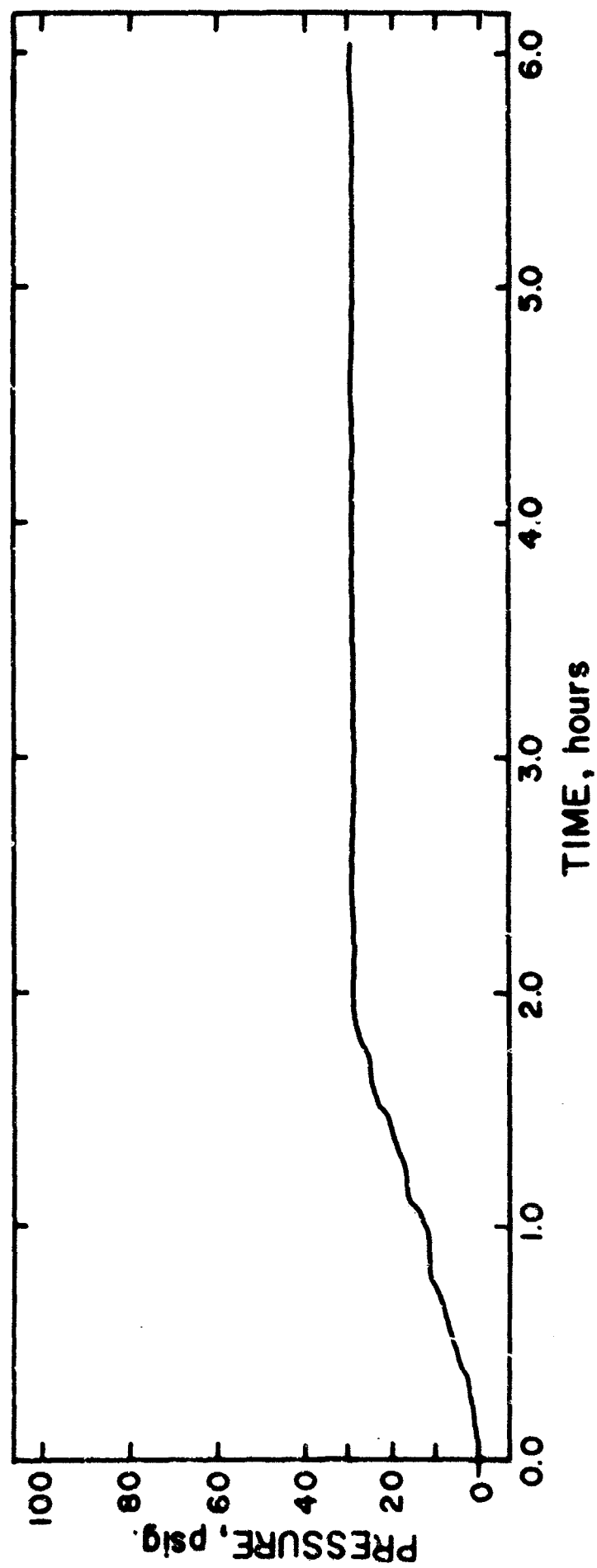


FIGURE 115. ELO-67-49. THERMAL STABILITY AT 700 DEG. F.

On the basis of the foregoing data, it is obvious that the addition of a continuous pressure measurement capability to the thermal stability apparatus provides much useful information. While sufficient data to permit any firm conclusions are not yet available at this stage of the investigation, it may ultimately be revealed that some systems which are apparently stable from the standpoint of corrosiveness and bulk fluid properties may be found to be unsatisfactory by the criterion of pressure build-up. Rate of pressure build-up is an alternate criterion for evaluation of stability. None of the samples studied thus far suffered catastrophic breakdown after an initial period of apparent relative stability. The existence of such induction periods prior to decomposition is common in the case of oxidative degradation and may prove to be of importance with respect to thermal decomposition as well.

4. CHEMICAL AND PHYSICAL PROPERTIES OF EXPERIMENTAL LUBRICANTS

Tables XXIII through XLIV and Figure 116 summarize chemical and physical measurements made during the current reporting period on a variety of experimental fluids and greases.

5. FUTURE WORK

The fixation of atmospheric nitrogen by combination with oxygen in a spark discharge or an active surface at elevated temperatures is a well known phenomenon. That this occurs in automotive internal combustion engines is a primary cause of the air pollution due to that source. The interaction of such nitrogen oxides with lubricating fluids has been used as an index of lubricant degradation by L. Gardner. (Reference 7) That author made quantitative measurements of infrared absorption in the 6.1 micron region to determine the extent of formation of organic nitrates produced by interaction with nitrogen oxides in blow-by gases. The results of that work suggest the possibility of extending the scope of current corrosion and oxidation stability tests through the artificial introduction of small amounts

of nitrogen oxides to the air stream bubbled through the samples. This could easily be accomplished through the use of a controlled spark discharge in the entering air stream. Such a modification would provide an additional variable in the corrosion-oxidation testing program which would permit the simulation of actual operating conditions more nearly than is now possible.

While nitrogen fixation may be of greatest importance in reciprocating internal combustion engines using gasoline fuels, it seems likely that it can occur to some degree in any engine system. For this reason it is felt that an initial investigation of nitrogen fixation in various lubricating fluids should be made and, depending on the results of such an investigation, a study of the effects of nitrogen oxides on corrosion-oxidation tests should follow.

REFERENCES:

1. A. A. Krawetz, et al, Technical Documentary Report ASD-TDR-63-220, Physical and Chemical Properties of Fuels and Lubricants, Directorate of Materials and Processes, Aeronautical Systems Division, Air Force Systems Command, Wright-Patterson Air Force Base, Ohio, March 1963.
2. A. A. Krawetz, et al, Technical Documentary Report ML-TDR-64-27, Physical and Chemical Properties of Lubricants, Air Force Materials Laboratory, Research and Technology Division, Air Force Systems Command, Wright-Patterson Air Force Base, Ohio, March 1964.
3. A. A. Krawetz, et al, Technical Documentary Report AFML-TR-65-76, Physical and Chemical Properties of Lubricants, Air Force Materials Laboratory, Research and Technology Division, Air Force Systems Command, Wright-Patterson Air Force Base, Ohio, March 1965.
4. A. A. Krawetz, et al, Technical Documentary Report AFML-TR-66-27, Physical and Chemical Properties of Lubricants, Air Force Materials Laboratory, Research and Technology Division, Air Force Systems Command, Wright-Patterson Air Force Base, Ohio, February 1966.
5. A. A. Krawetz, et al, Technical Documentary Report AFML-TR-67-133, Part I, Physical and Chemical Properties of Fluids, Lubricants and Related Materials, Air Force Materials Laboratory, Directorate of Laboratories, Air Force Systems Command, Wright-Patterson Air Force Base, Ohio, March 1967.
6. R. E. Dolle, et al, Technical Documentary Report AFML-TR-65-358, Chemical, Physical and Engineering Performance Characteristics of a New Family of Perfluorinated Fluids, Air Force Materials Laboratory, Research and Technology Division, Air Force Systems Command, Wright-Patterson Air Force Base, Ohio, September 1965.
7. L. Gardner, Canadian Spectroscopy, 11 (1961).

TABLE XXIII

SAMPLE NUMBER MLO-64-4

Specification MIL-H-5606B

Flash Point, deg. F.	435
Fire Point, deg. F.	500
Copper Strip Corrosion (72 hours @ 250 deg. F.)	Moderate tarnish-2B
Pour Point, deg. F.	35 below 0
Rubber Swelling, % ("I" Rubber)	14.43
Evaporation Test (4 hours @ 150 deg. F.)	Passes - Oily, not hard or tacky
Specific Gravity @ 60/60 deg. F.	0.8862
Spontaneous Ignition Temperature, deg. F. (ASTM D 286)	680*

* Moderate amount of carbonaceous residue

FOAMING TEST

Temperature	Foaming Tendency: Foam volume, ml. at end of 5 min. blowing period	Foam Stability: Foam volume, ml. at end of 10 min. settling period
75 deg. F.	540	50 ml. after 10 minutes
200 deg. F.	45	30 ml. after 10 minutes
75 deg. F.	500	5 ml. after 10 minutes

TABLE XXIII-CONTINUED

SAMPLE NUMBER MLO-64-4

CORROSION AND OXIDATION STABILITY TEST
168 hours @ 250 deg. F. - MIL-H-5606B*

Tests on the Original Oil:

Viscosity @ 130 deg. F., cs.	34.64
Neutralization No., mg.KOH/g.	0.03

Tests on the Oxidized Oil:

Viscosity @ 130 deg. F., cs.	34.97
Neutralization No., mg.KOH/g.	0.07
Evaporation Loss, %	0.83
Appearance after oxidation:	Straw color; no precipitate
Increase in Viscosity, %	1.0
Increase in Neutralization No., mg.KOH/g.	0.04

Loss of Weight of Metals, mg./sq.cm:

Magnesium	0.00
Aluminum	0.00
Copper	0.00 **
Cadmium	0.00
Steel	0.00

* Air flow 5 ± 0.5 liters/hour. With reflux.

** Moderate tarnish-2E

TABLE XXIV

SAMPLE NUMBER MLO-34-5

Specification MIL-H-5606B

Flash Point, deg. F.	340
Fire Point, deg. F.	360
Copper Strip Corrosion (72 hours @ 250 deg. F.)	Moderate tarnish-2B
Pour Point, deg. F.	60 below 0
Rubber Swelling, % ("L" Rubber)	7.91
Evaporation Test (4 hours @ 150 deg. F.)	Passes - Oily, not hard or tacky
Specific Gravity @ 60/60 deg. F.	0.8804
Spontaneous Ignition Temperature, deg. F. ASTM D 286	640*

* Light carbonaceous residue

FOAMING TEST

<u>Temperature</u>	<u>Foaming Tendency: Foam volume, ml. at end of 5 min. blowing period</u>	<u>Foam Stability: Foam volume, ml. at end of 10 min. settling period</u>
75 deg. F.	515	10 ml. after 10 minutes
200 deg. F.	50	30 ml. after 10 minutes
75 deg. F.	490	15 ml. after 10 minutes

TABLE XXIV-CONTINUED

SAMPLE NUMBER MLO-64-S

CORROSION AND OXIDATION STABILITY TEST
168 hours @ 250 deg. F. - MIL-B-5606B*

Tests on the Original Oil:

Viscosity @ 130 deg. F., cs.	34.67
Neutralization No., mg.KOH/g.	0.09

Tests on the Oxidized Oil:

Viscosity @ 130 deg. F., cs.	45.74
Neutralization No., mg.KOH/g.	0.14
Evaporation Loss, %	0.72
Appearance after oxidation:	Moderate amber; no precipitate
Increase in Viscosity, %	31.9
Increase in Neutralization No., mg.KOH/g.	0.05

Loss of Weight of Metals, mg./sq.cm:

Magnesium	0.00
Aluminum	0.00
Copper	0.06 **
Chromium	0.07
Steel	0.00

- * Air flow 5 ± 0.5 liters/hour. With reflux.
** Dark tarnish-3A

TABLE XXV

SAMPLE NUMBER FLO-66-20

Evaporation, % (6½ hours @ 400 deg. I.)	21.5
Pour Point, deg. F.	10
Kinematic Viscosity @ 130 deg. F., cs.	112.13
Kinematic Viscosity @ 400 deg. F., cs.	1.42

TABLE XV-CONTINUED

SAMPLE NUMBER ELO-66-20

HYDROLYTIC STABILITY TEST
MIL-H-8445B - 48 hours @ 200 deg. F.

Corrosion:

1. Loss of weight of copper, mg./sq.cm:
 - a. Before brushing 1.23
 - b. After brushing 1.23
2. Appearance of copper:
 - a. Before brushing Slight etching
 - b. After brushing Slight etching

Resistance to Hydrolysis:

1. Viscosity @ 100 deg. F., cs.
 - a. Original sample 326.4
 - b. After test 325.4
 - c. % change -0.3
2. Neutralization No., mg.KOH/g:
 - a. Water layer 0.05
 - b. Organic layer
 - Original 0.22
 - After test 27.50
 - Increase 27.28
3. Insoluble material in oil layer, % 0.29
4. Color Lighter than 0.5

TABLE XXVI

	<u>SAMPLE NUMBER</u> <u>ELO-55-24</u>	<u>SAMPLE NUMBER</u> <u>ELO-55-25</u>
Kinematic Viscosity:		
@ 130 deg. F.	119.26	116.99
@ 210 deg. F.	15.25	15.06
@ 400 deg. F.	1.44	1.49

TABLE XXVII

SAMPLE NUMBER ELO-66-30

RUBBER DETERIORATION TEST
168 hours at 275 degrees F.
MIL-H-5606B

% swelling (shrinkage) of "L" Stock Rubber Specimens 7.45

DUROMETER HARDNESS

Durometer Hardness Before Test 72
Durometer Hardness After Test 74

ELONGATION

Elongation Before Test, in. 2.53
Elongation After Test, in.
 1st specimen 0.9
 2nd specimen 0.9
 3rd specimen 0.8
 Average 0.87
 Decrease 65.6

TENSILE STRENGTH

Tensile Strength Before Test, psi 3,084
Tensile Strength After Test, psi:
 1st specimen 1,426
 2nd specimen 1,577
 3rd specimen 1,366
 Average 1,456
 Decrease, % 52.78

TABLE XXVII-CONTINUED

SAMPLE NUMBER ELO-66-30

RUBBER DETERIORATION TEST
168 hours at 275 degrees F.
MIL-H-5606B

% swelling of "RAK-3" (labeled no post cure) Stock Rubber Specimens 3.36

DUROMETER HARDNESS

Durometer Hardness Before Test 85
Durometer Hardness After Test 89

ELONGATION

Elongation Before Test, in. 1.8
Elongation After Test, in:
 1st specimen 1.5
 2nd specimen 1.2
 3rd specimen 1.5
 Average 1.4
 Decrease 22.2

TENSILE STRENGTH

Tensile Strength Before Test, psi 2,387
Tensile Strength After Test, psi:
 1st specimen 1,877
 2nd specimen 1,651
 3rd specimen 1,877
 Average 1,801
 Decrease, % 24.6

TABLE XXVII-CONTINUED

SAMPLE NUMBER ELO-66-30

RUBBER DETERIORATION TEST
168 hours at 275 degrees F.
MIL-H-5606B

% swelling of "RAK-26" (labeled no post cure) Stock Rubber Specimens	0.36
% shrinkage of "RAK-26" (labeled no post cure) Stock Rubber Specimens	
1st specimen	0.50
2nd specimen	2.60

DUROMETER HARDNESS

Durometer Hardness Before Test	85
Durometer Hardness After Test	89

ELONGATION

Elongation Before Test, in.	2.0
Elongation After Test, in:	
1st specimen	1.3
2nd specimen	1.4
3rd specimen	1.3
Average	1.3
Decrease	35.0

TENSILE STRENGTH

Tensile Strength Before Test, psi	2,177
Tensile Strength After Test, psi:	
1st specimen	1,832
2nd specimen	1,802
3rd specimen	1,727
Average	1,787
Decrease, %	17.9

TABLE XXVII-CONTINUED

SAMPLE NUMBER KLO-66-30

RUBBER DETERIORATION TEST
168 hours at 275 degrees F.
MIL-H-5606B

% swelling of "RAK-26" (labeled post cure) Stock Rubber Specimens 0.36

% shrinkage of "RAK-26" (labeled post cure) Stock Rubber Specimens

1st specimen	5.56
2nd specimen	0.15

DUROMETER HARDNESS

Durometer Hardness Before Test	86
Durometer Hardness After Test	87

ELONGATION

Elongation Before Test, in.	1.4
Elongation After Test, in:	
1st specimen	1.4
2nd specimen	0.9
3rd specimen	1.6
Average	1.3
Decrease	7.2

TENSILE STRENGTH

Tensile Strength Before Test, psi	1,952
Tensile Strength After Test, psi:	
1st specimen	1,772
2nd specimen	1,486
3rd specimen	1,892
Average	1,716
Decrease, %	12.1

TABLE XXVIII

SAMPLE NUMBER ELO-66-34

RTD Panel Coking Test, mg. deposit

1308

CORROSION AND OXIDATION STABILITY TEST
72 hours @ 347 deg. F. - MIL-L-007808F*

Tests on the Original Oil:

Viscosity @ 100 deg. F., cs.	62.91
Neutralization No., mg.KOH/g.	0.04

Tests on the Oxidized Oil:

Viscosity @ 100 deg. F., cs.	89.62
Neutralization No., mg.KOH/g.	6.20
Evaporation Loss, %	1.00
Appearance after oxidation:	Dark reddish brown; no precipitate
Increase in Viscosity, %	42.4
Increase in Neutralization No., mg.KOH/g.	6.16
Sludge retained on 10 micron millipore filter, mg./100 ml.	**

Loss of Weight of Metals, mg./sq.cm:

Magnesium	9.38 ***
Aluminum	0.00
Copper	0.40 ****
Silver	0.01 *****
Steel	0.00 *****

- * Air flow 5 \pm 0.5 liters/hour. With reflux.
- ** Cannot be filtered thru 10 micron filter.
- *** Dull gray-etched.
- **** Bright etching.
- ***** Light brown stain.
- ***** Gold.

TABLE XXVIII-CONTINUED

SAMPLE NUMBER ELO-66-34

CORROSION AND OXIDATION STABILITY TEST
72 hours @ 400 deg. F. - MIL-L-007808F*

Tests on the Original Oil:

Viscosity @ 100 deg. F., cs.	62.91
Viscosity @ 210 deg. F., cs.	9.17
Neutralization No., mg.KOH/g.	0.04

Tests on the Oxidized Oil:

Viscosity @ 100 deg. F., cs.	91.59
Viscosity @ 210 deg. F., cs.	11.83
Neutralization No., mg.KOH/g.	4.24
Evaporation Loss, %	1.65
Appearance after oxidation:	Dark brown; moderate precipitate
Increase in Viscosity @ 100 deg. F., %	45.6
Increase in Viscosity @ 210 deg. F., %	29.0
Increase in Neutralization No., mg.KOH/g.	4.20
Sludge retained on 10 micron millipore filter, mg./100 ml.	**

Loss of Weight of Metals, mg./sq.cm:

Magnesium	13.32 ***
Aluminum	0.0
Copper	1.19 ****
Silver	0.02 *****
Steel	0.00 *****

* Air flow 5 ±0.5 liters/hour. With reflux.

** Cannot be filtered thru 10 micron filter.

*** Dull gray-etched.

**** Bright etching.

***** Light gold.

***** Gold and blue.

TABLE XXVIII-CONTINUED

SAMPLE NUMBER ELO-66-34

CORROSION AND OXIDATION STABILITY TEST*
48 hours @ 400 deg. F.**

Tests on the Original Oil:

Viscosity @ 100 deg. F., cs.	62.91
Viscosity @ 210 deg. F., cs.	9.17
Neutralization No., mg.KOH/g.	0.04

Tests on the Oxidized Oil:

Viscosity @ 100 deg. F., cs.	2015
Viscosity @ 210 deg. F., cs.	80.7
Neutralization No., mg.KOH/g.	15.10
Evaporation Loss, %	3.69
Appearance after oxidation:	Dark brown; very viscous
Increase in Viscosity @ 100 deg. F., %	3100
Increase in Viscosity @ 210 deg. F., %	780
Increase in Neutralization No., mg.KOH/g.	15.06
Sludge retained on 10 micron millipore filter, mg./100 ml.	***

Loss of Weight of Metals, mg./sq.cm:

Aluminum	(QQ-A-355)	0.00
Titanium	(MIL-T-CC9046B, 5% Mn)	0.00 ****
Silver	(MIL-S-13282)	0.1 *****
Steel	(Tool Steel-Type M-10)	0.00 ****
Copper	(QQ-C-576)	1.51 *****
Magnesium	(QC-M-44)	0.00

- * Washers in same configuration as in Micro Corrosion Oxidation.
- ** Air flow 130-150 liters/hour. Without reflux.
- *** Cannot be filtered thru 10 micron filter.
- **** Gold.
- ***** light gold.
- ***** Bright etching.

TABLE XXIX

SAMPLE WLFER ELO-86-51

Pour Point, deg. F.	46
Kinematic Viscosity:	
@ 50 deg. F., cs.	161.5
@ 100 deg. F., cs.	26.2
@ 130 deg. F., cs.	11.7
@ 210 deg. F., cs.	2.7
@ 400 deg. F., cs.	1.3
Neutralization Number, mg.KOH/g.	33.4
Flash Point, deg. F. (Cleveland Open Cup)	"
Specific Gravity @ 60/60 deg. F.	1.8895
Spontaneous Ignition Temperature, deg. F.	
ASTM D 286	1000+
Evaporation Test (6½ hours @ 400 deg. F.)	100
* Up to 570 deg. F. no flash point observed. At this temperature the sample boiled, leaving the bulb of the thermometer exposed.	

TABLE XXIX-CONTINUED

SAMPLE NUMBER ELO-65-51

HYDROLYTIC STABILITY TEST
MIL-H-8446B - 48 hours @ 200 deg. F.

Corrosion:

1. Loss of weight of copper, mg./sq.cm:
 - a. Before brushing 0.23
 - b. After brushing 0.23
2. Appearance of copper:
 - a. Before brushing Dark tarnish-3E
 - b. After brushing Dark tarnish-3E

Resistance to Hydrolysis:

1. Viscosity @ 100 deg. F., cs.
 - a. Original sample 25.20
 - b. After test 26.21
 - c. % change +6.63
2. Neutralization No., mg.KOH/g:
 - a. Water layer 3.45
 - b. Organic layer
 - Original 33.4
 - After test 27.5
 - Decrease 5.9
3. Insoluble material in oil layer, % 1.003
4. Color Lighter than 1.5

TABLE XXIX-CONTINUED

SAMPLE NUMBER LSC-66-51

VAPOR PRESSURE BY ISOTENISCOPE

<u>Temperature, deg. F.</u>	<u>P, mm Hg</u>
20	0.1 ₅
250	0.8
300	3.6
350	13.3
400	43
450	110
500	265
550	620
575	890

No decomposition was observed.

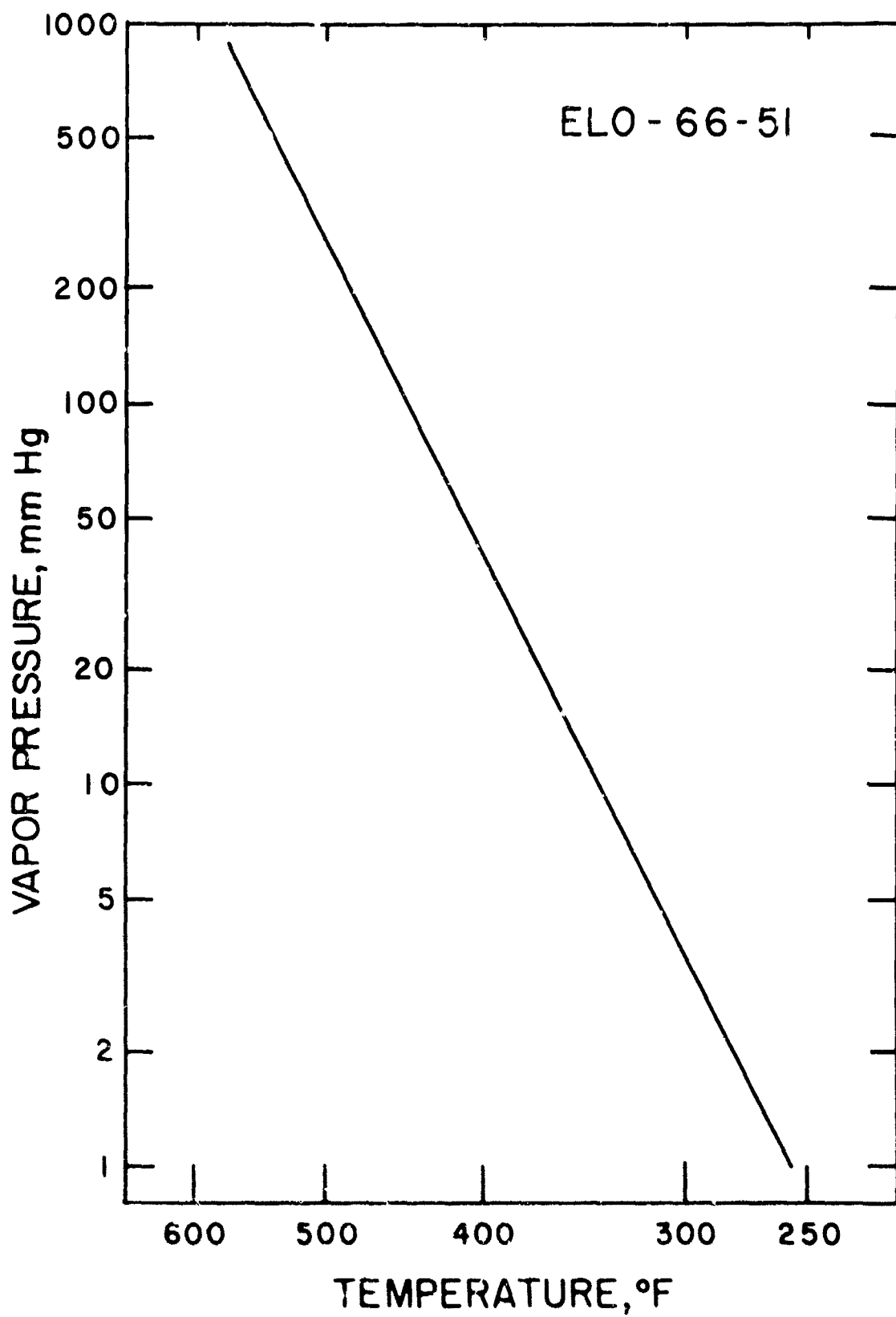


FIGURE 116. VAPOR PRESSURE OF ELO-66-51.

TABLE XXX

SAMPLE NUMBER ELO-66-109

Kinematic Viscosity, ASTM D 445-65.

a. @ 20 deg. F., cs.	2703
b. @ 100 deg. F., cs.	71.98
c. @ 210 deg. F., cs.	7.58

Flash Point, deg. F. (Cleveland Open Cup) 410

Fire Point, deg. F. 470

Pour Point, deg. F. 25 below 0

Spontaneous Ignition Temperature, deg. F.
(ASTM D 286) 685

Copper Strip Corrosion (72 hours @ 250 deg. F.)
MIL-H-5606B Dark tarnish-3B

Rubber Swelling, % ("L" Stock, MIL-H-5606B) 10.26

TABLE XXX-CONTINUED

SAMPLE NUMBER ELO-66-109

CORROSION AND OXIDATION STABILITY TEST
168 hours @ 250 deg. F. - MIL-H-5606B*

Tests on the Original Oil:

Viscosity @ 130 deg. F., cs.	31.88
Neutralization No., mg.KOH/g.	Less than 0.01

Tests on the Oxidized Oil:

Viscosity @ 130 deg. F., cs.	32.28
Neutralization No., mg.KOH/g.	0.04
Evaporation Loss, %	0.59
Appearance after oxidation:	Very light amber; no precipitate
Increase in Viscosity, %	1.3
Increase in Neutralization No., mg.KOH/g.	0.03+

Loss of Weight of Metals, mg./sq.cm:

Magnesium	0.00
Aluminum	0.00
Copper	0.00 **
Cadmium	0.01
Steel	0.00

* Air flow 5 ± 0.5 liters/hour. With reflux.
** Moderate tarnish-2E.

TABLE XXXI

SAMPLE NUMBER ELO-66-117

CORROSION AND OXIDATION STABILITY TEST
72 hours @ 347 deg. F. - MIL-L-007808F*

Tests on the Original Oil:

Viscosity @ 100 deg. F., cs.	62.73
Neutralization No., mg.KOH/g.	0.03

Tests on the Oxidized Oil:

Viscosity @ 100 deg. F., cs.	70.43
Neutralization No., mg.KOH/g.	2.39
Evaporation Loss, %	1.11
Appearance after oxidation:	Dark reddish brown; no precipitate
Increase in Viscosity, %	12.3
Increase in Neutralization No., mg.KOH/g.	2.36
Sludge retained on 10 micron millipore filter, mg./100 ml.	0.14

Loss of Weight of Metals, mg./sq.cm:

Magnesium	0.00
Aluminum	0.00
Copper	0.10 **
Silver	0.02 ***
Steel	0.00 ****

* Air flow 5 ± 0.5 liters/hour. With reflux.

** Moderate tarnish-2E, etched.

*** Light gold.

**** Purple and gold.

TABLE XXXI-CONTINUED

SAMPLE NUMBER ELO-66-117

CORROSION AND OXIDATION STABILITY TEST
72 hours @ 400 deg. F. - MIL-L-007808F*

Tests on the Original Oil:

Viscosity @ 100 deg. F., cs.	62.73
Viscosity @ 210 deg. F., cs.	9.14
Neutralization No., mg.KOH/g.	3.03

Tests on the Oxidized Oil:

Viscosity @ 100 deg. F., cs.	31.42
Viscosity @ 210 deg. F., cs.	11.00
Neutralization No., mg.KOH/g.	4.05
Evaporation Loss, %	2.53
Appearance after oxidation:	Dark brown; moderate precipitate
Increase in Viscosity @ 100 deg. F., %	29.8
Increase in Viscosity @ 210 deg. F., %	20.7
Increase in Neutralization No., mg.KOH/g.	4.02
Sludge retained on 10 micron millipore filter, mg./100 ml.	**

Loss of Weight of Metals, mg./sq.cm:

Magnesium	1.59 ***
Aluminum	0.00
Copper	0.86 ****
Silver	0.01 *****
Steel	0.00 *****

- * Air flow 5 ± 0.5 liters/hour. With reflux.
- ** Cannot be filtered thru 10 micron filter.
- *** Dull gray-etched.
- **** Bright etching.
- ***** Light gold.
- ***** Blue.

TABLE XXXI-CONTINUED

SAMPLE NUMBER ELO-66-117

CORROSION AND OXIDATION STABILITY TEST*
48 hours @ 400 deg. F.**

Tests on the Original Oil:

Viscosity @ 100 deg. F., cs.	62.73
Viscosity @ 210 deg. F., cs.	9.14
Neutralization No., mg.KOH/g.	0.03

Tests on the Oxidized Oil:

Viscosity @ 100 deg. F., cs.	93.29
Viscosity @ 210 deg. F., cs.	11.68
Neutralization No., mg.KOH/g.	3.18
Evaporation Loss, %	3.54
Appearance after oxidation:	Dark reddish brown; no precipitate
Increase in Viscosity @ 100 deg. F., %	48.7
Increase in Viscosity @ 210 deg. F., %	27.3
Increase in Neutralization No., mg.KOH/g.	3.15
Sludge retained on 10 micron millipore filter, mg./100 ml.	0.63

Loss of Weight of Metals, mg./sq.cm:

Aluminum	(QQ-A-355)	0.00
Titanium	(MIL-T-009046B, 8% Mn)	0.00 ***
Silver	(MIL-S-13282)	0.07
Steel	(Tool Steel-Type M-10)	0.00 ****
Copper	(QQ-C-576)	0.11 *****
Magnesium	(QQ-M-44)	0.00

* Washers in same configuration as in Micro Corrosion Oxidation.

** Air flow 130-0.5 liters/hour. Without reflux.

*** Light gold.

**** Gold.

***** Moderate tarnish-2D.

TABLE XXXII

SAMPLE NUMBER ELO-67-15

Copper Strip Corrosion (72 hours @ 250 deg. F.)
MIL-H-5606B

Moderate tarnish-2C

Kinematic Viscosity:

@ 0 deg. F., cs.	2,508
@ 100 deg. F., cs.	24.39
@ 130 deg. F., cs.	11.63
@ 210 deg. F., cs.	3.14
@ 275 deg. F., cs.	1.64

CORROSION AND OXIDATION STABILITY TEST
168 hours @ 250 deg. F. - MIL-H-5606B*

Tests on the Original Oil:

Viscosity @ 130 deg. F., cs.	11.63
Neutralization No., mg.KOH/g.	0.18

Tests on the Oxidized Oil:

Viscosity @ 130 deg. F., cs.	12.77
Neutralization No., mg.KOH/g.	0.31
Evaporation Loss, %	1.91
Appearance after oxidation:	Water white; no precipitate
Increase in Viscosity, %	9.8
Increase in Neutralization No., mg.KOH/g.	0.13

Loss of Weight of Metals, mg./sq.cm:

Magnesium	0.00
Aluminum	0.00
Copper	0.00 *
Cadmium	0.01
Steel	0.00

* Air flow 5 ± 0.5 liters/hour. With reflux.
** Dark tarnish-3B.

TABLE XXXIII

SAMPLE NUMBER ELO-67-16

Kinematic Viscosity:

@ 100 deg. F., cs.	71.83
@ 130 deg. F., cs.	31.90
@ 210 deg. F., cs.	7.62

Flash Point, deg. F. (Cleveland Open Cup) 420

Fire Point, deg. F. 465

Spontaneous Ignition Temperature, deg. F.
(ASTM D 286) 670

TABLE XXXIV

SAMPLE NUMBER ELO-57-21

Copper Strip Corrosion (72 hours @ 250 deg. F.)
MIL-H-5606B

Dark tarnish-3A

CORROSION AND OXIDATION STABILITY TEST
152 hours @ 250 deg. F. - MIL-H-5606B*

Tests on the Original Oil:

Viscosity @ 130 deg. F., cs.	11.93
Neutralization No., mg.KOH/g.	0.04

Tests on the Oxidized Oil:

Viscosity @ 130 deg. F., cs.	13.29
Neutralization No., mg.KOH/g.	0.07
Evaporation Loss, %	2.74
Appearance after oxidation:	Moderate amber; no precipitate
Increase in Viscosity, %	11.4
Increase in Neutralization No., mg.KOH/g.	0.03

Loss of Weight of Metals, mg./sq.cm:

Magnesium	0.00
Aluminum	0.00
Copper	0.00 **
Cadmium	0.01
Steel	0.00

- * Air flow 5 ± 0.5 liters/hour. With reflux.
- ** Dark tarnish-3B.

TABLE XXXV

SAMPLE NUMBER ELO-67-22

Kinematic Viscosity, ASTM D 445-65:

a. @ 100 deg. F., cs.	163.98
b. @ 210 deg. F., cs.	15.31

Saybolt Viscosity, ASTM D 88-56:

a. @ 100 deg. F., SUS	758
b. @ 210 deg. F., SUS	80.0

TABLE XXXVI

<u>SAMPLE MARKED</u>	<u>FLASH POINT, DEG. F.</u> <u>(CLEVELAND OPEN CUP)</u>	<u>FIRE POINT, DEG. F.</u>
ELO-67-23 1st sample	385	480
ELO-67-23 -22-67 (resubmitted)	405	485

TABLE XXXVI-CONTINUED

SAMPLE NUMBER ELO-67-23

Flash Point, deg. F.	375
Fire Point, deg. F.	480
Spontaneous Ignition Temperature, deg. F. ASTM D 296	720

TABLE XXXVII

SAMPLE NUMBER ELO-67-35

Flash Point, deg. F. (Cleveland Open Cup)	400
Fire Point, deg. F.	460

CORROSION AND OXIDATION STABILITY TEST
48 hours @ 347 deg. F., per MIL-E-27601 *

Tests on the Original Oil:

Viscosity @ 100 deg. F., cs.	25.54
Neutralization No., mg.KOH/g.	0.04

Tests on the Oxidized Oil:

Viscosity @ 100 deg. F., cs.	28.65
Neutralization No., mg.KOH/g.	2.56
Evaporation Loss, %	1.57
Appearance after oxidation:	Dark amber; no precipitate
Increase in Viscosity, %	12.2
Increase in Neutralization No., mg.KOH/g.	2.52

Loss of Weight of Metals, mg./sq.cm:

#350 Stainless Steel	0.00 **
#355 Stainless Steel	0.00 ***
#440 Stainless Steel	0.00 **
Copper	0.20 ****
Silver	0.01

Sludge retained on 10 micron millipore filter, mg./100 ml.	0.5
------------------------------------------------------------	-----

- * Air flow 5 ± 0.5 liters/hour. With reflux.
- ** Gold
- *** Light gold
- **** Dark tarnish 3B; bright etching

TABLE XXXVIII

SAMPLE NUMBER ELO-67-49

Spontaneous Ignition Temperature, deg. F.
(ASTM D 286)

735

TABLE XXXIX

SAMPLE NUMBER ELO-67-50

Specification MIL-H-5606B

Kinematic Viscosity:

a. @ -40 deg. F., cs.	2,286
b. @ 100 deg. F., cs.	16.94
c. @ 130 deg. F., cs.	10.03
d. @ 210 deg. F., cs.	3.73

Four Point, deg. F. Below 85 below 0

Flash Point, deg. F. (Cleveland Open Cup) 435

Fire Point, deg. F. 490

Spontaneous Ignition Temperature, deg. F.
(ASTM D 286) 675

Copper Strip Corrosion (72 hours @ 250 deg. F.) Dark tarnish-3B

FOAMING TEST

<u>Temperature</u>	<u>Foaming Tendency:</u>	<u>Foam Stability:</u>
	<u>Foam volume, ml. at end of 5 min. blowing period</u>	<u>Foam volume, ml. at end of 10 min. settling period</u>
75 deg. F.	Traces	0 after 3 seconds

Rubber Swelling, % ("L" Rubber) 6.70

Evaporation Test (4 hours @ 150 deg. F.) Passes - Oily, not hard or tacky

TABLE XXXIX-CONTINUED

SAMPLE NUMBER ELO-67-50

CORROSION AND OXIDATION STABILITY TEST
48 hours @ 347 deg. F., per MIL-H-27601A*

Tests on the Original Oil:

Viscosity @ 100 deg. F., cs.	17.01
Neutralization No., mg.KOH/g.	0.03

Tests on the Oxidized Oil:

Viscosity @ 100 deg. F., cs.	17.15
Neutralization No., mg.KOH/g.	0.49
Evaporation Loss, %	1.02
Appearance after oxidation:	Moderate amber; no precipitate
Increase in Viscosity, %	0.8
Increase in Neutralization No., mg.KOH/g.	0.46

Loss of Weight of Metals, mg./sq.cm:

#350 Stainless Steel	0.01 **
Titanium	0.00 **
#440 Stainless Steel	0.00 **
Copper	0.02 ***
Silver	0.00 **

Sludge retained on 10 micron millipore filter, mg./100 ml.	1.1
------------------------------------------------------------	-----

- * Air flow 5 ± 0.5 liters/hour. With reflux.
- ** Light gold
- *** Moderate tarnish-2E

TABLE XXXIX-CONTINUED

SAMPLE NUMBER ELO-67-50

CORROSION AND OXIDATION STABILITY TEST
168 hours @ 250 deg. F. - MIL-H-5606B*

Tests on the Original Oil:

Viscosity @ 130 deg. F., cs.	10.03
Neutralization No., mg.KOH/g.	0.05

Tests on the Oxidized Oil:

Viscosity @ 130 deg. F., cs.	10.03
Neutralization No., mg.KOH/g.	0.05
Evaporation Loss, %	0.76
Appearance after oxidation:	Straw color; no precipitate
Increase in Viscosity, %	0.5
Change in Neutralization No., mg.KOH/g.	0.00

Loss of Weight of Metals, mg./sq.cm:

Magnesium	0.00
Aluminum	0.00
Copper	0.02 **
Cadmium	0.01
Steel	0.00

- * Air flow 5 ± 0.5 liters/hour. With reflux.
** Moderate tarnish-2E.

TABLE XXXIX-CONTINUED

SAMPLE NUMBER ELO-67-50

SONIC SHEAR TEST - MIL-H-5606B

Properties of Reference Fluid

Viscosity @ 130 deg. F., cs:

a. Before irradiation	10.20
b. After irradiation of 30 ml. of fluid for 30 minutes	8.71
c. % change	-14.61

Viscosity @ -40 deg. F., cs:

a. Before irradiation	480.2
b. After irradiation of 30 ml. of fluid for 30 minutes	433.0
c. % change	-9.82

Properties of Sample

Viscosity @ 130 deg. F., cs:

a. Before irradiation	10.03
b. After irradiation of 30 ml. of fluid for 30 minutes	9.98
c. % change	-0.48

Viscosity @ -40 deg. F., cs:

a. Before irradiation	2,266
b. After irradiation of 30 ml. of fluid for 30 minutes	2,263
c. % change	-1.0

Neutralization No., mg.KOH/g.

a. Before irradiation	0.05
b. After irradiation of 30 ml. of fluid for 30 minutes	0.02
c. change	0.03

TABLE XI.

SAMPLE NUMBER ELO-67-54

Specification MIL-E-5606B

Pour Point, deg. F.	30 below 0
Acid Number, mg.KOH/g.	0.04
Specific Gravity @ 60/60 deg. F.	1.9182
Kinematic Viscosity:	
a. at -20 deg. F., cs.	1,795
b. at 100 deg. F., cs.	14.72
c. at 210 deg. F., cs.	2.70
Copper Strip Corrosion (72 hours @ 250 deg. F.)	Dark tarnish-3B

FOAMING TEST

<u>Temperature</u>	<u>Foaming Tendency: Foam volume, ml. at end of 5 min. blowing period</u>	<u>Foam Stability: Foam volume, ml. at end of 10 min. settling period</u>
75 deg. F.	20	0 after 25 seconds

VISCOSITY STABILITY (72 HOURS @ -20 DEG. F)

<u>HOURS</u>	<u>VISCOSITY, cs.</u>
0	1,795
3	1,814
24	1,823
48	1,823
72	1,825

TABLE XL-CONTINUED

SAMPLE NUMBER ELO-67-54

CORROSION AND OXIDATION STABILITY TEST
168 hours @ 250 deg. F. - MIL-E-5606B*

Tests on the Original Oil:

Viscosity @ 100 deg. F., cs.	14.72
Neutralization No., mg.KOH/g.	0.04

Tests on the Oxidized Oil:

Viscosity @ 100 deg. F., cs.	16.10
Neutralization No., mg.KOH/g.	0.04
Evaporation Loss, %	2.1
Appearance after oxidation:	Water white, no precipitate
Increase in Viscosity, %	9.4
Increase in Neutralization No., mg.KOH/g.	0.00

Loss of Weight of Metals, mg./sq.cm:

Magnesium	0.00
Aluminum	0.00
Copper	0.01 **
Cadmium	0.02
Steel	0.00

* Air flow 5 ± 0.5 liters/hour. With reflux.

** Moderate tarnish-2A

TABLE XLI

SAMPLE NUMBER MCG-85-303

MEAN HERTZ LOAD
Rock Island Arsenal Method

<u>Load, lbs.</u>	<u>Scar diameter, mm.</u>	<u>Corrected load, lbs.</u>
40	0.330	35.181
50	0.375	42.539
63	0.395	54.237
80	0.430	69.354 *
100	0.532	75.165 **
126	0.644	85.636
160	1.176	64.481
200	2.016	50.644
250	WELD	
		<u>Total A 479.837</u>

$$\frac{479.837 + 253.77}{10} = \frac{733.607}{10} = \text{Mean Hertz Load } 73.9$$

* No seizure

** Seizure

TABLE XLI-CONTINUED

SAMPLE NUMBER MCG-66-303
GREASE

Test Conditions: Temperature:	425 \pm 10 deg. F.
Cycles/minute	250
Angle of Oscillation, deg:	10
Load, lbs:	4000

Cycles to Failure

<u>Run</u>	<u>Cycles</u>
1	102,482
2	111,685
Average of runs 1 and 2	107,033

TABLE XLI-CONTINUED

SAMPLE NUMBER MCG-65-303, RUN NO. 1

OSCILLATING BEARING TEST
ADSRP-6 BEARINGS

425 deg. F., 4,000 lb. load; stopped automatically after
102,482 cycles; oscillation - 10^6 ; no relubrication.

Bottom Bearing:

Rollers	no fracture; heavy spalling; severe plastic deformation; heavy wear.
Inner Race	no fracture; heavy spalling; severe plastic deformation; heavy wear.
Outer Race	no fracture; heavy spalling; moderate plastic deformation; heavy wear.

Top Bearing:

Rollers	no fracture; moderate spalling; no plastic deformation; heavy wear.
Inner Race	no fracture; moderate spalling; no plastic deformation; heavy wear.
Outer Race	no fracture; light spalling; no plastic deformation; heavy wear.

Note: Thermocouples for measurement and control of temperature
were welded to the inner races of both bearings.

TABLE XLI-CONTINUED

SAMPLE NUMBER MCG-56-303, RUN NO. 2

OSCILLATING BEARING TEST
ADSRP-6 BEARINGS

425 deg. F., 4,000 lb. load; stopped automatically after
111,585 cycles; oscillation $\pm 10^\circ$; no relubrication.

Bottom Bearing:

Rollers	no fracture; heavy spalling; severe plastic deformation; heavy wear.
Inner Race	no fracture; heavy spalling; severe plastic deformation; heavy wear.
Outer Race	no fracture; heavy spalling; moderate plastic deformation; heavy wear.

Top Bearing:

Rollers	no fracture; heavy spalling; severe plastic deformation; heavy wear.
Inner Race	no fracture; heavy spalling; severe plastic deformation; heavy wear.
Outer Race	no fracture; moderate spalling; some plastic deformation; heavy wear.

Note: Thermocouples for measurement and control of temperature
were welded to the inner races of both bearings.

TABLE XLII

SAMPLE NUMBER MCG-66-334

MEAN HERTZ LOAD
Rock Island Arsenal Method

<u>Load, kg.</u>	<u>Scar diameter, mm.</u>	<u>Corrected load, kg.</u>
24	0.297 *	21.056
32	0.329	26.951
40	0.350	34.114
50	1.288	12.484
63	1.519	14.404
80	1.953	15.412
100	2.45	16.535
120	WELD	
		<hr/>
		Total A 140.960
$\frac{140.960 + 64.81}{10} = \text{Mean Hertz Load}$		20.6

* No seizure

TABLE XLII-CONTINUED

SAMPLE NUMBER MCG-66-334
GREASE

Test Conditions: Temperature:	125 \pm 10 deg. F.
Cycles/minute	250
Angle of Oscillation, deg:	10
Load, lbs:	4000

Cycles to Failure:

<u>Run</u>	<u>Cycles</u>
1	189,365
2	223,349
Average of runs 1 and 2	208,857

TABLE XLII-CONTINUED

SAMPLE NUMBER MCG-66-334, RUN NO. 1

OSCILLATING BEARING TEST
ADERP-6 BEARINGS

425 deg. F., 4,000 lb. load; stopped automatically after
189,365 cycles; oscillation - 10°; no relubrication.

Bottom Bearing:

Rollers	no fracture; moderate spalling; some plastic deformation; heavy wear.
Inner Race	no fracture; heavy spalling; severe plastic deformation; heavy wear.
Outer Race	no fracture; moderate spalling; some plastic deformation; heavy wear.

Top Bearing:

Rollers	no fracture; heavy spalling; severe plastic deformation; heavy wear.
Inner Race	no fracture; heavy spalling; severe plastic deformation; heavy wear.
Outer Race	no fracture; moderate spalling; some plastic deformation; heavy wear.

Note: Thermocouples for measurement and control of temperature
were welded to the inner races of both bearings.

TABLE XLII-CONTINUED

SAMPLE NUMBER MCG-66-334, RUN NO. 2

OSCILLATING BEARING TEST
ADSRP-6 BEARINGS

425 deg. F., 4,000 lb. load; stopped automatically after
228,349 cycles; oscillation $\pm 10^\circ$; no relubrication.

Bottom Bearing:

Rollers	no fracture; no spalling; no plastic deformation; moderate wear.
Inner Race	no fracture; no spalling; no plastic deformation; moderate wear.
Outer Race	no fracture; no spalling; no plastic deformation; moderate wear.

Top Bearing:

Rollers	no fracture; heavy spalling; severe plastic deformation; heavy wear.
Inner Race	no fracture; heavy spalling; severe plastic deformation; heavy wear.
Outer Race	no fracture; heavy spalling; severe plastic deformation; heavy wear.

Note: Thermocouples for measurement and control of temperature were welded to the inner races of both bearings.

TABLE XI.III

SAMPLE NUMBER MCG-66-335

MEAN HERTZ LOAD
Rock Island Arsenal Method

<u>Load, kg.</u>	<u>Scar diameter, mm.</u>	<u>Corrected load, kg.</u>
40	0.335	35.536
50	0.364 *	44.178
63	0.483	45.300
80	0.560	53.750
100	0.531	59.742
125	0.791	59.722
160	0.579	85.298
200	1.092	93.498
250	1.120	122.678
315	1.248	<u>150.080</u>
	Total A	769.700
400	1.519	165.454
500	WELD	<u> </u>
	Average B	84.727

$$769.700 + 84.727 + 40.57 = \frac{894.997}{10} = \text{Mean Hertz Load } 89.5$$

* No seizure.

TABLE XLIII-CONTINUED

SAMPLE NUMBER MCG-66-335
GREASE

Test Conditions: Temperature:	425 ± 10 deg. F.
Cycles/minute	250
Angle of Oscillation, deg:	10
Load, lbs:	4000

Cycles to Failure:

<u>Run</u>	<u>Cycles</u>
1	256,529
2	209,433
Average of runs 1 and 2	232,981

TABLE XLIII-CONTINUED

SAMPLE NUMBER MCG-66-335, RUN NO. 1

OSCILLATING BEARING TEST
ADSRP-6 BEARINGS

425 deg. F., 4,000 lb. load; stopped automatically after
256,529 cycles; oscillation - 10°; no relubrication.

Bottom Bearing:

Rollers	no fracture; no spalling; no plastic deformation; moderate wear.
Inner Race	no fracture; no spalling; no plastic deformation; moderate wear.
Outer Race	no fracture; no spalling; no plastic deformation; heavy wear.

Top Bearing:

Rollers	no fracture; no spalling; no plastic deformation; moderate wear.
Inner Race	no fracture; light spalling; no plastic deformation; moderate wear.
Outer Race	no fracture; light spalling; no plastic deformation; heavy wear.

Note: Thermocouples for measurement and control of temperature were welded to the inner races of both bearings.

TABLE XLIII-CONTINUED

SAMPLE NUMBER MCG-66-235, RUN NO. 2

OSCILLATING BEARING TEST
ADSRP-6 BEARINGS

425 deg. F., 4,000 lb. load; stopped automatically after
209,433 cycles; oscillation - 10°; no relubrication.

Bottom Bearing:

Rollers	no fracture; heavy spalling; severe plastic deformation; heavy wear.
Inner Race	no fracture; heavy spalling; severe plastic deformation; heavy.
Outer Race	no fracture; heavy spalling; moderate plastic deformation; heavy wear.

Top Bearing:

Rollers	no fracture; light spalling; no plastic deformation; moderate wear.
Inner Race	no fracture; light spalling; no plastic deformation; heavy wear.
Outer Race	no fracture; light spalling; no plastic deformation; heavy wear.

Note: Thermocouples for measurement and control of temperature
were welded to the inner races of both bearings.

TABLE XLIV

SAMPLE NUMBER M3-56-335

MEAN HERTZ LOAD
Rock Island Arsenal Method

<u>Load, kg.</u>	<u>Scar diameter, mm.</u>	<u>Corrected load, kg.</u>
40	0.336	35.536
50	0.364	44.176
63	0.378	57.894
80	0.413	72.581
100	0.462	86.396
126	0.497 *	110.966
150	0.903	83.976
200	1.071	95.331
250	WELD	
Total A		537.145
$\frac{456.30 + 587.15}{10} = 1044.04 = \text{Mean Hertz Load}$		104.4

* No seizure

TABLE XLIV-CONTINUED

SAMPLE NUMBER MCG-66-336
GREASE

Test Conditions: Temperature:	425 \pm 10 deg. F.
Cycles/minute	250
Angle of Oscillation, deg:	10
Load, lbs:	4000

Cycles to Failure:

<u>Run</u>	<u>Cycles</u>
1	228,375
2	141,222
3	150,295
Average of runs 1, 2 and 3	173,297

TABLE XLIV-CONTINUED

SAMPLE NUMBER MCG-66-336, RUN NO. 1

OSCILLATING BEARING TEST
ADSRP-6 BEARINGS

425 deg. F., 4,000 lb. load; stopped automatically after
228,375 cycles; oscillation $\pm 10^\circ$; no relubrication.

Bottom Bearing:

Rollers

no fracture;
heavy spalling;
severe plastic deformation;
heavy wear.

Inner Race

no fracture;
heavy spalling;
severe plastic deformation;
heavy wear.

Outer Race

no fracture;
heavy spalling;
severe plastic deformation;
heavy wear.

Top Bearing:

Rollers

no fracture;
some spalling;
no plastic deformation;
heavy wear.

Inner Race

no fracture;
some spalling;
no plastic deformation;
moderate wear.

Outer Race

no fracture;
moderate spalling;
no plastic deformation;
heavy wear.

Note: Thermocouples for measurement and control of temperature
were welded to the inner races of both bearings.

TABLE XLIV-CONTINUED

SAMPLE NUMBER MCG-66-336, RUN NO. 2

OSCILLATING BEARING TEST
ADSRP-6 BEARINGS

425 deg. F., 4,000 lb. load; stopped automatically after
141,222 cycles; oscillation - 10^0 ; no relubrication.

Bottom Bearing:

Rollers	no fracture; heavy spalling; severe plastic deformation; heavy wear.
Inner Race	no fracture; heavy spalling; severe plastic deformation; heavy wear.
Outer Race	no fracture; heavy spalling; severe plastic deformation; heavy wear.

Top Bearing:

Rollers	no fracture; some spalling; no plastic deformation; moderate wear.
Inner Race	no fracture; moderate spalling; no plastic deformation; heavy wear.
Outer Race	no fracture; moderate spalling; no plastic deformation; heavy wear.

Note: Thermocouples for measurement and control of temperature
were welded to the inner races of both bearings.

TABLE XLIV-CONTINUED

SAMPLE NUMBER MCG-66-336, RUN NO. 3

OSCILLATING BEARING TEST
ADSRP-6 BEARINGS

425 deg. F., 4,000 lb. load; stopped automatically after
150,295 cycles; oscillation $\pm 10^\circ$; no relubrication.

Bottom Bearing:

Rollers	no fracture; heavy spalling; severe plastic deformation; heavy wear.
Inner Race	no fracture; heavy spalling; severe plastic deformation; heavy wear.
Outer Race	no fracture; moderate spalling; moderate plastic deformation; heavy wear.

Top Bearing:

Rollers	no fracture; some spalling; no plastic deformation; moderate wear.
Inner Race	no fracture; some spalling; no plastic deformation; heavy wear.
Outer Race	no fracture; some spalling; no plastic deformation; heavy wear.

Note: Thermocouples for measurement and control of temperature
were welded to the inner races of both bearings.

UNCLASSIFIED

Security Classification

DOCUMENT CONTROL DATA - R 8 D

(Security classification of title, body of abstract and indexing annotation must be entered when the overall report is classified)

1. ORIGINATING ACTIVITY (Corporate author)		2a. REPORT SECURITY CLASSIFICATION	
Phoenix Chemical Laboratory, Incorporated 3953 W. Shakespeare Avenue Chicago, Illinois 60647		UNCLASSIFIED	
3. REPORT TITLE		2b. GROUP	
Physical and Chemical Properties of Fluids, Lubricants and Related Materials		NA	
4. DESCRIPTIVE NOTES (Type of report and inclusive dates)			
Final - 1 November 1966 to 31 October 1967			
5. AUTHOR(S) (First name, middle initial, last name)			
Krawetz, A. A. Krawetz, J. Krawetz, G. A., et al			
6. REPORT DATE		7a. TOTAL NO. OF PAGES	7b. NO. OF REFS
March 1968		218	7
8a. CONTRACT OR GRANT NO.		8b. ORIGINATOR'S REPORT NUMBER(S)	
AF 33(615)-3416		AFML-TR-67-133, Part II	
a. PROJECT NO. 7343		8c. OTHER REPORT NO(S) (Any other numbers that may be assigned this report)	
c. TASK NO. 734303		NA	
9. DISTRIBUTION STATEMENT			
This document is subject to special export controls and each transmittal to foreign government or foreign nationals may be made only with prior approval of the Fluid and Lubricant Materials Branch, MANL, Nonmetallic Materials Division, Air Force Materials Laboratory, Wright-Patterson Air Force Base, Ohio 45433.			
11. SUPPLEMENTARY NOTES		12. SPONSORING MILITARY ACTIVITY	
		Air Force Materials Laboratory Air Force Systems Command Wright-Patterson Air Force Base, Ohio	
13. ABSTRACT			
<p>Spontaneous ignition phenomena have been evaluated for eight experimental hydraulic fluids. The technique of thermoelectric flame detection has been used to determine the minimum spontaneous ignition temperature for each system in air at one atmosphere pressure. Differential thermal analysis has been employed for the study of the thermal and oxidative degradation of two experimental lubricants in the presence of several metal oxide catalysts. Six other lubricant systems without added catalytic agents have been subjected to differential thermal analysis to evaluate their resistance to thermal and oxidative decomposition. The standard MIL-H-27601A constant temperature thermal stability apparatus has been modified to permit the measurement and recording of pressures developed during the course of the test. Several materials have been evaluated by means of the modified procedure. The chemical and physical properties of various lubricants and hydraulic fluids have been determined. Emphasis has been directed but not exclusively confined to the study of properties which are related to the attainment of effective lubrication at elevated temperatures.</p> <p>This abstract is subject to special export controls and each transmittal to foreign government or foreign nations may be made only with prior approval of the Fluid and Lubricant Materials Branch, MANL, Nonmetallic Materials Division, Air Force Materials Laboratory, Wright-Patterson Air Force Base, Ohio 45433.</p>			

DD FORM 1473

UNCLASSIFIED

Security Classification

UNCLASSIFIED

Security Classification

KEY WORDS	LINK A		LINK B		LINK C	
	ROLE	WT	ROLE	WT	ROLE	WT
High temperature lubricants Hydraulic fluids and greases Differential thermal analysis Spontaneous ignition temperature Physical and chemical properties of fluids, lubricants and greases						

UNCLASSIFIED

Security Classification